IntechOpen

Silver Nanoparticles

Fabrication, Characterization and Applications

Edited by Khan Maaz

SILVER NANOPARTICLES - FABRICATION, CHARACTERIZATION AND APPLICATIONS

Edited by **Khan Maaz**

Silver Nanoparticles - Fabrication, Characterization and Applications
http://dx.doi.org/10.5772/intechopen.71247
Edited by Khan Maaz

Contributors

Neelu Chouhan, Parvathalu Kalakonda, Mudassar Abbas, Nida Naeem, Hina Iftikhar, Usman Latif, Raul Alberto Morales Luckie, Víctor Sanchez Mendieta, Sarai Carmina Guadarrama Reyes, Rogelio Schougall, Rafael Lopez Casatañares, Remziye Güzel, Gülbahar Erdal, Enrique Rocha, Jose Vega Baudrit, Hermicenda Perez Vidal, Zenaida Guerra Que, Jose Gilberto Torres Torres, María A. Lunagómez Rocha, Juan C. Arévalo Pérez, Ignacio Cuauhtémoc López, Alejandra E. Espinosa De Los Monteros Reyna, Durvel De La Cruz Romero, José G. Pacheco Sosa, Adib A. Silahua Pavón, Jorge S. Ferráez Hernández, Musibau Azeez, Felicia Durodola, Agbaje Lateef, Taofeek Yekeen, Amos Adubi, Margarita Miranda Hernadez, Andres A. Arocha Arcos, Sarai C Guadarrama-Reyes, Rogelio J Scougall-Vilchis, Markus Diantoro, Abdulloh Fuad, Nandang Mufti, Arif Hidayat, Hadi Nur, Atamjit Singh, Kirandeep Kaur, Yasemin Budama Kilinc, Rabia Cakir Koc, Tolga Zorlu, Burak Özdemir, Zeynep Karavelioglu, A. Can Egil, Serda Kecel-Gunduz, Adewumi Dada, Oluwasesan Micheal Bello, Folahan A. Adekola, Oluyomi Adeyemi, Charles Adetunji, Oluwakemi Josephine Awakan, Abiola Grace Femi-Adepoju, Magdalena Skonieczna, Dorota Hudy

Notice

First published in London, United Kingdom, 2018 by IntechOpen
eBook (PDF) Published by IntechOpen, 2019
IntechOpen is the global imprint of INTECHOPEN LIMITED, registered in England and Wales, registration number: 11086078, The Shard, 25th floor, 32 London Bridge Street
London, SE19SG – United Kingdom
Printed in Croatia

British Library Cataloguing-in-Publication Data
A catalogue record for this book is available from the British Library

Additional hard and PDF copies can be obtained from orders@intechopen.com

Silver Nanoparticles - Fabrication, Characterization and Applications
Edited by Khan Maaz

p. cm.

Print ISBN 978-1-78923-478-7

Online ISBN 978-1-78923-479-4

eBook (PDF) ISBN 978-1-83881-546-2

Meet the editor

Dr. Maaz Khan is working as a senior researcher in PINSTECH, Pakistan. He has done his PhD degree from Quaid-i-Azam University and postdoctorate degree from South Korea and China. He is working on fabrication of nanomaterials applying different chemical and electrochemical techniques and studying their structural, magnetic, optical, and electrical characterizations. He is the author of more than 80 articles in peer-reviewed journals and also the author and editor of many books in the field of materials science. Dr. Maaz is working as the editor in chief of the *Journal of Materials, Processing and Design* and executive editor of the *International Journal of Nano Studies & Technology* and also serving as an editorial board member of few more journals.

Contents

Preface

The book contains 14 chapters that describe fabrication, characterization, and application of silver nanoparticles. Various topics such as preparation of silver nanoparticles using wet chemical route and green synthesis of silver nanoparticles using plants and other organism derivatives; structural, chemical, electrical, optical, and photocatalytic properties, as well as their applications as electrochemical transducer and tougheners of alumina ceramics; antimicrobial, anticoagulant, and thrombolytic activities; and silver-based hybrid nanostructures for medical applications are discussed in detail in the book. Each chapter is written clearly and precisely that illustrates easier understanding of various phenomena reported in the book. This book is addressed to scientists in specialized fields, research students, postdoctoral fellows, and technical professionals.

The authors of the book are highly skilled in their field, and therefore this book provides up-to-date information about the concerned topics. The contents provide fundamental preparation needed for advanced research on silver nanoparticles and their applications. At the end of each chapter, references are included that can lead the readers to the best sources in the literature and help them to go into more details about the concerned topics.

I am grateful to all the authors for helping me to complete this project and also to the entire InTech's publishing team for making this project possible. I am very thankful to Mr. Julian Virag, Publishing Process Manager of the book, for his cooperative attitude during the entire reviewing and publishing processes. I hope that this book will provide an opportunity to the readers to strengthen their knowledge and capabilities in the fields related to silver nanoparticles and their applications.

Maaz Khan
Senior Researcher
Physics Division
Pakistan Institute of Nuclear Science and Technology
Islamabad, Pakistan

Section 1

Synthesis and Properties

Chapter 1

Synthesis of Silver Nanoparticles

Remziye Güzel and Gülbahar Erdal

Additional information is available at the end of the chapter

http://dx.doi.org/10.5772/intechopen.75363

Abstract

Nanoparticles of noble metals, especially the silver nanoparticles, have been widely used in different fields of science. Their unique properties, which can be incorporated into biosensor materials, composite fibers, cosmetic products, antimicrobial applications, conducting materials and electronic components, make them a very important subject to be studied by chemistry, biology, healthcare, electronic and other related branches. These unique properties depend upon size and shape of the silver nanoparticles. Different preparation methods have been reported for the synthesis of the silver nanoparticles, such as electron irradiation, laser ablation, chemical reduction, biological artificial methods, photochemical methods and microwave processing. This chapter aims to inform the synthesis methods of the silver nanoparticles.

Keywords: silver nanoparticles, physical methods, chemical methods, green synthesis, different shape

1. Introduction

Silver has too much of modern industrial uses and is considered a store of wealth. However, the story of this legendary precious metal begins with its use by ancient civilizations. Silver has many attributes that made it so valuable to early peoples. It is malleable, ductile, lustrous, resilient, conductive, antibacterial, and rare. Also, it was used as a precious commodity in currencies, ornaments, jewelry, electrical contacts and photography, among others. Although bulk silver is widely known for their brilliant surfaces and colors, there is a drastic color difference when the metal reduces in dimensions. Even though the craftsmen did not know nanoparticles in that period, the mixing of the metal chlorides with molten glass led to the formation of metallic nanoparticles of different shape and size, therefore the physical formats of the metal nanoparticles had interesting interactions with light and produced visibly beautiful colors. The metal chlorides materialized

and formed nanoparticles in the molten glass before cooling, making art, one of the first uses for nanotechnology. Nowadays, the nanoparticles are an important field of the modern research dealing with design, synthesis, and manipulation of particle structures ranging from approximately 1 to 100 nm. Nanoparticle research is currently an area of intense scientific research, due to a wide variety of potential applications in fields such as healthcare, cosmetics, food and feed, environmental health, mechanics, optics, biomedical sciences, chemical industries, electronics, space industries, drug-gene delivery, energy science, optoelectronics, catalysis, single electron transistors, light emitters, nonlinear optical devices, and photo-electrochemical area. The silver nanoparticles have been widely used in the fields of chemistry and related branches due to their high surface to volume ratio and excellent conducting capability. From electrical switches, solar panels to chemical-producing catalysts and antimicrobial activity, the silver nanoparticle is an essential component in many industries. Its unique properties make it nearly impossible to substitute and its uses contain a wide range of applications. At the same time, many of the consumer products that claim to contain nanomaterials contain nanosilver. Examples of the consumer products that include nanosilver including computers, mobile phones, automobile appliances, food packaging materials, food supplements, textiles, electronics, household appliances, cosmetics, medical devices, imaging techniques, and water and environment disinfectants. Most of these nanosilver-containing products are manufactured in North America, the Far East, especially in China, South Korea, Taiwan, Vietnam and India, the Russian Federation, and the Western Europe.

The knowledge of the silver nanomaterials synthesis methods is important due to an extensive application and area of use perspective. The main problem in synthesizing the silver nanoparticles is the control of their physical properties such as obtaining uniform particle size distribution, identical shape, morphology, nanoparticle coating or stabilizing agent, chemical composition or type and crystal structure. The methods can be classified and categorized that they follow common approaches and the differences such as reactants and the reaction conditions. Top-down versus bottom-up, green versus nongreen, and conventional versus nonconventional synthesis methods have been reported. The conventional synthesis methods contain the use of citrate, borohydride, two-phase systems (water-organic), organic reducers such as cyclodextrin, and micelles and/or polymer in the synthesis process. The unconventional methods contain laser ablation, radiocatalysis, vacuum evaporation of metal, irradiation, photolithography, electrodeposition and the electrocondensation. Top-down and bottom-up are the two synthesis approaches of metallic nanoparticles involving chemical, physical, and biological means. The common fabrication of the nanoparticles includes chemical and physical processes. The top-down approach uses macroscopic initial structures, which can be externally controlled in the processing of nanostructures. The nanoparticles synthesized by mechanical grinding of bulk metals and the addition of colloidal protecting agents are some examples of the top-down method. The bottom-up approaches contain the miniaturization of materials components (up to atomic level) with further self-assembly process. The reduction of metals, electrochemical methods, and decomposition are the examples of the bottom-up methods. In addition, the synthesis approaches can be classified as either green or non-green. Green synthetic systems use environmentally friendly agents such as sugars, plant extracts, bacteria and fungi to form and stabilize nanosilver.

It is important to measure nanosilver concentration, size, shape, surface charge, crystal structure, surface chemistry, and surface transformation in nanoparticle synthesis. The characterization

and detection techniques for the nanosilver contain transmission electron microscopy (TEM), scanning electron microscopy (SEM), electrospray scanning mobility particle sizer (ESMPS), zeta size analysis, atomic force microscopy (AFM), dynamic light scattering (DLS), Brunauer-Emmett-Teller analysis (BET), X-ray diffraction (XRD), X-ray photoelectron spectroscopy (XPS), X-ray absorption near edge structure (XANES), Fourier transform infrared spectroscopy (FTIR), Raman spectroscopy, nuclear magnetic resonance spectroscopy (NMR), inductively coupled plasma mass spectroscopy (ICP-MS), thermal gravimetric analysis (TGA), and atomic absorption spectroscopy (AAS).

2. Physical methods

The most important physical methods for the synthesis of the silver nanoparticles are evaporation-condensation, laser ablation, electrical irradiation, gamma irradiation, and lithography. Kimura and Bandow examined the measurement of the optical spectra of many metal colloid solutions and presented new preparation methods of metal colloids inorganic solvents without the chemicals such as redox reagents, polymers, electrolytes, glue or other kinds of colloid stabilizers. Three different preparation methods as the matrix isolation method, the gas flow-cold trap method, and the gas flow-solution trap method, were used to examine the synthesis of silver NPs [1]. The laser ablation method, which has several types of different applications, is another method to study the synthesis of silver nanoparticles (Ag-NPs). The laser ablation technique is a new useful and efficient method to prepare and obtain metal colloids in absence of chemical reagents. This method helps to control particle size of colloids by changing the number of laser pulses [2]. Pyatenko et al. produced silver nanoparticles by irradiating an Ag target with a 532 nm laser beam in pure water. This technique is successfully applied to produce small nanoparticles with a narrow size distribution in pure water without using any chemical additives by using a high-power laser and small laser beam spot sizes [3]. Sadrolhesseini et al. prepared a new method for the fabrication of silver nanoparticles which are dispersed in graphene oxide using the laser ablation and thermal effusivity of nanocomposite. This environmentally friendly method, which does not require any chemical agents, polymeric or surfactant stabilizers, works by releasing the nanoparticles inside liquid solution [4]. Tsuji et al. studied to perform to prepare Ag-NPs by laser ablation of a silver plate in polyvinylpyrrolidone (PVP) aqueous solutions and laser irradiation onto prepared colloidal solutions. This technique is seen as a remarkable technique due to its procedural simplicity and a very high rate of obtainability of nanoparticles of various species and materials such as metals, metal oxides semiconductors, and organic materials by the irradiation of intense laser light onto those materials settled in solvents [5]. The pulsed photoacoustic (PA) technique is another method to study the synthesis of the Ag-NPs in ethanol by laser ablation and determine the production rate laser pulse and concentration of synthesized Ag-NPs [6]. Researchers have studied mechanisms and processes such as plasma formation, dynamics of the cavitation bubble [7, 8], and also the influence of laser parameters and solvents on nanoparticles [9, 10].

Nanosphere lithography (NLS) is a simple and inexpensive nanofabrication method to produce large variety of nanoparticle (NP) structures and well-ordered 2D NP arrays. Jensen et al. studied the effect of solvent on the optical extinction spectrum of periodic arrays of surface-confined

silver nanoparticles fabricated by NSL and four separate samples of NP arrays. Jensen et al. have investigted four separate samples of nanoparticle arrays; three samples were obtained nanoparticles that are truncated tetrahedral in shape but that differ in out-of-plane height and one sample have nanoparticles that are oblate ellipsoidal in shape [11]. Jensen et al. also demonstrated that the localized surface plasmon resonance extinction maximum of a single nanoparticle material system, silver, can be continuously tuned throughout the visible, near-infrared, and mid-infrared regions of the electromagnetic spectrum [12].

3. Chemical method

3.1. Chemical reduction of silver nanoparticles

The size, shape, and surface morphology play an important role in controlling the chemical, physical, optical, and electronic properties of nanomaterials. The chemical reduction is one of the most commonly used methods for the synthesis of silver nanoparticles by inorganic and organic reducing agents. In general, different reducing agents such as sodium citrate, ascorbate, sodium borohydride ($NaBH_4$), elemental hydrogen, polyol process, Tollens reagent, N,N-dimethylformamide (DMF), and poly(ethylene glycol)-block copolymers, hydrazine, and ammonium formate are used for the reduction of the silver ions (Ag^+) in the aqueous or nonaqueous solutions.

3.2. Different shapes of silver nanoparticles synthesized with various chemical reductants

3.2.1. Synthesis of spherical silver nanoparticles

The spherical silver nanoparticles were synthesized using the reducing agents such as ascorbic acid, sodium citrate, $NaBH_4$, thiosulfate, and polyethylene glycol. In addition to that, the use of the surfactants such as citrate, polyvinylpyrolidone (PVP), cetyltrimethylammonium bromide (CTAB), and polyvinyl alcohol (PVA) for interactions with particle surfaces can stabilize particle growth and protect particles from sedimentation and agglomeration [13–17].

3.2.2. Synthesis of silver nanorods

Zhang et al. prepared silver nanorods by photoinduced synthesis (**Figure 1**). At first step, monodisperse spherical seed nanoparticles were prepared by irradiating silver nitrate, bis(p-sulfonatophenyl)-phenylphosphine dihydrate dipotassium salt (BSPP), trisodium citrate, and sodium hydroxide solutions with 254 nm light. Then, Silver nanorods were grown in the solution with the injection of silver seeds at the growth medium containing silver nitrate and sodium citrate and then irradiated for 24 h using a halogen lamp and a bandpass filter to selectively tune. This photomediated method provided an elegant method for controlling the architectural parameters of the resulting silver nanostructures [18]. Ojha et al. mixed the solution of $AgNO_3$ and citrate and added NaOH into the solution. Then solution of ice cold of $NaBH_4$ was added while stirring. To synthesize Ag nanorods of at three different aspect

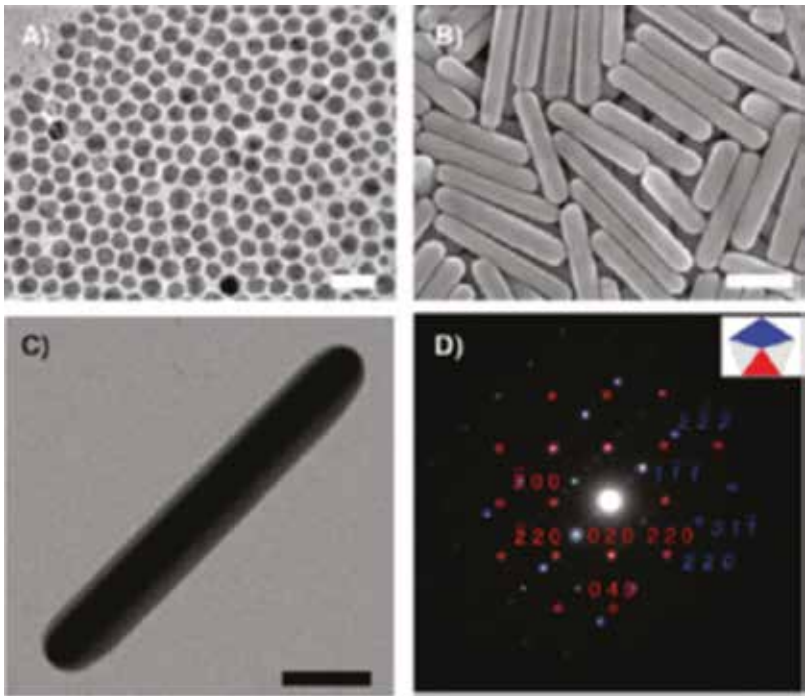

Figure 1. (A) TEM image of the silver seed nanoparticles. (B) SEM and (C) TEM images of silver nanorods synthesized with a bandpass filter centered at 600 ± 20 nm. (D) Selective-area electron diffraction (SAED) pattern of a single silver nanorod, showing the interpenetration. [100] (red) and [112] (blue) zone patterns (scale bars: 100 nm) [18].

ratios, three stock solutions of $AgNO_3$, ascorbic acid, and the surfactant cetyltrimethylammonium bromide (CTAB) were prepared separately. These stock solutions were mixed at certain quantities properly. Thereafter, 1.0, 0.5, and 0.25 ml of synthesized seed solution were added to set one, two and three, respectively, and at the end, NaOH solution was also added to each set. The color of each nanorod solutions depends on the seed concentrations added in the final solution [19]. Ajitha et al. prepared the aqueous solution containing $AgNO_3$ with sodium citrate dihydrate as stabilizer. Then, sodium borohydride (reducing agent) solution was injected to the above solution all at once while stirring vigorously. The solution color was changed to light yellow. The entire solution was heated under continuous stirring on magnetic stirrer. CTAB solution was prepared through heating stirring on a magnetic stirrer for dissolution of CTAB. Then, $AgNO_3$ and ascorbic acid solution were added. And then, the seed solution was added and at last, few drops of NaOH were added to maintain constant pH and stirred well. The synthesis temperature was varied from 30 to 70°C [20].

3.2.3. Synthesis of silver nanowires

Sun et al. studied silver nanostructrures that could be varied from nanoparticles and nanorods to long nanowires by adjusting the reaction conditions, including the ratio of PVP to silver nitrate, reaction temperature, and seeding conditions. They found that the large-scale synthesis of silver nanowires with diameters ranged from 30 to 40 nm, and lengths up to ~50 μm

[21]. Li et al. demonstrated that the diameter of Ag nanowires produced by a polyol synthesis could be controlled by adjusting the concentration of bromide. The silver nanowires with diameters of 20 nm and aspect ratios up to 2000 have obtained by adding 2.2 mM NaBr into $AgNO_3$ solution [22]. Gebeyehu et al. synthesized silver nanowire using a simple polyol method (**Figure 2**). They used polyvinylpyrrolidone as stabilizing and capping agent combined with sodium chloride and potassium bromide salts, ethylene glycol was used as both solvent and a reducing agent, and silver nitrate was used as a silver precursor. They determined that the diameter and uniformity of silver nanowires can be controlled by adjusting the concentration of $AgNO_3$ and [PVP] to [$AgNO_3$] molar ratio keeping the other parameters constant. AgNWs with diameters of 20 nm and aspect ratios >1000 were obtained by adding 30.5 mM $AgNO_3$ to a silver nanowire synthesis [23].

3.2.4. Synthesis of cubic silver nanoparticles

The synthesis of cubic silver nanoparticles was achieved by the reduction of silver nitrate using ethylene glycol in the presence of polyvinylpyrrolidone (PVP). In polyol process, ethylene glycol containing hydroxyl groups have functional structure as both solvent and reducing agent. Polyvinylpyrrolidone as capping agent was used to constitute the cubic shape. Molar ratio of the PVP and silver ions determines the shape of the product [24–26]. Siekkien et al. performed a faster method for synthesis of cubic silver nanoparticle by adding a trace amount of sodium sulfide (Na_2S) or sodium hydrosulfide (NaHS) to the conventional polyol synthesis (**Figure 3**). The reduction agent is important for the synthesis of NPs with different chemical compositions, sizes and morphologies, and controlled dispersities [27].

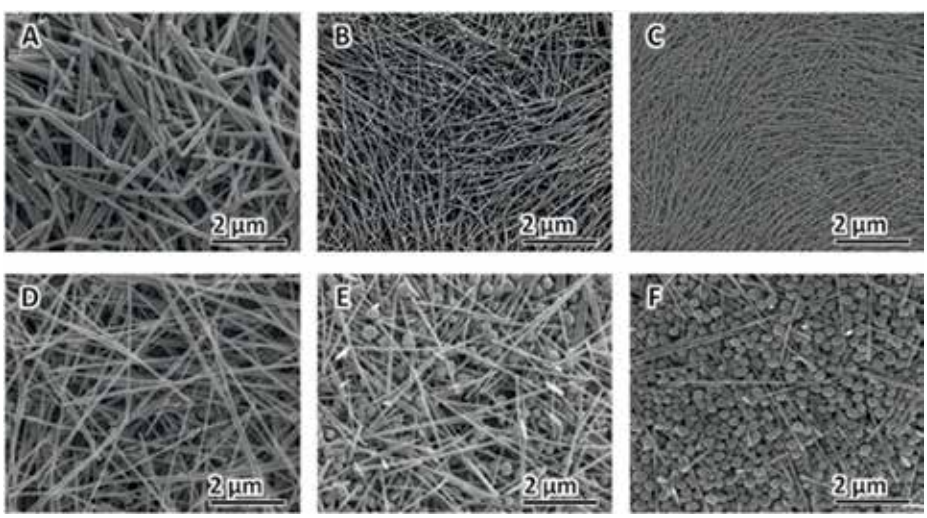

Figure 2. FE-SEM images of AgNWs synthesized at different [PVP] to [$AgNO_3$] molar ratio: (A) 2:1, (B) 4:1, (C) 6:1, (D) 8:1, (E) 10:1, and (F) 12:1 [23].

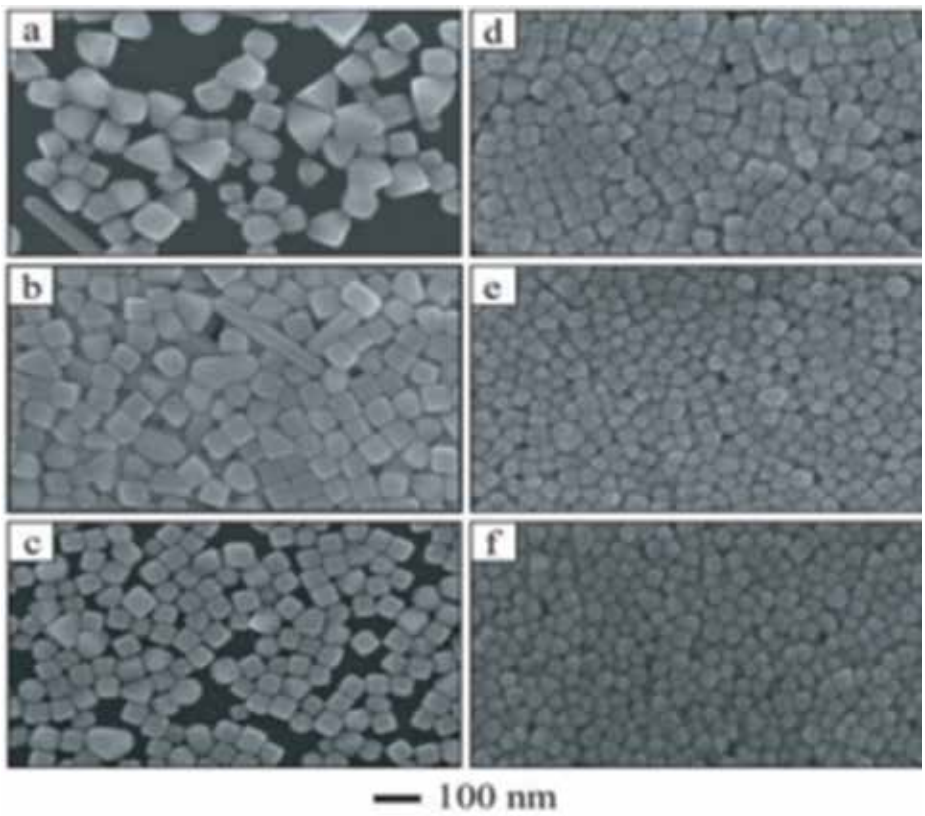

Figure 3. SEM images of reactions containing increasing molar ratios between the repeating unit of PVP and silver nitrate. The ratios of PVP to silver nitrate were (a) 0.77, (b) 1.15, (c) 1.5, (d) 1.9, (e) 2.3, and (f) 0.7 [27].

3.2.5. Synthesis of triangular silver nanoparticles

Zhang et al. prepared silver triangular bipyramids using the photoinduced reduction of 0.3 mM silver nitrate in aqueous solutions containing 1.5 mM sodium citrate, 0.3 mM bis(p-sulfonatophenyl) phenylphosphine dihydrate dipotassium salt (BSPP), and 0.005 M NaOH for 8 h using a 150 W halogen lamp and a bandpass filter (**Figure 4**). The samples were irradiated in the excitation wavelength range (500 ± 20, 550 ± 20, 600 ± 20, 650 ± 20 nm) [28]. Métraux and Mirkin used the chemical reduction method for the fabrication of silver nanoprisms. They synthesized silver nanoprisms at room temperature by using a mixture of $AgNO_3$/$NaBH_4$/polyvinylpyrrolidone/trisodium citrate/H_2O_2 in an aqueous solution as reagents [29].

3.3. Microemulsion techniques

Microemulsion includes a mixture of water, surfactant, and oil or a mixture of water, surfactant, co-surfactant, and oil. Many surfactants are available for the formation of the microemulsion in the preparation of the silver nanoparticles. Generally, many surfactants can be used

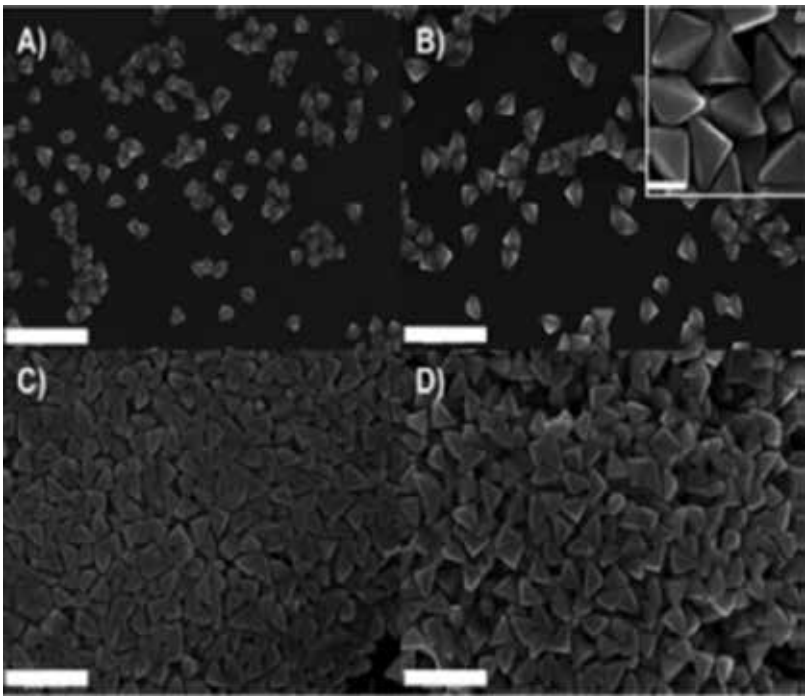

Figure 4. (A–D) SEM images of the triangular bipyramids (scale bar 300 nm) generated with the bandpass filter centered at 500 ± 20, 550 ± 20, 600 ± 20, and 650 ± 20 nm, respectively. Inset of (B): a higher-magnification view, scale bar 100 nm [28].

to form microemulsion, including anionic surfactants such as bis(2-ethylhexyl)sulfosuccinate, sodium dodecyl benzene sulfonate, and lauryl sodium sulfate, cationic surfactants such as cetyltrimethylammonium bromide, polyvinylpyrrolidone, and nonionic surfactants such as Triton X-100, etc. The water droplets covered by surfactant molecules act as micro-reactors and offer a unique micro-environment for the formation of nanoparticle [30–35].

3.4. Microwave-assisted techniques

The microwave synthesis methods provide the reduction of the silver nanoparticles with changeable rate microwave radiation in comparison to the conventional heating technique. Microwave-assisted technology, by accelerating chemical reactions from hours or days to minutes, provides quick results. Also, microwave irradiation provides uniform heating for the preparation of metallic nanoparticles and aids the ripening of these materials without aggregation [36–39].

4. Green synthesis

Biosynthesis of the nanoparticles has received considerable attention due to the growing need to develop environmentally beneficial technologies in material synthesis. To illustrate, a great

deal of effort has been put into the green synthesis of inorganic materials, especially metal nanoparticles using microorganisms and plant extracts. While microorganisms such as bacteria [40], algae [41], yeast [42], and fungi [43] are continued to be examined so far for the intra and extracellular synthesis of metal nanoparticles, the use of parts of the whole plant in analogous with nanoparticles synthesis methodologies is an exciting possibility which is newly explored. In the literature, various bacterial strains such as *Bacillus amyloliquefaciens* [44], *Acinetobacter calcoaceticus* [45], *Pseudomonas aeruginosa* [46], *Escherichia coli* [47] and *Bacillus licheniformis* [48] were used effectively for the synthesis of silver nanoparticles.

The benefits of using plants for the synthesis of the nanoparticles are that the plants are easily available and possess a large variety of active functional groups that can promote the reduction of silver ions. Most of the plant parts like leaves, roots, latex, bark, stem, and seeds are being used for the nanoparticle synthesis. Major compounds that ensure the reduction of the nanoparticles are biomolecules such as polysaccharides, tannins, saponins, phenolics, terpenoids, flavones, alkaloids, proteins, enzymes, vitamins, amino acids, and alcoholic component. The procedure for the nanoparticle synthesis of plants requires the collection of the part of the plant of interest from the available sites is done and then it is washed thoroughly several times with tap and distilled water to remove impurities of plants; followed with sterile distilled water to remove related wastes if any. Then, plant is dried clean and dry place in the shade for 10–15 days and then pulverized using a blender. For the plant broth preparation, an approximate amount of the dried powder is boiled with deionized distilled water. The resulting extraction is then filtered thoroughly until no insoluble material appears in the broth. Then a few mL of the plant extract is added to the silver nitrate solution whose concentration is kept at 1 mM. The reduction of Ag^+ to Ag^0 is confirmed by the color change of the solution. Its formation is confirmed by using UV-visible spectroscopy and transmission electron microscopy or scanning electron microscopy. The most important plants like *Alternanthera dentate* [49], *Cymbopogon citratus* [50], *Argyreia nervosa* [51], phlomis [52], *Aloe vera* [53], *Carica papaya* [54], *Nelumbo nucifera* [55], *Moringa oleifera* [56], *Ziziphora tenuior* [57], *Centella asiatica* [58], *Vitex negundo* [59], *Swietenia mahagoni* [60], *Boerhavia diffusa* [61], *Cocos nucifera* [62], *Brassica rapa* [63], *Melia dubia* [64], *Pogostemon benghalensis* [65], *Garcinia mangostana* [66], *Psoralea corylifolia* [67], *Portulaca oleracea* [68], *Trachyspermum ammi* [69], *Eclipta prostrate* [70], *Vitis vinifera* [71], *Thevetia peruviana* [72], *Calotropis procera* [73], *Premna herbacea* [74], *Ficus carica* [75], *Abutilon indicum* [76], *Terminalia chebula* [77], *Acorus calamus* [78], *Tinospora cordifolia* [79], *Ocimum tenuiflorum* [80], bamboo hemicelluloses [81], *Strychnos potatorum* [82], Pine, Persimmon, Ginkgo, Magnolia, and Platanus [83] used by researchers in green synthesis.

Many different plant extracts have been used in the synthesis of silver nanoparticles with the aim of producing Ag-NPs presenting different morphologies. TEM and SEM studies have shown that the presence of reducing agent in a plant-mediated synthesis of Ag-NPs, where the plant extract acts as reducing agents, shapes the nanoparticle during its growth. The use of medicinal plants in the synthesis of Ag-NPs is not only used for size and shape control, but also for providing plant antimicrobial properties to Ag-NPs. Tippayawat et al. reported a one-step hydrothermal method to prepare silver nanoparticles which is effective against gram-positive (*Streptococcus epidermidis*) and gram-negative (*Pseudomonas aeruginosa*). Reduction of Ag^+ ions to Ag^0 nanoparticles was performed in a medium of *Aloe vera* extract

in which no extra reducing agent was used. The silver nanoparticle sizes were found to be in a range of 70.70–192.02 nm and controllable by varying temperature and time conditions of the hydrothermal process (**Figure 5**) [53]. Kagithoju et al. achieved an economic and environmentally friendly green synthesis of silver nanoparticles using an aqueous leaf extract of *Strychnos potatorum* from 3 mM silver nitrate solution. The XRD and SEM analysis have shown the average particle size of nanoparticles as 28 nm as well as revealed their (mixed, i.e., cubic and hexagonal) structure. These nanoparticles have shown bactericidal activity against multidrug-resistant human pathogenic bacteria [82].

Song and Kim compared their extracellular synthesis of metallic silver nanoparticles by using five plant leaf extracts (Pine, Persimmon, Ginkgo, Magnolia, and Platanus). Magnolia leaf

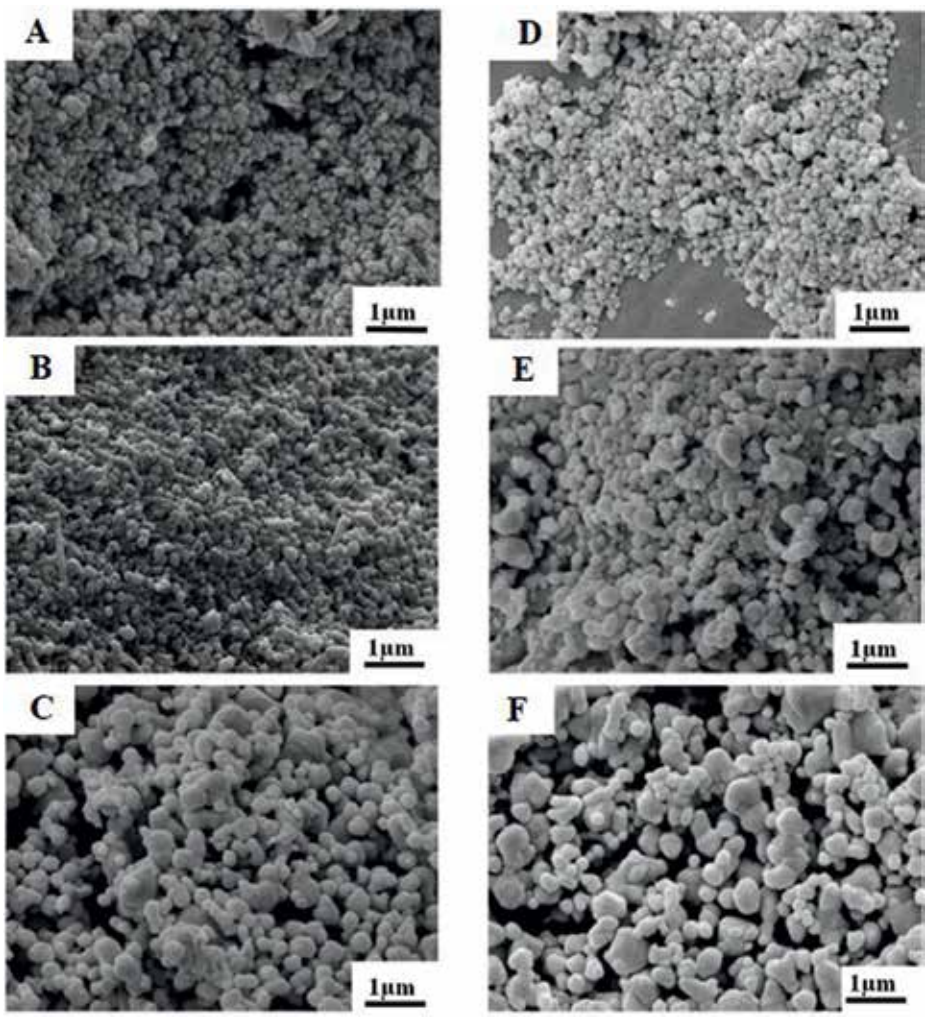

Figure 5. SEM images of Ag-NPs were obtained at (A) 100°C for 6 h, (B) 150°C for 6 h, (C) 200°C for 6 h, (D) 100°C for 12 h, (E) 150°C for 12 h, and (F) 200°C for 12 h [53].

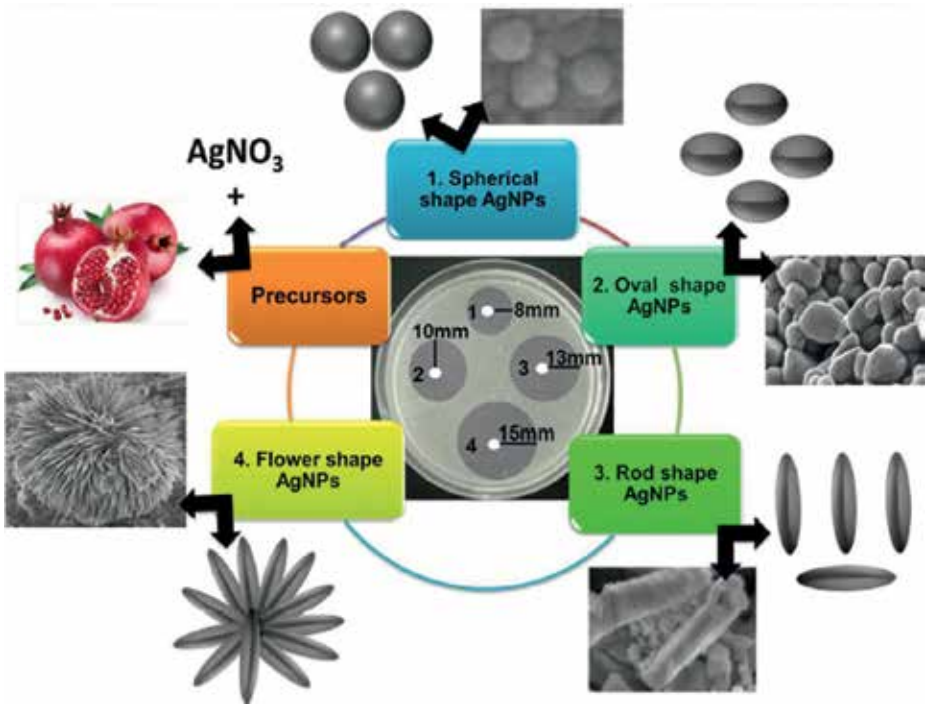

Figure 6. Green synthesis of different shape Ag-NPs and their antibacterial activity [84].

broth was the best reductive agent for the synthesis and conversion of the silver nanoparticles. More than 90% of the conversion was completed in 11 min by using Magnolia leaf broth at 95°C of reaction temperature. The average size of the nanoparticles, which was analyzed by TEM and SEM, ranges from 15 to 500 nm. The particle size was controlled by changing the reaction temperature, leaf broth concentration, and $AgNO_3$ concentration [83]. Roy et al. prepared four different shapes (spherical, oval, rod and flower shape) of silver nanoparticles (Ag-NPs) using pomegranate juice as a novel reducing agent via microwave-assisted synthesis. The Ag-NPs were characterized by UV-vis spectroscopy, XRD, SEM and TEM analysis. The synthesized Ag-NPs have shown a very rapid, effective, shape-specific and dose-dependent bacteriostatic/bactericidal effect towards four different bacterial strains. Among the four different shaped AgNPs, the flower shape AgNPs exhibited the best results and led to the fastest bactericidal activity against all the tested strains at similar bacterial concentrations (**Figure 6**) [84].

5. Conclusions

Silver nanoparticles can be obtained by physical, chemical, and biological synthesis methods. Hundreds of research articles reporting different synthesis methods for Ag-NP are published every year. Throughout this chapter, we have reviewed only some of the most

relevant works, dealing mostly with physical, chemical, and biological methods. In literature, all known applications for metallic silver may involve the use of nanosilver in place of silver to take advantage of nanosilver's unique properties. Despite all beneficial uses for nanosilver, its impact on the environment is concerning. These synthesis methods may require the use of different raw materials and yield reaction by using toxic products or wastes. But in recent years, also known as "green chemistry", an environmental-friendly approach has become a new option in chemistry, consisting of reduction and elimination of dangerous substantives for the design of products in the environment. However, as seen, there are numerous studies for the synthesis methods (green or nongreen) of the nanosilver in literature but the most commonly used methods in the industry are not yet known. For this reason, we suggest that researchers should be directed to work on the methods of synthesizing nanosilver used in the industry.

Author details

Remziye Güzel[1]* and Gülbahar Erdal[2]

*Address all correspondence to: guzel.remziye@gmail.com

1 Department of Chemistry, Dicle University, Diyarbakır, Turkey

2 Department of Medical Biology and Geneticts, Dicle University, Turkey

References

[1] Kimura K, Bandow S. The study of metal colloids produced by means of gas evaporation technique. I. Preparation method and optical properties in ethanol. Bulletin of the Chemical Society of Japan. 1983;**56**:3578-3584

[2] Tsuji T, Iryo K, Watanabe N, Tsuji M. Preparation of silver nanoparticles by laser ablation in solution: Influence of laser wavelength on particle size. Applied Surface Science. 2002;**202**:80-85

[3] Pyatenko A, Shimokawa K, Yamaguchi M, Nishimura O, Suzuki M. Synthesis of silver nanoparticles by laser ablation in pure water. Applied Physics A. 2004;**79**:803-806

[4] Sadrolhesseini AR, Noor ASM, Mahdi MA, Kharazmi A, Zakaria A, Yunus WMM, Huang NM. Laser ablation synthesis of silver nanoparticle in graphene oxide and thermal effusivity of nanocomposite. In: IEEE 4th International Conference on Photonics (ICP). 2013. pp. 62-65

[5] Tsuji T, Thang D-H, Okazaki Y, Nakanishi M, Tsuboi Y, Tsuji M. Preparation of silver nanoparticles by laser ablation in polyvinylpyrrolidone solutions. Applied Surface Science. 2008;**254**:5224-5230

[6] Valverde-Alvaa MA, García-Fernández T, Villagrán-Munizc M, Sánchez-Akéc C, Castañeda-Guzmáncr, Esparza-Alegríad E, Sánchez-Valdésecf, Sánchez Llamazarese JL, Márquez Herreraf CE. Synthesis of silver nanoparticles by laser ablation in ethanol: A pulsedphotoacoustic study. Applied Surface Science. 2015;**355**:341-349

[7] González MG, Liu X, Niessner R, Haisch C. Strong size-dependentphotoacoustic effect on gold nanoparticles by laser-induced nanobubbles. Applied Physics Letters. 2010;**96**: 174104

[8] Kudryashov SI, Lyon K, Allen SD. Photoacoustic study of relaxation dynamics in multibubble systems in laser-superheated water. Physical Review E. 2006;**73**:055301R (1-4)

[9] Osegura-Galindo DO, Machorro-Mejia R, Bogdanchikova N, Mota-Morales JD. Silver nanoparticles synthesized by laser ablation confined in urea choline chloride deep-eutectic solvent. Colloids and Interface Science Communications. 2016;**12**:1-4

[10] Galindo DOO, Utrera OH, Mejia RM, Aranda MAS. Silver nanoparticles by laser ablation confined in alcohol using an argon gas environment. JLMN-Journal of Laser Micro/ Nanoengineering. 2016;**11**(2):158-163

[11] Jensen TR, Duval ML, Kelly KL, Lazarides AA, Schatz GC, Van Duyne RP. Nanosphere lithography: Effect of the external dielectric medium on the surface plasmon resonance spectrum of a periodic array of silver nanoparticles. The Journal of Physical Chemistry. 1999;**103**:9846-9853

[12] Jensen TR, Malinsky MD, Haynes CL, Van Duyne RP. Nanosphere lithography: Tunable localized surface plasmon resonance spectra of silver nanoparticles. The Journal of Physical Chemistry B. 2000;**104**:10549-10556

[13] Malasis L, Deyfus R, Murphy RJ, Hough LA, Donnino B, Murray CB. One-step green synthesis of gold and silver nanoparticles with ascorbic acid and their versatile surface post-functionalization. RSC Advances. 2016;**6**:33092-33100

[14] Mikac L, Ivanda M, Gotic M, Mihelj T, Horvat L. Synthesis and characterization of silver colloidal particles with diffirent coating for SERS application. Journal of Nanoparticle Research. 2014;**16**(2748):1-13

[15] Wuithschick M, Paul B, Bienert R, Sarfraz A, Vainio U, Sztucki M, Kraehnert R, Strasser P, Rademann K, Emmerling F, Polte J. Size-controlled synthesis of colloidal silver nanoparticles based on mechanistic understanding. Chemistry of Materials. 2013;**25**:4679-4689

[16] Al-Thabaiti SA, Malik MA, Al-Youbi AAO, Khan Z, Hussain JI. Effects of surfactant and polymer on the morphology of advanced nanomaterials in aqueous solution. International Journal of Electrochemical Science. 2013;**8**:204-218

[17] Liang H, Wang W, Huang Y, Zhang S, Wei H, Xu H. Controlled synthesis of uniform silver nanospheres. Journal of Physical Chemistry C. 2010;**114**:7427-7431

[18] Zhang J, Langille MR, Mirkin CA. Synthesis of silver nanorods by low energy excitation of spherical plasmonic seeds. Nano Letters. 2011;**11**:2495-2498

[19] Ojha AK, Forster S, Kumar S, Vats S, Negi S, Fischer I. Synthesis of well–dispersed silver nanorods of different aspect ratios and their antimicrobial properties against gram positive and negative bacterial strains. Journal of Nanobiotechnology. 2013;**11**(42):1-7

[20] Ajitha B, Reddy YAK, Reddy PS. Influence of synthesis temperature on growth of silver nanorods. International Journal of Engineering Science. 2014;**3**(5):144-148

[21] Sun Y, Yin Y, Mayers BT, Herricks T, Xia Y. Uniform silver nanowires synthesis by reducing $AgNO_3$ with ethylene glycol in the presence of seeds and poly(vinyl pyrrolidone). Chemistry of Materials. 2002;**14**(11):4736-4745

[22] Li B, Ye S, Stewart IE, Alvarez S, Wiley BJ. Synthesis and purification of silver nanowires to make conducting films with a transmittance of 99%. Nano Letters. 2015;**15**(10):6722-6726

[23] Gebeyehu MB, Chala TF, Chang S-Y, Wu C-M, Lee J-Y. Synthesis and highly effective purification of silver nanowires to enhance transmittance at low sheet resistance with simple polyol and scalable selective precipitation method. RSC Advances. 2017;**7**:16139-16148

[24] Im SH, Lee YT, Wiley B, Xia Y. Large-scale synthesis of silver nanocubes: The role of HCl in promoting cube perfection and monodispersity. Angewandte Chemie International Edition. 2005;**44**:2154-2157

[25] Sun Y, Xia Y. Shape-controlled synthesis of gold and silver nanoparticles. Science. 2002a;**298**(5601):2176-2179

[26] Tao A, Sinsermsuksakul P, Yang PD. Polyhedral silver nanocrystals with distinct scattering signatures. Angewandte Chemie International Edition. 2006;**45**(28):4597-4601

[27] Siekkinen AR, McLellan JM, Chen J, Xia Y. Rapid synthesis of small silver nanocubes by mediating polyol reduction with a trace amount of sodium sulfide or sodium hydrosulfide. Chemical Physics Letters. 2006;**432**:491-496

[28] Zhang J, Li S, Wu J, Schatz GC, Mirkin CA. Plasmon-mediated synthesis of silver triangular bipyramids. Angewandte Chemie. 2009;**121**:7927-7931

[29] Me'traux GS, Mirkin CA. Rapid thermal synthesis of silver nanoprisms with chemically tailorable thickness. Advanced Materials. 2005;**17**(4):412-415

[30] Nourafkan A, Alamdari A. Study of effective parameters in silver nanoparticle synthesis through method of reverse microemulsion. Journal of Industrial and Engineering Chemistry. 2014;**20**:3639-3645

[31] Wani IA, Khatoon S, Ganguly A, Ahmed J, Ahmad T. Structural characterization and antimicrobial properties of silver nanoparticles prepared by inverse microemulsion method. Colloids and Surfaces B: Biointerfaces. 2013;**101**:243-250

[32] Chatre A, Solasa P, Sakle S, Thaokar R, Mehra A. Color and surface plasmon effects in nanoparticle systems: Case of silver nanoparticles prepared by microemulsion route. Colloids and Surfaces A: Physicochemical and Engineering Aspects. 2012;**404**:83-92

[33] Singha D, Barman N, Sahu K. A facile synthesis of high optical quality silver nanoparticles by ascorbic acid reduction in reverse micelles at room temperature. Journal of Colloids and Interface Science. 2014;**413**:37-42

[34] Sun YP, Atorngitjawat P, Meziani MJ. Preparation of silver nanoparticles via rapid expansion of water in carbon dioxide microemulsion into reductant solution. Langmuir. 2001;**17**(19):5707-5710

[35] Elmas ŞNK, Güzel R, Say MG, Ersöz A, Say R. Ferritin based bionanocages as novel biomemory device concept. Biosensors and Bioelectronics. 2018;**103**:19-25

[36] Pal A, Shah S, Devi S. Microwave-assisted synthesis of silver nanoparticles using ethanol as a reducing agent. Materials Chemistry. 2009;**114**:530-532

[37] Guo R, Li Y, Lan J, Jiang S, Liu T, Yan W. Microwave-assisted synthesis of silver nanoparticles on cotton fabric modified with 3-aminopropyltrimethoxysilane. Journal of Applied Polymer Science. 2013;**130**:3862-3868

[38] Wang B, Zhuang X, Deng W, Cheng B. Microwave-assisted synthesis of silver nanoparticles in alkalic carboxymethyl chitosan solution. Engineering. 2010;**2**:387-390

[39] Pal J, Deb MK, Deshmuk DK. Microwave-assisted synthesis of silver nanoparticles using benzo-18-crown-6 as reducing and stabilizing agent. Applied Nanoscience. 2014;**4**(4): 507-510

[40] Samadi N, Golkaran D, Eslamifar A, Jamalifar H, Fazeli MR, Mohseni FA. Intra/extracellular biosynthesis of silver nanoparticles by an autochthonous strain of Proteus mirabilis isolated from photographic waste. Journal of Biomedical Nanotechnology. 2009;**5**(3):247-253

[41] El-Rafie HM, El-Rafie MH, Zahran MK. Green synthesis of silver nanoparticles using polysaccharides extracted from marine macro algae. Carbohydrate Polymers. 2013;**96**:403-410

[42] Jha AK, Prasad K, Kulkarni AR. Yeast mediated synthesis of silver nanoparticles. International Journal of Nanoscience and Nanotechnology. 2008;**4**(1):17-21

[43] Bhainsa KC, D'Souza SF. Extracellular synthesis using the fungus Aspergillus fumigates. Colloids Surface B Biointerfaces. 2006;**47**:152-157

[44] Fouad H, Hongjie L, Yanmei D, Baoting Y, El-Shakh A, Abbas G, Jianchu M. Synthesis and characterization of silver nanoparticles using Bacillus amyloliquefaciens and Bacillus subtilis to control filarial vector Culex pipiens pallens and its antimicrobial activity, artificial cells. Nanomedicine and Biotechnology. 2017;**45**(7):1369-1378

[45] Singh R, Wagh P, Wadhwani S, Gaidhani S, Kumbhar A, Bellare J, Chopade BA. Synthesis, optimization, and characterization of silver nanoparticles from Acinetobacter calcoaceticus and their enhanced antibacterial activity when combined with antibiotics. International Journal of Nanomedicine. 2013;**8**:4277-4290

[46] Kumar CG, Mamidyala SK. Extracellular synthesis of silver nanoparticles using culture supernatant of *Pseudomonas aeruginosa*. Colloids Surface B Biointerfaces. 2011;**84**(2):462-466

[47] Koilparambil D, Kurian LC, Vijayan S, Shaikmoideen JM. Green synthesis of silver nanoparticles by *Escherichia coli*: Analysis of antibacterial activity. Journal of Water and Environmental Nanotechnology. 2016;**1**(1):63-74

[48] Kalimuthu K, Suresh Babu R, Venkataraman D, Bilal M, Gurunathan S. Biosynthesis of silver nanocrystals by *Bacillus licheniformis*. Colloids Surface B Biointerfaces. 2008;**65**(1):150-153

[49] Kumar DA, Palanichamy V, Roopan SM. Green synthesis of silver nanoparticles using Alternanthera dentata leaf extract at room temperature and their antimicrobial activity. Spectrochimica Acta Part A: Molecular and Biomolecular Spectroscopy. 2014;**127**:168-171

[50] Masurkar SA, Chaudhari PR, Shidore VB, Kamble SP. Rapid biosynthesis of silver nanoparticles using Cymbopogan Citratus (Lemongrass) and its antimicrobial activity. Nano-Micro Letters. 2011;**3**(3):189-194

[51] Thombre R, Parekh F, Patil N. Green synthesis of silver nanoparticles using seed extract of *Argyreia nervosa*. International Journal of Pharmacy and Biological Sciences. 2014;**5**(1):114-119

[52] Allafchian AR, Mirahmadi-Zare SZ, Jalali SAH, Hashemi SS, Vahabi MR. Green synthesis of silver nanoparticles using phlomis leaf extract and investigation of their antibacterial activity. Journal of Nanostructure Chemistry. 2016;**6**:129-135

[53] Tippayawat P, Phromviyo N, Boueroy P, Chompoosor A. Green synthesis of silver nanoparticles in aloe vera plant extract prepared by a hydrothermal method and their synergistic antibacterial activity. PeerJ. 2016;**4**:1-15

[54] Jain D, Daima HK, Kachhwaha S, Kothari S. Synthesis of plant-mediated silver nanoparticles using papaya fruit extract and evaluation of their antimicrobial activities. Digest Journal Nanomaterials Biostructures. 2009;**4**:557-563

[55] Santhoshkumar T, Rahuman AA, Rajakumar G, Marimuthu S, Bagavan A, Jayaseelan C. Synthesis of silver nanoparticles using Nelumbo nucifera leaf extract and its larvicidal activity against malaria and filariasis vectors. Parasitology Research. 2011;**108**:693-702

[56] Prasad TNVKV, Elumalai E. Biofabrication of Ag nanoparticles using *Moringa oleifera* leaf extract and their antimicrobial activity. Asian Pacific Journal of Tropical Biomedicine. 2011;**1**:439-442

[57] Sadeghi B, Gholamhoseinpoor F. A study on the stability and green synthesis of silver nanoparticles using Ziziphora tenuior (Zt) extract at room temperature. Spectrochimica Acta Part A: Molecular and Biomolecular Spectroscopy. 2015;**134**:310-315

[58] Rout A, Jena PK, Parida UK, Bindhani BK. Green synthesis of silver nanoparticles using leaves extract of *Centella asiatica* L. For studies against human pathogens. International Journal of Pharmacy and Biological Sciences. 2013;**4**(4):661-674

[59] Zargar M, Hamid AA, Bakar FA, Shamsudin MN, Shameli K, Jahanshiri F. Green synthesis and antibacterial effect of silver nanoparticles using Vitexnegundo L. Molecules. 2011;**16**:6667-6676

[60] Mondal S, Roy N, Laskar RA, Sk I, Basu S, Mandal D. Biogenic synthesis of Ag, Au and bimetallic Au/Ag alloy nanoparticles using aqueous extract of mahogany (Swietenia mahogani JACQ) leaves. Colloids and Surfaces B: Biointerfaces. 2011;**82**:497-504

[61] Nakkala JR, Mata R, Gupta AK, Sadras SR. Green synthesis and characterization of silver nanoparticles using Boerhaavia diffusa plant extract and their antibacterial activity. Industrial Crops and Products. 2014;**52**:562-566

[62] Mariselvam R, Ranjitsingh AJA, Usha Raja Nanthini A, Kalirajan K, Padmalatha C, Selvakumar MP. Green synthesis of silver nanoparticles from the extract of the inflorescence of *Cocos nucifera* (Family: Arecaceae) for enhanced antibacterial activity. Spectrochimica Acta Part A: Molecular and Biomolecular Spectroscopy. 2014;**129**:537-541

[63] Narayanan KB, Park HH. Antifungal activity of silver nanoparticles synthesized using turnip leaf extract (*Brassica rapa* L.) against wood rotting pathogens. European Journal of Plant Pathology. 2014;**140**:185-192

[64] Kathiravan V, Ravi S, Kumar SA. Synthesis of silver nanoparticles from Meliadubia leaf extract and their in vitro anticancer activity. Spectrochimica Acta Part A: Molecular and Biomolecular Spectroscopy. 2014;**130**:116-121

[65] Gogoi SJ. Green synthesis of silver nanoparticles from leaves extract of ethnomedicinal plants Pogostemon benghalensis (B) O.Ktz. Advances in Applied Science Research. 2013;**4**(4):274-278

[66] Veerasamy R, Xin TZ, Gunasagaran S, Xiang TFW, Yang EFC, Jeyakumar N. Biosynthesis of silver nanoparticles using mangosteen leaf extract and evaluation of their antimicrobial activities. Journal of Saudi Chemical Society. 2010;**15**:113-120

[67] Sunita D, Tambhale D, Parag V, Adhyapak A. Facile green synthesis of silver nanoparticles using *Psoralea corylifolia*. Seed extract and their in-vitro antimicrobial activities. International Journal of Pharmacy and Biological Sciences. 2014;**5**(1):457-467

[68] Firdhouse MJ, Lalitha P. Green synthesis of silver nanoparticles using the aqueous extract of *Portulaca oleracea* (L). Asian Journal of Pharmaceutical and Clinical Research. 2012;**6**(1):92-94

[69] Vijayaraghavan K, Nalini S, Prakash NU, Madhankumar D. One step green synthesis of silvernano/microparticles using extracts of *Trachyspermum ammi* and *Papaver somniferum*. Colloids and Surfaces B Biointerfaces. 2012;**94**:114-117

[70] Rajakumar G, Abdul Rahuman A. Larvicidal activity of synthesized silver nanoparticles using Eclipta prostrata leaf extract against filariasis and malaria vectors. Acta Tropica. 2011;**118**:196-203

[71] Gnanajobitha G, Paulkumar K, Vanaja M, Rajeshkumar S, Malarkodi C, Annadurai G, Kannan C. Fruit-mediated synthesis of silver nanoparticles using *Vitis vinifera* and evaluation of their antimicrobial efficacy. Journal of Nanostructure in Chemistry. 2013;**3**(67):1-6

[72] Rupiasih NN, Aher A, Gosavi S, Vidyasagar PB. Green synthesis of silver nanoparticles using latex extract of *Thevetia peruviana*: A novel approach towards poisonous plant utilization. Journal of Physics: Conference Series. 2013;**423**:1-8

[73] Gondwal M, Pant GJN. Biological evaluation and green synthesis of silver nanoparticles using aqueous extract of *Calotropis procera*. International Journal of Pharmacy and Biological Sciences. 2013;**4**(4):635-643

[74] Kumar S, Daimary RM, Swargiary M, Brahma A, Kumar S, Singh M. Biosynthesis of silver nanoparticles using Premna herbacea leaf extract and evaluation of its antimicrobial activity against bacteria causing dysentery. International Journal of Pharmacy and Biological Sciences. 2013;**4**(4):378-384

[75] Uluğ B, Türkdemir MH, Cicek A, Mete A. Role of irradiation in the green synthesis of silver nanoparticles mediated by fig (*Ficus carica*) leaf extract. Spectrochimica Acta Part A: Molecular and Biomolecular Spectroscopy. 2015;**135**:153-161

[76] Ashok Kumar S, Ravi S, Kathiravan V, Velmurugan S. Synthesis of silver nanoparticles using *A. indicum* leaf extract and their antibacterial activity. Spectrochimica Acta Part A: Molecular and Biomolecular Spectroscopy. 2015;**134**:34-39

[77] Edison TJI, Sethuraman MG. Instant green synthesis of silver nanoparticles using terminalia chebula fruit extract and evaluation of their catalytic activity on reduction of methylene blue. Process Biochemistry. 2012;**47**:1351-1357

[78] Nakkala JR, Mata R, Kumar Gupta A, Rani Sadras S. Biological activities of green silver nanoparticles synthesized with Acorous calamus rhizome extract. European Journal of Medicinal Chemistry. 2014;**85**:784-794

[79] Anuj SA, Ishnava KB. Plant mediated synthesis of silver nanoparticles using dried stem powder of *Tinospora cordifolia*, its antibacterial activity and its comparison with antibiotics. International Journal of Pharmacy and Biological Sciences. 2013;**4**:849-863

[80] Patil RS, Kokate MR, Kolekar SS. Bioinspired synthesis of highly stabilized silver nanoparticles using ocimum tenuiflorum leaf extract and their antibacterial activity. Spectrochimica Acta Part A: Molecular and Biomolecular Spectroscopy. 2012;**91**:234-238

[81] Peng H, Yang A, Xiong J. Green, microwave-assisted synthesis of silver nanoparticles using bamboo hemicelluloses and glucose in an aqueous medium. Carbohydrate Polymers. 2013;**91**:348-355

[82] Kagithoju S, Godishala V, Nanna RS. Eco-friendly and green synthesis of silver nanoparticles using leaf extract of *Strychnos potatorum* Linn.F. and their bactericidal activities. 3 Biotech. 2015;**5**:709-714

[83] Song JY, Kim BS. Rapid biological synthesis of silver nanoparticles using plant leaf extracts. Bioprocess and Biosystems Engineering. 2009;**32**:79-84

[84] Roy E, Patra S, Saha S, Mahduri R, Sharma PK. Shape-specific silver nanoparticles prepared by microwave assisted green synthesis using pomegranate juice for bacterial inactivation and removal. RSC Advances. 2015;**5**:95433-95442

Chapter 2

Silver Nanoparticles: Synthesis, Characterization and Applications

Neelu Chouhan

Additional information is available at the end of the chapter

http://dx.doi.org/10.5772/intechopen.75611

Abstract

Day by day augmenting importance of metal nanoparticles in the versatile fields like, catalyst, electronic, magnetic, mechanic, optical optoelectronic, materials for solar cell and fuel cell, medical, bioimaging, cosmetic, ultrafast data communication and optical data storage, etc, is increasing their value. Nanoparticles of alkali metals and noble metals (copper, silver, platinum, palladium, and gold, etc.) have a broad absorption band in the visible region of the electromagnetic spectrum of light, because the solutions of these metal nanoparticles show the intense color, which is absent in their bulk counterparts as well as their atomic level. The main cause behind this phenomenon is attributed to the collective oscillations of the free conductive electrons that are induced by an interaction with electromagnetic field. The whole incidence is known as localized surface plasmonic resonance. Out of these, we have selected the silver nanoparticles for the studies. In this article, we will discuss the synthesis, characterization, and application of the silver nanoparticles. Future prospective and challenges in the field commercialization of the nanosilver is also discussed.

Keywords: silver nanoparticles, particle size, localized surface plasmonic resonance (LSPR), characterization, application

1. Nanoparticles: an introduction

In a particle world, nanoparticles had attracted an immense attraction of the scientific world due to their large surface area to volume ratio and high reactivity with unmatchable properties. Greek Nano word used for "dwarf" means one-billionth. Nanoparticles can be served as a strong bridge between the bulk materials and atomic or molecular structures. A bulk material has constant physical properties regardless of their size and shape, but at the nanoscale, the

size, morphological substructure of the substance, and shape (as well as aspect ratios) are the major driving factors for changing their biological, chemical, and physical properties. Because at the nanoscale, the materials behave differently and they emerge with few novel characters in themselves, such as some of the materials become explosive (for example, aluminum) or their melting point changes (for example, silver and gold) or a new property is revealed (for example, nanosilver possess the antibacterial character and becomes an odor eater).

1.1. Salient features of nanomaterials

The novel properties of nano-objects occur due to the changes in size and scale. Surface area to volume ratio of the particle depends on the size and shape of an object; here, the size of the nanoparticle is very small in at least one dimension. Nanoparticles exhibited some extra phenomenon, i.e., random motion of the small particles, quantum tunneling, discreteness of energy, uncertainty of the matter, duality nature of mass, and energy for wave particles, etc. Moreover, the gravity becomes a markedly less significant force at the nanoscale, while the Vander Waals forces became incredibly strong. Therefore, the Vander Waals forces make the materials "sticky" [1]. Due to the reduction in the spatial dimension, confinement of these quasi particles in a particular crystallographic direction within a structure generally leads to changes in physical properties of the system in that direction. Some qualities (gravitational forces, vapour pressure and boiling point) of the nanoparticles decreases with their particle size and became insignificant at nanoscale because the electromagnetic force of protons is 10^{36} times stronger than gravitational forces. Here, quantum mechanics dominates in place of classical mechanics. Nanomaterials are changing their electrical, optical, surface-related, mechanical, and magnetic properties at nanoscale and exhibits some prominent effects that are associated with nanoparticles, as mentioned below.

1.1.1. Electrical properties

Because of the electrons that cannot move freely at nanolevel and their motion became restricted, this confinement at the nanoscale resulted in the changes in electrical properties, such as the bulk conductor/semiconductor materials behaving as superconductors or conductors at nanoscale. Similarly, nanogold/nanosilver (of size less than 10 nm) cannot conduct electricity.

1.1.2. Optical properties

Optical properties of nanomaterials are also size dependent. Electrons cannot move freely at the nanoscale and become restricted. The confinement of the electrons causes them to react to light differently. Gold appears golden at the macroscale, but the nanosized gold particles are red. Nanosized zinc oxide particles will not scatter visible light and bulk zinc oxide particles used for sun block as they scattered visible light and appear white. Quantum dots changes in their optical appearance as the size of the particles decreases creating different colors.

1.1.3. Surface properties

The surface-dominated properties such as melting point, rate of reaction, capillary action, and adhesion, are controlled by their surface area and due to high surface area of the nanomaterials,

these properties show drastic changes from their bulk counter parts. At the macro scale, gold has a melting point of 1064°C, but by decreasing the particle size from 100 to 10 nm diameter, its melting temperatures drops up to 100°C. As the size reduces to about 2 nm, the melting point decreases to about half of the melting point at the macroscale level [2, 3].

1.1.4. Mechanical properties

At nanolevel, the changes in mechanical properties of the material such as Young's modulus, tensile strength (four times larger), lower plastic deformation, more hardness, more brittle, grain boundaries deformations, decrease in elongation, lower density of dislocation moments, short distance of dislocation moments increases, are observed.

1.1.5. Magnetic properties

For nanomagnetic materials, each spin behaves as a small magnet for nanomaterials. The interaction between neighboring spins is dominated by the spin exchange interaction. Usually, most of the materials has $J < 0$ and are nonmagnetic (paramagnetic or diamagnetic) by nature. Similar to the paramagnets, the nanosuperparamagnets back to zero magnetization upon removing of the field. It happens because of their small size and not due to the inherently weak exchange between the individual moments.

1.1.6. Lotus effect

Lotus leaves are super hydrophobic due to high contact angle (122°) of water droplets to lotus leaf surface and presence of the needle-shaped wax tubes in these leaves, (a smaller-sized roughness region of 0.3–1.7 μm with D of 1.48) besides normal leaves pattern. Similarly, nanomaterials show the self-cleaning phenomena that are controlled by various parameters, i.e., surface fractal dimension, surface morphology, and dynamic-wetting behaviors, responsible for the super hydrophobic character in them [4].

A rough surface of lotus leaves was etched into polydimethylsiloxane (PDMS) and a negative PDMS template was made, and then, the negative template was used to make a positive PDMS reproduced as a replica sheet of the original lotus leaf. These positive PDMS templates exhibit the extreme water repellency (superhydrophobic) along with the same surface structural features as the lotus leaves shown in **Figure 1a–d** and **f**. Four classes of surfaces are revealed on the grounds of surface wettability and their contact angles are shown in **Figure 1g** [5, 6]. The chief applications of lotus effect are in making of non-wettable rain wear/sails for boats, paints for kitchen roofs/walls that make them soot-free, windows in high-rise buildings, glass for greenhouses avoiding their expensive and cumbersome cleaning, water-repellant fibers for garments, sanitary products in bathrooms/toilets and windshields motor vehicle for reducing sticking of dirt matter and easier cleaning, etc.

1.1.7. Localized surface plasmon resonance (LSPR)

When plasmonic material (nanosphere is small in comparison to the wavelength of light, and the light has a frequency close to that of the SP, then the SP will absorb energy) is exposed to

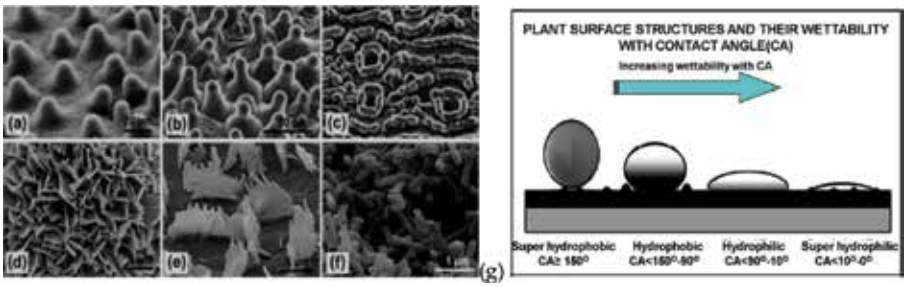

Figure 1. (a) SEM images of superhydrophobic plant leave surfaces, showing the different type of epidermal cells (a–c) and various types of epicuticular wax crystals (d–f) on leaves of *Euphorbia myrsinites* (a, d), *Xanthosoma robustum* (b, e), and *Taxus baccata* (c, f). Lotus effect associated with lotus leaves and (g) the four classes of surface wettability types of leaf surface based on their interaction with aqueous droplets [5, 6].

sunlight, free electrons of the nanoparticle of noble metals are integrated with the photon energy that produces subwaves and conducting electrons in oscillating mode [7, 8]. These collective oscillations (excitation) offer a localized surface plasmonic resonance (LSPR). LSPR adds the benefits of the enhanced local heating effect, LSPR-powered e/h generation, enhanced UV-Vis absorption, reduced e/h diffusion length, enhanced local electric effect and molecular polarization effect, quantum tunneling effect, high catalytic effect, and to the main photocatalytic unit. Hence, NPs of noble metals act as the thermal redox reaction-active centers on the catalyst that can trap, scatter, and concentrate light [9–11], and enhance the number of active sites and the rate of electron–hole formation by providing a fast lane for charge transfer on the semiconductor surface. Cu, Ag, Au, Pt, Pd, and their alloys Cu–Ag, Cu–Au, Cu–Ag–Au, are few examples of NPs of the noble metals with SPR. This phenomenon results in numerous physical effects including tailorable absorption of light (from UV to near-IR), local heating, and proficient charge transfer. Therefore, photoexcitation leads to a smooth electron transfer between the semiconductor carrier/supports and the noble-metal NPs. NPs of Ag, or Au (< 10 nm), are the most commonly used plasmonic materials.

1.1.8. The quantum confinement effect

The quantum confinement effect is observed for the particles having particle size less than the wavelength of the electron. If the motion of randomly moving electron is to be restricted in a specific energy levels (discreteness) then the motion of electron confined in three dimensions, two dimensions and one dimension, result in the particles having the shape of quantum dots, nanowire/rods and nanosheets, respectively. As the size of a particle decreases up to a nanoscale, the decrease in confining dimension makes the energy levels discrete, which widens up their band gap and band gap energy. If the size of the quantum dot is smaller than the Bohr's radius of the charge carrier (excitons, electron, hole quasi-particles of semiconductors), then the confinement observed here leads to a transition from continuous to discrete energy levels [12]. Although the physical properties of a quantum dots are not affected by quantum confinement, their optical absorption and emission can be tuned via the quantum size effect.

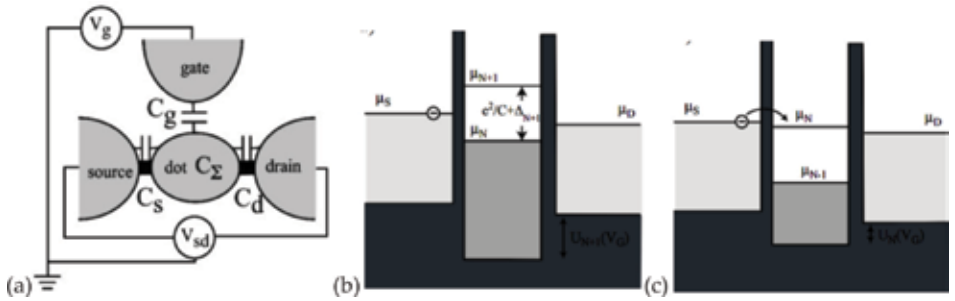

Figure 2. (a) Schematic diagram of typical arrangement of electrodes (quantum dot (QD) surrounded with source, drain and gate) for a single electron transistor. Energy diagram for a quantum dot, where the two tunnel barriers connected the QD to the source and drain contacts. (b) Electron transport is blocked and the dot contains a fixed number of N electrons. (b) Number of electrons on the QD can vary between N and N−1, result in rise a peak in the conductance because the gate voltage was tuned in order to align the chemical potential of the QD with that of source and drain [15].

1.1.9. Coulomb blockade

The phenomenon of Coulomb blockade can also be observed for a very small device (like a quantum dot) at the temperature which has to be low enough (~1 Kelvin ≅ 3 He refrigerators) so that the characteristic charging energy (the energy that is required to charge the junction with one elementary charge) is larger than the thermal energy of the charge carriers. But the small sized quantum dots of only few nanometers has quality to observe Coulomb Blockade from the liquid helium temperature up to room temperature (**Figures 2a–2c**) [13–15].

During the Coulomb Blockade phenomenon, the electrons inside this quantum sized device will create a strong coulomb repulsion that prevent other electrons to flow, resulting in the device will no longer follow Ohm's law as shown in **Figures 2a–2c**. When very few electrons are involved and an external static magnetic field is applied, Coulomb blockade provides the ground for spin blockade (also called Pauli blockade) and valley blockade [16, 17] which includes quantum mechanical effects due to spin and orbital interactions, respectively, between the electrons.

2. Present, past, and future of nanoparticles

History of mankind is a pursuit of color. Even in the Stone Age, people made use of pigments in paintings. In the Middle Age, the ancient Egyptians used nanotechnology but they did not understand as such in detail, but they prepared colloidal dispersion as inks and other useful products like paintings, dying hair, etc. Long ago before the beginning of the "Morden nano-era," people were well encountered with various nanosized objects and nanolevel processes, and they were using them in practice without due knowledge of the nature of these objects and processes. Thus, people were indulged in nanotechnology subconsciously, without proper understanding of the reason behind them. The secrets of nano-antiques were passed from generation to generation, without getting into the reasons behind their acquired unique

properties. Thousands of primeval knew to cultivate and process the natural fabrics, such as flax, cotton, wool, and silk, in developing the fabric of typical nanoporous materials with pores size of 1–20 nm. They were able to cultivate them and process into fine fabric product. These special fabrics possessed a developed network of pores with the size of 1–20 nm, i.e., they are typical nanoporous materials. Due to their nanoporous structure, the natural fabrics possess high-utilitarian properties as they absorb sweat well, quickly swell, and dry. Since ancient times, Egyptian people were mastered with the ways of making bread, wine, beer, cheese, and other foodstuffs, where the critical fermentation processed at nanolevel. Ph. Walter conducted a study on the hair samples from ancient Egyptian burial sites. He found that the primeval Egyptians used a nanoparticle of galenite (5 nm sized PbS) made of paste of lime, lead oxide, and small amount of water to dye hair in black. The dyeing paste reacted with sulfur of keratin, to obtain a few nanometer-sized galenite particles, to provide even and steady dyeing. The British museum possess Lycurgus Cup that was made by Roman artists in the 4th century AD, as an outstanding glass work of the primordial Rome. The impression of the Tsar of Edons (Lycurgus, **Figure 3a**) is embossed on the bowl and it shows unusual optical properties. In natural light, the bowl is green (**Figure 3b**), and if illuminated from within cup, it turns red (**Figure 3b**). The analysis of fragments of the bowl was done in 1959, by General Electric Motors for the first time, which reflected that the bowl consists of usual soda-lime-quartz glass with about 1% of gold and silver, and also 0.5% of manganese. The researchers discovered particles of gold and silver from 50 to 100 nanometers in size using an electronic microscope (**Figure 3c**), responsible for the unusual coloring of the bowl. In 2007, Harry [18] explained this phenomenon by the effects of plasmon excitation of electrons with metal nanoparticles. The Medieval Age manufacturing of multi-colored-stained glass windows (due to the gold and other metal nanoparticles) of church in Europe, are also a good example of high perfection engineering. During the battles of the European knights against Muslims, they faced the extraordinary strength of the blades of Muslims warriors in fights for the first time that was made of an ultra-strong Damascus steel (nanofibrous structure). After the discovery of electron microscopy in 1857, Michal Faraday discovered the colloidal gold in different colors: ruby, green, violet, or blue [19]. Thereafter, Albert Einstein explained the existence of colloidal dispersion in terms of Brownian motion. The above theory was experimentally confirmed by Jean-Baptize Perrin, which was awarded by Nobel Prize in 1926 [20].

Figure 3. (a) Dichroic Lycrugus cup made in 4th century AD and (b) in direct light it resembles jade with an opaque greenish-yellow tone, but when light shines through the glass (transmitted light) it turns to a translucent ruby color. (c) Transmission electron microscopy (TEM) image of a silver-gold alloy particle within the glass of the Lycurgus Cup [21].

3. Why silver nanoparticles preferred over the available nanoparticles?

Metal nanoparticles (MNPs) exhibit novel and size-related physico-chemical properties significantly different from their bulk counterpart [22]. The unique properties of MNPs have been an ambassador of their potential uses in medicine, catalysis, optics, cosmetics, renewable energies, inks, microelectronics, medical imaging, environmental remediation, and biomedical devices [23–28]. Besides, Ag-NPs exhibit a broad spectrum of bactericidal and fungicidal activity [29]. Therefore, the use of MNPs became exceptionally trendy for the wide range of consumer goods, including plastics, soaps, pastes, food, and textiles, to enhance their market value [30–32]. Among the wide range of metal nanoparticles, silver nanoparticles (Ag-NPs or nanosilver) were the most popular, due to their unique physical, chemical, and biological properties when compared to their macroscaled counterparts [33]. The advantage of the nanosilver over the other noble metals with respect to their physico-chemical properties are: small loss of the optical frequency during the surface-plasmon propagation [34], non-toxic, high electrical and thermal conductivity, stability at ambient conditions, low cost than the other noble metals such as gold and platinum, high-primitive character, wide absorption of visible and far IR region of the light, surface-enhanced Raman scattering, chemical stability, catalytic activity, and non-linear optical behavior (**Figure 4a–c**). Moreover, they exhibit a broad spectrum of high antimicrobial activity (bactericidal and fungicidal activity) attracting the scientists and technologists with much interest to develop nanosilver-based disinfectant products [35].

LSPR region of Ag, Au, and Cu in the visible and near-infrared wavelength range of sunlight is exhibited in **Figure 5a** [38]. The comparative UV/Vis diffuse-reflectance spectra of AgCl, Ag@AgCl, and N-TiO_2, are demonstrated by the **Figure 5b** that reflected the Ag@AgCl with plasmonic Ag molecules covers the wide range visible wavelength than other systems. The large effective scattering cross section, plasmon resonance with unique colors of the individual silver nanoparticles, as well as their non-bleaching properties have significant potential for single molecule labeling-based biological assays [40, 41]. Metal nanoparticles are also used in various near-field optical microscopic applications [42, 43] on the heels of augmented signal output due to their efficient scattering properties. Currently, nanosilver technologies have appeared in a variety of manufacturing processes and end products. There are many consumer products and applications which are utilizing nanosilver in consumer products

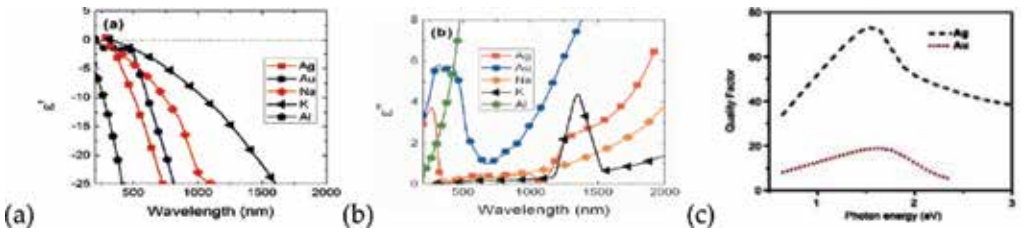

Figure 4. (a) Real and (b) imaginary part of permittivities of the metal candidates Ag, Au, Na K, and Al [36]. (c) Quality factor of plasmon resonances of a metal nanostructure as a function of plasmon frequency for two commonly used metals: silver (dashed line) and gold (dotted line) [37].

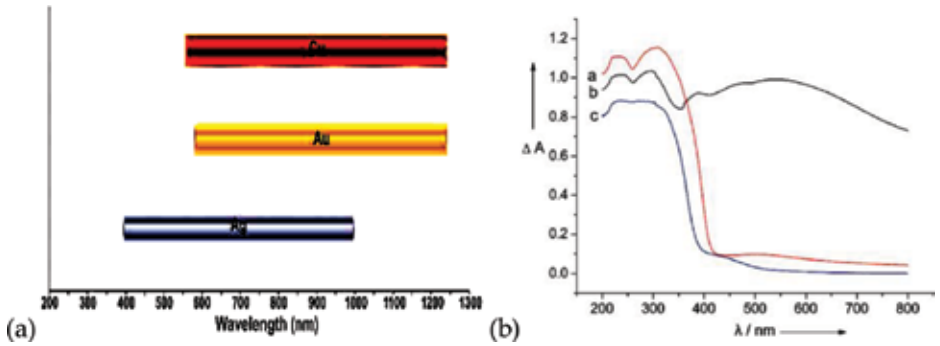

Figure 5. (a) Localized surface plasmon resonance of Ag, Au, and Cu that covers most of the visible and near-infrared wavelength range of sunlight [38]. (b) Comparative UV/Vis diffuse-reflectance spectra of (a) AgCl, (b) Ag@AgCl, and (c) N-TiO_2 [39].

(soap, shampoo, textile, disinfecting medical devices and home appliances to water treatments) with the highest degree of commercial value.

4. Silver nanoparticles: a plasmonic material for optical applications

During the LSPR, the light exposure in the UV-Visible wavelength range to the noble metal NPs (<10 nm), induced collective oscillations of their valence electrons [44]. The oscillating electron cloud (called localized surface plasmon/hot electrons) has the lifetime of femtoseconds order. After the lifetime, the population of hot electron started decaying via the radiative and non-radiative routes [45]. In radiative decay, they released radiations and in non-radiative decay, they were converted into photons and electron-hole pairs by inter-band/intra-band excitations that populated in conduction bands of the SP, as shown in **Figure 6**.

Surface plasmon resonance (SPR) has two different forms: (i) propagating part: surface plasmon polaritons (SPP) and (ii) stationary part: localized SPR (LSPR) [46]. The SPP traveled through resonantly excited charge oscillations on the surface of thin metal films, whereas LSPR represents

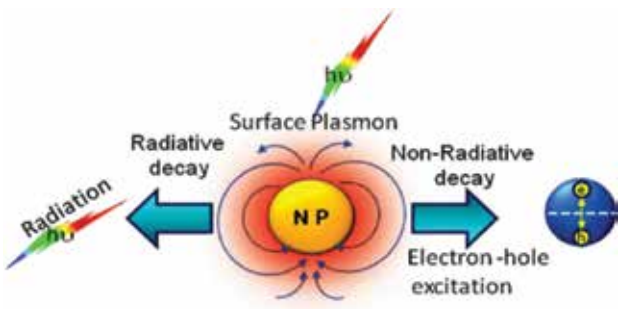

Figure 6. Schematic representation of radiative (left) and non-radiative (right) decay of the SP NP. The intra-band excitation within the conduction band results the non-radiative decay.

the non-propagating collective oscillation of the surface electrons in metal nanostructures. By utilization of SPP and LSPR in plasmonic nanostructures, the solar energy conversion efficiency of semiconductors can be improved via two paths [46]: photonic enhancement (or light trapping) and plasmonic energy transfer enhancement. In patterned plasmonic nanostructures, multiple times efficient scattering of the incident light increases the optical path length along with the light absorption direction in thin semiconductor layers [46, 47]. The previous part (SPP) contributes to enhance the energies above the band gap of a semiconductor, whereas the latter (LSPR) can induce charge separation in the semiconductor by absorbing light at the energies below the band gap [44, 48] due to the large local-field enhancement and absorption cross-section. The LSPR-induced charge separation can occur by transferring the plasmonic energy from the metal to the semiconductor via (i) direct electron transfer (DET) [49] and/or (ii) plasmon-induced resonant energy transfer (PIRET) [48]. This is referred to as plasmonic energy transfer enhancement [46] and is strong in small metal nanoparticles with small scattering cross-sections. The efficiency of the DET process depends open the relative energy of the hot electron to the height of the Schottky barrier at the interface Therefore, the semiconductor must be in close contact with the plasmonic metal. In contrast, PIRET proceeds non-radiatively based on the near-field dipole-dipole interaction between the plasmonic metal and the semiconductor [48]. PIRET allows the light absorption and the charge separation and does not require direct contact or band alignment, but its efficiency is controlled by the spectral overlap between the semiconductor's absorption band edge and the LSPR absorbance [48]. The good example of utilizing propagating (SPP) and localized (LSPR) plasmon modes is hematite nanorod array grown on a long-range-ordered plasmonic gold nanohole array pattern by combating the scattering/absorption trade-off, illustrated in **Figure 7**, where the hematite nanorods have been acted as "fiber optics miniature" to create the incarcerated modes, to trap the incident light, and to enhance the light absorption [50].

The size, shape, and composition of plasmonic NP affects the optical properties, i.e., absorption phenomena in the semiconductor, charge transport, and energetics of the semiconductor photoelectrodes as illustrated in **Figure 8** [51].

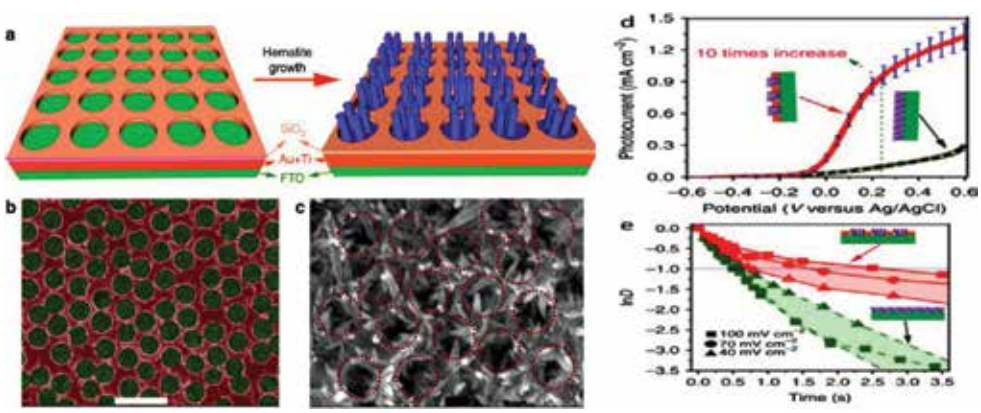

Figure 7. Architecture and microstructure of plasmonic photoanode. (a) Scheme for the growth of the hematite nanorod array on the Au nanohole array. (b, c) Scanning electron microscopic images of the Au nanohole array without (b) and with (c) the hematite nanorods. Scale bars, 1 mm (b) and 200 nm (c) [50].

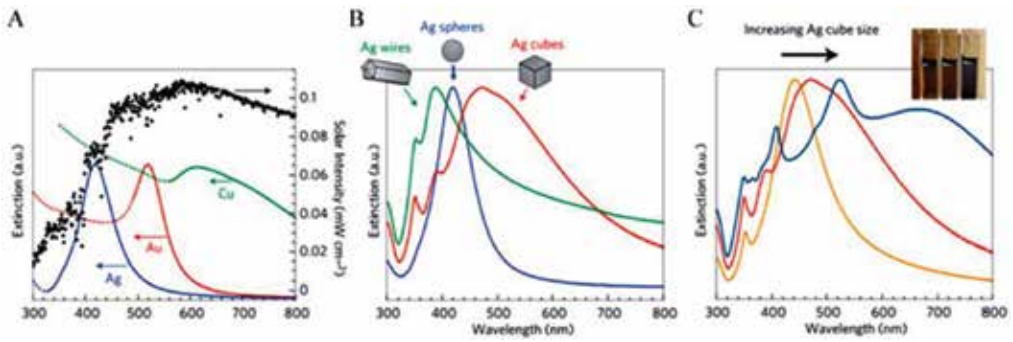

Figure 8. (A) Normalized extinction spectra of spherical Ag-NPs (38 ± 12 nm in diameter), Au NPs (25 ± 5 nm) and CuNPs (133 ± 23 nm). The solar radiation (air mass 1.5G) spectrum was taken from the National Renewable Energy Laboratory and is shown in black (http://rredc.nrel.gov/solar/spectra/am1.5/). Dashed portions of the metal extinction curves represent the inter-band transitions without surface plasmon resonance. (B) Normalized extinctions spectra of Ag-NPs with the wire (d = 90 ± 12 nm with >30 aspect ratio), cube (d = 79 ± 12 nm), and sphere (d = 38 ± 12 nm) shapes. (C) Normalized extinction spectra for Ag nanocubes as a function of size as 56 ± 8 nm (orange), 79 ± 13 nm (red), and 129 ± 7 nm (blue) edge lengths. The ethanolic suspension of the three different nanocube samples is shown in inset (reprinted with permission from Ref. [51]).

The energy of electron-electron as well as electron-phonon coupling was ultimately being converted into heat which will further thermalize the hot electrons. In the most of the cases, nonradiative (formation of electron and holes) plasmonic decay paralyzed the thermalization process that results in the efficiency minimization of the devices [52]. It not only limits the propagation length of plasmonic waveguides but also reduces the optical absorption of the metal that declines the overall performance of the device. The hot carriers generated from nonradiative plasmon decay offers new avenues to exploit the absorption losses. Although the much efforts have been devoted to alleviate the plasmon nonradiative decay, recent research has exposed the new prospectives by utilizing this energy in the areas [44, 53] such as in photothermal heat generation [45], photovoltaic devices [53, 54], photocatalysis [55, 56], driving material phase transitions [57, 58], photon energy conversion [59, 60] and photodetection [51, 61], and solar steam generation [62–64]. Most significantly, the decay of hot electrons can lead to the localized heating in the plasmonic nanostructures and making them good candidates for nanoscale heat sources [45, 65] that can be used in cancer therapy for destroying cancer cells [66]. On the contrary, hot electrons can be captured before thermalization by an adjacent semiconductor, to provide a novel photo-electrical energy conversion or chemical energy. The transformations from Plasmon energy to chemical energy occurred in four ways to drive the chemical reactions, i.e., (i) light scattering (radiative decay, **Figure 9A**), (ii) hot electron injection (HEI, **Figure 9B**), (iii) light concentration (**Figure 9C**), and (iv) Plasmon-induced resonance energy transfer (PIRET, **Figure 9D**). Light scattering by radiative decay can enhance the effective optical path length in the semiconductor. This leads to enhance the absorption of light and generation of charge carriers that can drive the chemical reactions [65].

Recently, a combination of a chiral metamaterial with hot electron injection was demonstrated in circularly polarized light detector [62, 67], where the chiral metamaterial can perfectly absorb the circularly polarized light which is the complimentary component of the largely

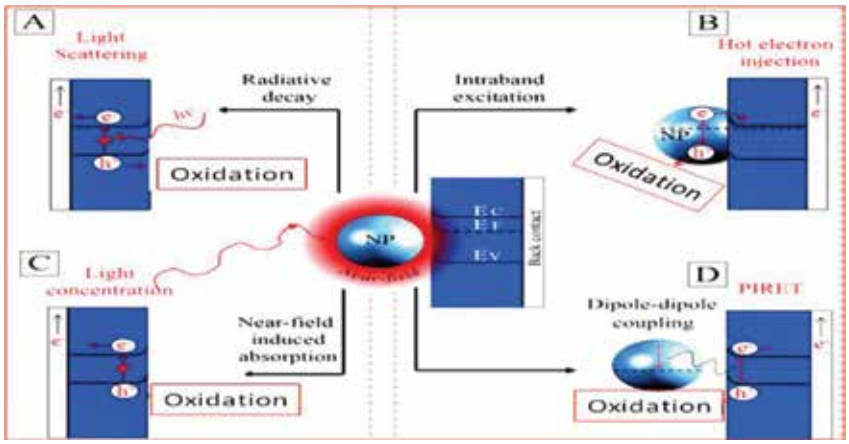

Figure 9. Schematic presentation of the transformations from Plasmon energy to chemical energy occurred in four ways (A) light scattering (radiative decay; LS), (B) hot electron injection (intra-band excitation; HEI), (C) light concentration (near field induced absorption; LC) and (D) plasmon-induced resonance energy transfer (dipole-dipole coupling; PIRET).

reflecting device. Therefore, it can be also selectively generate the hot electrons and produce a photocurrent signal depending upon the handedness of the light [62]. This ultracompact detector avoids the complexity of conventional circularly polarized light detectors, where a quarter wave-plate/polarizer were used.

In order to obtain the mechanistic insights into the structure-functionality relationship of the plasmonic NP/semiconductor composites, the decoupling of plasmon-induced and non-plasmon-induced effects are promising way to improve activity. Resonant enhancement in the polarizability of the materials with a negative real dielectric function (assuming a relatively small imaginary part) is responsible for plasmonic excitations in the metal nanoparticles.

The scattering cross section of a spherical gold NP is almost vanished when its radius decreased from 35 nm (**Figure 10A**) to 10 nm (**Figure 10B**), while the absorption and excitation

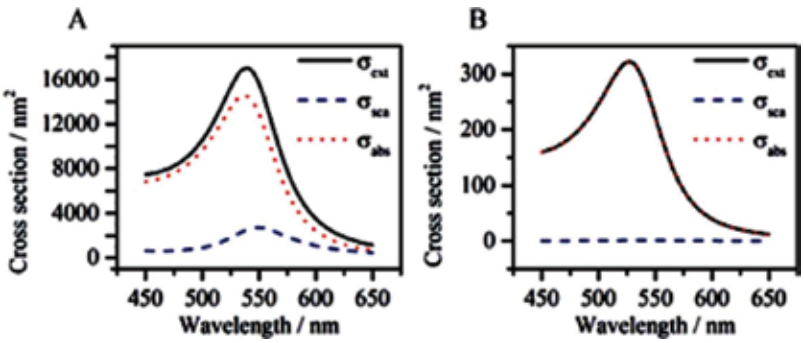

Figure 10. Extinction (black), scattering (blue) and absorption spectra (red) of a gold NP with a radius of 35 nm (A) and a radius of 10 nm (B) calculated using Mie theory. In both cases, the refractive index of the environment is 1.33 [68].

cross section are decreased to a lesser extent for the same compound. Thus, small NPs are used for applications where only non-radiative decays are desired.

5. Synthesis methods of silver nanoparticles

Recently, many techniques have been used for the synthesis of Ag-NPs by using chemical, physical, photochemical, and biological methods. Each method has its pros and cons with common problems of cost, scalability, uniform particle size, and the size distribution. Traditionally, metal nanoparticles are produced by physical methods like ion sputtering or pulsed laser ablation and chemical methods such as reduction, solvothermal synthesis, hydrothermal, sol-gel methods, and so on. However, recently, the environmentally friendly synthesis methods (by using natural products) have been developed under the branch of "green syntheses." Depending upon the selected path of synthesis and different experimental conditions, the silver NPs of different morphology, sizes, and shapes can be obtained. Nevertheless, the most important criteria is the size distribution that should be achieved as narrow as possible for the target-specific applications [69]. Four important methods (chemical, physical, photochemical, and biological) for the synthesis of nanoparticles are discussed as follows.

5.1. Chemical method

Among the existing methods, the chemical methods have been most common used for the production of Ag-NPs. The chemical reduction of metal ions is the most universal and easy route for the preparation of the metal nanoparticles. The chemical transformation of the silver ions into the silver nanostructures can occurred using photochemical method, [70, 71] wet chemical synthesis with [72] or without templates, [73] by employing liquid crystal, [74] polymer templates,[75] solution-based methodologies such as aspartate reduction [76] and starch-mediated reduction, etc [77]. Generally, the chemical synthesis process of the Ag-NPs in solution usually employs the following three main components: (i) metal precursors (for formation of AgNPs: $AgNO_3$ $AgClO_4$, AgCl, $(PPh_3)_3AgNO_3$, CF3CooAg), (ii) reducing agents, and (iii) stabilizing/capping agents. Few of the representative reducing agents are: $NaBH_4$, glucose, N,N-dimethyformamide, N_2H_4, sodium citrate, polyols, (such as ethylene glycol, diethylene glycol or a mixture of them), formaldehyde, etc., [78–83]. It is known that the different reductants are powered by different degree of reducibility that can play an important role in deciding the final shape of nanostructures. Moreover, these reductants favor the growth of nanocrystals along its different facets ((100) (111) or (110) facets). Unprotected metal colloids are highly vulnerable to the irreversible aggregation due to their small size. Therefore, the protective agents such as thiols, amines, polymers (e.g., polyvinylpyrrolidone PVP, polyvinyl alcohol PVA), polyelectrolytes (sodium oleate, oleic acid, etc.) [84–86], surfactants (cetyl trimethyl ammonium bromide (CTAB), sodium dodecyl sulfate, and cetyl trimethyl ammonium chloride (CTAC)), etc., can be added to suppression aggregation. The formation of colloidal solutions from the reduction of silver salts involves four stages, i.e., nucleation, incubation, subsequent growth, and Ostwald ripening. It is also revealed that the size and the shape of synthesized Ag-NPs are strongly

dependent on these stages. Furthermore, for the synthesis of monodispered Ag-NPs with uniform size distribution, all nuclei are required to form at the same time. In this case, all the nuclei are likely to have the same or similar size, and then they will have the same subsequent growth. The initial nucleation and the subsequent growth of initial nuclei can be controlled by adjusting the reaction parameters such as reaction temperature, pH, precursors, reduction agents, and stabilizing agents. These capping agents spontaneously adsorbed on the particle surface prevent their agglomeration, resulting in instable particle. In a typical experiment, aqueous 0.5 M $AgNO_3$ (0.8 mL) was mixed well with aqueous 0.4 M poly[(2-ethyldimethylammonioethyl methacrylate ethyl sulfate)-*co*-(1-vinylpyrrolidone)] (PQ11) (3 mL), and the resulting solution was hydrothermally treated at 100°C for 60 min. The spontaneous formation of the AgNPs can be attributed to the direct redox reaction between the PVP part of PQ11 and Ag^+, because there are no other reducing agents involved in the reaction system. As-formed dark brown colored colloidal-silver dispersion turned into yellow color (characteristic of spherical shaped AgNPs) on dilution. Usually, the bulk Ag show 4d → 5sp inter-band transitions, which are represented by the characteristic peak at 320 nm [87] in its UV-Vis spectrum (**Figure 11**). But the nano dispersion of silver display red shift and the peak at 320 nm shifted to 416 nm that corresponds to the dipole resonance of silver nanospheres.

5.1.1. Polyol process

Monodispersed solution of silver nanocubes were synthesized in large quantities by reducing silver nitrate with ethylene glycol in the presence of the capping agent polyvinylpyrrolidone (PVP) [79], which is an example of the so-called polyol process. In this case, ethylene glycol served as both reducing agent and solvent. It shows that the presence of PVP and its molar ratio relative to silver nitrate along with other additive formaldehyde, NaOH, played important roles in finalizing the geometric shape and size of the product. It suggested that it is possible to tune the size of silver nanocubes by controlling the experimental conditions.

5.1.2. Precursor injection technique

In the precursor injection method, the injection rate and the reaction temperature were important factors for producing uniform-sized Ag-NPs with a reduced size [81]. The injection of the

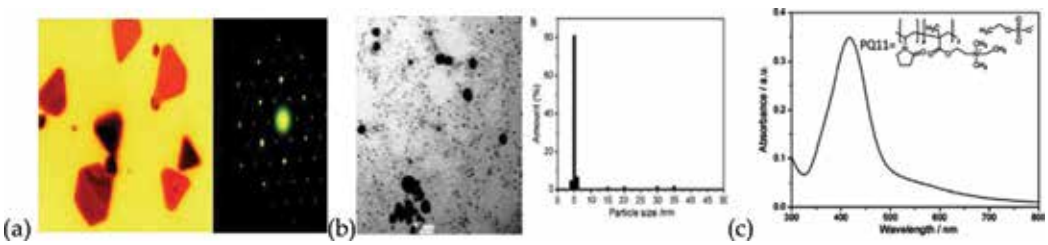

Figure 11. (a) Polygonal (mainly triangular) silver nanoprisms were synthesized by boiling $AgNO_3$ in *N, N*-dimethyl formamide and PVP, [88] (b) TEM image of as-formed silver colloids and the corresponding particle size distribution histogram and (c) UV-Vis spectrum of 150-fold diluted PQ-11 supported Ag NP solution of the dispersion synthesized at 100°C and 60min [89].

precursor solution into a hot solution is an effective mean to induce rapid nucleation in a short period of time, ensuring the fabrication of Ag-NPs with a smaller size and a narrower size distribution. Spherical Ag-NPs with a controllable size and high monodispersity were synthesized under the polyol process with the help of the modified precursor injection technique. Ag-NPs of the size 17 $\pm$ 2 nm were obtained at an injection rate of 2.5 mLs^{-1} along with the reaction temperature 100°C. Nearly, monodisperse Ag-NPs have been prepared in a simple oleylamine-liquid paraffin system [82] by using this technique.

5.2. Physical method

In the physical synthesis process of Ag-NPs, usually, the physical energies (thermal, ac power, and arc discharge) are utilized to produce Ag-NPs with a narrow size particle distribution. This approach can permit us to produce large quantities of Ag-NPs samples in a single process. Under the physical methods, the metallic NPs can be generally fabricated by evaporation-condensation process that could be carried out in a tube furnace at atmospheric pressure. The large space of tube furnace, consumption of large amount of energy, raising the environmental temperature around the source material and a lot of time for achieving thermal stability, are the few drawbacks of the method. Another physical method of synthesis of Ag-NPs is a thermal decomposition method that used to synthesize the powdered Ag-NPs [90]. In particular case, Ag-NPs (particles with particle size of 9.5 nm with a standard deviation of 0.7 nm) were formed by thermal decomposition of a Ag^{1+}–oleate complex, at high temperature of 290°C. This indicates that the Ag-NPs were prepared with a very narrow size distribution. Jung et al. [91] reported a small ceramic heater (with a local heating area) for synthesizing the metal NPs and by evaporating the source materials under the flow of carrier gas, i.e., air. It had been reported that the geometric mean diameter, the geometric standard deviation, and the total concentration of spherical NPs without agglomeration increases with the temperature of the surface of the heater. The testimony given by Tien et al. [92] reveal the fabrication technique for the Ag-NPs by employing the electrical discharge machining (EDM) without addition of any surfactants. Where, pure silver wires were submerged in deionized water and treated as electrodes. The stability of suspension, concentration of particles, particle size, solution properties, electric conductivity, and pH are the factors that may affect the synthesis of NPs by enhancing the complex interactions to the nanofluid, in the form of van der Waals combination force and electrostatic Coulomb repulsion force. Metallic Ag-NPs of the 10 nm size and ionic silver of approximate concentrations 11–19 ppm were obtained by silver rod at the consumption rate ~ $100mgmin^{-1}$. More recently, Siegel et al. [93] reported an unconventional approach for the physical synthesis of gold-NPs and Ag-NPs by the direct metal sputtering into the liquid medium (glycerol-to-water).

5.3. Photochemical synthesis

The photo-induced synthesis of Ag-NPs has two main approaches: that is the photophysical (top down) and photochemical (bottom up) ones. In former way, NPs could be prepared by the fragmentation of the bulk metals and followed by generation of the NPs from ionic

precursors. The NPs are formed by the direct photoreduction of a metal ion using photochemically generated intermediates, such as excited molecules and radicals, which are often known as photosensitization of NPs [94, 95]. The main advantages of the photo-induced process are: clean process, high spatial resolution, convenience of use, the controllable in-situ reducing agents generation; the formation of NPs can be triggered by the photo irradiation, (iii) enables one to fabricate the NPs in various mediums including emulsion, surfactant micelles, polymer films, glasses, cells, etc [94]. The direct photo-reduction process of $AgNO_3$ takes place in the presence of sodium citrate (NaCit) using different light thermal sources (UV, white, blue, cyan, green, and orange) at room temperature [96]. This light-induced process results in a metallic colloid with size and shape powered distinctive optical properties of the particles. Reproducible UV photo-activation method is used for the preparation of the stable Ag-NPs in aqueous TritonX-100 (TX-100) [97], where TX-100 molecules play a dual role: (i) as an reducing agent and (ii) as a NPs stabilizer through template/capping action. The addition of surfactant solution to TX-100 and silver precursor helps in carrying out the NPs growth process by controlling the diffusion (by decreasing the diffusion/mass transfer coefficient of the system) to improve the NPs size distributions (by increasing the surface tension at the solvent–NPs interface). The Ag-NPs (size 2–8 nm) can also be synthesized in a basic aqueous $AgNO_3$ solution and carboxymethylated chitosan (CMCTS) under UV light irradiation. CMCTS is a biocompatible water-soluble derivative of chitosan and served as a reducing agent for silver cation and a stabilizing agent for Ag-NPs (stable for more than 6 months), simultaneously [98]. This method is used to fabricate a high-yield metal nanostructures and composite materials at low cost. Few alternative approaches, such as laser ablation at the solid–liquid interface and combination of the reducing agent and sunlight, are also used for metal nanostructure fabrication. The three-dimensional metal NPs are produced using laser ablation and are applicable in the field of a light-driven actuator, bioimaging, and three-dimensional processing [99]. The photo-induced silver nanoprisms/nanodecahedrons have been the synthesis by controlling the concentration of sodium citrate and sunlight (ultraviolet light). At the lower concentration of citrate ($\leqslant 5.0 \times 10^{-4}$ M), silver nanoprisms are converted into nanodecahedrons silver by increasing the concentration of citrate as shown in **Figure 12**. Although the intensity of light affects the shape of the NPs, the lighting power density did not influence the shape conversion except for reaction rate [100].

Figure 12. Photo-induced synthesis of silver nanoprisms and nanodecahedrons by controlling the concentration of sodium citrate and sunlight [100].

5.4. Biological synthesis

Usually, wet-chemical or physical method is used to prepare the metal nanoparticles. However, the chemicals used in pbhysical and chemical methods are generally expensive, harmful and inflammable but the bogenic methods are a cost effective, energy saver and having enviornmentally benign protocols technique for green synthesis of silver nanoparticles from different microorganisms (yeast, fungi and bacteria, etc) and plant tissues (leaves, fruit, latex, peel, flower, root, stem, etc) as shown in **Figure 13**. Pytochemicals (lipids, protiens, polyphenols, carboxylic acids, saponins, aminoacids, polysachccarides amino cellulose, enzymes, etc.) present in plants are used as reducing and capping agent. The use of agro waste and micro-orgamisms materials not only reduces the cost of synthesis but also minimizes the need of using hazardous chemicals and stimulates "green synthesis" way for synthesizing nanoparticles [101, 102].

This method of biosynthesis is very simple, requiring less time and energy in comparison to the physical and chemical methods with predictable mechanisms. The other advantages of biological methods are the availability of a vast array of biological resources, a decreased time requirement, high density, stability, and the ready-to-soluble as-prepared nanoparticles in water [103]. Therefore, biogenic synthesis of metal NPs unwraps up enomorus opportunities for the use of biodegradable or waste materials.

Figure 13. Biogenic synthesis of metal nanoparticle of various shape and size using microorganisms and plant tissues extracts.

6. Characterization tools for analysis of silver nanoparticles

At the nanoscale, particle-particle interactions are either dominated by weak Vander Waals forces, stronger polar and electrostatic interactions or covalent interactions. Characterization of nanoparticles is vital part of determination of the phase purity, shape, size, morphology, electronic transition plasmonic character, atomic environment and surface charge, etc. By using advanced analytical techniques such as electron microscopic techniques (atomic force microscopy (AFM), electron energy loss spectroscopy (EELS), surface enhanced Raman scattering (SERS), scanning electron microscopy (SEM) and transmission electron microscopy (TEM) and their corresponding energy-dispersive X-ray spectroscopy (EDX), and selected area electron diffraction (SAED for crystallinity). Properties like surface morphology, size, and overall shape are determined by electron microscopy techniques and

elemental composition by SEM-/TEM-/EELS-supported EDX. Optical analysis techniques such as Fourier transform infrared (FTIR) spectroscopy, fluorescence correlation spectroscopy (FCS, diffusion coefficients, hydrodynamic radii, average concentrations, and kinetic chemical reaction), X-ray diffraction (XRD for phase purity with crystal parameters and particle size), diffuse light scattering (DLS can probe the size distribution of small particles), UV-Vis spectroscopy (band gap, particle size electronic interaction), XPS (X-ray photon spectroscopy, surface environment of elemental arrangement), Raman spectroscopy (it provides submicron spatial resolution average size and size distribution through analysis of the spectral line broadening and shift), nuclear magnetic resonance (NMR can detect structure, compositions, diffusivity of nanomaterials, dynamic interaction of species under investigation), small-angle X-ray scattering (SAXS; from 0.1° to 3° can evaluate the size distribution, shape, orientation, and structure of a variety of polymers and nanomaterials), zeta potential with a value of ±30 mV is generally chosen to infer particle stability. Above analysis can be used to determine the properties of nanomaterials such as the size distribution, dispersibility, average particle diameter, charge affect the physical stability and the in vivo distribution of the nanoparticles. Few of above are discussed below.

6.1. X-ray diffraction spectroscopy (XRD)

The crystalline structure, size, and shape of the unit cell and the crystallite size of a material can be determined using X-ray diffraction spectroscopy (XRD). Usually, X-ray diffraction peaks were observed at $2\theta = 38.00°$, 44.16°, 64.40°, and 77.33°, which correspond to (111), (200), (220), and (311) Bragg's reflections of the face-centered cubic (fcc) structure of metallic silver, respectively (standard JCPDS card No. 04-0783 or 87-0597). The crystalline size of the particulate can be estimated by using the Debye-Scherrer formula $d = 0.89\lambda\ \beta\cos\theta$, where d is the particle size, λ is the wavelength of X-ray radiation (1.5406 Å), β is the full-width at half-maxima (FWHM) of the strongest peak (in radians) of the diffraction pattern and 2θ is the Bragg angle [104].

6.2. Scanning electron microscopy (SEM)

In this technique the whole sample is analyzed by scanning with a focused fine beam of electrons and electrostatic or electromagnetic lenses to generate images of much higher resolution. Surface morphology of the sample is determined by the help of the secondary electrons emitted from the sample surface.

6.3. Transmission electron microscope (TEM)

In TEM analysis, an incident beam of electrons is transmitted through an ultra-thin sample which interacts with the sample and transforms into unscattered electrons, elastically scattered electrons, or inelastically scattered electrons. The scattered or unscattered electrons are focused by a series of electromagnetic lenses and then projected on a screen to generate a electron diffraction, amplitude-contrast image, a phase-contrast image, or a shadow image of varying darkness according to the density of unscattered electron. Transmission electron microscopy

techniques can provide direct imaging, diffraction and spectroscopic information, chemical composition, either simultaneously or in a serial manner, of the specimen with an atomic or a sub-nanometer spatial resolution. High-resolution TEM imaging, when combined with nanodiffraction, scanning tunneling microscopy (STM), atomic resolution electron energy-loss spectroscopy, and nanometer resolution X-ray energy dispersive spectroscopy techniques, is critical to the fundamental studies of importance to nanoscience and nanotechnology.

Different surface structures can be obtained from various synthesis routes. Surface morphology of the nano-structural features of silver are examined using above electron microscopic techniques. Electron microscopy images of single-crystal Ag-NPs (cubes, bars, wires, and bipyramids) grown in ethylene glycol in the presence of PVP and Br− at different proportions, are demonstrated in the **Figure 14A–D**. Silver triangular nanoplates, prepared by are demonstrated by the **Figure 14E** and **F** Asymmetric Silver "Nanocarrot" Structures, were synthesized by using wet chemical method using CF3COOAg as precursor, PEG as reducing agent, and PVP as capping agent are depicted in the **Figure 14G–I** [105, 106].

6.4. Scanning tunneling microscopy (STM)

STM uses quantum tunneling current to generate electron density images at the atomic scale for conductive/semiconductive surfaces and biomolecules attached on conductive substrates [107]. A sharp scanning tip, an xyz-piezo scanner controlling the lateral and vertical movement of the tip, a coarse control unit positioning the tip close to the sample within the tunneling range, a vibration isolation stage and feedback regulation electronics are the basic parts of the STM instrumentation. Its working on the generic principle for, i.e., to bring a susceptible probe in close proximity to the surface of an object measured to monitor the reactions of the probe [108].

6.5. Atomic force microscopy (AFM)

The AFM can investigate the size, shape, structure, sorption, dispersion, and aggregation of nanomaterials. It is based on a physical scanning of samples at sub-micron level (contact or noncontact mode) using a probe tip of atomic scale and offers ultra-high resolution (>100 times

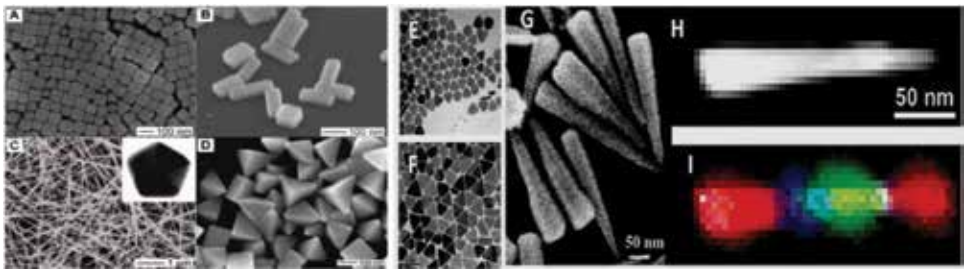

Figure 14. Electron microscopy images of single-crystal Ag nanocrystals: (A) nanocubes prepared in ethylene glycol with PVP as a capping agent in DMF; (B) nanobars prepared in ethylene glycol in the presence of PVP and Br−; (C) pentagonal nanowires prepared in ethylene glycol in the presence of PVP in DMF; (D) bipyramids prepared in ethylene glycol in the presence of PVP, where TEM image represented by E, F, and G and the EELS spectrum of the asymmetric silver nanocarrot, were represented by H&I [105, 106].

better than the optical diffraction) in particle size measurement. One of the principal advantages of this nondestructive technique is that it felicitates the imaging of the non-conducting samples without any specific pretreatment and without causing appreciable harm to the surface. The major drawbacks of this technique is (i) the size of the cantilever tip is generally larger than the dimensions of the nanomaterials to be examined that led to unfavorable overestimation of the lateral dimensions of the samples [109, 110], (ii) AFM also lacks the capability of the detecting or locating specific molecules; however, this disadvantage has been eliminated by recent progress in single-molecule force spectroscopy with an AFM cantilever tip carrying a ligand.

6.6. Electron energy-loss spectroscopy (EELS)

In looking to the better understanding of the atomic processes in solids, their emerging demand for new imaging, diffraction and spectroscopy methods with high-spatial resolution. That demand has been reinforced by the growing interest of human being in nanomaterials. Although, the transmission electron microscopy (TEM) can provide the structural information with excellent spatial resolution (down to atomic dimensions) through high-resolution TEM imaging and electron diffraction technique, electron energy-loss spectroscopy offers unique possibilities for the nanoscale thin materials (plasmonic) analysis. Due to the broad range of inelastic interactions of the high energy electrons with the specimen atoms, ranging from phonon interactions to ionization processes, EELS and their combination with TEM offers the facility to map the elemental composition of a specimen for studying the physical and chemical properties of a wide range of biological and non-biological materials. Moreover, the energy distribution of all the inelastically scattered electrons provides the information [111] about the local environment of the atomic electrons for the universal dispersions of surface plasmons in flat nanostructures, [112] 3D distribution of the surface plasmons around a metal nanoparticle [113] and exotic nanostructures are shown in **Figure 15** [114].

6.7. UV-Visible spectroscopy analysis

In decades past, synthesis of silver nanostructures has been an active research area because of their excellent optical properties such as surface-enhanced Raman scattering (SERS) and

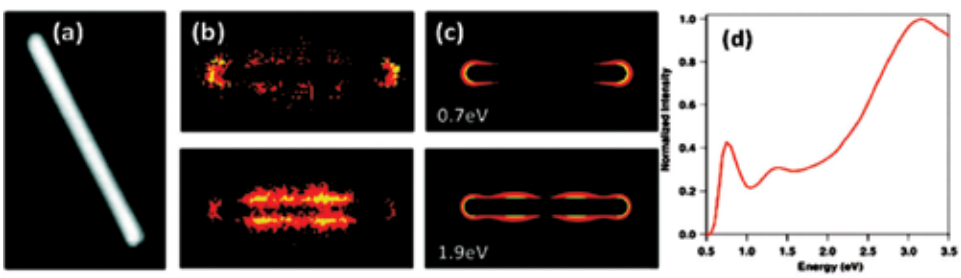

Figure 15. EELS data and corresponding electrodynamic calculation for rod. (a) Annular dark field (ADF) image of rod with high aspect ratio 9.6, (b) multivariate statistical analysis (MVSA)) score images, (c) discrete dipole approximation (DDA) calculated electric field plots displaying the field generated by a plane wave optical excitation at the energies and polarization given on each plane, and (d) summed EEL spectrum [114].

surface plasmonic resonance, which strongly depend on size, shape, and composition, and can be checked by the help of the optical analyses like XPS and UV-Visible spectroscopy analysis. Although, the change in color of precursor silver ion to silver nanoparticles was visually observed, the absorption measurements were carried out using UV-Visible spectrophotometer to check the stability of silver nanoparticles. Characteristic UV-Vis spectrum peak of bulk Ag appears at 320 nm due to the inter-band 4d → 5sp transitions [87]; and the red shift in this peak to around 420 nm was observed due to the occurring of the plasmonic resonance phenomenon in the nano-dispersion of silver metal. Effect of shape and size on optical properties of the silver nanoparticle is reflected by **Figure 16**.

UV-Vis spectroscopy also used for particle size determination of silver nanoparticles, using Mie scattering theory. The full width at half maxima of the optical spectra (Lorentz-shaped peak; Ω) can be used to calculate the particle size of stable suspension by using following equation [116, 117]:

$$D = \frac{\left(\epsilon_0 + 2n^2\right) c\, m\, U_F}{2N_c e^2 \omega} \tag{1}$$

where, w is full width at half maxima of the Lorentz shaped peak, and ϵ_0, n, c, m, U_F, N_c, e, and D, are the frequency independent dielectric constant, refractive index of water, velocity of light, mass of electron, electron velocity at the Fermi energy, number of electrons per unit volume, the electron charge and diameter of the particle, respectively.

6.8. Surface-enhanced Raman scattering spectroscopy (SERS)

SERS can be employed as a sensitive and selective technique for identification of molecules. Strong electromagnetic fields are generated due to the localized surface plasmon resonance (LSPR) of nano-noble metals, when they are exposed to visible light. If the Raman scatterer is placed near these intensified electromagnetic fields of nano-noble metals, the induced-dipole

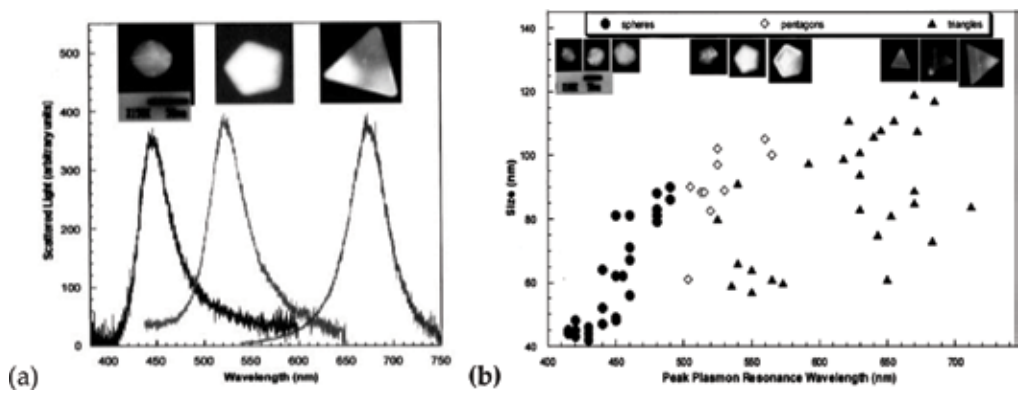

Figure 16. (a) optical spectra of the individual silver nanoparticles of different shape spherical (Blue emission), pentagon (Green emission) and triangular (Red emission) as reflected from their typical high resolution TEM images. (b) Plot of the lateral size of TEM images vs the wavelength of the plasmonic resonance spectral peak for a spherical (dark circle; 85%) pentagon (empty rectangle; 5%) and triangular (dark triangle; 5%) particles [115].

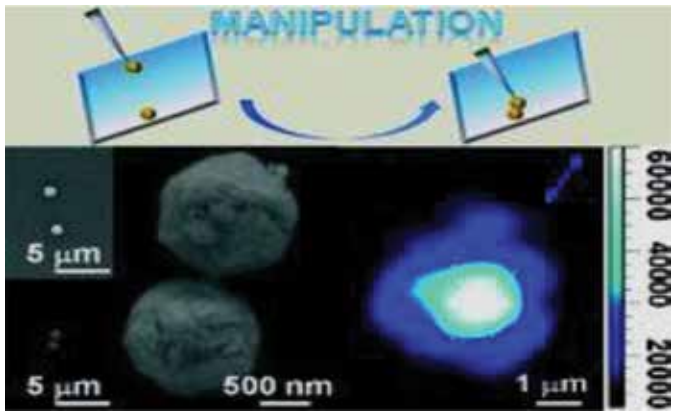

Figure 17. SEM images of a self-assembled dimmer of flower-like silver mesoparticles along with their corresponding Raman images at the axis parallel to the dimer axis of the detected particles with high SERS quality [118].

increases that results in the increase of intensity of the inelastic scattering. Similar relations can hold-good for the extinction and scattering cross sections of the nanoparticle. If the extinction and scattering cross sections of the nanoparticle at resonant wavelengths are maximized, it represents the spectroscopic signature of exciting the LSPR. A SER spectrum also provides the accurate information about molecular structure and the local environment in condensed phases than any other electronic spectroscopy technique.

A typical example of the surface-enhanced Raman scattering (SERS) is reflected by **Figure 17**, where the coupling effect still dominates the SERS and the flower-like silver mesoparticle dimer image with the large hot areas is ≈10 to 100 times greater than the individual mesoparticles [118].

7. Applications of the silver nanoparticles

Metal nanocatalysts of different shapes and sizes like quantum dots, nanotubes, nanofibres, nanolithographs, self-assemble processing devices, nanoparticles, and nanofibres, have immense significance. They have bright future in broad research areas of high-tech applications in the field of information of storage, computing, medical and biotechnology, energy, sensors, photonics, communication, and smart materials. The size and shape of the nanometal is a critical criteria to target-specific applications that may be achieved by keeping size distribution as narrow as possible. Nanometals has enormous potential to serve all facets of life for building big future from small things, as they acquire the goodness of both homogeneous and heterogeneous catalysts. At present, the pretty command over the morphologies of silver nanoparticles has received immense attention of researchers due to their considerable budding applications in almost all fields. In the present context, they have attracted the interest of the people due to their unique physical, chemical, and biological properties in compared to their massive counterparts. Silver nanoparticles are also studied by material scientists who investigate their integration into other materials in order to obtain enhanced properties, for example, in solar cells where silver

nanoparticles are used as plasmonic light traps. These properties make them valuable in other applications such as catalyst [119, 120], inks, microelectronics, medical, imaging, health products, and waste management. Antifungicidal activities making them extremely popular in a diverse range of consumer/medical products, including plastics, soaps, pastes, food, cosmetics, medicine, highly sensitive surface-enhanced Raman spectroscopy (SERS) application [121–123], water treatment and textiles, etc., that boost their market value [124]. Moreover, the nanofibre can be very effective in attracting and trapping small particles because it is "sticky" due to its large surface area. This makes nanofibres excellent materials for use in filtration [125]. Moreover, silver nanoparticles accounts for more than 23% of available nano-products in the market. It includes the share of different facets of life, i.e., 52.61% health and fitness, 10.44% cleaning, 10.04% food, 6.02% household equipments, 4.02% medicine, 3.21% electronic devices, 2.01% toys, and 11.65% others [126]. Out of the versatile applications of nanosilver in diverse phases of life, few are discussed below.

7.1. Medical: diagnosis and treatment of aliment

The silver nanoparticles exhibit a broad spectrum of antibactericidal, antiviral, anti-inflmmatory, antiangiogenic, anti-tumor, and anti-oxidativeproperties along with the biological and chemical sensing, imaging, drug carrier, and diagnosis of the cancer/HIV/AIDS [127–131]. When the researchers directed near-infrared laser light through the mice's skin and at the tumors, the resonant absorption of energy in the embedded nanoshells raised the temperature of the cancerous tissues from about 37°C to about 45°C. The photothermal heating killed the cancer cells while leaving the surrounding healthy tissue unharmed. In the mice treated with nanoshells, all signs of cancer disappeared within 10 days; in the control groups, the tumors continued to grow rapidly [132].

Silver nanotechnology, emerging as a fast growing technology in the field of orthopedics due to its antimicrobial properties. Therefore, silver nanoparticles can be used in orthopedic applications such as trauma implants, tumor prostheses, bone cement, and hydroxyapatite coatings to prevent the biofilm formation. Bio film formation is a major source of morbidity in orthopedic surgery. The promising results with *in vitro* and *in vivo* studies of the use of AgNPs in this field reduce the risk of infection in an effective and biocompatible manner [133].

7.2. Food industry

Silver nanoparticles are already utilized for various applications in areas such as food supplements, food packaging, and functional food ingredients. To protect the food from dust, gases (O_2, CO_2), light, pathogens, moisture nanocomposite LDPE films containing Ag and ZnO nanoparticles packaging, would be a safer, inert; cheaper to produce, easy to dispose and reuse-way. Nanocomposite LDPE films containing Ag and ZnO nanoparticles were prepared by melt mixing in a twin screw extruder. Packages prepared from the above films were used to carry/store fresh orange juice, fresh meat (highly perishable commodity) to avoid the proliferation of undesirable microorganisms and also to provide desired texture to the food, encapsulate food components (e.g., control the release of flavors), increase the bioavailability of nutritional components [134].

7.3. Catalyst

In recent years, one of the most important applications of the AgNPs has been observed in catalysis of chemical reactions. Nanosilver catalysts' with their unique reactivity and selectivity, stability, as well as recyclability in catalytic reactions with atom-economy and environmental benign nature, increases the interest in nanosilver-mediated organic synthesis in the last few years. Nanosilver of different shapes and sizes catalyzed many organic transformations such as cyclization, Michael addition, alkylation, alkynylation, oxidation, cross-coupling reaction, A^3-coupling reaction, reduction, Friedal-crafts, Diel-Alder reaction, and many more [135]. Researchers are fascinated to silver nanoparticles, since it has enabled unprecedented or low selective transformations to highly reactive and chemoselective catalysis for various nanosilver-catalyzed reactions. For example, kinetically difficult reduction of p-nitrophenol is not possible even in presence of strong reducing agent $NaBH_4$ and month long aging. But, by the addition of AgNPs in the same reaction mixture, it made the reaction possible by formation of the p-aminophenol [136]. Studies in this field, revealed the strong potential of nanosilver catalysis in the total synthesis of natural products and pharmaceutical molecules [137].

7.4. Air disinfection (biosols filter)

Bioaerosols are airborne biological origins such as viruses, bacteria, fungi, which are capable of causing infectious, allergenic, or toxigenic diseases. Large quantities of these bioaerosols were accumulated on the filters of heating, ventilating, and air-conditioning (HVAC) systems [138]. It often resulted in the low quality of indoor air. The WHO estimated that 50% of the biological contamination present in indoor air comes from filter-medium after air filtration, which can add on microbial growth. These pathogens generate mycotoxins which are dangerous to human health. To reduce the microbial growth in air filters, Ag-deposited-activated carbon filters (ACF) were effectively used for the removal of bioaerosols. Antibacterial activity analysis of Ag-coated ACF filters was checked for *Bacillus subtilis* and *E. coli* [138]. It was found that above two bacteria were completely inhibited the physical properties of ACF filters such as pressure drop and filtration efficiency with in 10 and 60 min, respectively.

7.5. Drinking water purification

Studies supported that the silver nanoparticle (AgNP) can work as an excellent antiviral, antimicrobial, and disinfectant agents. The results obtained showed that silver nanoparticles in surface water, ground water, and brackish water are stable. However, in seawater conditions, AgNP tend to aggregate. The comparison of AgNP-impregnated ceramic water filters and ceramic filters impregnated with silver nitrate was made. The results showed that AgNP-impregnated ceramic water filters are more appropriate for this application due to the lesser amount of silver desorbed compared with silver nitrate-treated filters without disturbing the water chemistry conditions and performance of the filters. Quaternary ammonium functionalized silsesquioxanes-treated ceramic water filter desorbed less from the filters and achieved higher bacteria removal than the filters impregnated with AgNP. This indicates that

the quaternary ammonium functionalized silsesquioxanes compound could be considered as a substitute for silver nanoparticles due to its lower price and higher performance [139].

7.6. General/health care

Nanosilver products such as beauty soap, hair shampoo and conditioner, body cleanser, tooth brush, sanitizer, facial masksheets, skin care line, makeupline, wetwipes, disinfectant spray, wash and laundry detergent, etc., have been influence our daily life at great extent [140]. Silver nanoparticles can also be incorporated in manufacturing of the toothpaste or oral care gels. Silver nanoparticles with particle size less than 15 nm and concentration of 0.004% w/w showed maximum efficiency to prevent the growth of bacteria that causes unpleasant oral smells and dental cavities [141].

The nanoproduct can also be used in dyeing of cosmetic foundations, eye shadows, powders, lipsticks, inks, varnishes, or eyebrow pencils. According to Ha et al., the products with metal nanoparticles, unlike the conventionally used metallic pigments, are not harmful to human health, and may even have health benefits [142].

A soap with silver nanoparticles as one of the ingredients was prepared; and in 2013, the method for its preparation was patented [143]. Nia had used the silver nanoparticles to improve the plant growth of the plants (citrus fruits, grains, and oleaceae trees) [144]. Silver nanoparticles-treated structure of textile materials [145] were used for antimicrobal activities protected clothing. The authors reported that the silver nanoparticles coated nylon fibers used in making of floor coverings/carpets that helps to secure them against bad odors and the growth of pathogenic microorganisms [146].

8. Challenges and perspectives

The commercial use of the engineered nanomaterials, with at least one-dimension of 100 nm or less, is increasing in the area of fillers, opacifiers, consumer/medical products (including plastics, soaps, pastes, food, cosmetics, medicine, drug carriers, and highly sensitive SERS application), catalysts, semiconductors, textile, waste water treatment, microelectronics, bioimaging, etc. Materials at nano-level may induce some specific physical or chemical interactions with their environment. As a result, they perform exceptional changes in the properties like conductivity, reactivity, and optical sensitivity, in comparison to their massive counterparts, which may enhance the processes such as dissolution, redox reactions, or the generation of reactive oxygen species (ROS). These processes may be accompanied by biological effects that would not be produced by larger particles of the same chemical composition. The nanomaterials are responsible for the possible undesirable interactions with biological systems and the environment which might generate toxicity. Therefore, there is an urgent requirement to establish the principles, procure the test procedures to ensure safe manufacture and commercial use of nanomaterials [147] to stop the uncontrolled release of nanoparticles to the environment through waste disposal, and to incorporate the nanowaste and nanotoxicology in the waste management. Thus, the bioaccumulation and toxicity of the nanoparticles may

become important environmental issues. Although the amount of the nanoparticles in commercial products are lower than those present in soluble form but the toxicity resulting from their intrinsic nature (e.g., their size, shape, or density) may be significant. Moreover, the major challenge in the treatment of nanowaste is the current need of the time. Not only the proper understanding of its chemical, physical, and biological properties, but it also requires the apt number of studies on the impact (short- and long term effects) of these new materials on biological and environmental systems (acutely lacking area). It is necessary to have basic information from companies about the level and nature of nanomaterials produced or emitted and about the expectation of the life cycle time of nanoproducts as a basis to estimate the level of nanowaste in the future. Without the knowledge of how to use, store, facilitate the separation, and recovery of recyclable and non-recyclable nanomaterials, the development of the regulations in this field is difficult. Moreover, Ag metal has strong affinity toward the elements, i.e., O, Cl, S, and organic compounds (particularly, the thiol group containing compound) and oxidation capacity that shorten the lifetime of Ag-NPs in the environment. The kinetics of Ag-NPs corrosion increases with decreases in particle size. Sulfidation (significant amount of the sulfide ion present in polluted water) is the most probable corrosion process for metallic AgNPs undergo because of the very high stability of Ag_2S. However, the mechanisms with the kinetics of the oxidation of Ag_2S-NPs in to Ag_2SO_4, on contact with air or microbial transformation, is needed to be deal with as Ag_2SO_4 ($Ksp = 1.2 \times 10^{-5}$) is considerably more soluble than Ag_2S ($Ksp = 5.92 \times 10^{-51}$). Furthermore, in comparison to the unsulfidized AgNPs and Ag ion, the toxicity of Ag_2S-NPs has shown limited acute toxicity because sulfidation momentously decreases the solubility [148]. Recently, the plasmonic materials are in fashion because of their efficiency in optoelectronic materials; for example, in a recent report, the hot electron transfer from a plasmon-induced interfacial charge-transfer transition induced the quantum efficiency of the device up to 20% independent of incident photon energy [149]. In addition to above, a better understanding of the hot carrier generation, transport, emission and relaxation timescale, engineering of semiconductor-hot electron interface is still needed for better designing of the efficient hot carrier devices [150–153]. Beside all the challenges, the future of silver nanoparticles is bright because of their potential use in biomedical applications as long lasting and enhanced antifungal, antibacterial, disinfection properties along with their utilization in drug delivery, diagnosis, bioimaging, biosensoring, etc. Moreover, their role as an effective molecular sieve, metallic sorbent, and catalyst for the removal of the environmental pollutions are commendable. There is great hope for the application of Ag-NPs in the versatile field of computers and informatics, cosmetics, textile, food, and medicine. Although a lot of work is done in this field, the full potential of silver nanoparticles is yet to come into lime light with better understanding of their mechanism and long lasting impact on environment and waste management.

9. Chapter summary

The chapter started with a brief introduction of the nanomaterials along with their historical existence without in-depth knowledge. The importance of the silver NPs over other nanometals was established on the account of their properties such as surface-enhanced plasmonic character,

cost, stability, and so on. The synthesis methods and advanced characterization tools were also discussed in keeping AgNPs in the mind. The applications of these competent nanoparticles along with their goodness and special qualities are also described in the chapter. In the end, the challenges and future prospective of this up-bringing area were discussed.

Author details

Neelu Chouhan

Address all correspondence to: niloochauhan@hotmail.com

Department of Pure and Applied Chemistry, University of Kota, Kota, Rajasthan, India

References

[1] Available form: https://www.sciencelearn.org.nz/resources/1676-novel-properties-emerge-at-the-nanoscale

[2] Booker R, Boysen E. Nanotechnology for Dummies. 1st ed. Hoboken NJ: Wiley Publishing; 2005. 40 p. ISBN: 13: 978-0-7645-8368-1

[3] Bonner JT. Why size matters. In: Stevens SY, Sutherland LAM, Krajccik J, editors. The Big Ideas of Nanoscale Science and Engineering. Princeton, NJ: Princeton University Press; 2009. pp. 4-5 (80 p). ISBN 978-1-935155-07-2

[4] Yamamoto M, Nishikawa N, Mayama H, Nonomura Y, Yokojima S, Nakamura S, Uchida K. Theoretical explanation of the lotus effect: Superhydrophobic property changes by removal of nanostructures from the surface of a lotus leaf. Langmuir. 2015; **31**(26):7355-7363. DOI: 10.1021/acs.langmuir.5b00670

[5] Ensikat HJ, Ditsche-Kuru P, Christoph Neinhuis C, Barthlott W. Superhydrophobicity in perfection: The outstanding properties of the lotus leaf. Beilstein J Nanotechnol. 2011;**2**: 152-161. DOI: 10.3762/bjnano.2.19

[6] Koch K, Bhushan B, Barthlott W. Diversity of structure, morphology and wetting of plant surfaces. Soft Matter. 2008;**4**(10):1943-1963. DOI: 10.1039/B804854A

[7] Maier SA. Plasmonics Fundamentals and Applications. 1.st ed. New York: Springer; 2007. pp. 21-34, 65-88. eISBN 978-0387-37825-1

[8] Lal S, Link S, Halas NJ. Nano-optics from sensing to waveguiding. Nature Photonics. 2007;**1**(11):641-648. DOI: 10.1038/nphoton.2007.223

[9] Wang X, Yu JC, Yip HY, Wu L, Wong PK, Lai SY. A mesoporous Pt/TiO_2 nanoarchitecture with catalytic and photocatalytic functions. Chemistry – A European Journal. 2005;**11**(10):2997-3004. DOI: 10.1002/chem.200401248

[10] Cao XB, Gu L, Zhuge LJ, Gao WJ, Wang WC, Wu SF. Template-free preparation of hollow Sb2S3 microspheres as supports for Ag nanoparticles and photocatalytic properties of the constructed metal–semiconductor nanostructures. Advanced Functional Materials. 2006;**16**(7):896-902. DOI: 10.1002/adfm.200500422

[11] Virkutyte J, Varma RS. Fabrication and visible light photocatalytic activity of a novel $Ag/TiO_{2-x}N_x$ nanocatalyst. New Journal of Chemistry. 2010;**34**(6):1094-1096. DOI: 10.1039/C0NJ00268B

[12] Takagahara T, Takeda K. Theory of the quantum confinement effect on excitons in quantum dots of indirect-gap materials. Physical Review B. 1992;**46**:15578(R). DOI: 10.1103/PhysRevB.46.15578

[13] Couto Jr OD, Puebla J, Chekhovich EA, Luxmoore IJ, Elliott CJ, Babazadeh N, Skolnick MS, Tartakovskii AI, Krysa AB. Charge control in InP/(Ga, In) P single quantum dots embedded in Schottky diodes. Physical Review B. 2011;**84**(12):125301. DOI: 10.1103/PhysRevB.84.125301

[14] Shin SJ, Lee JJ, Kang HJ, Choi JB, Yang SR, Takahashi Y, Hasko DG. Room-temperature charge stability modulated by quantum effects in a nanoscale silicon island. Nano Letters. 2011;**11**(4):1591-1597. DOI: /abs/10.1021/nl1044692

[15] Beenakker CWJ. Theory of Coulomb-blockade oscillations in the conductance of a quantum dot. Physical Review B. 1991;**44**:1646. DOI: 10.1103/PhysRevB.44.1646

[16] Prati E. Valley blockade quantum switching in silicon nanostructures. Journal for Nanoscience and Nanotechnology. 2011;**11**(10):8522-8526. DOI: 10.1166/jnn.2011.4957

[17] Crippa A, Tagliaferri ML, Rotta D, De Michielis M, Mazzeo G, Fanciulli M, Wacquez R, Vinet M, Prati E. Valley blockade and multielectron spin-valley Kondo effect in silicon. Physical Review B. 2015;**92**(3):035424. DOI: 10.1103/PhysRevB.92.035424

[18] Harry A. Atwater, the promise of Plasmonics. Scientific American. 2007;**296**:56-62. DOI: 10.1038/scientificamerican0407-56

[19] Farady M. The Bakerian Lecture: Experimental Relations of Gold (and Other Metals) to Light. Philosophical Transactions of the Royal Society. 1857;**147**:145-181. Bibliography code: 1857RSPT.147.145F

[20] Perrin JB. Nobel Lecture: Discontinuous Structure of Matter. Nobelprize.org. Nobel Media AB 2014. Web. Jan 17, 2018. Available from: http://www.nobelprize.org/nobel_prizes/physics/laureates/1926/perrin-lecture.html

[21] Sharma M, Pathak M, Roy B, Ojha H. Green synthesis of gold nanoparticles using *Cinnamomum verum*, *Syzygium aromaticum* and *Piper nigrum* extract. Asian Journal of Chemistry. 2017;**29**(8):1693-1696. DOI: 10.1007/BF03215599

[22] Ju-Nam Y, Lead JR. Manufactured nanoparticles: An overview of their chemistry, interactions and potential environmental implications. Science of the total environment. 2008;**400**(1):396-414. DOI: 10.1016/j.scitotenv.2008.06.042

[23] McConnell WP, Novak JP, Brousseau LC, Fuierer RR, Tenent RC, Feldheim DL. Electronic and optical properties of chemically modified metal nanoparticles and molecularly bridged nanoparticle arrays. The Journal of Physical Chemistry B. 2000;**104**(38): 8925-8930. DOI: 10.1021/jp000926t

[24] Collier CP, Saykally RJ, Shiang JJ, Henrichs SE, Heath JR. Reversible tuning of silver quantum dot monolayers through the metal-insulator transition. Science. 1997; **277**(5334):1978-1981. DOI: 10.1126/science.277.5334.1978

[25] De M, Ghosh PS, Rotello VM. Applications of nanoparticles in biology. Advanced Materials. 2008;**20**(22):4225-4241. DOI: 10.1002/adma.200703183

[26] Lu AH, Salabas EE, Schüth F. Magnetic nanoparticles: Synthesis, protection, functionalization, and application. Angewandte Chemie International Edition. 2007;**46**(8):1222-1244. DOI: 10.1002/anie.200602866

[27] Ghosh Chaudhuri R, Paria S. Core/shell nanoparticles: Classes, properties, synthesis mechanisms, characterization, and applications. Chemical Reviews. 2011;**112**(4):2373-2433. DOI: 10.1021/cr100449n

[28] Monteiro DR, Gorup LF, Takamiya AS, Ruvollo-Filho AC, de Camargo ER, Barbosa DB. The growing importance of materials that prevent microbial adhesion: Antimicrobial effect of medical devices containing silver. International Journal of Antimicrobial Agents. 2009;**34**(2):103-110. DOI: 10.1016/j.ijantimicag.2009.01.017

[29] Ahamed M, AlSalhi MS, Siddiqui MK. Silver nanoparticle applications and human health. Clinica Chimica Acta. 2010;**411**(23):1841-1848. DOI: 10.1016/j.cca.2010.08.016

[30] García-Barrasa J, López-de-luzuriaga JM, Monge M. Silver nanoparticles on zinc oxide thin film: An insight in fabrication and characterization. Central European Journal of Chemistry. 2011;**64**:9-17. DOI: 10.2478/s11532-010-0124-x

[31] Fabrega J, Luoma SN, Tyler CR, Galloway TS, Lead JR. Silver nanoparticles: Behaviour and effects in the aquatic environment. Environment International. 2011;**37**(2):517-531. DOI: 10.1016/j.envint.2010.10.012

[32] Dallas P, Sharma VK, Zboril R. Silver polymeric nanocomposites as advanced antimicrobial agents: Classification, synthetic paths, applications, and perspectives. Advances in Colloid and Interface Science. 2011;**166**(1):119-135. DOI: 10.1016/j.cis.2011.05.008

[33] Sharma VK, Yngard RA, Lin Y. Silver nanoparticles: Green synthesis and their antimicrobial activities. Advanced Colloidal Interface Science. 2009;**145**:83-96. DOI: 10.1016/j.cis.2008.09.002

[34] Gong HM, Zhou L, Su XR, Xiao S, Liu SD, Wang QQ. Illuminating dark plasmons of silver nanoantenna rings to enhance exciton–plasmon interactions. Advanced Functional Materials. 2009;**19**(2):298-303. DOI: 10.1002/adfm.200801151

[35] Krutyakov YA, Kudrinskiy AA, Olenin AY, Lisichkin GV. Synthesis and properties of silver nanoparticles: Advances and prospects. Russian Chemical Reviews. 2008;**77**(3): 233-257. DOI: 10.1070/RC2008v077n03ABEH003751

[36] West PR, Ishii S, Naik GV, Emani NK, Shalaev VM, Boltasseva A. Searching for better plasmonic devices. Laser & Photonics Reviews. 2000;**2010**:1-13. DOI: 10.1002/lpor.200900055

[37] Oulton RF. Surface plasmon lasers: Sources of nanoscopic light. Materials Today. 2012; **15**(1):26-34. DOI: 10.1016/S1369-7021(12)70018-4

[38] Sharma B, Frontiera RR, Henry AI, Ringe E, Van Duyne RP. SERS: Materials, applications, and the future. Materials Today. 2012;**15**(1):16-25. DOI: 10.1016/S1369-7021(12) 70017-2

[39] Wang P, Huang B, Dai Y, Whangbo MH. Plasmonic photocatalysts: Harvesting visible light with noble metal nanoparticles. Physical Chemistry Chemical Physics. 2012;**14**(28): 9813-9825. DOI: 10.1039/C2CP40823F

[40] Schultz S, Smith DR, Mock JJ, Schultz DA. Single-target molecule detection with nonbleaching multicolor optical immunolabels. Proceedings of the National Academy of Sciences. 2000;**97**(3):996-1001. DOI: 10.1073/pnas.97.3.996

[41] Schultz S, Mock J, Smith DR, Schultz DA. Nanoparticle based biological assays. Journal of Clinical Ligand Assay. 1999;**22**(2):214-216. scholars.duke.edu/display/pub798936

[42] Silva TJ, Schultz S, Weller D. Scanning near-field optical microscope for the imaging of magnetic domains in optically opaque materials. Applied Physics Letters. 1994;**65**(6): 658-660. DOI: 10.1063/1.112261

[43] Sqalli O, Bernal MP, Hoffmann P, Marquis-Weible F. Improved tip performance for scanning near-field optical microscopy by the attachment of a single gold nanoparticle. Applied Physics Letters. 2000;**76**(15):2134-2136. DOI: 10.1063/1.126277

[44] Mie G. Beiträge zur Optik trüber Medien, speziell kolloidaler Metallösungen. Annalen der Physik. 1908;**330**(3):377-445. DOI: 10.1002/andp.19083300302

[45] Sönnichsen C, Franzl T, Wilk T, von Plessen G, Feldmann J, Wilson OV, Mulvaney P. Drastic reduction of plasmon damping in gold nanorods. Physical Review Letters. 2002; **88**(7):077402. DOI: 10.1103/PhysRevLett.88.077402

[46] Valenti M, Dolat D, Biskos G, Schmidt-Ott A, Smith WA. Enhancement of the photoelectrochemical performance of $CuWO_4$ thin films for solar water splitting by plasmonic nanoparticle functionalization. The Journal of Physical Chemistry C. 2015;**119**(4):2096-2104. DOI: 10.1021/jp506349t

[47] Chen HM, Chen CK, Chen CJ, Cheng LC, Wu PC, Cheng BH, Ho YZ, Tseng ML, Hsu YY, Chan TS, Lee JF. Plasmon inducing effects for enhanced photoelectrochemical water splitting: X-ray absorption approach to electronic structures. ACS Nano. 2012;**6**(8):7362-7372. DOI: 10.1021/nn3024877

[48] Erwin WR, Zarick HF, Talbert EM, Bardhan R. Light trapping in mesoporous solar cells with plasmonic nanostructures. Energy & Environmental Science. 2016;**9**(5):1577-1601. DOI: 10.1039/C5EE03847B

[49] Piot A, Earl SK, Ng C, Dligatch S, Roberts A, Davis TJ, Gómez DE. Collective excitation of plasmonic hot-spots for enhanced hot charge carrier transfer in metal/semiconductor contacts. Nanoscale. 2015;**7**(18):8294-8298. DOI: 10.1039/C5NR01592H

[50] Li J, Cushing SK, Zheng P, Meng F, Chu D, Wu N. Plasmon-induced photonic and energy-transfer enhancement of solar water splitting by a hematite nanorod array. Nature Communications. 2013;**4**:2651. DOI: 10.1038/ncomms3651

[51] Linic S, Christopher P, Ingram DB. Plasmonic-metal nanostructures for efficient conversion of solar to chemical energy. Nature Materials. 2011;**10**(12):911-921. DOI: 10.1038/nmat3151

[52] Cushing SK, Wu N. Progress and perspectives of plasmon-enhanced solar energy conversion. The Journal of Physical Chemistry Letters. 2016;**7**(4):666-675. DOI: 10.1021/acs.jpclett.5b02393

[53] Haro M, Abargues R, Herraiz-Cardona I, Martínez-Pastor J, Giménez S. Plasmonic versus catalytic effect of gold nanoparticles on mesoporous TiO_2 electrodes for water splitting. Electrochimica Acta. 2014;**144**:64-70. DOI: 10.1016/j.electacta.2014.07.146

[54] Quinten M. Optical Properties of Nanoparticle Systems. Wiley-VCH Verlag GmbH & Co. KGaA; Weinheim, Germany, 2011. pp. 55-74. ISBN: 978-3-527-41043-9

[55] Pathak NK, Pandey GK, Ji A, Sharma RP. Study of light extinction and surface plasmon resonances of metal nanocluster: A comparison between coated and non-coated nanogeometry. Plasmonics. 2015;**10**(6):1597-1606. DOI: 10.1007/s11468-015-9978-2

[56] Huang X, El-Sayed IH, Qian W, El-Sayed MA. Cancer cell imaging and photothermal therapy in the near-infrared region by using gold nanorods. Journal of the American Chemical Society. 2006;**128**(6):2115-2120. DOI: 10.1021/ja057254a

[57] Kadkhodazadeh S, de Lasson JR, Beleggia M, Kneipp H, Wagner JB, Kneipp K. Scaling of the surface plasmon resonance in gold and silver dimers probed by EELS. The Journal of Physical Chemistry C. 2014;**118**(10):5478-5485. DOI: 1021 jp500288s

[58] Nordlander P, Oubre C, Prodan E, Li K, Stockman MI. Plasmon hybridization in nanoparticle dimers. Nano Letters. 2004;**4**(5):899-903. DOI: 10.1021/nl049681c

[59] Jain PK, Huang W, El-Sayed MA. On the universal scaling behavior of the distance decay of plasmon coupling in metal nanoparticle pairs: A plasmon ruler equation. Nano Letters. 2007;**7**(7):2080-2088. DOI: 10.1021/nl071008a

[60] Quinten M, Leitner A, Krenn JR, Aussenegg FR. Electromagnetic energy transport via linear chains of silver nanoparticles. Optics Letters. 1998;**23**(17):1331-1333. DOI: 10.1364/OL.23.001331

[61] Stiles PL, Dieringer JA, Shah NC, Van Duyne RP. Surface-enhanced Raman spectroscopy. Annual Review of Analytical Chemistry. 2008;**1**:601-626. DOI: 10.1146/annurev.anchem.1.031207.112814

[62] Belkin M, Chao SH, Jonsson MP, Dekker C, Aksimentiev A. Plasmonic nanopores for trapping, controlling displacement, and sequencing of DNA. ACS Nano. 2015;**9**(11):10598-10611. DOI: 10.1021/acsnano.5b0417

[63] Zhang L, Herrmann LO, Baumberg JJ. Size dependent plasmonic effect on $BiVO_4$ photoanodes for solar water splitting. Scientific Reports. 2015;**5**:16660. DOI: 10.1038/srep16660

[64] Callahan DM, Munday JN, Atwater HA. Solar cell light trapping beyond the ray optic limit. Nano letters. 2012;**12**(1):214-218. DOI: 10.1021/nl203351k

[65] Kelly KL, Coronado E, Zhao LL, Schatz GC. The optical properties of metal nanoparticles: The influence of size, shape, and dielectric environment. Journal of Physical Chemistry B. 2002;**107**:668-677. DOI: 10.1021/jp026731y

[66] Atwater HA, Polman A. Plasmonics for improved photovoltaic devices. Nature Materials. 2010;**9**(3):205-213. DOI: 10.1038/nmat2629

[67] Mtangi W, Tassinari F, Vankayala K, Vargas Jentzsch A, Adelizzi B, Palmans AR, Fontanesi C, Meijer EW, Naaman R. Control of electrons' spin eliminates hydrogen peroxide formation during water splitting. Journal of the American Chemical Society. 2017;**139**(7):2794-2798. DOI: 10.1021/jacs.6b12971

[68] Valenti M, Jonsson MP, Biskos G, Schmidt-Otta A, Smith WA. Plasmonic nanoparticle – semiconductor composites for efficient solar water splitting. Journal of Materials Chemistry A. 2016;**4**:17891-17912. DOI: 10.1039/c6ta06405a

[69] Rauwel P, Rauwel E, Ferdov S, Singh MP. Chapter 1: Silver Nanoparticles: Synthesis, Properties, and Applications in the book Advances in Materials Science and Engineering. 2015. pp. 624394 (2 pages). DOI: 10.1155/2015/624394

[70] Jin R, Cao Y, Mirkin CA, Kelly KL, Schatz GC, Zheng JG. Photoinduced conversion of silver nanospheres to nanoprisms. Science. 2001;**294**(5548):1901-1903. DOI: 10.1126/science.1066541

[71] Jin R, Cao YC, Hao E, Metraux GS, Schatz GC, Mirkin CA. Controlling anisotropic nanoparticle growth through plasmon excitation. Nature. 2003;**425**:487-490. DOI: 10.1038/nature02020

[72] Hao E, Kelly KL, Hupp JT, Schatz GC. Synthesis of silver nanodisks using polystyrene mesospheres as templates. Journal of the American Chemical Society. 2002;**124**(51):15182-15183. DOI: 10.1021/ja028336r

[73] Pastoriza-Santos I, Liz-Marzon LM. Synthesis of silver nanoprisms in DMF. Nano Letters. 2002;**2**:903-905. DOI: 10.1021/nl025638i

[74] Wang L, Chen X, Zhan J, Chai Y, Yang C, Xu L, Zhuang W, Jing B. Synthesis of gold nano-and microplates in hexagonal liquid crystals. The Journal of Physical Chemistry B. 2005;**109**(8):3189-3194. DOI: 10.1021/jp0449152

[75] Kim JU, Cha SH, Shin K, Jho JY, Lee JC. Preparation of gold nanowires and nanosheets in bulk block copolymer phases under mild conditions. Advanced Materials. 2004;**16**(5):459-464. DOI: 10.1002/adma.200305613

[76] Shao Y, Jin Y, Dong S. Synthesis of gold nanoplates by aspartate reduction of gold chloride. Chemical Communications. 2004;**9**:1104-1105. DOI: 10.1039/B315732F

[77] Sarma TK, Chattopadhyay A. Starch-mediated shape-selective synthesis of au nanoparticles with tunable longitudinal plasmon resonance. Langmuir. 2004;**20**(9):3520-3524. DOI: 10.1021/la049970g

[78] Pal T, Maity DS, Ganguly A. Use of a silver-gelatin complex for the determination of micro-amounts of hydrazine in water. The Analyst. 1986;**111**(12):1413-1415. DOI: 10.1039/AN9861101413

[79] Link S, Wang ZL, El-Sayed MA. Alloy formation of gold-silver nanoparticles and the dependence of the plasmon absorption on their composition. The Journal of Physical Chemistry B. 1999;**103**(18):3529-3533. DOI: 10.1021/jp990387w

[80] Pastoriza-Santos I, Liz-Marzán LM. Formation of PVP-protected metal nanoparticles in DMF. Langmuir. 2002;**18**(7):2888-2894. DOI: 10.1021/la015578g

[81] Fievet F, Lagier JP, Figlarz M. Preparing monodisperse metal powders in micrometer and submicrometer sizes by the polyol process. MRS Bulletin. 1989;**12**:29-34. DOI: 10.1557/S0883769400060930

[82] Yamamoto T, Wada Y, Sakata T, Mori H, Goto M, Hibino S, Yanagida S. Microwave-assisted preparation of silver nanoparticles. Chemistry Letters. 2004;**33**(2):158-159. DOI: 10.1246/cl.2004.158

[83] Chou KS, Ren CY. Synthesis of nanosized silver particles by chemical reduction method. Materials Chemistry and Physics. 2000;**64**(3):241-246. DOI: 10.1016/S0254-0584(00)00223-6

[84] Chen SF, Zhang H. Aggregation kinetics of nanosilver in different water conditions. Advances in Natural Sciences: Nanoscience and Nanotechnology. 2012;**3**(3):035006. DOI: 10.1088/2043-6262/3/3/035006/meta

[85] Dang TM, Le TT, Fribourg-Blanc E, Dang MC. Influence of surfactant on the preparation of silver nanoparticles by polyol method. Advances in Natural Sciences: Nanoscience and Nanotechnology. 2012;**3**(3):035004. DOI: 10.1088/2043-6262/3/3/035004/meta

[86] Patil RS, Kokate MR, Jambhale CL, Pawar SM, Han SH, Kolekar SS. One-pot synthesis of PVA-capped silver nanoparticles their characterization and biomedical application. Advances in Natural Sciences: Nanoscience and Nanotechnology. 2012;**3**(1):015013. DOI: 10.1088/2043-6262/3/1/015013/meta

[87] Henglein A. Physicochemical properties of small metal particles in solution: "microelectrode" reactions, chemisorption, composite metal particles, and the atom-to-metal transition. The Journal of Physical Chemistry. 1993;**97**(21):5457-5471. DOI: 10.1021/j100123a004

[88] Pastoriza-Santos I, Liz-Marzán LM. Synthesis of silver nanoprisms in DMF. Nano Letters. 2002;**2**(8):903-905. DOI: 10.1021/nl025638i

[89] Lu W, Liao F, Luo Y, Chang G, Sun X. Hydrothermal synthesis of well-stable silver nanoparticles and their application for enzymeless hydrogen peroxide detection. Electrochimica Acta. 2011;**56**(5):2295-2298. DOI: 10.1016/j.electacta.2010.11.053

[90] Lee DK, Kang YS. Synthesis of silver nanocrystallites by a new thermal decomposition method and their characterization. ETRI Journal. 2004;**26**(3):252-256. DOI: HJTODO_2004_v26n3_252

[91] Jung JH, Oh HC, Noh HS, Ji JH, Kim SS. Metal nanoparticle generation using a small ceramic heater with a local heating area. Journal of Aerosol Science. 2006;**37**(12):1662-1670. DOI: 10.1016/j.jaerosci.2006.09.002

[92] Tien DC, Tseng KH, Liao CY, Huang JC, Tsung TT. Discovery of ionic silver in silver nanoparticle suspension fabricated by arc discharge method. Journal of Alloys and Compounds. 2008;**463**(1):408-411. DOI: 10.1016/j.jallcom.2007.09.048

[93] Siegel J, Kvítek O, Ulbrich P, Kolská Z, Slepička P and Švorčík V. Progressive approach for metal nanoparticle synthesis. Materials Letters. 2012;**89**:47-50. DOI: 10.1016/j.matlet.2012.08.048

[94] Sakamoto M, Fujistuka M, Majima T. Light as a construction tool of metal nanoparticles: Synthesis and mechanism. Journal of Photochemistry and Photobiology C: Photochemistry Reviews. 2009;**10**(1):33-56. DOI: 10.1016/j.jphotochemrev.2008.11.002

[95] Christy AJ, Umadevi M. Synthesis and characterization of monodispersed silver nanoparticles. Advances in Natural Sciences: Nanoscience and Nanotechnology. 2012; **3**(3):035013. DOI: 10.1088/2043-6262/3/3/035013/meta

[96] Sato-Berrú R, Redón R, Vázquez-Olmos A, Saniger JM. Silver nanoparticles synthesized by direct photoreduction of metal salts. Application in surface-enhanced Raman spectroscopy. Journal of Raman Spectroscopy. 2009;**40**(4):376-380. DOI: 10.1002/jrs.2135

[97] Ghosh SK, Kundu S, Mandal M, Nath S, Pal T. Studies on the evolution of silver nanoparticles in micelle by UV-photoactivation. Journal of Nanoparticle Research. 2003; **5**(5–6):577-587. DOI: 10.1023/B:NANO.0000006100.25744.fa

[98] Huang L, Zhai ML, Long DW, Peng J, Xu L, Wu GZ, Li JQ, Wei GS. UV-induced synthesis, characterization and formation mechanism of silver nanoparticles in alkalic carboxymethylated chitosan solution. Journal of Nanoparticle Research. 2008;**10**(7): 1193-1202. DOI: 10.1007/s11051-007-9353-0

[99] Sakamoto M, Fujistuka M, Majima T. Light as a construction tool of metal nanoparticles: Synthesis and mechanism. Journal of Photochemistry and Photobiology C: Photochemistry Reviews 2009;**10**(1):33-56. DOI: 10.1016/j.jphotochemrev.2008.11.002

[100] Tang B, Sun L, Li JL, Zhang M, Wang X. Sunlight-driven synthesis of anisotropic silver nanoparticles. Chemical Engineering Journal. 2015;**260**:99-106. DOI: 10.1016/j.cej.2014.08.044

[101] Chouhan N, Ameta R, Meena RK. Biogenic silver nanoparticles from Trachyspermum ammi (Ajwain) seeds extract for catalytic reduction of p-nitrophenol to p-aminophenol in excess of $NaBH_4$. Journal of Molecular Liquids. 2017;**230**:74-84. DOI: 10.1016/j.molliq.2017.01.003

[102] Roy N, Gaur A, Jain A, Bhattacharya S, Rani V. Green synthesis of silver nanoparticles: An approach to overcome toxicity. Environmental Toxicology and Pharmacology. 2013; **36**(3):807-812. DOI: 10.1016/j.etap.2013.07.005

[103] Thakkar KN, Mhatre SS, Parikh RY. Biological synthesis of metallic nanoparticles. Nanomedicine: Nanotechnology, Biology and Medicine. 2010;**6**(2):257-262. DOI: 10.1016/j.nano.2009.07.002

[104] Scherrer P. Bestimmung der Größe und der inneren Struktur von Kolloidteilchen mittels Röntgenstrahlen. Nachrichten von der Gesellschaft der Wissenschaften zu Göttingen. Mathematisch-Physikalische Klasse. 1918;**1918**:98-100. DOI: eudml.org/doc/59018

[105] Wiley B, Sun YG, Xia YN. Synthesis of silver nanostructures with controlled shapes and properties. Accounts of Chemical Research. 2007;**40**:1067-1076. DOI: 10.1021/ar7000974

[106] Liang H. Rossouw D, Zhao H, Cushing SK, Shi H, Korinek A, Xu H, Rosei F, Wang W, Wu N, Botton GA, Ma D. Asymmetric silver "Nanocarrot" structures: Solution synthesis and their asymmetric plasmonic resonances. Journal of the American Chemical Society. 2013;**135**:9616-9619. DOI: 10.1021/ja404345s

[107] Miles MJ, Master T. Mc, HJ, Lambert N, Scanning tunneling microscopy of biomolecules. Journal of Vacuum Science & Technology A: Vacuum Surfaces and Films. 1990;**8**(1):698-702. DOI: 10.1116/1.576986

[108] Chi L, Röthig C. Scanning probe microscopy of nanoclusters. In: Wang ZL, editor. Characterization of Nanophase Materials. Weinheim, Germany: Wiley-VCH, Verlag GmbH; 2000:133-163. DOI: 10.1002/3527600094.ch5

[109] Gmoshinski IV, Khotimchenko SA, Popov VO, Dzantiev BB, Zherdev AV, Demin VF, Buzulukov YP. Nanomaterials and nanotechnologies: Methods of analysis and control. Russian Chemical Reviews. 2013;**82**(1):48. DOI: 10.1070/RC2013v082n01ABEH004329/meta

[110] Tiede K, Boxall ABA, Tear SP, Lewis J, David H, Hassellöv M. Detection and characterization of engineered nanoparticles in food and the environment. Food Additives & Contaminants: Part A. 2008;**25**:795-821. DOI: 10.1080/02652030802007553

[111] Schmidt FP, Ditlbacher H, Hohenester U, Hohenau A, Hofer F, Krenn JR. Universal dispersion of surface plasmons in flat nanostructures. Nature Communications. 2014;**5**: 3604. DOI: 10.1038/ncomms4604

[112] Nicoletti O, de La Peña F, Leary RK, Holland DJ, Ducati C, Midgley PA. Three-dimensional imaging of localized surface plasmon resonances of metal nanoparticles. Nature. 2013;**502**(7469):80-84. DOI: 10.1038/nature12469

[113] Schmidt FP, Ditlbacher H, Hohenester U, Hohenau A, Hofer F, Krenn JR. Dark plasmonic breathing modes in silver nanodisks. Nano Letters. 2012;**12**(11):5780-5783. DOI: 10.1021/nl3030938

[114] Guiton BS, Iberi V, Li S, Leonard DN, Parish CM, Kotula PG, Varela M, Schatz GC, Pennycook SJ, Jon P. Camden correlated optical measurements and plasmon mapping of silver nanorods. Nano Letters. 2011;**11**(8):3482-3488. DOI: 10.1021/nl202027h

[115] Mock JJ, Barbic M, Smith DR, Schultz DA, Schultz S. Shape effects in plasmon resonance of individualcolloidal silver nanoparticles. The Journal of Chemical Physics. 2002; **116**(15):6755-6759. DOI: 10.1063/1.1462610

[116] Baia L, Simon S. UV-VIS and TEM assessment of morphological features of silver nanoparticles from phosphate glass matrices. In: Méndez-Vilas A, Díaz J, editors. Modern Research and Educational Topics in Microscopy. 2007:576-583. DOI: 10.1.1.605.2338

[117] Seney CS, Gutzman BM, Goddard RH. Correlation of size and surface-enhanced Raman scattering activity of optical and spectroscopic properties for silver nanoparticles. The Journal of Physical Chemistry C. 2008;**113**(1):74-80. DOI: 10.1021/jp805698e

[118] Liang H, Li Z, Wang Z, Wang W, Rosei F, Ma D, Xu H. Enormous surface-enhanced raman scattering from dimers of flower-like silver mesoparticles. Small. 2012;**8**(22):3400-3405. DOI: 10.1002/smll.201201081

[119] Butun S, Sahiner N. A versatile hydrogel template for metal nano particle preparation and their use in catalysis. Polymer. 2011;**52**(21):4834-4840. DOI: 10.1016/j.polymer.2011.08.021

[120] Harish S, Sabarinathan R, Joseph J, Phani KL. Role of pH in the synthesis of 3-aminopropyl trimethoxysilane stabilized colloidal gold/silver and their alloy sols and their application to catalysis. Materials Chemistry and Physics. 2011;**127**(1):203-207. DOI: 10.1016/j.matchemphys.2011.01.060

[121] Cao Y, Li D, Jiang F, Yang Y, Huang Z. Engineering metal nanostructure for SERS application. Journal of Nanomaterials. 2013;**2013**:01-12. DOI: 10.1155/2013/123812

[122] Botta R, Upender G, Sathyavathi R, Rao DN, Bansal C. Silver nanoclusters films for single molecule detection using surface enhanced Raman scattering (SERS). Materials Chemistry and Physics. 2013;**137**(3):699-703. DOI: 10.1016/j.matchemphys.2012.10.022

[123] Zhu SQ, Zhang T, Guo XL, Wang QL, Liu X, Zhang XY. Gold nanoparticle thin films fabricated by electrophoretic deposition method for highly sensitive SERS application. Nanoscale Research Letters. 2012;**7**(1):613. DOI: 10.1186/1556-276X-7-613

[124] Rauwel P, Rauwel E, Ferdov S, Singh MP. Silver nanoparticles: Synthesis, properties, and applications. Advances in Materials Science and Engineering. 2015;**2015**:624394 (2 p). DOI: 10.1155/2015/624394

[125] Zhang T, Song YJ, Zhang XY, Wu JY. Synthesis of silver nanostructures by multistep methods. Sensors. 2014;**14**:5860-5889. DOI: 10.3390/s140405860

[126] Fauss E. The Silver Nanotechnology Commercial Inventory. Charlottesville, VA: University of Virginia; 2008. Available from: http://www.nanoproject.org

[127] Alivisatos P. The use of nanocrystals in biological detection. Nature Biotechnology. 2004; **22**(1):47-52. DOI: 10.1038/nbt927

[128] Hong Y, Huh YM, Yoon DS, Yang J. Nanobiosensors based on localized surface plasmon resonance for biomarker detection. Journal of Nanomaterials. 2012;**2012**:111. DOI: 10.1155/2012/759830

[129] Tripp RA, Dluhy RA, Zhao Y. Novel nanostructures for SERS biosensing. Nano Today. 2008;**3**(3):31-37. DOI: 10.1016/S1748-0132(08)70042-2

[130] Samanta A, Maiti KK, Soh KS, Liao X, Vendrell M, Dinish US, Yun SW, Bhuvaneswari R, Kim H, Rautela S, Chung J. Ultrasensitive near-infrared Raman reporters for SERS-based in vivo cancer detection. Angewandte Chemie International Edition. 2011;**50**(27):6089-6092. DOI: 10.1002/anie.201007841

[131] Kumar A, Boruah BM, Liang XJ. Gold nanoparticles: Promising nanomaterials for the diagnosis of cancer and HIV/AIDS. Journal of Nanomaterials. 2011;**2011**:22. DOI: 10.1155/2011/202187

[132] Atwater HA. The promise of plasmonics. Scientific American. 2007;**296**(4):56-62. DOI: 10.1038/scientificamerican0407-56

[133] Brennan SA, Ní Fhoghlú C, Devitt BM, O'Mahony FJ, Brabazon D, Walsh A. Silver nanoparticles and their orthopaedic applications. Bone & Joint Journal. 2015;**97-B**:582-589. DOI: 10.1302/0301-620X.97B5.33336

[134] ZhiLiang J, Yuan C, AiHui L, HuiLin T, NingLi T, FuXin Z. Silver nanoparticle labeled immunoresonance scattering spectral assay for trace fibrinogen. Science in China Series B. 2007;**50**:345-350. DOI: 10.1007/s11426-007-0064-2

[135] Dong XY, Gao ZW, Yang KF, Zhang WQ, Xu LW. Nanosilver as a new generation of silver catalysts in organic transformations for efficient synthesis of fine chemicals. Catalysis Science & Technology. 2015;**5**(5):2554-2574. DOI: 10.1039/C5CY00285K

[136] Chouhan N, Ameta R, Meena RK. Biogenic silver nanoparticles from Trachyspermum ammi (Ajwain) seeds extract for catalytic reduction of p-nitrophenol to p-aminophenol in excess of $NaBH_4$. Journal of Molecular Liquids. 2017;**230**:74-84. DOI: 10.1016/j.molliq.2017.01.003

[137] Bhosale MA, Bhanage BM. Silver nanoparticles: Synthesis, characterization and their application as a sustainable catalyst for organic transformations. Current Organic Chemistry. 2015;**19**(8):708-727. DOI: 10.2174/1385272819666150207001154

[138] Yoon KY, Byeon JH, Park CW, Hwang J. Antimicrobial effect of silver particles on bacterial contamination of activated carbon fibers. Environmental Science & Technology. 2008;**42**(4):1251-1255. DOI: 10.1021/es0720199

[139] Hongyin Z. Application of Silver Nanoparticles in Drinking Water Purification. 2013. Open Access Dissertations. Paper 29. DOI: http://digitalcommons.uri.edu/oa_diss/29

[140] Rai M, Birla S, Ingle A, et al. Nanosilver: An inorganic nanoparticle with myriad potential applications. Nanotechnology Reviews. 2014;**3**(3):281-309. DOI: 10.1515/ntrev-2014-0001

[141] Holladay RJ. Toothpaste or tooth gel containing silver nanoparticles coated with silver oxide. US 20130017236 A1

[142] Ha TH, Jeong JY, Jung BH, Kim JK, Lim YT, Cosmetic pigment composition containing gold or silver nano-particles. WO 2007011103 A1

[143] Zhao Z, Zhang B, Lin K. Nano-silver antibacterial liquid soap and preparation method thereof. CN102860923 B

[144] Nia JR. Nanosilver for preservation and treatment of diseases in agriculture field. US 0075818 A1

[145] Zhang G, Liu Y, Gao X, Chen Y. Synthesis of silver nanoparticles and antibacterial property of silk fabrics treated by silver nanoparticles. Nanoscale Research Letters. 2014;**9**:216-223. DOI: 10.1186/1556-276X-9-216

[146] Montazer M, Hajimirzababa H, Rahimi MK, Alibakhshi S. Durable anti-bacterial nylon carpet using colloidal nano silver. Fibres & Textiles in Eastern Europe. 2012;**4**(93):96-101. DOI: http://www.fibtex.lodz.pl/article757.html

[147] Nel A, Xia T, Mädler L, Li N. Toxic potential of materials at the nanolevel. Science. 2006; **311**(5761):622-627. DOI: 10.1126/science.1114397

[148] Levard C, Hotze EM, Lowry GV, Brown Jr GE. Environmental transformations of silver nanoparticles: Impact on stability and toxicity. Environmental Science & Technology. 2012;**46**(13):6900-6914. DOI: 10.1021/es2037405

[149] Wu K, Chen J, McBride JR, Lian T. Efficient hot-electron transfer by a plasmon-induced interfacial charge-transfer transition. Science. 2015;**349**:632-635. DOI: 10.1126/science.aac5443

[150] Kumarasinghe CS, Premaratne M, Bao Q, Agrawal GP. Theoretical analysis of hot electron dynamics in nanorods. Scientific Reports. 2015;**5**:12140. DOI: 10.1038/srep12140

[151] Harutyunyan H, Martinson AB, Rosenmann D, et al. Anomalous ultrafast dynamics of hot plasmonic electrons in nanostructures with hot spots. Nature Nanotechnology. 2015; **10**:770-774. DOI: 10.1038/nnano.2015.165

[152] Saavedra JR, Asenjo-Garcia A, García de Abajo FJ. Hot-electron dynamics and thermalization in small metallic nanoparticles. ACS Photonics. 2016;**3**(9):1637-1646. DOI: 10.1021/acsphotonics.6b00217

[153] Méjard R, Verdy A, Petit M, Bouhelier A, Cluzel B, Demichel O. Energy-resolved hot-carrier relaxation dynamics in monocrystalline plasmonic nanoantennas. ACS Photonics. 2016;**3**(8):1482-1488. DOI: 10.1021/acsphotonics.6b00033

Chapter 3

Synthesis and Optical Properties of Highly Stabilized Peptide-Coated Silver Nanoparticles

Parvathalu Kalakonda and Sreenivas Banne

Additional information is available at the end of the chapter

http://dx.doi.org/10.5772/intechopen.76829

Abstract

The interaction between the silver nanoparticle and peptide surfaces has been of increased interest for the applications of bionanotechnology and tissue engineering. In order to completely understand such interactions, we have examined the optical properties of peptide-coated silver nanoparticles. However, the effect of peptide binding motif upon the silver nanoparticles surface characteristics and physicochemical properties of these nanoparticles remains incompletely understood. Here, we have fabricated sodium citrate stabilized silver nanoparticles and coated with peptide IVD (ID_3). The optical properties of these peptide-capped nanomaterials were characterized by UV-visible, transmission electron microscopy (TEM), and z-potential measurement. The results indicate that the interface of silver nanoparticles (AgNP)-peptide is generated using ID_3 peptide and suggested that the reactivity of peptide is governed by the conformation of the bound peptide on the silver nanoparticle surface. The interactions of peptide-nanoparticle would potentially be used to fabricate specific functionality into the various peptide-capped nanomaterials and antibacterial applications.

Keywords: silver nanoparticles, peptide, Z-potential, physicochemical properties

1. Introduction

Over the last few years, the fabrication and synthesis of stable silver nanoparticles are the most leading active areas of research in the field of bionanotechnology due to their wide range of applications in areas such as biosensing, biotechnology, biolabeling, biomedical, and antibacterial applications [1–8]. The properties of nanoparticles would be modified by capping certain functional groups to change their biocompatibility and stability in many biological

systems [9, 10]. The major challenge is maintaining the size control and distribution of these particles into the biological environment. The nanoparticles' size plays a very important role and it should be of a suitable size between 20 and 100 nm to avoid the negative charge and renal clearance [11]. The physical and chemical properties of nanoparticles can be changed rapidly by the adsorption of proteins which enable them to help cellular internalization [12]. In addition, opsonization can result in an undesired cellular uptake, nanoparticle aggregation, and an immune system response [13].

The available methods for creating "stealth" nanoparticles that resist nonspecific protein adsorption include surface modification by polyethylene glycol (PEG) [14], polysaccharides [15], mixed charge self-assembly [16], and polymers [17, 18]. An attractive way for stealth coatings is to study the use of natural materials such as peptides: they are biocompatible, biodegradable, well-studied, non-immunogenic, and multifunctional materials [19]. Over the last few years, antibacterial peptides have become huge interesting diagnosis tools for improving new techniques for the production of novel antibiotics in the treatment of human infections [20]. The antimicrobial activity of AgNP nanoparticles has been communicated extensively in the area of killing Gram-negative and Gram-positive bacteria [21, 22]. Silver nanoparticles are more toxic element to microorganism compared to other metals and they exhibit slow toxicity into cells. They have an advantage of lower propensity to induce microbial resistance [23, 24]. The protein-coated nanoparticles have been well studied to fabricate stable systems in buffered saline systems (PBS) [25, 26]. However, by improving the nanoparticles stability in complex fluids, we can use as undiluted human serum is very challenging than in buffered saline solution due to the presence of huge proteins. And also, the interactions between peptides and peptide-bound nanoparticles were not yet well studied. It is very important to investigate nanoparticles properties in complex fluids before performing in vivo experiments. Developing peptide-coated-AgNP materials that are stable in complex fluids increases in vivo applications. In addition to possessing stealth properties, it is very useful to incorporate specific interactions of peptide with nanoparticles for biomedical technology applications. The peptide sequences have a particular molecular recognition for receptors on various cell types. However, additional conjugation steps are important to change peptide targeting sequences onto stealth particles which contain synthetic polymers such as PEG [27, 28]. Peptide capping offers many advantages due to their sequence and can be applied off for the existing peptide sequence [29, 30]. Combining the s-peptide sequence with a targeting moiety leads to specific interactions with maintaining a low fouling background, and the complex fluids increase the stability of nanoparticles by peptide coating.

In this work, we have examined a synthetic peptide of IVD (ID3) [31]. The sequence mimics is important and the surfaces of proteins have adapted to avoid nonspecific adsorption. This leads to improve the stability of nanoparticles in complex fluids. Here, charge neutrality is balanced by leaving the N-terminus amine which is free ion, and it contributes to an extra positive charge to the peptide. The peptide sequence was attached to nanoparticles such as AgNP through a surface anchoring via covalent bonding. The zeta potential and optical spectroscopy (UV-visible) results indicate that peptide-anchored silver nanoparticles show high stability in complex fluids. The functional peptide always contains biomolecular recognition. Moreover, the advantages of this system are easily fabricated in a one-step process by mixing silver nanoparticles and self-assembling peptides.

http://dx.doi.org/10.5772/intechopen.76829

2. Experimental section

2.1. Materials and methods

Peptide (ID_3) with confirmed amino acid analysis was purchased from the American Peptide Company. Silver nitrate ($AgNO_3$) and citric acid tri-sodium salt dehydrate were purchased from Fisher Scientific (Waltham, MA). The peptide content varied between 70 and 85%, and the ID_3 peptide was acetylated at the N-terminus. All solvents were purchased from Sigma-Aldrich Co.

2.1.1. Synthesis

Silver nanoparticles were synthesized by reduction method. Hundred milligrams of silver nitrate was dissolved in 500 ml of aqueous solution. It was vigorously stirred and heated to a steaming point. To synthesize about 20–30-nm diameter AgNPs, 10–15-mL solution of sodium citrate was quickly added while steaming the AgNP solution. The solution was heated for another 10–15 min, and the final solution was allowed to cool naturally to room temperature (shown in **Figure 1**).

2.1.2. Peptide-coated AgNPs

Peptide-anchored silver nanoparticles were prepared by mixing citrated-capped AgNP with 0.5-mM peptide concentration in aqueous solution. The solution was stirred for about 10 min, and the self-assembled process was made for 20 h to get a uniform coating.

2.1.3. Characterization of silver nanoparticles

UV-visible absorption spectra were recorded at room temperature from 300 to 800 nm range. Fluorescence emission spectra were collected using a Horiba Fluoromax-4 spectrofluorometer. The chemical compositions of AgNPs solution were collected using a Fourier transform infrared spectroscopy ranging from 4000 to 400 cm^{-1}. The silver nanoparticles size and morphology of particles were determined by TEM using a Tecnai G2 F20. Samples were prepared by evaporating a 10-μL solution of AgNPs onto carbon-supported copper grids. For the determination of particle size, 300 particles were counted from multiple pictures from different areas of the TEM grid using Image J software analysis. The zeta potential of the particles was

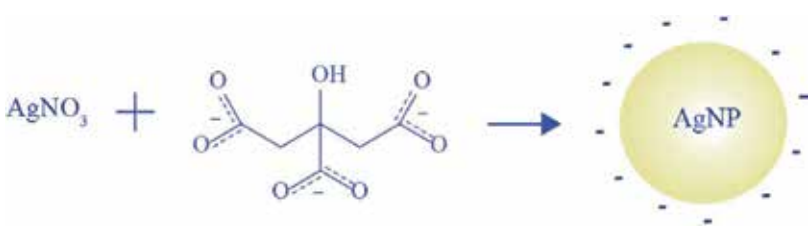

Figure 1. Schematic of silver nanoparticles (AgNPs) synthesis.

analyzed by using the Zetasizer Nano-ZS device. The measurements were carried out at room temperature at 25°C in aqueous solution. The zeta potential was calculated from the electrophoretic mobility based on the Smoluchowski theory.

3. Results and discussion

The peptide-capped-AgNPs size was analyzed by transmission electron microscopy (TEM) (**Figure 2**). The diameter and size distribution of the AgNPs were measured using TEM image analysis software and verified by image J software. The diameter of the silver nanoparticles was approximately observed to be 27 ± 2.0 nm (**Figure 2**), and it was measured by statistical analysis. The images of nanoparticles are shown in **Figure 2(a)–(c)** and peptide-anchored AgNPs images are also shown in **Figure 3(a)** and **(b)**. The peptide anchoring does not influence the size of silver nanoparticles. On the basis of the HR-TEM images, and the constant silver core diameter, it is evident that peptide-anchored-AgNPs remain mono-disperse even after peptide-anchoring process (**Figure 3**).

The HR-TEM image (**Figures 2** and **3**) of AgNPs showed that the fringe spacing of AgNP was 2.4 Å, which corresponded to the spacing between the plane of face-centered cubic (fcc) silver. The selected area of the diffraction pattern (SEAD) of silver nanoprism (**Figure 2(d)**) indicated that the entire nanoparticle was a single crystalline structure [32–34]. The SEAD pattern was

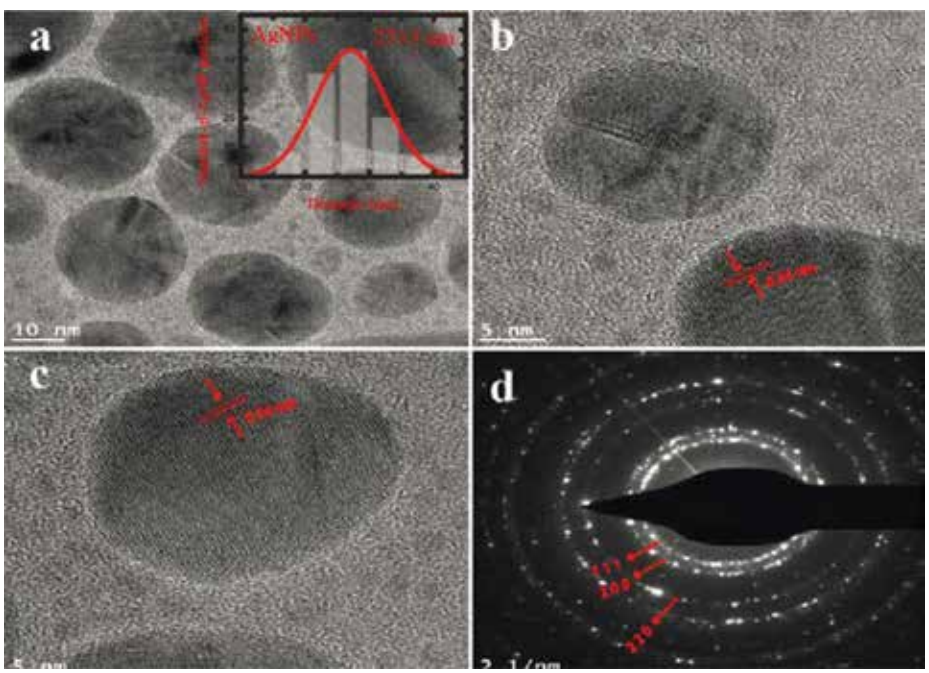

Figure 2. The TEM images of silver nanoparticles dispersion (a–c) and a selected area of the diffraction pattern of gold nanoparticles (d), and the insert shows the diameter distribution of AgNPs (a).

http://dx.doi.org/10.5772/intechopen.76829

indexed according to planes of (111) and (200) reflection, and the crystal structure of silver is FCC on the basis of the d-spacing 2.4 and 2.04 Å. The d-spacing was also calculated from diffraction pattern. The HR-TEM image of peptide-anchored AgNPs showed (**Figure 3**) that the nano-thin layer of peptide anchoring was observed.

The FTIR spectra of citrate-stabilized AgNPs were performed to know the anchoring molecules present on the surface of AgNPs (**Figure 4**). FTIR spectrum shows absorption bands at 3350, 2914, 2855, 2354, 1740, 1632, 1455, 1377, 1242, and 1040 cm^{-1} and indicating the presence of anchoring agent on the AgNPs surface. The bands at 3350 cm^{-1} in the spectra indicate an O–H stretching vibration in the presence of alcohol. The bands at 2914 and 2855 cm^{-1} regions arising from C–H stretching of the aromatic groups were found. The band at 1740 cm^{-1} was assigned to the C–C band stretching. The band at 1632 cm^{-1} in the spectra indicates C–C and C–N stretching in the presence of proteins [35]. The band at 1455 cm^{-1} was indicated for N–H stretch vibration in the presence of amide linkages of peptides. These functional groups have

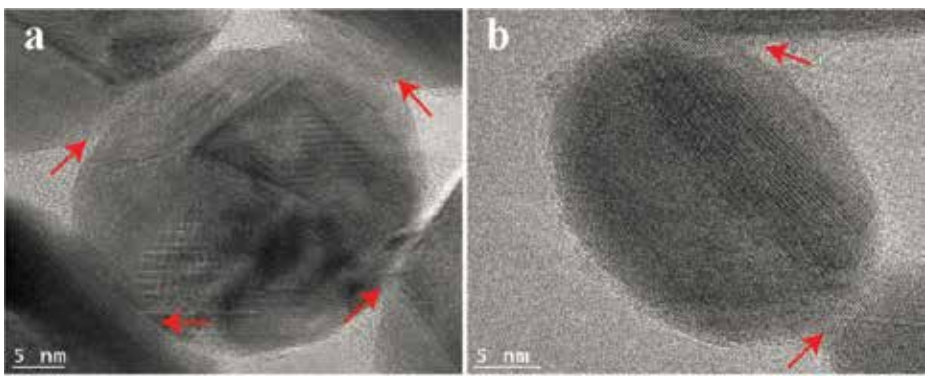

Figure 3. HR-TEM image of peptide-coated AgNPs.

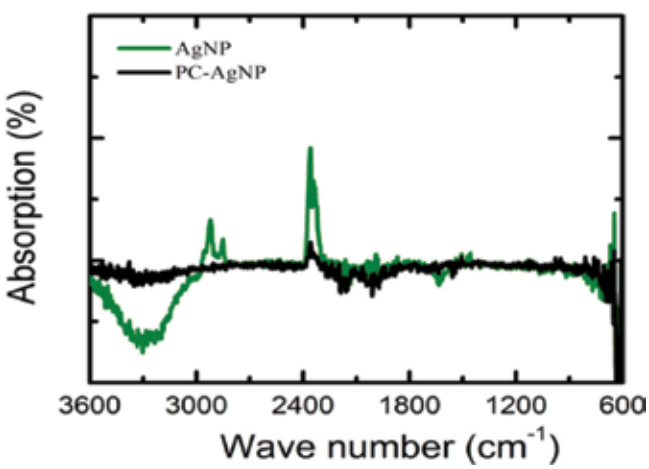

Figure 4. FTIR spectra of silver nanoparticles.

an important role in stability and anchoring of AgNP as reported in the previous studies [35]. The bands at 1455 and 1040 cm^{-1} were assigned for N–H and C–N stretch vibration of the proteins, respectively. The peptide-anchored AgNP particles spectra were also collected by using FTIR and observed that the peaks were suppressed. It may be due to a thin nano-layer anchoring covered on the nanoparticles surface.

The citrated-AgNPs show a Plasmon band at 529 nm (**Figure 5(a)**) with the help of UV-visible spectra. The particle diameter and size can also be identified from the concentration of silver nanoparticles solution [36–38]. The surface Plasmon absorption spectrum of AgNPs as the function of concentration is shown in **Figure 5(a)**. The intensity of absorption spectra increases as increasing the AgNP concentration. The trend was consistent with the changes indicating the surface of Plasmon band of AgNPs. For peptide (ID_3)-anchored AgNPs, the Plasmon band absorbance shifts to a higher wavelength of 404-nm region (**Figure 5(b)**).

The hydrodynamic diameter of peptide-anchored-AgNPs was measured by Zetasizer as 27 ± 2 nm. Zeta potential measurements indicate that the charge of the Cit-AgNP is −40 ± 2 mV (**Figure 6**) in a water medium and the charge of peptide-anchored-AgNPs is −13 ± 1 mV. The differences of charge are observed between citrated-AgNPs and PC-AgNPs in UV-visible region, and TEM and zeta potential measurements show evidence that the peptide is effectively anchored on the surface of AgNPs. The shift to a higher Plasmon band and the hydrodynamic diameter size increase by about 1–2 nm after the addition of a peptide which is consistent with the formation of a peptide layer on the surface of nanoparticles [18]. Also, the reduction of charge from −40 to −13 mV (**Figure 6**) indicates the displacement of negatively charged citric acid by the positive charge of the peptide. The small amount of negative charge still remaining on the PC-AgNPs is most likely due to a few residual citrate molecules on the surface even after ligand exchange.

The stability of peptide-anchored nanoparticles in phosphate-buffered saline is the first phenomenon for developing robust, biocompatible systems. However, if the particles are to be utilized in more complex environments, such as in vivo, then harsher conditions need to be analyzed.

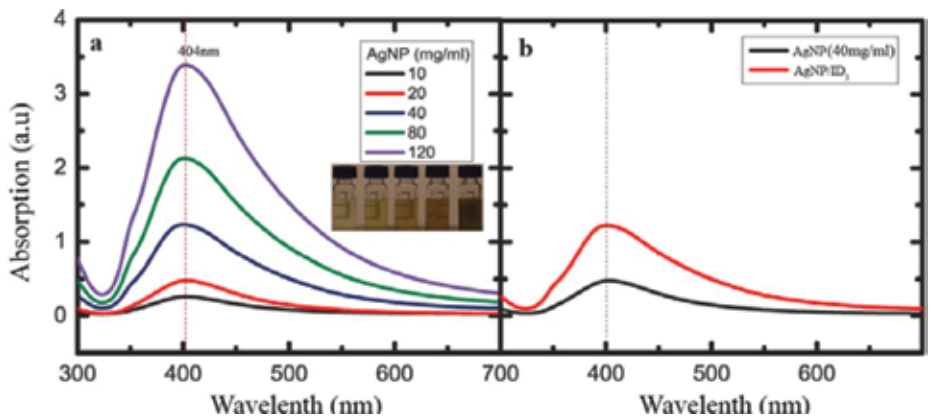

Figure 5. (a) Absorption spectra with a peak intensity of AgNPs at different concentrations. (b) Absorption spectra of AgNPs and $AgNP/ID_3$ at 30 mg/ml AgNP concentration.

Particle stability was assessed by monitoring the hydrodynamic diameter of nanoparticles using the UV–visible, TEM, and DLS. As seen in **Figure 7**, PC-AgNPs maintain the same hydrodynamic diameter (27 ± 2) after exposure to 15 wt% NaCl, 1 mg/ml lysozyme, and PBS solutions.

We examined the peptide-anchored AgNP stability under high salt conditions. Most of the nanoparticles aggregate when the salt was increased due to the screening of electrostatic repulsion. However, zwitterionic and mixed charge materials can resist aggregation of

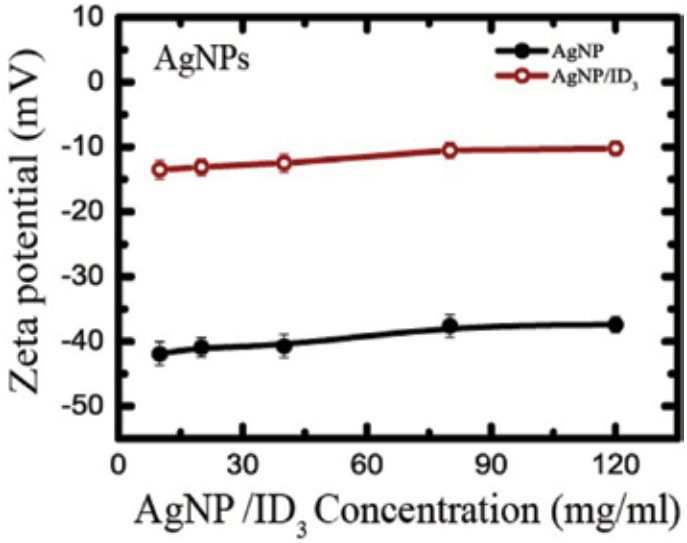

Figure 6. (a) The zeta potential of AgNPs and AgNP/ID_3 as a function of concentration.

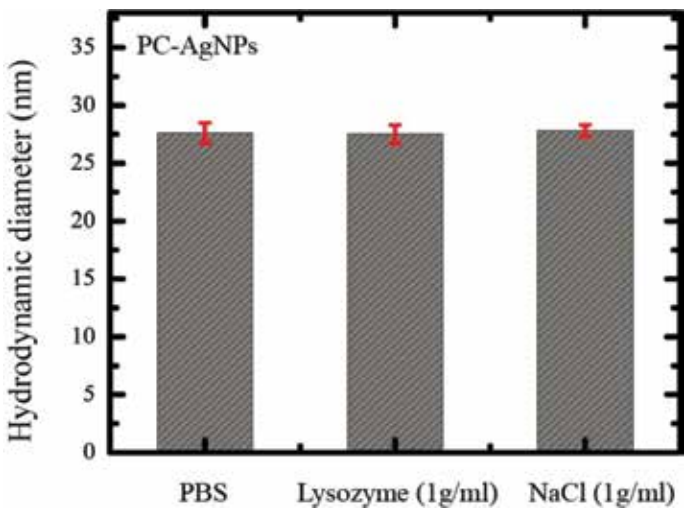

Figure 7. DLS measurements of the hydrodynamic diameter (volume percentage) (nm) of PC-AgNPs after exposure to PBS, 1 mg/mL lysozyme in PBS, and 15 wt% NaCl solution for 50 min. Each data point represents an average value/standard deviation from three independent measurements.

nanoparticles due to the presence of a strongly bound surface hydration layer [17, 18]. In addition, to examining particle stability in PBS medium, the stability of peptide-anchored AgNPs was also measured at higher salt concentrations. Peptide-anchored silver nanoparticles maintain stability even at 15 (wt%) salt concentration. These results indicate that the thin nano-peptide layer formed on the surface of silver nanoparticles (AgNPs).

4. Conclusion

In summary of results, the synthesis and characterization of peptide-anchored silver nanoparticles was demonstrated. The peptide-anchored nanomaterials were generated through a simple reduction approach, which helps a general synthetic route that produces particles of a similar size using peptides anchoring. The AgNPs were generally spherical with a relatively narrow size distribution. Peptide-anchored AgNPs show high stability in a high salt concentration. The results suggest that the reactivity of the peptide on AgNPs surface is governed by more details as indicated by the peptide structure. These results would be useful in the development of functional nanoparticles that exploit surface-based activity in the area of drug delivery and various bionanotechnology applications.

Acknowledgements

The authors would like to thank WPI, USA, and IISc, Bangalore, India, for the financial support.

Author details

Parvathalu Kalakonda[1]* and Sreenivas Banne[2]

*Address all correspondence to: parvathalu.k@gmail.com

1 Department of Chemistry, Chongqing University, Chongqing, People's Republic of China

2 Department of Materials Science and Engineering, Carnegie Mellon University, Pittsburgh, Pennsylvania, USA

References

[1] Baptista P, Pereira E, Eaton P, Doria G, Miranda A, Gomes I, Quaresma P, Franco R. Gold nanoparticles for the development of clinical diagnosis methods. Analytical and Bioanalytical Chemistry. 2008;**391**(3):943-950

[2] Dykman LA, Khlebtsov NG. Gold nanoparticles in biology and medicine: Recent advances and prospects. Acta Naturae. 2011;**3**(2):34-55

[3] Yeh YC, Creran B, Rotello VM. Gold nanoparticles: Preparation, properties, and applications in bionanotechnology. Nanoscale. 2012;**4**(6):1871-1880

[4] Han M, Gao X, Su JZ, Nie S. Quantum-dot-tagged microbeads for multiplexed optical coding of biomolecules. Nature Biotechnology. 2001;**19**(7):631-635

[5] Huang X, El-Sayed IH, Qian W, El-Sayed MA. Cancer cell imaging and photothermal therapy in the near-infrared region by using gold nanorods. Journal of the American Chemical Society. 2006;**128**(6):2115-2120

[6] Mirkin CA, Letsinger RL, Mucic RC, Storhoff JJ. A DNA-based method for rationally assembling nanoparticles into macroscopic materials. Nature. 1996;**382**(6592):607-609

[7] Moreno-Manas M, Pleixats R. Formation of carbon−carbon bonds under catalysis by transition-metal nanoparticles. Accounts of Chemical Research. 2003;**36**(8):638-643

[8] Salem AK, Searson PC, Leong KW. Multifunctional nanorods for gene delivery. Nature Materials. 2003;**2**(10):668-671

[9] Peng ZA, Peng X. Nearly monodisperse and shape-controlled CdSe nanocrystals via alternative Routes: Nucleation and growth. Journal of the American Chemical Society. 2002;**124**(13):3343-3353

[10] Puntes VF, Krishnan KM, Alivisatos AP. Colloidal nanocrystal shape and size control: The case of cobalt. Science. 2001;**291**(5511):2115-2117

[11] Choi CHJ, Zuckerman JE, Webster P, Davis ME. Transcytosis and brain uptake of transferrin-containing nanoparticles by tuning avidity to transferrin receptor. In: Proceedings of the National Academy of Sciences of the United States of America. 2011;**108**(16):6656-6661

[12] Albanese A, Chan WC. Effect of gold nanoparticle aggregation on cell uptake and toxicity. ACS Nano. 2011;**5**(7):5478-5489

[13] Karmali PP, Simberg D. Interactions of nanoparticles with plasma proteins: Implication on clearance and toxicity of drug delivery systems. Expert Opinion on Drug Delivery. 2011;**8**(3):343-357

[14] Larson TA, Joshi PR, Sokolov K. Preventing protein adsorption and macrophage uptake of gold nanoparticles via a hydrophobic shield. ACS Nano. 2012;**6**(10):9182-9190

[15] Kodiyan A, Silva EA, Kim J, Aizenberg M, Mooney DJ. Rigidity of two-component hydrogels prepared from alginate and poly(ethylene glycol)−diamines. ACS Nano. 2012;**6**(6):4796-4805

[16] Liu XS, Chen YJ, Li H, Huang N, Jin Q, Ren KF, Ji J. Tumor-Targeting and microenvironment-responsive smart nanoparticles for combination therapy of antiangiogenesis and apoptosis. ACS Nano. 2013;**7**(7):6244-6257

[17] Yang W, Zhang L, Wang SL, White AD, Jiang SY. Functionalizable and ultra stable nanoparticles coated with zwitterionic poly(carboxybetaine) in undiluted blood serum. Biomaterials. 2009;**30**(29):5617-5621

[18] Zhang L, Xue H, Gao CL, Carr L, Wang JN, Chu BC, Jiang SY. Maging and cell targeting characteristics of magnetic nanoparticles modified by a functionalizable zwitterionic polymer with adhesive 3,4-dihydroxyphenyl-l-alanine linkages. Biomaterials. 2010;**31**(25):6582-6588

[19] Collier JH, Segura T. Designing ECM-mimetic materials using protein engineering. Biomaterials. 2011;**32**(18):4198-4204

[20] Yoganathan V. Evaluation of the effects of antimicrobial peptides on endodontic pathogens In Vitro. Otago: Otago; 2012. p. 131

[21] Ansari MA, Khan HM, Khan AA. Anti-biofilm efficacy of silver nanoparticles against MRSA and MRSE isolated from wounds in a tertiary care hospital. Biologie et Médecine. 2011;**3**(2):141-146

[22] Naqvi SZ, Kiran U, Ali MI, Jamal A, Hameed A, Ahmed S, et al. Combined efficacy of biologically synthesized silver nanoparticles and different antibiotics against multidrug-resistant bacteria. International Journal of Nanomedicine. 2013;**8**:3187-3195. DOI: 10.2147/IJN.S49284. [PubMed: 23986635]

[23] Kora AJ, Arunachalam J. Bactericidal potential of silver nanoparticles synthesized using cell-free extract of *comamonas acidovorans*: In vitro and in silico approaches. World Journal of Microbiology and Biotechnology. 2011;**27**(5):1209-1216. DOI: 10.1007/s11274-010-0569-2

[24] Alizadeh H, Salouti M, Shapouri R. Actericidal effect of silver nanoparticles on intramacrophage brucella abortus. Jundishapur Journal of Microbiology. 2014;**7**(3):e9039

[25] Levy R, Thanh NTK, Doty RC, Hussain I, Nichols RJ, Schiffrin DJ, Brust M, Fernig DG. Ational and combinatorial design of peptide capping ligands for gold nanoparticles. Journal of the American Chemical Society. 2004;**126**(32):10076-10084

[26] Olmedo I, Araya E, Sanz F, Medina E, Arbiol J, Toledo P, Alvarez-Lueje A, Giralt E, Kogan MJ. Bioconjugate Chemistry. 2008;**19**(6):1154-1163

[27] Arosio D, Manzoni L, Araldi EM, Scolastico C. Cyclic RGD functionalized gold nanoparticles for tumor targeting. Bioconjugate Chemistry. 2011;**22**(4):664-672

[28] Kim YH, Jeon J, Hong SH, Rhim WK, Lee YS, Youn H, Chung JK, Lee MC, Lee DS, Kang KW, Nam JM. Tumor targeting and imaging using cyclic RGD-PEGylated gold nanoparticle probes with directly conjugated iodine-125. Small. 2011;**7**(14):2052-2060

[29] Scari G, Porta F, Fascio U, Avvakumova S, Dal Santo V, De Simone M, Saviano M, Leone M, Del Gatto A, Pedone C, Zaccaro L. Multidentate peptide for stabilization and facile bioconjugation of gold nanoparticles. Bioconjugate Chemistry. 2012;**23**(3):340-349

[30] Sun L, Liu D, Wang Z. Functional gold nanoparticle-peptide complexes as cell-targeting agents. Langmuir. 2008;**24**(18):10293-10297

[31] Reithofer MR, Lakshmanan A, Ping AT, Chin JM, Hauser CA. In situ synthesis of size-controlled, stable silver nanoparticles within ultrashort peptide hydrogels and their antibacterial properties. Biomaterials. 2014;**35**(26):7535-7542

[32] Chen S, Cao Z, Jiang S. Ultra-low fouling peptide surfaces derived from natural amino acids. Biomaterials. 2009;**30**(29):5892-5896

[33] Khan MAM, Kumar S, Ahamed M, Alrokayan SA, AlSalhi MS. Structural and thermal studies of silver nanoparticles and electrical transport study of their thin films. Nanoscale Research Letters. 2011;**6**(1):434

[34] Lin K, Yi J, Hu S, Sun J, Zheng J, Wang X, Ren B. Intraband Hot-Electron photoluminescence from single silver nanorods. ACS Photonics. 2016;**3**(7):1248-1255

[35] Prakash P, Gnanaprakasam P, Emmanuel R, Arokiyaraj S, Saravanan M. Green synthesis of silver nanoparticles from leaf extract of Mimusops elengi, Linn. for enhanced antibacterial activity against multi drug resistant clinical isolates. Colloids and Surfaces B: Biointerfaces. 2013;**108**:255-259

[36] Mogensen KB, Katrin K. Quantum size effects in the optical properties of ligand stabilized aluminum nanoclusters. The Journal of Physical Chemistry C. 2014;**118**(48): 28075-28083

[37] Kalakonda P, Banne S. Synthesis and optical properties of highly stabilized peptide-coated gold nanoparticles. Plasmonics. August 2017;**12**(4):1221-1225

[38] Kalakonda P, Banne S. Synthesis and optical properties of highly stabilized peptide-coated silver nanoparticles. Plasmonics. 2017;**12**(4):121-122. https://doi.org/10.1007/s11468-017-0628-8

Chapter 4

Synthesis, Characterization and Antimicrobial Properties of Silver Nanocomposites

Mudassar Abbas, Nida Naeem, Hina Iftikhar and Usman Latif

Additional information is available at the end of the chapter

http://dx.doi.org/10.5772/intechopen.74623

Abstract

Nanoparticles and polymers in their respective fields have contributed greatly in the form of science and hence in daily life application products. But due to lack in emerging technologies for developing silver nanocomposites with polymers and other materials, the nanoparticle-based products have conquered little less attention. Hereby, an effort is made to put a light on already developed functional materials containing silver nanoparticles and also to look forward their scope in daily life applications. A little more insight into antimicrobial properties of such materials will also be elaborated. Finally, the optimal amounts of silver that cannot be health hazardous to living being especially human and overall environmental impacts of Nanocomposites are presented.

Keywords: silver nanoparticles, functional materials, antimicrobial properties, polymers

1. Introduction

Today the nanoscience can easily be presumed as the key feature of modern world technology. Thereforth, due to assorted field of utilizations, it is playing pivotal role in material science industry [1]. Its applications can monetarily expand the properties and estimations of material preparing and items. The nanomaterials are prepared either by incorporating into the core matrix of the material or via polishing over the surface of designed materials. The wide spread application of nanomaterials ranges from catalysis to electronics and optics as well as in magnetics alongside the health and environment applications [2]. Yet the future of nanotechnology in material applications lies in territories where the new standards will be joined into strong, multifunctional material frameworks without bartering the intrinsic material properties.

Silver nanoparticles are domineering among the most important and entrancing nanomaterials among a few metallic nanoparticles that are engaged with the biomedical applications. They exhibit excellent antibacterial, antifungal, anti-inflammatory and antiviral properties generously or either after reacting with specific elements to impart such functional properties [3]. To an extent, the silver nanoparticles can be utilized against a broad variety of infections [4]. The use of silver nanoparticles is not restricted to the medical field only; they have been also used as self-cleaning, UV protection, improving durability and opto-electronics.

Silver is stable in pure water and air environments but the surrounding of ozone, hydrogen sulfide or sulfur if present in air or water may bring about silver tarnishing because of the formation of silver sulfide [5]. Apart from conventional Ag^{+}, silver is available in three other oxidation states: Ag^{0}, Ag^{2+}, Ag^{3+}. However, the last two are unstable and rarely found in the sea-going condition. Silver has numerous isotopes but with molecular weight 107 is the most commonly existing. Even though intense poisonous quality of silver in the condition is subject to the accessibility of free silver particles, analyses have appeared that these convergences of Ag^{+} particles are too low to lead toxicity. Metallic silver appears to posture the negligible hazard to wellbeing, while solvent silver mixes are all the more promptly consumed and can possibly deliver unfriendly effects [6]. The decrease in the measure of silver to nano-sized silver expands its capacity to control microscopic organisms and growths. Because of the extensive surface region of nanomaterials prompt the expanded contact with microbes and growths which builds its affectivity. Nano-silver, when in contact with microorganisms and their growth, unfavorably influences the cell digestion of the electron exchange structures

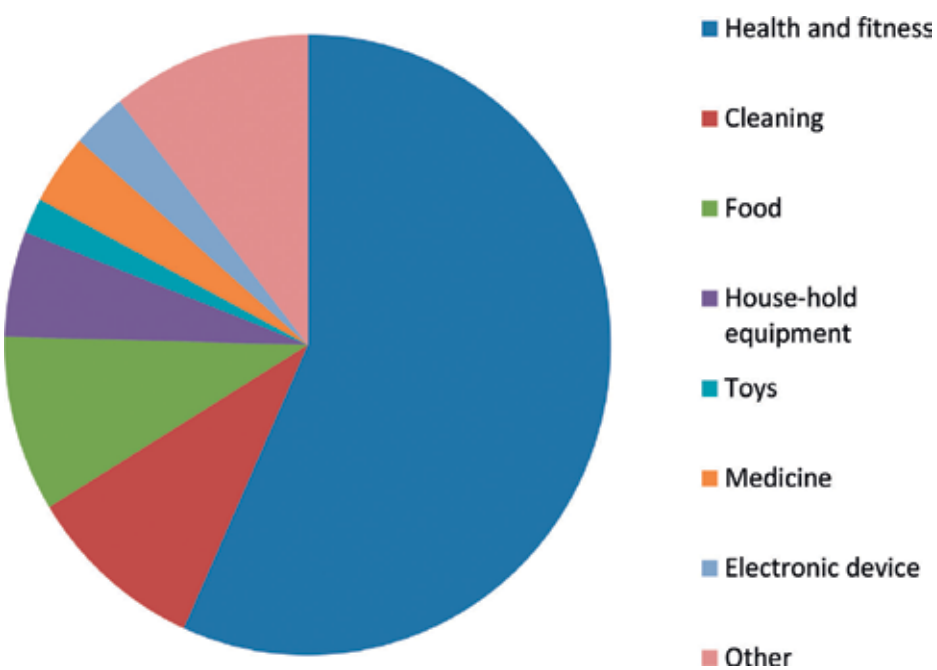

Figure 1. Application of silver nanoparticles in different fields.

http://dx.doi.org/10.5772/intechopen.74623

and cause the substrate movement in the microbial cell film [7]. Microscopic organisms and growths causes irritation, contamination, smell, wounds, the utilization of nano-silver subdue the expansion of microscopic organisms and parasites [8]. Nano-silver have been generally utilized because of its antibacterial microbial movement for the advancement of items containing silver incorporate nourishment contact materials, (for example, containers, bowls and cutting sheets), scent safe materials, gadgets and family unit apparatuses, beautifying agents and individual care items, therapeutic gadgets, water disinfectants, room splashes, children's toys, newborn child items and health supplement [9] (**Figure 1**).

2. Synthesis of silver nanoparticles

The nanoparticles of silver can be synthesized by various physical, chemical, biological and other methods. The most prevalent chemical methodologies contain the chemical reduction by using a range of several inorganic and organic reducing agents, physicochemical reduction, radiolysis and electrochemical methods [10]. The vast majority of these techniques are still in the development stage as well experienced some complications in silver nanoparticles stability and accumulation, morphology, size and size distribution [11]. Moreover, for the produced silver nanoparticles, the extraction and purification are still significant concerns for further applications. Besides, silver nanoparticles prepared through biological-, irradiation- and Tollen's method and in presence of polyoxomerales and polysaccharides method can also be incorporated into functional materials [12].

In the biological method, the synthesis of silver nanoparticles takes place through the reduction of the silver ion by the help microorganisms extracts [13]. The extracts of the microorganisms at a time can behave as both the capping agents as well as reducing agent. The preparation of silver nanoparticles by using polysaccharides along with water as the capping agent is recognized as polysaccharide technique [14]. The nanoparticles of silver can also be synthesized by using numerous irradiation methods like UV-irradiation, microwave, gamma rays and through sonochemical methods [15]. These nanoparticles can also fabricated by the Tollen's method and polyoxomerales procedures. The stable spherical silver nanoparticles with a diameter 0.5–150 nm are also created at the several concentration of silver nitrate using the biosynthesis procedure [16]. These methods have many advantages than chemical, physical and the microbial synthesis because in this procedure no hazardous chemicals are being used. Fundamentally, the green synthesis is considered to be an environmental friendly as well the cost effective substitute to the physical and chemical procedures.

The plant extract is the most common reducing agent in the green synthesis [17]. Generally, the silver ions face reduction in aqueous solution to produce different nanometer diameter sized colloidal silver. Herein, the silver ions also get reduced to silver atoms which then rise into the oligomer clusters. Later these clusters support to advance the colloidal silver particles. Fabrication of silver nanoparticles follows the three chief principles that are, the selection of solvent medium, and selection of environment friendly reducing agent along with the choice of the harmless substances to stabilize the nanoparticles of silver. A huge collection of secondary metabolites is created in plants that have the redox capability for the biosynthesis of silver

nanoparticles. So, the silver nanoparticles are produced from Ag+ ion by the bio reduction by the help of plant metabolites [18]. The uniform silver nanoparticles of controlled size can also be synthesized by using the microemulsion procedures [19]. The nanoparticles preparation in the two-phase aqueous organic schemes is centered onto the preliminary spatial split-up of the reactants of metal precursor and reducing agent into the two immiscible segments. The interface between the two fluids and the strength of inter-phase transference between the two phases, which is intermediated by the quaternary alkyl-ammonium salt, influence the level of interactions between the metal precursors and the reducing agents. The metal clusters formed at the interface are stabilized, due to their coated surface with stabilizer molecules arising in the non-polar aqueous medium, and shifted to the organic medium by the inter-phase transporter [20]. The major drawbacks of this process are the use of highly poisonous organic solvents. Consequently, the large amounts of surfactant and the organic solvent must be disconnected and removed from the final product. On the other hand, the colloidal nanoparticles prepared in no aqueous media for conductive inks are well-dispersed in a low vapor pressure organic solvent, to readily wet the surface of polymeric substrate without any accumulation [21].

The nanoparticles of silver can be produced through the wide range of the irradiation methods [22]. The silver nanoparticles of well-defined shape and size can be produced by the laser irradiation of the surfactant along with an aqueous solution of the silver salt. Moreover, laser is being used in the photo-sensitization synthetic method of producing the silver nanoparticles by using benzo-phenone. At the short irradiation periods, the low laser powers formed the nanoparticles of about 20 nm, whereas an improved irradiation power created the silver nanoparticles of the size about 5 nm. Mercury lamp and laser can be used as the light sources for the production of the silver nanoparticles. In the visible light irradiation method, the photo-sensitized growth of silver nanoparticles using thiophene (sensitizing dye) and silver nanoparticle formation by illumination of [Ag(NH3)]+ in ethanol are being used [23].

Among all available methods, the basic route for the syntheses of nanoparticles is defined by keeping in mind the parameters like availability of chemicals, natural extract and available instruments, the demanded size and shape of nanoparticles and most importantly the use of nanoparticles in a particular application. In our laboratory, we prepared the solvent-free synthesis of oleophlic nanoparticles from silver nitrate and oleyl amine [24]. The direct heating of reaction mixture for 20 min at 165°C yielded the nanoparticles of average 68 nm upon dispersal in ethanol. The ultra-refined nanoparticles were incorporated in the polymerization of dicyclopentadiene and polymers were evaluated against their activity for microbes. Another example constitutes the manufacturing of fluff pulp using sonochemically impregnated silver nanoparticle and the materials was compared for their antimicrobial properties against the conventionally used sodium borohydride reducing agent [16].

3. Application of silver nanoparticles in functional materials

Silver nanoparticles represent the manifest nano-products and are now generally utilized as a part of medicinal applications, including wound dressing, diagnosis, water filtration, electronics, optics, and pharmacological treatment [15]. Since the shape, size, and synthesis of silver nanoparticles can affect their capability and conceivable dangers to human wellbeing,

broad research is expected to completely comprehend their amalgamation, portrayal, and conceivable harmfulness. Herein, we present an outline of silver nanoparticles amalgamated materials for utilizations in different fields.

Nano-silver has high electrical and thermal conductivity alongside the improved optical properties that prompts different applications in hardware. In nano-electronics, silver nanowires are utilized as nano-connectors and electrodes. Other applications include opto-electronics, nano-electronics, (for example, single-electron transistors and electrical connectors), information stockpiling gadgets, the readiness of dynamic waveguides in optical gadgets high thickness recording gadgets, intercalation materials for batteries, making small scale interconnects in coordinated circuits (IC) and fundamental capacitors [25].

For the access of clean water, a feasible treatment of the combination of filtration along with disinfection is recommended. Revealing in Nanotechnology, analysts have built up a layer channel in view of silver nanostructures that are connected to cellulose filaments. Driven by gravity, the framework gives a rapid yet modest and sturdy alternative for the cleansing of water [26]. The silver nanostructures gradually break down and discharge silver particles, which have been utilized as antibacterial operators for a considerable length of time. In such a way, debased water can be purged averting basic sicknesses, for example, cholera or gastroenteritis. This gives a shabby, protected, compact and simple to-utilize water-purification framework.

Similarly, it is equally utilized with conjunction of copper ions as a protection measured against colonization of Legionella spp. Silver nanoparticles are right now being tried in various trial purpose of-utilization (POU) treatment frameworks and ionic silver has been researched for its potential use as an optional disinfectant (to lessen levels of chlorine) in drinking-water supplies. Silver particles (in mix with both copper and chlorine) have also been examined for use in swimming pool sterilization [27].

The production of metal-polymer involves multiple procedures. Due to harmful steps and difficulty in managing the nanoparticles for even distribution in the large medium, less work has been done using ex-situ process. Besides this, in-situ method has been appreciated for linking the beneficial properties of all the materials involving in the process and metal NPs formed through it has provided numerous uses. According to the latest research study, different polymer amalgams have been tried for fabrication of metal nanoparticles. The technique of in-situ method in polymer matrixes majorly deals with uniform solution, direct photo-reduction and photo-sensitization [28]. Basically photo-reduction of the metal and reduction of their salts/ions takes place to generate M^0. The main approach for synthesis of the Ag nanoparticles involves the reaction between silver cations and shortly lived specie formed by photo-generation. Two photo-induction reactions are performed to formulation the basic radicals.

Another process involves the photo-initiation by acryl-phosphine (photo-initiator) that encourages the synthesis of silver nanoparticles by the reduction of $AgNO_3$ and fundamental polymerization of acrylic resin. Hence, speedy production of metallic silver and radical initiation of the crosslinking polymerization takes place at the same time when irradiation of Irgacure 819 is reacted with polyethylene-glycol di-acrylate monomer in the presence of $AgNO_3$. Change in color of the solution was observed by the UV-Visible absorption that clarifies the synthesis of silver nanoparticles [29].

A wide range of actinic wavelengths and photo- reduction media were tried for fabrication of silver nanoparticles through photo-induction method. **Table 1** describes the photo-indicator and their chemical structures that have been tried for this respective purpose. In another example, by mixing of silver cations and dye, two processes i.e.; photo-reduction and photo-initiation are simultaneously carried out. Ag nanoparticles were uniformly dispersed in the polymer mixture and photo-polymerization process was carried without any interruption. This single step process for synthesis of silver nanoparticles proves to be new method for production in polymer matrixes. Apart from the synthesis of nanoparticles in spherical form by photo-induced method, the production of the NPs in other distinctive geometrics is thought-provoking matter still left for working [30].

Among the numerous conductive materials like; nickel, palladium, gold, copper, graphite, silver, and carbon fibers, only silver exhibits the best properties due to its brilliant conductivity as well chemical durability and also ability to manufacture the different shapes of the nanostructures with modified substrates. For increasing the conductivity, a ribbon shaped silver nanostructures is formed by the fabrication of the metallic ribbons where the cotton fabric is being used as a substrate. By these techniques a solution of a solution of PVP and $AgNO_3$ in ethylene-glycol (EG) is sprayed onto the cotton fabric surface and dried at about 160±5°C for 8 min [31]. The nano-porous structure of cotton can act as a nano-reactor and hence a good pattern to control the shape of nano-structure is produced. These ribbons are further characterized by SEM micrographs. Therefore, the technique provides a geometrically organized method to synthesize in-situ nanoribbons onto the fabric models [32].

The conducting polyaniline produced in the existence of the oxidizing agent potassium dichromate by the chemical oxidation process helped in producing silver composites using various compositions of silver nitrate ($AgNO_3$) into the polyaniline. The surface morphology of the composites was investigated utilizing Scanning electron magnifying instrument (SEM) demonstrate that Ag molecule are implanted in the chain of polyaniline to form the different phases. The powder X-beam diffraction (XRD), Spectrograph recommends the semi-crystalline behavior of the materials. It was additionally discovered that the electrical conductivity of PANI/Ag nanocomposite was around 100 times higher than that of the pure polyaniline. The arrangement of PANI as the semiconducting polymer with the silver as the noble metal can

Dentistry	The silver-loaded SiO_2 nanocomposite resin filler used as an additive in the polymerizable dental constituents
Neurosurgery	The coating of the catheter for the drainage of cerebrospinal fluid
Eye care	Nano-silver used in the coating of contact lenses
Anesthesiology	Used in the coating of the breathing mask also in endotracheal tube for the mechanical ventilatory maintenance
Diagnostics	Nano-silver pyramids for improved bio-detection Ultrasensitive and ultrafast stage for clinical tests for analysis of myocardial localized necrosis Fluorescence-based RNA detecting Magnetic center/shell Fe_3O_4/Au/Ag nanoparticles with turnable plasmonic properties

Table 1. Coatings of silver nanoparticles in different medical domains.

produce the hybrid material which behaves as the semiconductor at the low temperature and as the metal at relatively high temperatures [33].

Polyvinylpyrolidone is one of the largest contributors for polymer based nanoparticle synthesis. In a particular example, silver nanoparticles- polyvinylpyrolidone (PVP) composite comprising the 100 ppm of silver has been synthesized in the powder in the textile applications by utilizing the sonochemical method comprising the sonication and reduction with the tri-sodium citrate followed by the spray drying. The synthesized PVP coated silver nano-powder is characterized by using the atomic absorption spectra, UV-visible spectra, energy dispersion analysis of X-ray and transmission electron microscope. As well the EDX measurements confirm the presence of silver in the synthesized powder. The silver nanoparticles of the size of 50–60nm are present in the nano-powder. By exhaustion method, silver nano-powder can be applied onto the cotton and wool fabric for imparting the antibacterial efficacy. A clear zone of inhibition was observed in both of the treated cotton and wool fabrics against the microorganisms [34].

Nano-silver is being utilized in paper industry by DocuGuard and many others. The use of silver nanoparticle-based paper for the protection of the hospital case notes as well the medical files against the production of bacteria. Future applications include the business stationery, brochures, envelopes, as well the book-binding materials. Nano-silver can be used in the commercial water-purification schemes where polymers and fibers containing silver nanoparticle for stronger antimicrobial applications. Due to such antibacterial properties, nano-silver is also being used in the interior of the automobiles such as steering wheels and in building materials such as sanitary tubing and coverings. Nano-silver can also be used for the preservation of wood to resist mold and mildew. MTR Corporation in Hong Kong reports the use of silver nanoparticles in combination with titanium dioxide coating to improve the hygiene by spraying it onto the surfaces in MTR train stations, inside train compartments, as well as MTR managed shopping malls, staff offices along with recreational services [35].

The accumulation of the coated silver nanoparticles to the matrix of polypropylene by the extrusion process signifies a stimulating solution that increases the protection against the bacteria of both nature Gram-negative like *S. aureus* and Gram-positive like *E. coli*. Some of the silver nanoparticles disclosed inside the Polypropylene film which obstructs the antibacterial activity however the general outcome was the high antibacterial effectiveness. Typical organic biocides have limited their applications due to low heat resistance, high decomposability, short life and high toxicity. One feasible alternative are inorganic biocides such as polymers composites. Presence of silver nanoparticles also slightly increases the thermal stability of PP-AgNPs (Polypropylene-silver nanoparticles) compounds therefore assisting the easy processing; this could be done to the interaction between polypropylene chains and (PVP) surfactant-coated silver nanoparticles. Reduction (%) CFU assay exhibited positive biocide outcomes for *S. aureus* and for *E. coli* bacteria. No cytotoxicity effect is produced onto the polypropylene film having silver nanoparticles (AgNPs) [36].

Water soluble biopolymers in combination with AgNP were expected to produce new antimicrobial activities. A stream of natural polymers has been employed for the preparation process of polymeric AgNP nanocomposites. Polyvinyl alcohol (PVA) represent a nontoxic, synthetic and water soluble polymer used in stabilization in nanoparticles synthesis and their

blend with chitosan exhibits antimicrobial activity against pathogenic bacteria in food packaging preparation. Films of AgNPs/PVA/CS were synthesized using solution casting method. Solutions of equal weights of PVA and CS were prepared using double distilled water with constant stirring at 60°C. The homogeneous solution was casted into Petri dishes and left to dry at 50°C for 3 days to form the desired film with a thickness from about 0.5–1.0 mm, and then the films were stripped off the dish. After the FTIR and XRD analysis, the results indicate that the nanocomposite samples show better film properties than that of pristine polymer blend without silver nanoparticles [37].

4. Application of nanotechnology in textiles

Nanotechnology has appeared to be the paramount technology for the abundant applications that could cover an extensive range of the industries [3]. The increased efficiency has subsequently added the definite value of products in textile industry. Development of the smart, nano-textiles has the great potential to revolutionize the production of the fibers, nonwovens or woven fabrics and functionality of the clothing in all forms of the textile products [38]. Silver nanoparticles are being widely used in apparel applications that include a wide range of functional properties. The fabrics containing engineered nano-silver are also being used to kill odor causing bacteria in socks and sports clothing.

The nano-fibers of silver are of the great importance recently in view of the double advantages from silver particles and nano-fibers. Silver nanoparticles are widely utilized for biomedical applications because of the antibacterial and antiviral properties [39]. The nanocomposites of Ag (0)-polymer has been manufactured by the various techniques by introducing the precursors of the salts of silver into the polymer network followed by the method of chemical reduction or by laser ablation furthermore processing to form the silver-embedded fibers or silver-bonded polymer micelles [40]. Depending onto the preparation process of the silver particles, the Ag (0)-polymer nanocomposites synthesis can be one stage or two stages. In the one-step process, the silver precursor and the polymer that functions as the stabilizer for the solver nanoparticles segment the same solvent. The selective solvents must be used in this method so the precursor and the polymer can be melted. Additionally, the ethanol and methanol are usually used as a solvent and these solvents should reduce the silver precursors into the nanoparticles of silver. After the homogeneous solution scheme is attained, the solution is then further subjected toward the electro-spinning for the production of silver nanoparticle-containing the nano-fibers [41]. Whereas, in two-step process the conversion of silver precursors into the silver nanoparticles involves an extra step instead of reduction in presence of solvent. Usually silver nitrate is introduced into the polymer solution. After achieving the homogeneous dispersion, the solution is subjected to chemical reduction or laser ablation. The plasma treatment has been described as an operative way to produce the silver nanoparticle in the solution of nylon 6. The chemical reduction has similarly employed to make the silver nanoparticles in the solution of polypyrrole (PPy). At the second stage, electro-spinning is employed to create the silver particles suspended polymer solution into the nano-fiber composites [42].

Though the one-step process is simpler and needs the less treatments as well processing as compared to the two-step process. For the two-step process, since the reduction of silver particle and nano-fiber formation are accomplished into the two separated steps, solvent is not needed in that process that is for reducing the silver precursors and more possibilities of solution structures. Electro-spinning is an adaptable and solid procedure to deliver smaller scale or nano-fibers. Electro-spinning is a fiber framing process, where a high voltage is utilized to make an electrically charged jet of polymer arrangement or soften from the needle. At the point when the voltage is sufficiently high, the electrostatic powers beat the surface pressure of the polymer, and the stream is extended and goes toward the collecting plate. The polymer solidifies among the movement toward the collecting plate, frequently providing the nanometer scale filaments [43]. Nano-fiber development by electro-spinning is influenced by the spinning parameters including arrangement properties as well the concentration, hydrostatic pressure of the capillary tube, the electric potential at the capillary tip, the tip-to-collector distance and the conditions of chamber [44]. By the electro-spinning, the nano-fibers embedded with the silver nanoparticles can be organized, and the morphology can be controlled by the parameters of electro-spinning process. With benefits of the antibacterial and fungicidal properties of silver nanoparticles and high surface-to-volume proportion of nano-fibers, the utilization of the silver-containing nano-fibers extends from biomedical applications to optical materials [45].

The synthesis of the composite film was accomplished by the addition of 100 μl of the different concentrations of silver nitrate ($AgNO_3$) [46] to the solution of chitosan in the presence of 1% acetic acid. The temperature of this reaction plays a significant role as it strongly influences the particle size and silver nanoparticles dispersion into the solution of chitosan [47]. These films were produced by the solvent cast method pouring the finishing solution into the plastic petri dish and allowing the solvent to vaporize. The confirmation of the silver nanoparticles in the metallic state carried out by the XRD and XPS measurements [48].

Silver wires can be directly organized from the aqueous silver nitrate by depositing the reduced silver nanoparticles (AgNPs) onto the self-assembled, 1-D wires of tetra-anilines (TeAN-ES) that are doped with nitric acid which also act as a reducing agent [49]. Nano-silver is utilized for the coating materials, for example, fused in wound dressings, diabetic socks, frameworks, sanitization materials in healing centers, therapeutic materials and so forth.

Nano-silver can be used to cover the wound pads for bandages with assorted sizes for treatment of cuts, burns and scratches. Any antibacterial spray or ointment, (for example, Neosporin) should not be used as it might hinder the silver's fixing properties. Despite the fact that researchers and wellbeing experts have cautioned about the ascent of “supergerms,” organisms that have turned out to be impervious to anti-infection medications, microbes appear not able develop a protection from silver. The bandage pad is basically absorbed colloidal silver and is permitted to dry. The nanoparticles of silver impregnate the gauze material and will give against microbial protection when the wrap is connected to an injury. Silver restricts the microorganisms in no less than three courses: by connecting with the cell film, authoritative to the DNA of cells and hindering the digestion of the microscopic organisms. It lessens the development of several distinct sorts of microbes, including some that do not regularly respond to

pharmaceutical antibacterial specialists. Since silver obstructs the development and spread of germs through various instruments, it is hard for microbes to develop protection. Dissimilar to some different metals, silver is not toxic to the body—just too wounding organisms. It is additionally not addictive, and is exceptionally hard to overdose on. Notwithstanding many years of handy utilize, late logical examinations on people and creatures have demonstrated that injuries treated with silver heal at a speedier rate than those treated without silver [50] The antibacterial properties were brought into the bandages by drop-cast technique, utilizing 2 and 5% concentrations by weight of silver nanoparticles in water. To decide the measure of the silver nanoparticles and their dispersion over the wraps, Scanning Electron Microscopy was utilized. In the SEM can be watched that more nanoparticles were saved in the bandages with the less concentrated dispersions (2%) [51]. For a specific example for bandage preparations and in order to determine the antibacterial properties, *Escherichia coli* (*E. Coli*) bacteria were used. The bacteria cells were grown into the liquid at 37°C and 250 rpm overnight. After that, the piece of bandages with 0% (blank sample), 2% and 5 % silver nanoparticles were placed into the solution containing E.Coli bacteria and left another 24 h at 37°C.

Silver nanoparticles (AgNPs) are utilized as a part of antimicrobial applications, containing an extensive collection of the consumer goods and apparel. This advanced fiber protection, based upon the nanotechnology also provides the oil and water resistant properties to the textiles. In general, an invisible film is produced onto the surface around the fibers by the product. Resultantly, the dry dirt cannot adhere to the material and the liquid cannot be soaked up by the fibers. Water, coffee and fatty substances are repelled from the treated textiles. Even extreme soiling can be removed certainly without any trace [25].

It is ideal for the clothes made up of wool, silk, synthetics and leather. It can be applied on every textile from finest silk to hard wearing cotton on different garments such as uniforms, hiking clothes costumes, sports jackets, suits, jackets, blouses, shirts, track suits, ties, rain coats, trousers, jeans, anoraks, ski clothing, motorcycle clothing, adventure wear and snowboard clothing [52].

The main advantages of the silver nano coatings

- Environmentally friendly
- Harmless to skin
- Easy handling
- Breathability remains
- Dry cleaning resistant
- Ironing resistant
- Suitable for all textiles
- Long lasting sealing of textiles
- Prevents tea, coffee and ketchup stains etc.

- Simply wash off contaminants
- Washing stable up to 40°C
- The look, texture and breathability of the material remains
- Long lasting protection for the textiles against dirt water and grease

5. Characterization of silver nanoparticles

The synthesized nanoparticles of silver can be characterized by various electron microscopic and absorption spectroscopic techniques [53]. The major among them are atomic force microscopy (AFM), scanning electron microscopy, dynamic light scattering (DLS), transmission electron microscopy (TEM), X-ray photoelectron spectroscopy, X-ray diffraction analysis, UV-visible spectroscopy and Fourier transformation infrared spectroscopy (FTIR). The UV-visible spectroscopy is the most convenient and feasible method for detection of nanosilver as the typical peak of 385–450 nm range predicts the presence of nanoparticles. The powder form of silver nanoparticles is used for capturing SEM image and X-ray diffraction pattern is used to obtain the structural image of the prepared nanoparticles and to determine the size of the nanoparticles [54]. Atomic force microscopy is used for observing the surface morphology and the size of consequential silver nanoparticles [55]. The sample is dropped onto the new cleaved mica pieces and dried overnight. This study of nanoparticles of silver that are deposited onto the mica pieces is executed in a microscope VEECO or Multimode Nano-scope IIIa [56]. At times, after synthesis, the nanoparticles are also examined under scanning electron microscopy (SEM) VEGA3 TESCAN, which provides the clear image of the nanoparticles synthesized [57] and morphological structures of nanoparticles are exposed. Scanning electron microscopy depiction not just provides the structural depiction but also provides the nanoparticles' size in the specimen to recognize whether the nanoparticles are in range of the nano-scale or above [53] (**Figure 2**).

Dynamic light scattering (also known as Photon Correlation Spectroscopy) is an important technique, mostly used in recognizing the distribution pattern of the size of very small particles present in the suspension or in the solution. This light scattering (Malvern) technique is being used to recognize the size distribution pattern of the silver nanoparticles synthesized biologically or other methods [58]. Transmission electron microscopy (TEM) demonstrates the crystal structure, shape as well as the size of the nano- particles [59]. The grid for this analysis is arranged by placing a drop of the nanoparticle suspension on a carbon-coated copper grid and allowing the water to evaporate inside a vacuum dryer. The grid covering with the silver nanoparticles is scanned by the Transmission Electron Microscope [60]. Similarly, the X-ray beam photoelectron spectroscopy (XPS) estimations have been done to clear up the surface compound conditions of the nanoparticles. Silver nanoparticles are explored by XPS to describe the idea of the surfactant chemisorbed to the surface. It is utilized to inspect the valence of the subsequent silver nanoparticles while it also gives the additional information with respect to the structure of the silver nanoparticles encapsulated into the organic linkages [61].

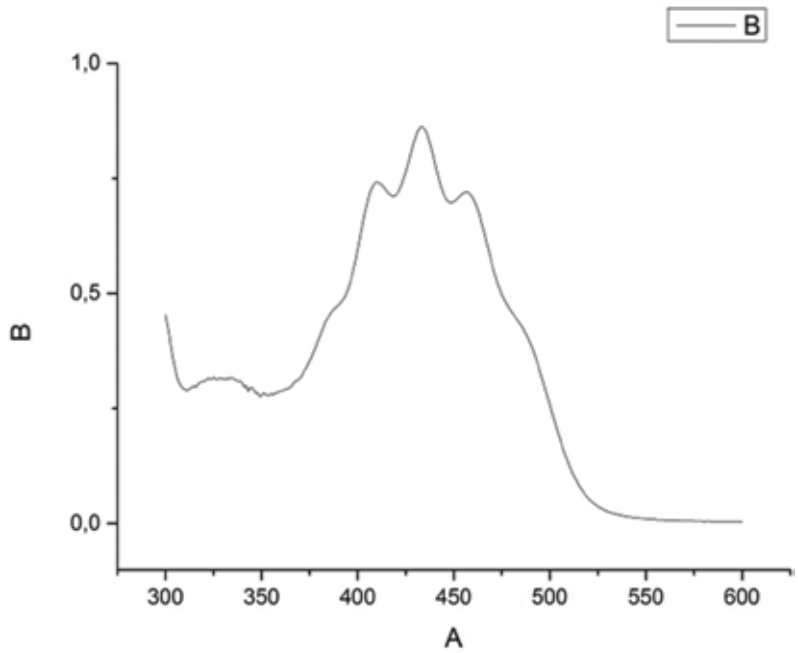

Figure 2. The exemplary UV-visible spectra of silver nanoparticles prepared from orange juice.

In contrast the crystal structure and respective particle size is calculated via X-ray diffraction analysis [62]. The diffracted intensities are recorded from 35.01 to 79.99° at 2θ angles. The crystalline size is calculated from the half-height width of the diffraction peak of XRD pattern by using the Debye-Scherrer equation [63].

$$D = \frac{K\lambda}{\beta cos\theta} \quad (1)$$

where *D* is the crystalline size, *Å*, K is the crystalline-shape factor, λ is the X-beam wavelength, θ is the watched crest point, degree [64], β is the X-beam diffraction expanding, radian.

The change of the color into the reaction combination of the metal ion solution during nanoparticle formation is generally recorded by the visual observation. The synthesized nanoparticles of silver are confirmed by sampling the aqueous component of two hour after the reaction and the absorption maxima was scanned by the UV-Vis spectrophotometer at the wavelength of 325–825 nm onto the Beckman Du-50 Spectrophotometer [65]. The absorption as well into the visible range directly reflects the perceived the color of the chemical convoluted in the whole synthesis process [56]. For the measurements of FTIR, the synthesized silver nanoparticles arrangement is centrifuged at 10000 rpm for 30 min. The pellet is washed thrice with 5 ml of deionized water to dispose of the free proteins or chemicals that are not topping the silver nanoparticles. The pellet is then dried by utilizing vacuum drier to measure the recording through FTIR [66] (**Figure 3**).

http://dx.doi.org/10.5772/intechopen.74623

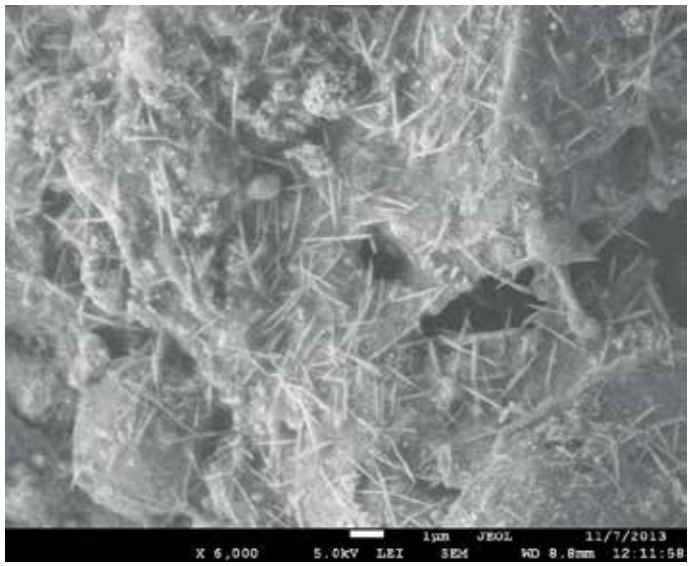

Figure 3. The SEM images of silver nanoparticles from Sumbla plant.

6. Antibacterial properties

Both, the Gram-positive and Gram-negative microorganisms are successfully killed by nano-silver, so it can call as executing agent including the anti-toxin safe strains [67]. Gram-negative microscopic organisms are the microbes which hold the shade of the stain even in the wake of washing with liquor acetone or alcohol as well include genera, for example, Salmonella Acinetobacter, Escherichia, Vibrio and Pseudomonas [68]. The Acinetobacter species are related with nosocomial diseases, i.e., contaminations that are the consequence of treatment in a doctor's facility or a human services benefit unit, however auxiliary to the patient's unique condition. Gram-positive microscopic organisms are those which lose the shade of the stain after wash with liquor or acetone and incorporate some outstanding genera, for example, Staphylococcus, Listeria, Bacillus, Enterococcus, Streptococcus and Clostridium [69]. Anti-toxin safe microbes are the microscopic organisms that are not controlled or murdered by anti-toxins which incorporate strains, for example, *Staphylococcus aureus*, and Enterococcus faecium, methicillin-safe and vancomycin-safe [70]. To improve the antibacterial action of different antibiotics, penicillin G, amoxicillin, erythromycin, clindamycin and vancomycin against *Staphylococcus aureus* and *Escherichia coli*, the silver nanoparticles assumes to be an extremely evident part. The antimicrobial movement of silver nanoparticles relies upon their size and Gram-positive microorganisms [71]. The little-sized nanoparticles with a vast surface range to volume proportion give a more effective intends to antibacterial action even at low fixation. Additionally, the antimicrobial action of silver nanoparticles relies on the fixation and shape [72]. The diverse shapes silver nanoparticles of circular, pole formed, truncated triangular nano-plates have been created by manufactured progressions [73]. Because of their

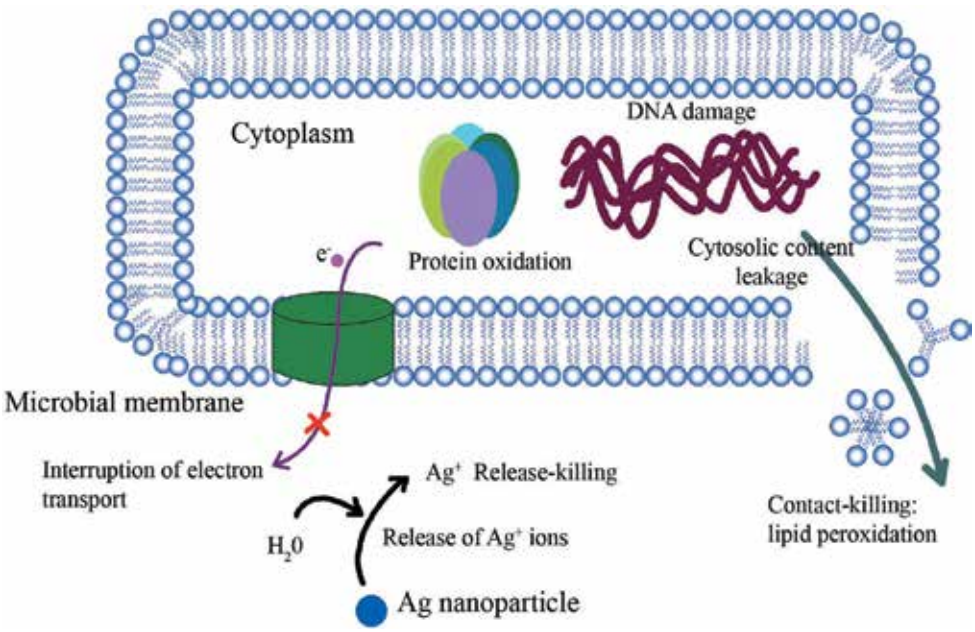

Figure 4. Silver nanoparticles rupturing the cell membrane.

expansive surface zone to volume proportions, truncated triangular silver nano-plates show the most grounded antibacterial action [74] (**Figure 4**).

6.1. Factors affecting the antimicrobial activity of silver nanoparticles

Silver nanoparticles are right now utilized as a part of the type of colloids, comprising mostly of diffused nano-metric silver particles, a stabilizing element and also act as a solvent [75]. Biological action of silver nanoparticles relies upon the morphology and physicochemical properties of the nanoparticles, and in addition the particular qualities of microorganisms which are dealt with by silver nanoparticles [76]. One can recognize various elements influencing the antimicrobial action, for example, shape, size and zeta (ζ) potential of the metal particles which impact the surface properties of the particles and the stabilizer, the pH of the suspension, ionic quality contaminants and so forth [77].

6.2. Mechanism of antibacterial activity of silver nanoparticles

Usually it is broadly recognized that the main antibacterial effect of silver nanoparticles or silver nanoparticles-based materials is due to the partial oxidation of nanoparticles and due to the release of the silver ions (Ag+) [78]. Later on the oxidation takes place, resulting the following actions that can happen either separately or simultaneously;

1. The uptake of the free silver ions (Ag+) followed by the interference of ATP production and DNA replication

2. Silver nanoparticles and silver ions (Ag+) interaction takes place with the bacterial proteins, by disrupting the synthesis of protein
3. Silver nanoparticles directly damage the cell membranes, interacting with the peptidoglycan wall cell and the plasmatic membrane causing cell-lysis [79].

7. Conclusion

In sum, the exploration of silver nanoparticle and related materials is established in this chapter. The availability, comparatively inexpensive price, ease of formation of nanoparticles and related materials and less toxic nature of silver as compared to other transition metals make silver and its nanoparticles special place in material science applications. The nanoparticles either prepared through natural extract or via synthetic routes from commercially available chemicals in laboratory both are of equal benefits when utilized in the development of functional materials. The polymers, emulsions, resins, natural extracts, carbohydrates, materials for water cleaning application, electronics, textiles and all related applications specially human health and environment make silver nanoparticles an essential addition.

Acknowledgements

Authors pay thanks to Higher Education Commission of Pakistan for providing funding for this project under project number HEC/NRPU/3422.

Author details

Mudassar Abbas[1]*, Nida Naeem[1], Hina Iftikhar[1] and Usman Latif[2]

*Address all correspondence to: mudassirabbas@yahoo.com

1 School of Textile and Design, University of Management and Technology, Lahore, Pakistan

2 Interdisciplinary Research Center in Biomedical Materials, COMSATS Institute of Information Technology, Lahore, Pakistan

References

[1] Perez DP, editor. Silver Nanoparticles. Rijeka: InTech Publishers; 2010

[2] Zhang P, Wyman I, Hu J, Lin S, Zhong Z, Tu Y. Silver nanowires: Synthesis technologies, growth mechanism and multifunctional applications. Materials Science and Engineering. 2017:1-23

[3] Goswami L, Kim K-H, Deep A, Das P, Sundar S, Kumar S, Adelodun AA. Engineered nano particles: Nature, behavior and effect on the environment. Journal of Environmental Management. 2017;**196**:297-315

[4] Ahamed M, Alsalhi MS, Siddiqui MKJ. Silver nanoparticle applications and human health. Clinical Chemica Acta. 2010;**411**(23):1841-1848

[5] Zhang P, Wyman I, Hu J, Lin S, Zhong Z, Tu Y. Silver nanowires: Synthesis technologies, growth mechanism and multifunctional applications. Materials Science and Engineering. 2017:1-23

[6] Mcgillicuddy E, Murray I, Kavanagh S, Morrison L, Fogarty A, Cormican M, Dockery P, Prendergast M, Rowan N, Morris D. Silver nanoparticles in the environment: Sources, detection and ecotoxicology. The Science of the Total Environment. 2017;**575**:231-246

[7] Duran N, Marcato DP, Alves LO, De Souza G, Esposito E. Mechanical aspect of biosynthesis of silver nanoparticles by several *Fusarium oxysporum* strains. Journal of Nanobiotechnology. 2005;**3**:8-15

[8] Marcato PD, Conti MR, Alves OL, Costa FTM, Brocchi M, Durán N. Potential use of silver nanoparticles on pathogenic bacteria, their toxicity and possible mechanisms of action. Journal of Brazillian Chemical Society. 2010;**21**:6949-6959

[9] Zahra Q, Fraz A, Anwar A, Awais M, Abbas MA. Mini review on the synthesis of Ag-nanoparticles by chemical reduction method and their biomedical applications. NUST Journal of Engineering Sciences. 2016;**9**(1):1-7

[10] Pal S, Tak YK, Song JM, Pal S. Does the antibacterial activity of silver nanoparticles depend on the shape of the nanoparticle? A study of the gram-negative bacterium *Escherichia coli*. Applied and Environmental Microbiology. 2007;**73**(6):1712-1720

[11] Singh MRJ, Bajaj R, Kaur H, Kaur H, Kaur N. Chemo-bio synthesis of silver nanoparticles. Journal of Nano Research. 2016;**4**(3):1-4

[12] Banerjee S, Loza K, Prymak O, Epple M. Structural evolution of silver nanoparticles during wet-chemical synthesis. Chemical Materials. 2014;**26**(2):951-957

[13] Logeswari P, Silambarasan S, Abraham J. Synthesis of silver nanoparticles using plants extract and analysis of their antimicrobial property. Journal of Saudi Chemical Society. 2015;**19**(3):311-317

[14] Vikas S, Selwal KK, Selwal MK. Nanosilver: Potent antimicrobial agent and its biosynthesis. African Journal of Biotechnology. 2014;**13**(4):546-554

[15] Shafqat S, Munir C, Abbas M. The sonochemical impregnation of silver particles into fluff pulp for enhanced antimicrobial efficacies. NUST Journal of Engineering Sciences. 2013;**6**(1):10-14

[16] Fayaz AM, Balaji K, Girilal M, Yadav M, Kalaichelvan MP, Venketesan R. Biogenic synthesis of silver nanoparticles and their synergistic effect with antibiotics: A study against

gram-positive and gram-negative bacteria. Nanomedicine: Nanotechnology, Biology, and Medicine. 2010;**6**(1):103-109

[17] Mano PM, Selvi BK, Paul JAJ. Green synthesis of silver nanoparticles from the leaf extracts of euphorbia hirta and nerium indicum. Digest Journal of Nanomaterials and Biostructures. 2011;**6**(2):869-877

[18] Naurani SJ, Saha CK, Khan MAR, Sunny SMH. Silver nanoparticles synthesis, properties, applications and future perspectives: A short review. International Journal of Electrical and Electronics Engineering. 2015;**10**(6):117-126

[19] Zhang W, Qiao X, Chen J. Synthesis and characterization of silver nanoparticles in AOT microemulsion system. Chemical Physics. 2006;**330**(3):495-500

[20] Amin M, Anwar F, Ramzan M, Ashraf S. Green synthesis of silver nanoparticles through reduction with Solanum Xanthocarpum L. Berry extract: Characterization, antimicrobial and urease inhibitory activities against helicobacter pylori. International Journal of Molecular Sciences. 2015;**13**:9923-9941

[21] Roy CN, Macgregor-ramiasa N, Zilm P. Chocolate silver nanoparticles: Synthesis, antibacterial activity and cytotoxicity. Journal of Colloid and Interface Science. 2006:1-25

[22] Natalia PL, Borsarelli CD, Rey V, Veglia AV. Synthetic routes for the preparation of silver nanoparticles a mechanistic. Perspective. 2015;**6**:13-46

[23] Whan CJ, So JH. Polyurethane–Silver fibers prepared by infiltration and reduction of silver nitrate. Materials Letters. 2006;**60**:2653-2656

[24] Abbas M, Leitgeb A, Klienbeger J, Slugovc C. Solvent-free synthesis of silver-nanoparticles and their use as additive in poly (Dicyclopentadiene). Journal of the Chemical Society of Pakistan. 2013;**35**(2):35-362

[25] Bonsak J, Jeyanthinath M, Marstein ES, Mahalingam U. Chemical synthesis of silver nanoparticles for solar cell applications. Phisica Status Solidic. 2011;**8**(3):924-927

[26] Hong X, Wen J, Xiong J, Hu Y. Silver nanowire-carbon fiber cloth nanocomposites synthesized by UV curing adhesive for electrochemical point-of-use water disinfection. Chemosphere. 2016;**154**:537-545

[27] Nicolle ST, Stefaniak AB, Vance ME, Rogers K, Mwilu S, Lebouf RF, Schwegler-berry D, Willis R, Thomas TA, Marr LC. Characterization of silver nanoparticles in selected consumer products and its relevance for predicting children's potential exposures. International Journal of Hygiene and Environmental Health. 2015:21831-21813

[28] Adit D, Wagle S, Jacobsen S, Melandsø F. Using silver nano-particle ink in electrode fabrication of high frequency copolymer ultrasonic transducers: Modeling and experimental investigation. Textile Engineering and Fashion Design Blog. 2015;**23**(2):9210-9227

[29] Usha M, Roy AS, Kundu SK, Roy S. Mesoporous polyacrylic acid supported silver nanoparticles as an efficient catalyst for reductive coupling of nitrobenzenes and

alcohols using glycerol as hydrogen source. Journal of Colloid and Interface Science. 2016;**472**:202-209

[30] Hiroshl H, Yoshida A, Kurakake A. Photoreduction of silver ion in aqueous and alcoholic solutions. The Journal of Physical Chemistry. 1976;**80**(25):2728-2731

[31] Sunghyun N, Parikh DV. Importance of poly (ethylene glycol) conformation for the synthesis of silver nanoparticles in aqueous solution. Journal of Nanoparticle Research. 2011;**13**(7):3755-3764

[32] Gulina LB, Tolstobrov EV, Tolstoi VP. Silver nanoribbons synthesized on a silicon surface by the 'layer-by-layer' technique. Russian Journal of General Chemistry. 2010;**80**(6):1149-1151

[33] Rajasekhar M, Marimuthu J, Nithya M. Synthesis and characterization of silver nano composite polyaniline. International Journal of Engineering Research and Applications. 2011;**6**(5):1-3

[34] Harifi T, Montazer MA. Review on textile sonoprocessing: A special focus on sonosynthesis of nanomaterials on textile substrates. Ultrasonics Sonochemistry. 2010;**23**:1-10

[35] Dankovich TA, Gray DG. Bactericidal paper impregnated with silver nanoparticles for point-of-use water treatment. Environmental Science and Texhnology. 2011;**45**(5): 1992-1998

[36] Wankhede YB, Kondawar SB, Thakare SR, More PS. Synthesis and characterization of silver nanoparticles embedded in polyaniline nanocomposite. Advanced Materials Letters. 2013;**4**(1):89-93

[37] Olayinka OJ, Dare EO, Adetunji OR, Adedeji OO, Ogungbesan SO. Synthesis and characterization of chitosan-silver nanocomposite film. Nano Hybrids and Composites. 2016;**11**:22-29

[38] Bhattacharyya M, Joshi A. Nanotechnology–A new route to high-performance functional textiles. Textile Progress. 2011;**43**(3):155-233

[39] Boroumand MA, Namvar F, Moniri M, Tahir P, Azizi S, Mohamad R. Nanoparticles biosynthesized by fungi and yeast: A review of their preparation, properties, and medical applications. Molecules. 2015;**20**:16540-16565

[40] Mahboubeh R, Mortazavi SA, Yazdi FT. Silver nanocomposite and its antimicrobial effect in reducing microbial load of cakes. International Journal of Agriculture and Crop Sciences. 2014;**7**(8):430-432

[41] Xupin Z, Cheng B, Kang W, Xu X. Electrospun chitosan/gelatin nanofibers containing silver nanoparticles. Carbohydrate Polymers. 2010;**82**(2):524-527

[42] Goudarzir EH, Montazer M, Laftifi M, Akbar A, Aghaji G. Electrospinning of chitosan/sericin/PVA nanofibers incorporated with in situ synthesis of nano silver. Carbohydrate Polymers. 2010;**113**:231-239

[43] Seon KE, Kim SH, Lee CH. Electrospinning of polylactide fibers containing silver nanoparticles. Macromolecular Research. 2010;**18**(3):215-221

[44] Urrutia A, Rivero PJ, Goicoechea J, Rodrígue Y, Arregui FJ, Matias R. Silver Nanoparticles Loaded Electrospun Nanofibers for Humidity Optical Fiber Sensing; 2012

[45] Khan N. Applications of electrospun nanofibers in the biomedical field. SURG. 2012;**5**(2): 63-73

[46] David L, Espuche E, Lyon D. Structure and morphology of nanocomposite films prepared from polyvinyl alcohol and silver nitrate: Influence of thermal treatment. Journal of Polymer Science. 2007;**35**(13):2657-2672

[47] Kumar-krishnan S, Prokhorov E, Hernández-iturriaga M, Mota-morales JM, Vázquez-lepe M, Kovalenko Y, Sanchez IC, Luna-bárcenas G. Chitosan/silver nanocomposites: Synergistic antibacterial action of silver nanoparticles and silver ions. European Polymer Journal. 2015;**67**:242-251

[48] Govindan S, Nivethaa EAK, Saravanan R, Narayanan V, Stephen A. Synthesis and characterization of chitosan-silver nanocomposite. Applied Nanoscience. 2012;**2**(3):299-303

[49] Parikh DV, Fink T, Rajasekharan K, Sachinvala ND, Calamari TA, Parikh AD. Antimicrobial silver/sodium carboxymethyl cotton dressings for burn wounds. Textile Research Journal. 2005;**75**(2):134-138

[50] Pourjavadi A, Soleyman R. Novel silver Nano-wedges for killing microorganisms. Materials Research Bulletin. 2011;**46**(11):1860-1865

[51] Nurani SJ, Saha CK, Khan AR. Silver nanoparticles synthesis, properties, applications and future perspectives: A short review Sharif Masnad Hossain Sunny. Journal of Electrical and Electronics Engineering. 2015;**10**(6):117-126

[52] Khan Z, Ijaz J, Adil A. Preparation and characterization of silver nanoparticles using aniline. Arabian Journal of Chemistry. 2013;**10**(2):1-6

[53] Kumar A, Ghosh A. Biosynthesis and characterization of silver nanoparticles with bacterial isolate from gangetic- alluvial soil. International Journal of Biotechnology and Biochemistry. 2016;**12**(2):95-102

[54] Klapetek P, Valtr M, Ne D, Salyk O, Dzik P. Atomic force microscopy analysis of nanoparticles in non-ideal conditions. Nanoscale Research Letters. 2011:1-9

[55] Kumari J, Baunthiyal M, Singh A. Characterization of silver nanoparticles synthesized using urtica dioica Linn leaves and their synergistic effects with antibiotics. Journal of Radiation Research and Applied Science. 2015;**9**(3):217-227

[56] Min J. SEM/EDX and XRD characterization of silver nanocrystalline thin film prepared from organometallic solution precursor. Journal of Mining and Metallurgy. 2009;**49**(1): 91-95

[57] Hellmers J, Riefler N, Wriedt T, Eremin YA. Light scattering simulation for the characterization of sintered silver nanoparticles. Journal of Quantitative Spectroscopy and Radiative Transfer. 2008;**108**(8):1363-1373

[58] Hussain JI, Kumar S, Hashmi AA, Khan Z. Silver nanoparticles: Preparation, characterization, and kinetics. Advanced Materials Letters. 2011;**2**(3):188-194

[59] Srivastava G, Narayan RP, Kumar P. Synthesis and characterization of silver nanoparticles using transmission electron microscopy (TEM) and nanoparticle tracking analysis (NTA) technique. Journal of Biological Sciences and Medicine. 2017;**3**(1):1-4

[60] Kumar A, Ghosh A. Biosynthesis and characterization of silver nanoparticles with bacterial isolate from gangetic-alluvial soil. International Journal of Biotechnology and Biochemistry. 2016;**12**(2):95-102

[61] Satish B, Ahmadipour M, Narisngam S, Kalagadda VR, Chidurala SC. Extensive studies on X-ray diffraction of green synthesized silver nanoparticles. Advances in Nanoparticles. 2015;**4**(1):1-10

[62] Hussain IJ, Kumar S, Hashmi AA, Khan Z. Silver nanoparticles: Preparation, characterization and kinetics. Advanced Materials. 2011;**2**(3):188-194

[63] Min J. SEM/EDX and XRD characterization of silver nanocrystalline thin film prepared from organometallic solution precursor. Journal of Mining and Metallurgy. 2015;**49**(1):91-95

[64] Kumar BD, Bar W, Sarkar P, Sahoo GP, De SP, Misra A. Synthesis and UV-vis spectroscopic study of silver nanoparticles in aqueous SDS solution. Journal of Molecular Liquids. 2009;**145**(1):33-37

[65] Lim J, Park WH. Preparation and characterization of gelatin nanofibers containing silver nanoparticles. International Journal of Molecular Sciences. 2014;**15**:6857-6879

[66] Haase A, Mantion A, Graf P, Plendl J, Thuenemann AF, Meier W, Taubert A, Luch A. A novel type of silver nanoparticles and their advantages in toxicity testing in cell culture systems. Archives of Toxicology. 2012;**867**:1089-1098

[67] Ibrahim HMM. Green synthesis and characterization of silver nanoparticles using banana peel extract and their antimicrobial activity against representative microorganisms. Journal of Radiation Research and Applied Science. 2015;**8**(3):265-275

[68] Ouay BL, Francesco S. Antibacterial activity of silver nanoparticles: A surface science insight. Nano Today. 2015;**10**(3):339-354

[69] Hyeong-seon L, Ryu D-S, Choi S-J, Lee D-S. Antibacterial activity of silver-nanoparticles against *Staphylococcus aureus* and *Escherichia Coli*. Korean Journal of Microbiolology Biotechnology. 2011;**39**(1):77-85

[70] Juanni C, Li S, Luo J, Wang R, Ding W. Enhancement of the antibacterial activity of silver nanoparticles against phytopathogenic bacterium *Ralstonia solanacearum* by stabilization. Journal of Nanomaterials. 2016:1-15

[71] Simoncic B, Tomsic B. Structures of novel antimicrobial agents for textiles–A review. Textile Research Journal. 2010;**80**(16):1721-1737

[72] Hungund BS, Dhulappanavar GR, Ayachit NH. Comparative evaluation of antibacterial activity of silver nanoparticles biosynthesized using fruit juices. Nanomaterials and Nanoscience. 2015;**6**(2):1-6

[73] Juanni C, Li S, Luo J, Wang R, Ding W. Enhancement of the antibacterial activity of silver nanoparticles against phytopathogenic bacterium *Ralstonia solanacearum* by stabilization. Journal of Nanomaterials. 2016:1-15

[74] Rai M, Ingle RP, Paralikar R, Gupta I, Medici S, Carolina AS. Recent advances in use of silver nanoparticles as antimalarial agents. International Journal of Pharmaceutics. 2017:1-44

[75] Bankura KP, Maity D, Mollick MMR, Mondal D, Bhowmick B, Bain MK, Chakraborty A, Sarkar J, Acharya K, Chattopadhyay D. Synthesis, characterization and antimicrobial activity of dextran stabilized silver nanoparticles in aqueous medium. Carbohydrate Polymers. 2012;**89**(4):1159-1165

[76] Humberto P. Antimicrobial polymers with metal nanoparticles. International Journal of Molecular Sciences. 2015;**16**:2099-2116

[77] Li R, Chen J, Cesario TC, Wang X, Yuan JS, Peter MR. Synergistic reaction of silver nitrate, silver nanoparticles, and methylene blue against bacteria. PNAS. 2016;**113**(48): 13612-13617

[78] Singh M, Mallick AK, Banerjee M, Kumar R. Loss of outer membrane integrity in gram-negative bacteria by silver nanoparticles loaded with camellia Sinensis leaf phytochemicals: Plausible mechanism of bacterial cell disintegration. Bulletin of Materials Science. 2016;**39**(7):1871-1878

[79] Thombre R, Vinaya S, Thaiparambil E, Zende S, Mehta S. Antimicrobial activity and mechanism of inhibition of silver nanoparticles against extreme Halophilic archaea. Frontiers in Microbiology. 2016;**7**:1-17

Applications

Chapter 5

Application of Silver Nanoparticles for Water Treatment

Zenaida Guerra Que, José Gilberto Torres Torres,
Hermicenda Pérez Vidal,
María A. Lunagómez Rocha, Juan C. Arévalo Pérez,
Ignacio Cuauhtémoc López,
Durvel De La Cruz Romero,
Alejandra E. Espinosa De Los Monteros Reyna,
José G. Pacheco Sosa, Adib A. Silahua Pavón and
Jorge S. Ferráez Hernández

Additional information is available at the end of the chapter

http://dx.doi.org/10.5772/intechopen.74675

Abstract

In recent past development of silver nanoparticles and their application in the treatment of wastewaters is becoming a major area of research. It is mainly applicable to the removal of three major pollutants like pesticides, heavy metals, and microorganisms. Variety of synthesis techniques have been reported for preparation and characterization of silver nanoparticles. In our research, we synthesized Ag nanoparticles supported on ZrO_2 and ZrO_2-CeO_2 by a "deposit-precipitation method" as the first step and later sequentially synthesized Ag-Au supported on ZrO_2 and ZrO_2-CeO_2 by Redox method. Catalysts were evaluated in catalytic wet air oxidation (CWAO) of methyl tert-butyl ether and phenol. The CWAO is a liquid phase process for the treatment of organic pollutants operating at temperatures in the range of 100–325°C at 5–200 bar pressures. The selectivity and efficient of catalysts were evaluated by total organic carbon (TOC) and high-performance liquid chromatograph (HPLC). Ideally, the total mineralization of pollutants into CO_2 and H_2O is preferred.

Keywords: silver nanoparticles, wastewaters, catalytic wet air oxidation, phenol, MTBE

1. Introduction

1.1. Refractory organic compounds in wastewater

Many factors have contributed to the deterioration of our environment, among them the exponential growth of the world population, the industrial sector excessive exploitation of the natural resources on earth, the generation of waste as a result of the activities by the aforementioned and the irrational consumption of the domestic sector. A large number of anthropogenic activities generate wastewater as a product of the processes that are carried out by the chemical, petrochemical, pharmaceutical, textile, agriculture and domestic sectors [1].

The conventional processes applied for water treatment have not been effective enough which can be evidenced worldwide showing that there are high concentrations of toxic, dangerous substances of the carcinogenic type, teratogenic and mutagenic, in surface and groundwater bodies of fresh water.

Freshwater is the most valuable resource we have since all the metabolic processes of the human body (reproduction, growth, development) are regulated by the presence of this fundamental substance. It is for these reasons that water pollution is a severe environmental problem, which is why strict water quality regulations have been implemented [2, 3].

In domestic, industrial, service or wastewater there are refractory organic compounds that by their chemical constitution are not susceptible to microorganisms in the aerobic digester to take advantage of it to obtain energy. Refractory molecules are organic compounds that are present in aqueous residues, formed by solid non-sedimentable particles of colloidal size, which as they are not biodegradable or even toxic thus cannot be treated by conventional methods since they show resistance to biological degradation from microorganisms, therefore, after the application of conventional treatments, remain present [4, 5]. These organic compounds tend to resist conventional methods of wastewater treatment [6]. The current conventional technologies available for wastewater treatment, whose processes can be physical, chemical and biological are very diverse and have been used to remove aqueous pollutants [7].

In general, conventional processes are frequently classified as preliminary, primary, secondary (biological) and tertiary treatments. Specifically, the biological treatment is designed to eliminate the dissolved organic load of the waters using microorganisms. The microorganisms used are responsible for the degradation of organic matter. The aerobic treatment of wastewater converts organic pollutants into wastewater in a good amount of excess sludge and oxidizes the remainder with oxygen to carbon dioxide [8, 9]. The treatments depend on the aerobic or anaerobic organics, for example, the *Ochrobactrum cytisi* is an aerobic bacterium used to degrade methyl tert-butyl ether (MTBE). In the aerobic mechanism, oxygen is essential for successful operation of the systems [10].

In most applications of conventional wastewater treatment, the complete oxidation of organic pollutants to carbon dioxide and water is difficult to achieve due to the formation of even more refractory intermediates such as short chain carboxylic acids. As a consequence, the combination of processes has a great potential benefit, chemical treatment of advanced oxidation (unconventional) and then the conventional biological that could be a more efficient way

to reduce pollution; this has been presented as a strategy. For such a case, chemical oxidation is needed to destroy persistent molecular structures, remove high ecotoxicity and improve solubility in water [9, 11].

1.2. Environmental impact of refractory organic compounds

The persistent or refractory organic pollutants, such as phenols and derivatives, polycyclic aromatic hydrocarbons (PAHs), polychlorinated by phenyls (PCBs), pesticides or even other organic compounds, are very slowly metabolized or otherwise degraded. Since long, plant protection products, substituted phenols, non-biodegradable chlorinated solvents, PAHs, PCBs, and surfactants are recognized as examples of relevant substances, because of the environmental damage they cause [2, 7].

The Phenol and phenolic compounds are harmful from the human health; they can cause tissue detachment, necrosis, digestive delay, kidneys and liver damage. Furthermore, if the discharge is at very low concentrations, they are highly dangerous to aquatic life and transfer a particularly unpleasant smell and taste [9, 12]. MTBE is a suspected human carcinogen by the US Environmental Protection Agency, which is hazardous to human health [10]. Therefore, it is essential to treat water contaminated properly with refractory organic compounds before being discharged to freshwater bodies.

1.3. Non-conventional treatment for the degradation of refractory organic compounds

The unconventional treatment methods include membrane separation, adsorption by activated carbon, the Fenton Process, oxidation using H_2O_2/UV, advanced oxidation processes (AOPs) and chemical oxidation technologies. The environmental technologies play an important role in de-coupling environmental from economic growth. Advanced treatment technologies have been demonstrated to remove various potentially harmful compounds that could not be effectively removed by conventional treatment process [8, 9, 13, 14].

The objective of oxidative treatment processes is frequently to rapidly convert organic molecules to carbon dioxide, water, and innocuous products by exploiting chemical principals in order to surmount the kinetic restraints, which are responsible for the slowness of some of the reactions. AOPs have been roughly defined as near ambient temperature treatment processes based on highly reactive radicals, especially the hydroxyl radical (.OH). The .OH radical is among the strongest oxidizing species used in water and wastewater treatment and offers the potential to greatly accelerate the rates of contaminant oxidation. The generation of OH, radicals are commonly accelerated by combining ozone (O_3), hydrogen peroxide (H_2O_2), titanium dioxide (TiO_2), heterogeneous photocatalysis, UV radiation, ultrasound, and (or) high electron beam irradiation [15].

Besides, the Catalytic Wet Air Oxidation process (CWAO) has been adopted for wastewater with very low concentrations of contaminants that cannot be incinerated or very high concentrations that cannot be biologically treated. The main efforts in research are frequently directed to reach the total oxidation of organic effluents in wastewater under less severe conditions in the presence of homogeneous or heterogeneous catalysts [16, 17].

CWAO is regarded one of the most important industrial processes to destroy hazardous, toxic and non-biodegradable organic compounds present in wastewater streams. The process involves the use of a trickle-bed or slurry reactors operating at temperatures in the range of 100–325°C at 5–200 bar pressures, with oxygen as oxidant agent, using a supported catalyst [18–20].

1.4. Silver nanoparticles supported applied in the degradation of organic matter

Currently, efforts have been directed to conduct studies of silver nanoparticles (NPS) in organic matter oxidation due to the persistence of certain molecules after conventional degradation treatments, or to their partial oxidation to obtain precursors for other valuable products in the industry.

Noble metals have been widely used in the CWAO of model compounds, as well as in real wastewater due to their excellent catalytic activities. One of these metals is the finely dispersed nanometer-sized silver particles that have been studied by various authors, as an ideal feature for outstanding catalytic properties [21–24].

Metal nanoparticles have been widely studied because they have excellent optical, mechanical, electrical, magnetic, and chemical properties. These properties are generally the product of the large surface area possessed by the nanoparticles due to the reduction in size. Recently, metallic nanoparticles have turned out to be very attractive for their commercial development, which is why their production has increased in different industries such as aeronautics, agriculture, food, automotive, biomedical, cosmetic, pharmaceutical, computer, textile, catalysis, among others [25, 26].

Metals such as gold, silver, palladium, and copper are used for the manufacture of nanoparticles of different shapes and sizes. The techniques and conditions when the synthesis is performed the nanoparticles are directly influenced by the morphology and physical–chemical properties of these. Of all the metal NPS, in this chapter, we will discuss silver and gold for their catalytic application.

2. Silver nanoparticles supported on metal oxides for the catalytic wet air oxidation of refractory organic compounds

The technology used for the mineralization of refractory organic matter, has different types of treatments, which we will discuss this chapter, it will be focused on the CWAO, which is based on a reaction in the presence of oxygen on the problem molecule (phenol, MTBE) in which is used inorganic catalysts, at a certain pressure and specific temperature, with the aim of the total or almost total degradation of the pollutant.

2.1. Silver nanoparticles supported applied in the degradation of organic matter

Organic matter is composed mainly of proteins, carbohydrates, and fats, biodegradable organics measured in terms of biochemical oxygen demand (BOD) and chemical oxygen demand

(COD). If there is untreated discharge to the environment, its biological stabilization can cause the depletion of natural oxygen sources and the quality of fresh water in available sources [9].

The silver nanoparticles, in particular, are exceptional due to their excellent optical, thermal, catalytic, electromagnetic, adsorbent and antimicrobial properties, which differ greatly to the properties that silver presents in volumetric sizes. This is due to the reduction in size which produces an increase in the surface area in relation to the volume, as well as the shape of the nanoparticle [27–30]. The optical properties of nanoparticles strongly depend on the particle size and the refractive index of the medium. The dependencies of these properties with respect to particle size can be of two kinds, due to the increase in energy caused by the quantum confinement of the system or by the resonance of the surface plasmon [30, 31]. The surface plasmons are defined as the collective oscillation of conduction electrons on the surface of the particle, as a result of the interaction with the electric field of electromagnetic radiation [31, 32].

2.2. Au-Ag bimetallic nanoparticles supported in oxide

The supported bimetallic gold-silver nanoparticles have been reported in various reactions of CO oxidation, photoreaction of phenol degradation among others. In addition to the chemical relationship between the metals, the proportions of the mesoporous support in the case of mixed oxides have a remarkable effect on the catalytic activity [33–37]. Many experiments show that the modification of the structure of the support surface or the morphology can result in the improvement of the catalytic activity in case of the oxidation of CO [34, 38]. Modifying nanoparticle systems with such characteristics are procedures that require a deep study of the physicochemical properties of the materials in question, Au-Ag nanoparticle alloys which is a system that is currently studied for oxidation systems and has peculiarities that are of special scientific attention For example, particle size no longer plays a key role in the determination of catalytic activity, while the composition of the Au:Ag ratio becomes important [34]. However, this type of mixed nanoparticle has been studied as "inert" systems and it is not clear how it affects the support in the alloy particle, size and catalytic activity [37].

That is why our research group was interested in working with noble metals (Ag, Au) and evaluating them in CWAO, since it has been little studied, despite its interesting properties in catalytic oxidation. Next, we present the most relevant synthesis methods, results and conclusions of Ag and Au-Ag nanoparticles supported on ZrO_2 and ZrO_2-CeO_2 for the degradation of phenol and MTBE.

3. Synthesis, characterization and catalytic activity of silver nanoparticles

The NPS of Ag^0 can be manufactured using a large number of methods such as electric, chemical reduction, photochemistry, among others [39]. The reduction technique is the most economical and used method due to its large-scale manufacturing and easy handling [40–42].

From these methods, our research group decided to carry out different strategies: (1) sol–gel method to obtain simple (ZrO_2) and mixed (ZrO_2-CeO_2) supports, (2) deposit-precipitation with NaOH for the synthesis of NPS of Ag, (3) with urea to obtain the bimetallic materials, (4) sequential deposit precipitation method to introduce the Au and obtain the bimetallic (Au-Ag), and (5) oxide-reduction method to introduce a second metal (Au) and obtain bimetals. The materials were evaluated in the catalytic activity using probe molecules: phenol and MTBE.

3.1. Synthesis of silver monometallic catalysts for deposition-precipitation using NaOH

Brackets of simple zirconium oxides (Zr) and mixed oxides (Zr-Ce) were initially prepared by the sol-gel method. After addition of the metal (Ag) by the deposition-precipitation method which is a modification of the precipitation methods in solution. It consists of the conversion of a highly soluble metal precursor into another substance of low solubility, which precipitates specifically on the support and not in the solution [43].

3.2. Synthesis of Au-Ag bimetallic catalysts for sequential deposition-precipitation using urea

The materials that were synthesized have a 1:1 molar ratio of Ag:Au.

The addition of the second metal (Au) was done by the deposit-precipitation method, with a slight modification to the synthesis process, this is because the second metal is gold, these gold nanoparticles are very sensitive to the preparation method, the choice of the support or the treatment conditions, for which the deposit-precipitation process with urea was chosen [44].

At the end of the synthesis of the catalysts, materials with a weight concentration of 1.4% silver supported in the oxides were obtained.

3.3. Synthesis of Au-Ag bimetallic catalysts by recharge or redox

The selective deposition of Au on the surface of nanoparticles of a primary oxide-supported metal has been performed by a redox method that is based on the reduction of the second metal ions with hydrogen adsorbed on the surface of first metal or with itself [45].

The bimetallic catalysts were prepared by the recharge method, reducing $HAuCl_4^-$ (from $HAuCl_4$) with pre-adsorbed hydrogen on the silver surface. An amount of 2 g silver monometallic catalyst supported on zirconia and mixed oxides of pre-reduced zirconia-ceria was introduced into a reactor under nitrogen flow and was activated at 400°C for 1 h under a hydrogen atmosphere. Next, the solution of the gold precursor, previously degassed under a stream of nitrogen, was introduced onto the catalyst, taking an amount sufficient to synthesize a 1:1 molar ratio. After a reaction time of 1 h under hydrogen bubbling at room temperature, the bimetallic catalyst is dried with hydrogen at room temperature, then at 100°C (heating rate 2°C/min) overnight. Finally, the five bimetallic catalysts synthesized were reduced under a stream of hydrogen at 400°C for 1 h, with a heating rate of 2°C/min [45–47].

3.4. Degradation of pollutants (methyl tert-butyl ether and phenol) by catalytic wet air oxidation over Ag/ZrO_2-CeO_2

All catalysts were tested in a high-pressure stainless steel batch reactor (Parr Instruments) equipped with sampling valve, magnetically driven stirrer, gas supply system and temperature controller. The Catalytic Wet Air Oxidation reaction was carried out as follows: using a reaction volume of 300 mL of an aqueous solution with a concentration of 440 ppm and 1 g/L of the monometallic catalyst. After the reactor was heated at 100°C to reach the desired temperature, pure oxygen (O_2) at 8 bar was added under stirring. The catalysts were previously reduced at 400°C during 3 h with an H_2 flow (60 ml/min). The reaction was performed for 60 min. The samples in the effluent were taken at intervals of 10 min through 1 h, and the MTBE content (C), intermediate content and Total Organic Carbon (TOC) were analyzed. MTBE content and intermediate content were measured with High-Performance Liquid Chromatograph (HPLC). Total Organic Carbon (TOC) of the samples was measured with a TOC 5000 Shimadzu Analyzer. The conversion of MTBE and phenol, respectively, for the different materials and the TOC was calculated using:

$$X_{pollutant} = \frac{C_0 - C_{60}}{C_0} \times 100\%$$

$$X_{TOC} = \frac{TOC_0 - TOC_{60}}{TOC_0} \times 100\%$$

where TOC_0 is Total organic carbon at t = 0 (ppm), C_0 is the MTBE or Phenol concentration at t = 0 (ppm), C_{60} is the MTBE or Phenol concentration at t = 1 h of reaction (ppm), TOC_{60} is total organic carbon at t = 1 h of reaction (ppm). So the selectivity was calculated according to following equation [48].

$$S_{CO_2} = \frac{X_{TOC}}{X_{mtbe}} \times 100$$

The initial rate (r_i) was calculated from the MTBE or phenol conversion as a function of time, using the following equation:

$$r_i = \left(\frac{\Delta_{mtbe}(\%)}{\Delta t\, m_{cat}}\right) \left([pollutant]_i \right.$$

where $\frac{\Delta_{mtbe}(\%)}{\Delta t}$, $\frac{\Delta_{phenol}(\%)}{\Delta t}$ is the conversion at initial time; $[pollutant]_I$ = initial concentration of the pollutant and m_{cat} = mass of catalyst ($g_{cat}L^{-1}$).

3.5. Characterization of monometallic nanoparticles (Ag) y bimetallic of Au-Ag supported on Simple and mixed oxides of ZrO_2 and ZrO_2-CeO_2

In **Table 1** the materials studied are listed, the nomenclature is Ag/ZrO_2-Cex and Au-Ag/ZrO_2-Cex, where X = % cerium.

Nomenclature	Supports and catalysts	Synthesis method					Molecular probe	
		Sol–Gel	Deposit-precipitation			Redox method		
			NaOH	Urea	Urea: sequential		MTBE	Phenol
	Supports							
S1	ZrO_2	x						
S2	ZrO_2-Ce0.5	x						
S3	ZrO_2-Ce1	x						
S4	ZrO_2-Ce5	x						
S5	ZrO_2-Ce10	x						
S6	ZrO_2-Ce15	x						
S7	ZrO_2-Ce20	x						
	Monometallic							
M1	Ag/ZrO_2		x				x	x
M2	Ag/ZrO_2-Ce0.5		x					x
M3	Ag/ZrO_2-Ce1		x					x
M4	Ag/ZrO_2-Ce5		x				x	x
M5	Ag/ZrO_2-Ce10		x				x	x
M6	Ag/ZrO_2-Ce15		x				x	x
M7	Ag/ZrO_2-Ce20		x				x	x
	Bimetallic							
B1-U*	Au-Ag/ZrO_2			x	x			x
B2-U*	Au-Ag/ZrO_2-Ce0.5			x	x			x
B3-U*	Au-Ag/ZrO_2-Ce1			x	x			x
B4-U*	Au-Ag/ZrO_2-Ce5			x	x			x
B5-U*	Au-Ag/ZrO_2-Ce10			x	x			x
B6-U*	Au-Ag/ZrO_2-Ce15			x	x			x
B7-U*	Au-Ag/ZrO_2-Ce20			x	x			x
B1-R*	Au-Ag/ZrO_2					x	x	
B2-R*	Au-Ag/ZrO_2-Ce5					x	x	
B3-R*	Au-Ag/ZrO_2-Ce10					x	x	
B4-R*	Au-Ag/ZrO_2-Ce15					x	x	
B5-R*	Au-Ag/ZrO_2-Ce20					x	x	

S = supports (1–7), Mx = monometallic, By-U* = bimetallic from urea y Bz-R = bimetallic by the redox method. x = 1–7, y = 1–7, z = 1–5.

Table 1. Method of synthesis of Ag and Ag-au/ZrO_2-Cex, and catalytic evaluation: phenol and MTBE.

The real properties were determined by the Brunauer-Emmett-Teller method (BET) and the average pore diameter was estimated by the BJH method. The real values of the supports (S1 and S7) indicate that the specific area did not vary significantly (S_{BET} 72–63 m^2/g) when increasing the cerium content and the average pore diameter was 3.6 and 3.3 nm. When depositing Ag (M1 and M7) it was 68 and 49 m^2/g, respectively, and, with Au, samples B1 and B7 were 69 and 62 m^2/g. There are no significant changes in these properties in the synthesized materials. All the isotherms were of the type IV characteristics of well-defined mesoporous systems. The shape of the hysteresis loop was H_2 type according to the IUPAC classification. All materials have a unimodal pore size distribution.

In the X-ray diffraction patterns (XRDs) of the supports (**Figure 1**), diffraction planes (101), (110), (112) and (211) are observed, having as the main peak the plane (101) located at 30.11° on a 2θ de scale; these planes are characteristic of the tetragonal phase of ZrO_2 with a spatial group of *P42/nmc* and reported cell parameters of a = b = 3.612 Å and c = 5.212 Å and angles for $\alpha = \beta = \gamma = 90°$ [49].

As the concentration of ceria increases in the surface of ZrO_2 it stabilizes the tetragonal phase of it and this is easily appreciated when taking as reference the material Au-Ag/ZrO_2 in which a small peak is observed in 28.41° in 2θ, characteristic of the monoclinic phase of ZrO_2 [50], this peak disappears in the materials synthesized with a concentration of 5% CeO_2 (Au-Ag/ZrO_2-Ce5) at 20% CeO_2.

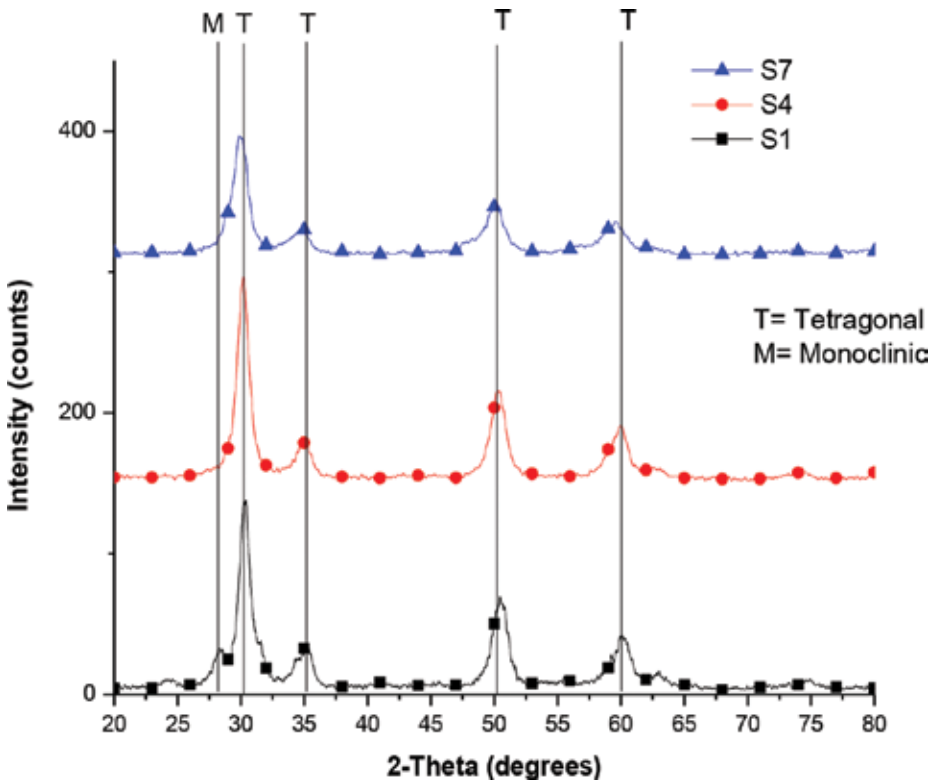

Figure 1. X-ray diffraction pattern of S1, S4 and S7 supports.

The average crystal size was calculated using the Scherrer equation [51]. The results indicate that the crystal average decreased when CeO_2 of 9.50 nm was added in ZrO_2 at 8.36 nm in ZrO_2-Ce0.5 and, 6.33 nm in ZrO_2-Ce20 (S7). When the Ag was supported in these materials values of 8.36, 8.04 and 6.52 nm were recorded in Ag/ZrO_2, Ag/ZrO_2-Ce0.5 and Ag/ZrO_2-Ce20, respectively, and, when introducing the second metal (Au) in these bimetallic materials the values were as follows: 9.09, 8.36, and 6.33 nm. The estimated average crystallite size varies depending on the concentration of cerium in the structure of ZrO_2 in the case of supports, but changes when depositing the Ag on the surface of the material, the smaller average size of the crystal was for the materials S7, M7, and B7. In the bimetals (Au-Ag) the size of the crystallites does not vary much in relation to the supports. If they are of a larger size, they decreased in size, this is due to the sequential precipitation deposition method, which not only deposits the second metal (Au) in the system's matrix but also redisperses the entire system, recovering the crystal size of the support.

The crystalline phases of the support (S1–S7) and the monometallic catalysts (M1–M7) are similar, and there are no differences in the diffraction peaks (**Figure 2**), so the amount of Ag that was deposited on the support formed no agglomerations of the metal, forming silver nanoparticles well dispersed in the material, this is corroborated by the UV-Vis with DRS (surface plasmon) and the TPD of H_2 of the materials.

In the XRD diffractograms of the bimetallic materials (**Figure 3**), a small peak could be observed at 38.33° in 2θ, attributed to the diffraction of silver or gold, of which the two elements have

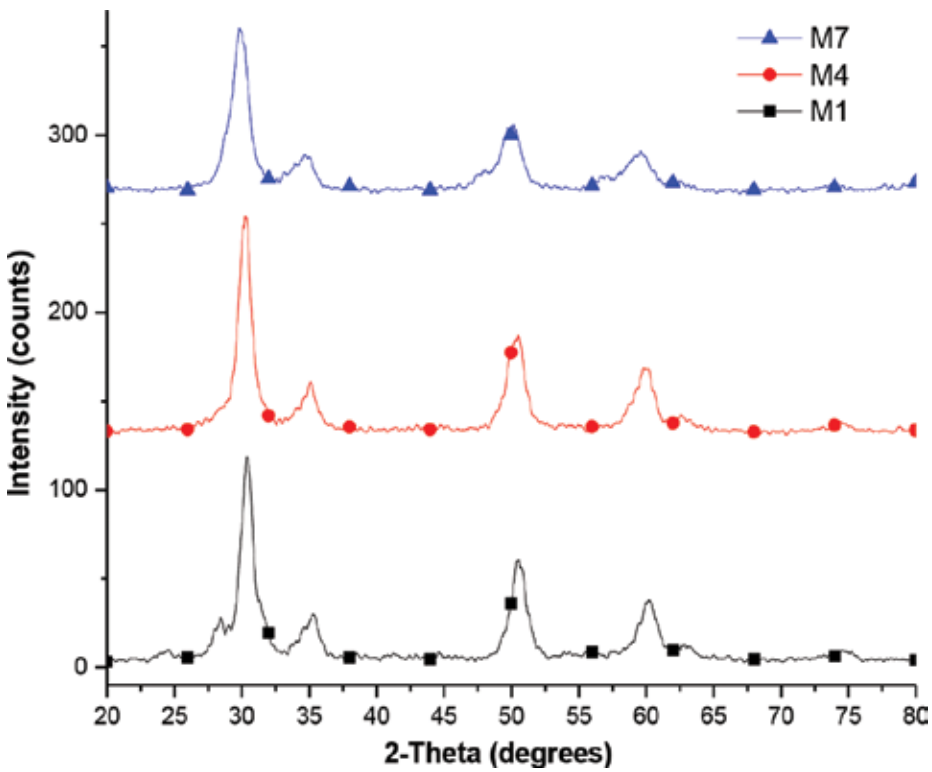

Figure 2. X-ray diffraction of M1, M4 and M7, monometallic catalysts.

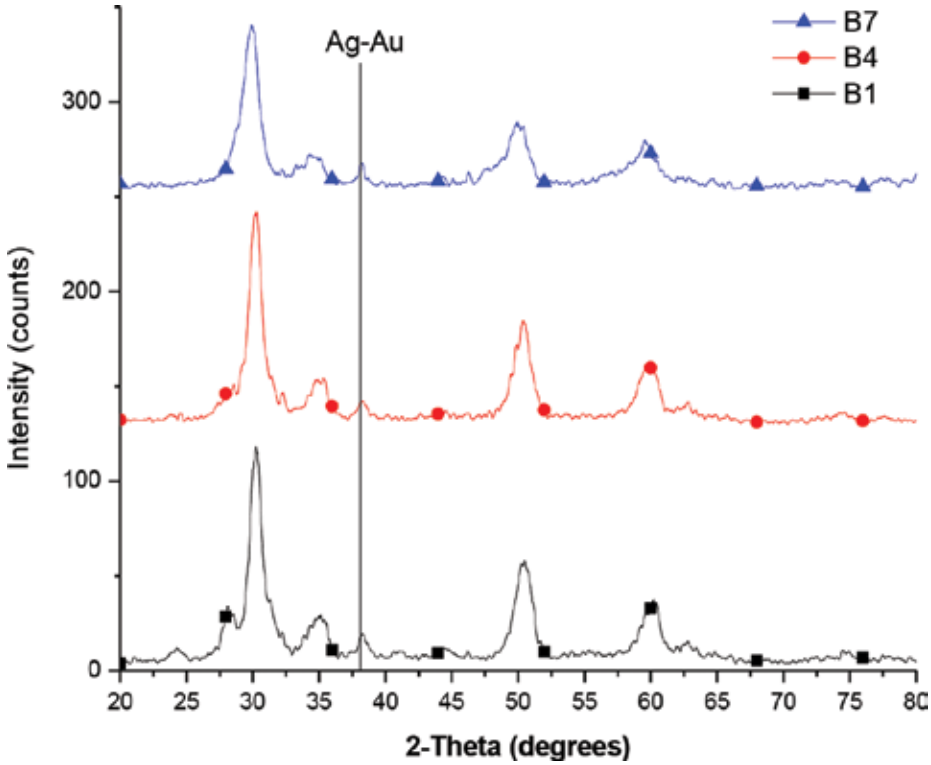

Figure 3. X-ray diffraction pattern of B1, B4 and B7, bimetallic catalysts.

diffraction peaks in the same region due to having a similar crystalline structure (fcc, cubic centered on the faces). Since the concentration of silver is relatively low (1.4% by weight), the equipment does not detect peaks in the DRXs in the monometallic, but when depositing the gold 1:1 molar, the concentration of the metals together reaches ~4% by weight.

Below are the TPD of H_2, TPD-NH_3, and TPR-H_2

3.5.1. H_2 of TPD

The accessibility of the silver and silver-gold catalysts was determined from the thermogram area of the H_2 of TPD, assuming a stoichiometry H:Ag = 1 and H:Au = 1 [52]. The TPD-H_2 method allows the calculation of the dispersion of the metal deposited on the surface of the support, as well as an estimate of the average size of the metallic crystals on the surface.

The values of percent dispersion and average crystal size for the monometallic and bimetallic catalysts prepared on the ZrO_2 carriers modified with ceria are presented in **Table 2**.

The dispersion percentage of the monometallic materials M1, M4 and M7, increases as the aggregate of cerium increases in the ZrO_2 surface of 26 > 28 > 80%, which indicates a better dispersion of the silver promoted by this promoter, and smaller sizes of metallic glass for the M7 monometallic catalyst. Bimetallic catalysts (B1, B4, B7) tend to increase in size, which is expected when a second metal is deposited on the surface, but this does not occur in material

Catalyst	μmol of H_2/g catalyst	TPCM (nm)*	%D**
M1	34	7.3	26.2
M4	37	6.7	28.5
M7	104	2.4	80.1
B1	37	9.1	14.8
B4	169	2.0	67.5
B7	29	11.6	11.6

*TPCM = Average size of metallic crystallite**%D = dispersion percentage.

Table 2. Monometallic catalysts (M1, M4, and M7) and bimetallic catalysts (B1, B4, and B7): μmol H_2/g, average crystal size, and dispersion percentage.

B4 where it decreases possibly due to the strong metal support interaction that exists to that concentration of ceria in the material. As it was observed in the maximum desorption temperature that was of 366°C for the material B1, on the other hand in the material B4 it is of 446° C followed by a peak at 256°C.

The B7 material increases its average size of metallic crystal in relation to its monometallic counterpart (M7) and presents peaks of desorption at 423°C followed by one at 294°C which suggests very strong interactions between the support and the metals deposited in its surface.

3.5.2. NH_3 of TPD

This technique is used in catalysis to determine the number and type of acidic sites available on the surface of the catalyst. Desorption at a programmed temperature of ammonia is based on the chemisorption of a gas on a solid and the subsequent desorption of that gas by a progressive increase in temperature.

Monometallic materials show some acidity, but the most notable is M7, which presents ammonia desorption peaks at a temperature of 435°C and is due to strong acid sites; the percentage of acidity of the sites have 69.9% for strong acid sites. In the case of bimetallic catalysts, the deposit of Au on the surface of the monometallic material changes the acidity of M4 to desorption sites of a higher temperature for the case of its bimetallic counterpart B4.

For bimetallic materials, the appearance of strong acid sites is due to the deposition of the second metal to the surface of the monometallic material. The addition of second metal (Au) can modify the active sites of mono-metallic material. This change can be shown through TPD-NH_3 when increasing the number of moderate and strong acid sites. An alternative modification can be done through addition of promoter CeO_2 in the support. In this study we synthesized supports with different CeO_2 content, increasing gradually when ceria is present in high concentration enhance strong metal-support interaction effect.

It has been reported that the addition of Au by the precipitation deposition method increases the oxygen reducibility of ceria [52]. In general, the capacity to store oxygen of the systems

containing CeO_2 results from the change in the associated oxidation state that is reversible in the case of materials with Ceria in a very general way is $2CeO_2 \leftrightarrow Ce_2O_3 + ½\ O_2$ [53], so that denotes the importance of the oxygen kinetics incorporated or removed from the CeO_2 structure promoted by the Au is a crucial step in the formation of stronger acid sites.

3.5.3. H_2 of TPR

The studies of the programmed temperature reduction were made to the materials M7, B7, M4, and M7. In B7 material, two reduction peaks predominate, one at 130° C and the other at 200°C corresponding to the metal on the surface of the material, because there are oxidized species of silver (AgO and Ag_2O) and Gold (Au_2O and Au_2O_3) in The surface of the metal will be reduced to the aforementioned temperatures. Another peak that is observed is at 275°C which may be due to the reduction of the Ag_2O on the surface of the support, this peak of reduction indicates that on the surface of the support the silver is oxidized easily due to the strong interaction with CeO_2, in the literature it is indicated that the ceria is reduced at two temperatures 770 and 1100 K [54], not appearing in the ranges of analysis of the samples, this is corroborated by UV-Vis and TPD of H_2. Associated with the small cerium crystal and its reduction temperature, it is clear to note that this helps the material to have a better oxidation–reduction on the surface contributing oxygen to the system and increasing its catalytic activity.

The monometallic materials are easily oxidized even after the thermal treatment with Hydrogen, where two reduction peaks are shown at 66 and 158°C for the M7 material. The peaks of the silver as the support without Ceria (material M1) in relation to those that do have the promoter, present peaks at lower temperatures than for the monometallic ones.

3.6. Catalytic evaluation (phenol, MTBE)

3.6.1. Phenol

In the group of M catalysts the best nanomaterial was M7 which corresponds at Ag/ZrO_2-Ce20 for degradation of phenol. The conversion of phenol was followed through Gas chromatography and Total Organic Carbon. M7 has 30% of conversion of phenol and 25% of TOC. The rest of the M catalyst has lower values. The reasons for this behavior are explained basically through TPD-NH_3. M7 has a higher percentage of strong acid sites than the rest of his other counterparts. M7 has 69.9% of strong acid sites and M4 and M1 0%. As they know the adsorption of molecules over a strong acid site is more stable than the adsorption over a weak acid site.

In the group of B-U* catalysts the best nanomaterial was B7 which corresponds at Ag-Au/ZrO_2-Ce20 for degradation of phenol. The conversion of phenol was followed through Gas chromatography and Total Organic Carbon. B7 has 61% of conversion of phenol and 40% of TOC. The rest of the B-U* catalyst has lower values. The reasons for this behavior are explained basically through TPD-NH_3. M7 has a higher percentage of strong acid sites than the rest of his other counterparts. B7 has 47.9% of strong acid sites and B4 35%. As they know the adsorption of molecules over a strong acid site is more stable than the adsorption over a weak acid site. Thus, the bimetallic catalyst B7 overcomes the monometallic catalyst M7. Therefore it is the most active for CWAO reaction of phenol, mineralizing intermediaries in a more efficient way.

The B7 catalyst showed the highest conversion of all the catalysts. B7 has 61% of conversion of phenol and 40% of Total Organic Carbon (TOC), which is highly consistent with the accessibility data for the Ag-Au active sites obtained by the acidity study obtained by TPD-NH_3, in which this catalyst presented the values higher in the percentage of strong acidity. When Au is added to the solid, the conversion of the model molecule increases in the case of the M4 and M7 catalysts. However, catalyst M1 decreased its catalytic activity by depositing gold (material B1) and had greater selectivity to CO_2 production. The bimetallic catalyst B7 prepared by the sequential deposition-precipitation technique has the highest conversion (61%) compared to the catalyst B1 (16%). In catalyst B7 there is a higher conversion of phenol and the highest selectivity to CO_2. Therefore, the increase in oxidation and conversion to CO_2 can be explained by an adequate relationship between the acid function of the support and the metallic function of the system.

3.6.1.1. Degradation of phenol (TOC)

The results of metallic dispersion of the monometallic materials (M1-M7) indicate a decrease in the average crystal size in relation to the increase in Ceria concentration. Despite the size, it was not a determinant factor in the degradation, where the monometallic M4 (6.7 nm) has higher conversion than the M7 (2.4 nm). The deposit of the gold to the monometallic catalyst increases the crystal size and increases the degradation of the phenol for the catalyst (B7). It was observed that the increase in the degradation and mineralization of phenol due to the addition of gold to the system promotes the oxidation change of CeO_2, causing structural and electronic defects in bimetallic materials. This is also corroborated in the analysis of the acidity in the material.

The increase in the activity promoted by gold in the catalysts with a greater amount of ceria shows that gold facilitates the reduction of CeO_2, causing superoxide species in the surface and increases the oxidative-reductive capacity of the promoter. Various authors [38, 51, 55] have studied the alloy of Ag-Au in catalytic reactions, and have proposed that the natural adsorption of oxygen by silver is favored by the presence of gold. This implies that the adsorption of oxygen and its subsequent activation by gold creates superoxide species (O_2) on the surface of the bimetallic nanoparticles; which, besides being catalytically active, have a strong metal-support interaction, which favors the catalytic activity.

3.6.2. MTBE

Results from Ag/ZrO_2-CeO_2 catalysts with 5, 10, 15 and 20% ceria the MTBE conversion has values between 52 and 90%, being the Ag/ZrO_2-Ce15 catalyst the most active with 90% MTBE conversion.

In TOC conversion for monometallic catalysts (**Figure 4**) it is strongly distinguished the effect of ceria dopant on the conversion of intermediates, because at a high content of cerium oxide (15–20%) it results in high percentages of TOC conversion (69 and 80%), so the reaction rate is faster for the conversion of intermediates and therefore, the concentration of the intermediate compounds is degraded more efficiently. According to the reported by Cervantes et al. [19], this latter result is controlled by the relative abundance of Ce^{+4}.

http://dx.doi.org/10.5772/intechopen.74675

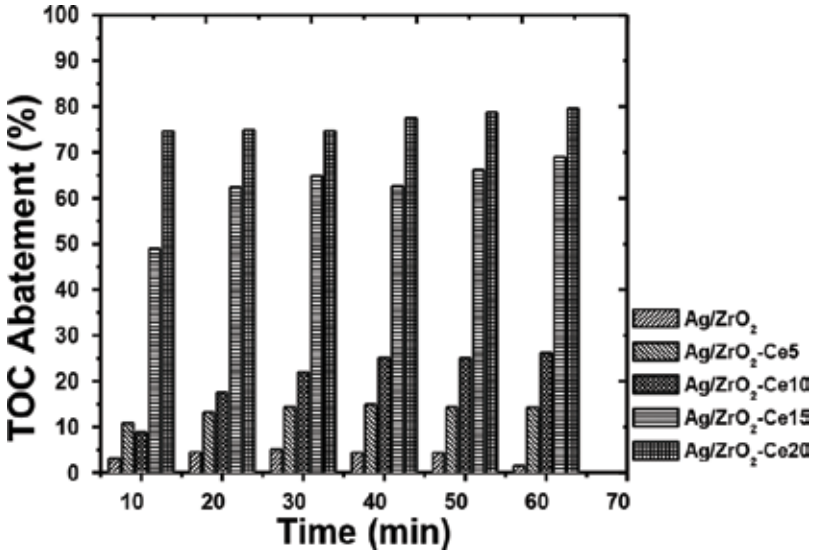

Figure 4. TOC abatement as a function of the time for silver supported catalysts.

This activity results demonstrate the effect of the ceria content on the effectiveness of the MTBE degradation process for the supported Ag nanoparticles. With the characterization studies hydrogen temperature programmed desorption and UV-Vis, we verified the high metal dispersion of the silver when in the materials there was a high concentration of ceria since they reached values of between 49 and 61%, the latter value being assigned to the catalyst Ag/ZrO_2-Ce15.

In this study, it was found that one of the essential steps to carry out the oxidation process by the active phase of the supported silver catalysts is the adsorption of molecular oxygen on the surface of the metallic crystallite. The spectra for reduced Ag/ZrO_2, and several Ag/ZrO_2-Cex containing catalysts it is important to point out that the most intense plasma absorption is for the Ag/ZrO_2-Ce15. This finding suggests that this catalyst should contain the larger proportion of metallic silver. In other words, Ag/ZrO_2-Ce15 has more abundance of Ag^0 nanoparticles compared to their monometallic counterparts. This result shows better performance of chemisorption of oxygen over Ag/ZrO_2-Ce15 and Ag/ZrO_2-Ce20 than the rest of catalyst.

The results of XPS revealed the importance of ceria in the improvement of silver properties. **Figure 5** shows XPS of $Ce_{3d\ 5/2}$ and $Ce_{3d\ 3/2}$ core levels for calcined and H_2-reduced samples and according to several similar studies, the slightly negative shift of Binding Energies was attributed that cerium is mainly in the Ce^{+4} oxidation state, with a certain increase in the Ce^{+3}. For the samples prepared for our study, the $Ce_{3d\ 5/2}$ of Ag/ZrO_2-Ce20 is 0.3 eV smaller than of ZrO_2-Ce20, indicating a greater abundance of Ce^{+3} species, after doping of silver. In this way, we show the presence of oxygen vacancies in the ceria, in the materials with the highest percentage of ceria.

The results showed that in the Ag_{3d} region consisted of two peaks which corresponded to $Ag_{3d\ 5/2}$ and $Ag_{3d\ 3/2}$ and it was determined that The $Ag_{3d\ 5/2}$ binding energies of Ag/ZrO_2 and

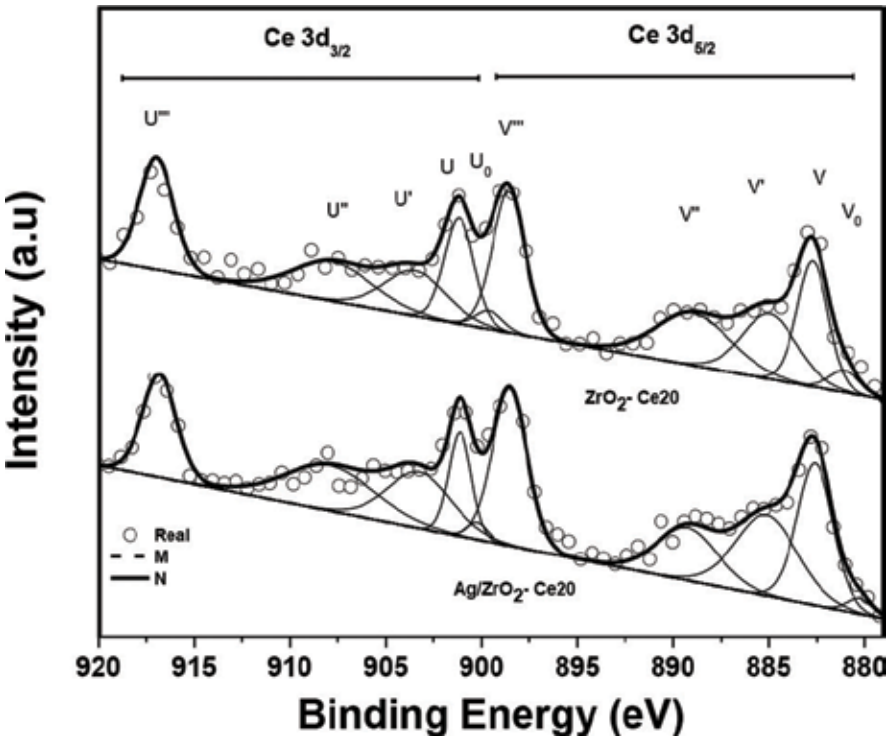

Figure 5. XPS Ce 3D spectra for ZrO_2-Ce20 support and Ag/ZrO_2-Ce20 catalyst.

Ag/ZrO_2-Ce20 were 368.2 and 368.5 eV, respectively. These results demonstrate that only one form of Ag is present, in the form of Ag0. This is because we did not observe any peak corresponding to the oxidized silver species located around 367.7 eV.

The ceria through the oxygen vacancies exerts an interaction between the support and Ag nanoparticles, which allows the silver to become more metallic, increasing the degree of reduction state of silver. This behavior was observed when there is a higher percentage of ceria in the catalysts synthesized, in the case of Ag/ZrO_2-Ce20. That is why the catalysts Ag/ZrO_2-Ce15 and Ag/ZrO_2-Ce20 showed better activity or degradation efficiency of CWAO for MTBE.

With respect to the bimetallic catalysts synthesized by the redox method (Au-Ag/ZrO_2-Cex), CWAO tests were performed under the same conditions presented for the monometallic.

Results from **Table 3** show that on Au-Ag/ZrO_2-Ce5 the MTBE conversion has value 86% and TOC conversion of 68%, being the Au-Ag/ZrO_2-Ce5 the most active catalyst.

Table 3 shows the activity and selectivity for the catalyst Wet-Air Oxidation of MTBE after 60 min of reaction. MTBE conversion (X_C), TOC abatement (X_{TOC}) and intermediate concentration (Acetone) as a function of the time for gold-silver supported catalysts.

Catalysts	X_C (%)[a]	X_{TOC} (%)[a]	C (mmol/l)[a]	r_1[a] (mmol $h^{-1}g_{met}^{-1}$)	Selectivity to CO_2[a]
Ag-Au/ZrO_2	78	61	n.d.	2310	78
Ag-Au/ZrO_2-(5%)CeO_2	86	68	n.d.	2580	79
Ag-Au/ZrO_2-(10%)CeO_2	77	68	n.d.	2340	88
Ag-Au/ZrO_2-(15%)CeO_2	81	59	n.d.	2430	73
Ag-Au/ZrO_2-(20%)CeO_2	86	61	n.d.	2580	71
Without catalyst	51	16	6	—	31

[a]Obtained after 1 h of reaction, n.d. not detected.

Table 3. Activity and selectivity for the catalyst of MTBE after 60 min of reaction.

The values determined by TOC in the MTBE CWAO of bimetallic catalysts, it is observed that the effect of the ceria is minimized, and when depositing the gold (2.5%), it is possible to improve the TOC of Au-Ag/ZrO_2, Au-Ag/ZrO_2-Ce5 and Au-Ag/ZrO_2-Ce10, the opposite being for Au-Ag/ZrO_2-Ce15 and Au-Ag/ZrO_2-Ce20.

The XPS results showed that For the pure Ag/ZrO_2 and Ag/ZrO_2-20% CeO_2, the binding energy (BEs) of $Ag_{3d\ 5/2}$ were 368.243 and 368.355 eV, which is slightly higher than that of bulk metallic Ag (368.1–386.5 eV). Moreover, for the bimetallic catalyst, the BE $Ag_{3d\ 5/2}$ were 368.22 eV for Ag-Au/ZrO_2, 368.23 eV for Ag-Au/ZrO_2-10% CeO_2 and 367.36 eV for Ag-Au/ZrO_2-Ce20. This implies that through allowing gold, the silver has a greater tendency to lose electrons. Therefore, the doping ceria of support affected the degree of reduction of silver in the Ag-Au system. The relative abundance of Ag^0/Ag^{+1} were 49.14/50.86, obtained after deconvolution of Ag_{3d} of Ag-Au/ZrO_2-Ce20.

For the bimetallic catalyst, the XPS analysis of Au_{4f} shifted to slightly higher values compared Ag-Au/ZrO_2 (83.9455 eV) and Ag-Au/ZrO_2-Ce10 (83.9604 eV), but closer to that of the bulk metallic Au (84 eV). But, for the Ag-Au/ZrO_2-Ce20, the BE Au_{4f} was 84.7392 eV. The relative abundance of Au^0/Au^{+1} were 89.74/10.26, obtained after deconvolution of Au_{4f} of Ag-Au/ZrO_2-Ce20. This implies that promoter Ce, in high loading, can inhibit the formation of Ag^0 and Au^0 species, in the bimetallic catalyst. It is because of that the catalyst Au-Ag/ZrO_2-Ce5 shows better activity or degradation efficiency of CWAO for MTBE.

4. Conclusions

The addition of CeO_2 to the ZrO_2 system varied the textural and electronic properties, corroborated by physisorption of N_2 and UV-Vis; increasing the surface area of the support and its capacity of oxide-reduction of the system.

The monometallic nanoparticles by the method deposit precipitation (DP) with NaOH gives excellent results obtaining nanoparticles less than 10 nm, even reaching 2.4 nm for the case

of the material Ag/ZrO_2-Ce20 (M7). The DP method with urea for the bimetals, improved the particle size (2 nm in the B4-U*), although the oxidation is not modified by the size of the nanoparticles.

The addition of Au by the precipitation method with urea modifies the active sites of monometallic material, dispersing the gold in nanometric sizes, not greatly modifying the surface area of the monometallic system, this is corroborated by the TPD-NH_3. The dynamic interaction between Au and CeO_2 modifies the properties of ceria.

For the degradation of phenol, the best catalytic material was Au-Ag/ZrO_2-Ce20 (B7-U*) with a composition of 1.4% Ag and a ratio of Au: Ag molar 1:1 supported in ZrO_2-CeO_2 (20% by weight), due to the strong metal-support interaction that modifies the structure of CeO_2, creating strong acid sites that promote the mineralization of phenol in a catalytic wet oxidation reaction.

A higher percentage of ceria greater vacancies of oxygen and there is an interaction between the support and the silver nanoparticles, allowing the Ag to be reduced to its metallic state. In the monometallic Ag/ZrO_2-CeO_2 catalysts with 5, 10, 15 and 20% ceria, the MTBE conversion was from 52 to 90%; the most active was Ag/ZrO_2-Ce15. The bimetallic catalyst Ag/ZrO_2-Ce5 (B2-R*) was the best in the degradation of CWAO for MTBE, because those containing higher Ce content (Ag-Au/ZrO_2-20% CeO_2) the relative abundance of Au^0/Au^{+1} obtained from the deconvolution of Au_{4f} was 89.74/10.26, which suggests that Ce at high concentrations inhibits the formation of Ag^0 and Au^0 species in bimetallic catalysts.

Author details

Zenaida Guerra Que, José Gilberto Torres Torres, Hermicenda Pérez Vidal*,
María A. Lunagómez Rocha, Juan C. Arévalo Pérez, Ignacio Cuauhtémoc López,
Durvel De La Cruz Romero, Alejandra E. Espinosa De Los Monteros Reyna,
José G. Pacheco Sosa, Adib A. Silahua Pavón and Jorge S. Ferráez Hernández

*Address all correspondence to: hermicenda.perez@ujat.mx

Laboratory of Catalytic Nanomaterials Applied to the Development of Energy Sources and Environmental Remediation, Applied Science and Technology Research Center of Tabasco (CICTAT), Juarez Autonomous University of Tabasco, DACB, Cunduacan, Tabasco, Mexico

References

[1] Gehringer P, Sampa MHO, Ham B, Kim Y, Kim J, Kang H, Shin K, Salimov RA. Status of industrial scale radiation treatment of wastewater and its future. In: Proceedings of a Consultants Meeting of the International Atomic Energy Agency (IAEA); 13-16 October 2003; Daejon, Vienna: IAEA; 2004. pp. 1-18

[2] Wei H, Yan X, He S, Sun C. Catalytic wet air oxidation of pentachlorophenol over Ru/ZrO_2 and Ru/$ZrSiO_2$ catalysts. Catalysis Today. 2013;**201**:49-56

[3] European Commission. 2000. The Water Framework Directive. EC Directive 2000/60/EEC

[4] Glaze WH, Kang JW, Chapin DH. The chemistry of water treatment processes involving ozone, hydrogen-peroxide and ultraviolet-radiation. Ozone: Science & Engineering. 1987;**9**:335-352

[5] Luan M, Jing G, Piao Y, Liu D, Jin L. Treatment of refractory organic pollutants in industrial waste water by wet air oxidation. Arabian Journal of Chemistry. 2017;**10**:S769-S776

[6] Zhou H, Smith DW. Advanced technologies in water and wastewater treatment. Journal of Environmental Engineering and Science. 2002;**1**:247-264

[7] Debellefontaine H, Chakchouk M, Foussard JN, Tissot D, Striolo P. Treatment of organic aqueous wastes: Wet air oxidation and wet peroxideoxidation. Environmental Pollution. 1996;**92**:155-164

[8] Kulkarni SJ, Kaware JP. Review on research for removal of phenol from wastewater. International Journal of Science and Research Publications. 2013;**4**:1-5

[9] Chindris A. Degradation of refractory organic compounds in aqueous wastes employing a combination of biological and chemical treatments [Thesis]. Cagliari: University of Cagliari; 2010

[10] Lin C-W, Cheng Y-W, Tsai S-L. Influences of metals on kinetics of methyl tert-butyl ether biodegradation by *Ochrobactrum cytisi*. Chemosphere. 2007;**69**:1485-1491

[11] Zheng C, Zhao L, Zhou X, Fu Z, Li A. Treatment Technologies for Organic Wastewater. Rijeka, Croatia: In Tech Open; 2013. pp. 249-286

[12] Massa P, Ivorra F, Haure P, Medina Cabello F, Fenoglio R. Catalytic wet air oxidation of phenol aqueous solutions by 1% Ru/CeO_2-Al_2O_3 catalysts prepared by different methods. Catalysis Communications. 2007;**8**:424-428

[13] Kim K-H, Ihm S-K. Heterogeneous catalytic wet air oxidation of refractory organic pollutants in industrial wastewaters: A review. Journal of Hazardous Materials. 2011;**186**:16-34

[14] Shahidi D, Roy R, Azzouz A. Advances in catalytic coxidation of organic pollutants prospects for thorough mineralization by natural clay catalysts. Applied Catalysis, B: Environmental. 2015;**174-175**:277-292

[15] Herney-Ramirez J, Vicente MA, Madeira LM. Heterogeneous photo-Fenton oxidation with pillared clay-based catalysts for waste water treatment: A review. Applied Catalysis, B: Environmental. 2010;**98**:10-26

[16] Li N, Descorme C, Besson M. Application of $Ce_{0.33}Zr_{0.63}Pr_{0.04}O_2$ supported noble metal catalysts in the catalytic wet air oxidation of 2-chlorophenol: Influence of there action conditions. Applied Catalysis, B: Environmental. 2008;**80**:237-247

[17] Delgado JJ, Chen X, Pérez-Omil JA, Rodríguez-Izquierdo JM, Cauqui MA. The effect of reaction conditions on the apparent deactivation of Ce-Zr mixed oxides for the catalytic wet oxidation of phenol. Catalysis Today. 2012;**180**:25-33

[18] Cuauhtémoc I, Del Angel G, Torres G, Lafaye G, Navarrete J, Angeles-Chavez C, Padilla JM. Synthesis and characterization of $Rh/Al2O_3$-CeO_2 catalysts: Effect of the Ce^{+4}/Ce^{+3} ration on the MTBE removal. Journal of Ceramic Processing Research. 2009;**10**:512-520

[19] Cervantes A, Del Angel G, Torres G, Lafaye G, Barbier J Jr, Beltramini JN, Cabañas-Moreno JG, Espinoza de los Monteros A. Degradation of methyl tert-butyl ether by catalytic wet air oxidation over Rh/TiO_2-CeO_2 catalysts. Catalysis Today. 2013;**212**:2-9

[20] Guerra-Que Z, Torres-Torres G, Pérez-Vidal H, Cuauhtémoc-López I, Beltramini JN, Espinoza de los Monteros A, Frías-Márquez DM. Silver nanoparticles supported on zirconia-ceria for the catalytic wet air oxidation of methyl tert-butyl ether. RSC Advances. 2017;**7**:3599-3613

[21] Chen D, Qu Z, Shen S, Li X, Shi Y, Wang Y, Fu Q, Wu J. Comparative studies of silver based catalyst supported on different supports for the oxidation of formaldehyde. Catalysis Today. 2011;**175**:338-345

[22] Shimizu K-I, Kawachi H, Komai S-I, Yoshida K, Sasaki Y, Satsuma A. Carbon oxidation with Ag/Ceria prepared by self-dispersion of Ag power into nano-particles. Catalysis Today. 2011;**175**:93-99

[23] Alabbab S, Adil SF, Assal ME, Khan M, Al warthan A. Gold and silver nanoparticles supported on manganese oxide: Synthesis, characterization and catalytic studies for selective oxidation of benzyl alcohol. Arabian Journal of Chemistry. 2014;**7**:1192-1198

[24] Ruiz-Trejo E, Boldrin P, Medley-Hallam JL, Darr J, Atkinson A, Brandon NP. Partial oxidation of methane using silver/gadolinia-doped ceria composite membranes. Chemical Engineering Science. 2015;**127**:269-275

[25] Almendáres A, González J. Nanomateriales: Su crecimiento, caracterización estructural y tendencias. Ideas CONCYTEG. 2011;**72**:772-787

[26] Salman H, Godlisten N, Imran S, Sung S, Nadir A, Suleman T, Manwar H, Wookeun B, Hee T. Aminated polyethersulfone-silver nanoparticles (AgNPs-APES) composite membranes with controlled silver ion release for antibacterial and water treatment applications. Materials Science and Engineering. 2016;**62**:732-745

[27] Noritomi H, Umezawa Y, Miyagawa S, Kato S. Preparation of highly concentrated silver nanoparticles in reverse micelles of sucrosefatty acid esters through solid-liquid extraction method. Advances in Chemical Engineering and Science. 2011;**1**:299-309

[28] Zhiya S, Joy D, Jizhong Z, Yang L. Contradictory effects of silver nanoparticles on activated sludge wastewater treatment. Journal of Hazardous Materials. 2018;**341**:448-456

[29] Uma P, Fuangfa U. Simultaneous adsorption of silver nanoparticles and silver ions on large pore mesoporous silica. Journal of Environmental Chemical Engineering. 2018;**66**:596-603

[30] Delgado-Beleño Y, Martinez-Nuñez C, Cortez-Valadez M, Flores-López N, Flores-Acosta M. Optical properties of silver, silver sulfide and silver selenide nanoparticles and antibacterial applications. Materials Research Bulletin. 2018;**99**:385-392

[31] Majles M, Dehghani Z, Sahraei R, Nabiyouni G. Non-linear optical properties of silver nanoparticles prepared by hydrogen reduction method. Optics Communications. 2009; **283**:1650-1653

[32] Noginov M, Zhu G, Bahoura M, Adegoke J, Small C, Ritzo B, Drachev V, Shalaev V. The effect of gain and absorption on surface plasmons in metal nanoparticles. Applied Physics B: Lasers and Optics. 2007;**86**:455-460

[33] Wang A, Hsieh Y, Chen Y, Mou C. Au–Ag alloy nanoparticle as catalyst for CO oxidation: Effect of Si/Al ratio of mesoporous support. Journal of Catalysis. 2006;**237**:197-206. DOI: 10.1016/j.jcat.2005.10.030

[34] Liu J-H, Wang A-Q, Chi Y-S, Lin H-P, Mou C-Y. Synergistic effect in an Au-Ag alloy nanocatalyst: CO oxidation. The Journal of Physical Chemistry. B. 2005;**109**:40-43. DOI: 10.1021/jp044938g

[35] Wang J, Zhu W, He X, Yang S. Catalytic wet air oxidation of acetic acid over different ruthenium catalysts. Catalysis Communications. 2008;(13):2163-2167. DOI: 10.1016/j.catcom.2008.04.019

[36] Grunwaldt J, Maciejewski M, Becker OS, Fabrizioli P, Baiker A. Comparative study of Au/TiO_2 and Au/ZrO_2 catalysts for low-temperature CO oxidation. Journal of Catalysis. 1999;**186**:458-469

[37] Schubert M. CO oxidation over supported gold catalysts—"inert" and "active" support materials and their role for the oxygen supply during reaction. Journal of Catalysis. 2001;(1):113-122. DOI: 10.1006/jcat.2000.3069

[38] Wang A, Liu J, Lin S, Lin T, Mou C. A novel efficient Au–Ag alloy catalyst system: Preparation, activity, and characterization. Journal of Catalysis. 2005;**1**:186-197. DOI: 10.1016/j.jcat.2005.04.028

[39] Hayelom D, Adhena A, Hailemariam K, Tekilt G. Synthesis paradigm and applications of silver nanoparticles (AgNPs), a review. Sustainable Materials and Technologies. 2017; **13**:18-23

[40] Akter M, Tajuddin Sikder MD, Mostafizur Rahman MD, AtiqueUllah AKM, Binte Hossain KF, Banik S, Hosokawa T, Saito T, Kurasaki M. A systematic review on silver nanoparticles-induced cytotoxicity: Physicochemical properties and perspectives. Journal of Advanced Research. DOI: 10.1016/j.jare.2017.10.008

[41] Kalantari K, Muhammad Afifi AB, Bayat S, Shameli K, Yousefi S, Mokhtar N, Kalantari A. Heterogeneous catalysis in 4-nitrophenol degradation and antioxidant activities of silver nanoparticles embedded in tapioca starch. Arabian Journal of Chemistry. In press. DOI: 10.1016/j.arabjc.2016.12.0182017

[42] Passos de Aragao A, De Oliveira TM, Veras Queremes P, Gomes Perfeito ML, Carvalho Araújo M, Sousa Santiago JA, Cardoso VS, Quaresma P. Green synthesis of silver nanoparticles using the seaweed *Gracilaria birdiae* and their antibacterial activity. Arabian Journal of Chemistry. In press. DOI: http://dx.doi.org/10.1016/j.arabjc.2016.04.014

[43] Regalbuto J. Catalyst Preparation. Science and Engineering. 2nd ed. CRC Press, Taylor & Francis. 2007. 488 p

[44] García JA, Arreola Sanchez R, Ríos Enríquez MA, Rentería Tapia VM, Valverde Aguilar G. Estudio del desempeño de un catalizador $Au/TiO_2/SiO_2$ en la reaccion de oxidación de CO. Revista Mexicana de Física. México. 2011;**2**:30-35

[45] Redina E, Greish A, Novikov R, Strelkova A, Kirichenko O, Tkachenko O, Kapustin G, Sinev I, Kustov L. $Au/Pt/TiO_2$ catalysts prepared by redox method for the chemo selective 1,2-propanediol oxidation to lactic acid and NMR spectroscopy approach for analyzing the product mixture. Applied Catalysis, A: General. 2015;**491**:170-183

[46] Pieck CL, Marecot P, Barbier J. Preparation of $Pt\text{-}Re/Al_2O_3$ catalysts by surface redox reactions. I. Influence of operating variables on Re deposit in the presence of hydrochloric acid. Applied Catalysis, A: General. 1996;**134**:319-329

[47] Astruc D. Nanoparticles and Catalysis. Wiley-VCHVerlag GmbH; 1999

[48] Luck F. Wet air oxidation: Past, present and future. Catalysis Today. USA. 1999;**1**:81-91. DOI: 10.1016/S0920-5861(99)00112-1

[49] Igawa N, Ishii Y. Crystal structure of metastable tetragonal zirconia up to 1473 K. Journal of the American Ceramic Society. 2001;**5**:1169-1171. DOI: 10.1111/j.1151-2916.2001.tb00808.x

[50] Ranga Rao G, Ranjan Sahu H. XRD and UV-Vis diffuse reflectance analysis of CeO_2–ZrO_2 solid solutions synthesized by combustion method. Proceedings of the Indian Academy Of Science. 2001;**5-6**:651-658

[51] Shah A, Qureshi R, Latif-ur R, Synthesis Z-u R. Characterization and applications of bimetallic (Au-Ag, Au-Pt, Au-Ru) alloy nanoparticles. Reviews on Advanced Materials Science. 2012;**30**:133-149

[52] Fu Q, Kudriavtseva S, Saltsburg H, Flytzani-Stephanopoulos M. Gold–ceria catalysts for low-temperature water-gas shift reaction. Chemical Engineering Journal. 2003;**1**:41-53

[53] Rao GR, Fornasiero P, Monte RD, Kašpar J, Vlaic G, Balducci G. Reduction of NO over partially reduced metal-loaded CeO_2–ZrO_2 solid solutions. Journal of Catalysis. 1996;**254**:1-9

[54] Trovarelli A. Catalytic properties of ceria and CeO^{2-} containing materials. Catalysis Reviews. 1996;**4**:439-520. DOI: 10.1080/01614949608006464

[55] Zhang L, Zhang C, He H. The role of silver species on $Ag\ Al_2O_3$ catalysts for the selective catalytic oxidation of ammonia to nitrogen. Journal of Catalysis. 2009;**1**:101-109

Chapter 6

Antibacterial Effect of Silver Nanoparticles *Versus* Chlorhexidine Against *Streptococcus mutans* and *Lactobacillus casei*

Raul Alberto Morales Luckie,
Rafael Lopez Casatañares, Rogelio Schougall,
Sarai Carmina Guadarrama Reyes and
Víctor Sanchez Mendieta

Additional information is available at the end of the chapter

http://dx.doi.org/10.5772/intechopen.76183

Abstract

The porpoise of the study was to evaluate the antibacterial effect of silver nanoparticles (Ag-NPs) *versus* chlorhexidine (CHX) against *Streptococcus mutans and Lactobacillus casei*. Three different reducing agents were used for the synthesis and characterization of Ag-NPs: sodium borohydride ($NaBH_4$), a chemical method, and *Heterotheca inuloides* (Hi) and *Camellia sinensis* (Cs), two eco-friendly methods. The synthesized substance was deposited on deciduous teeth. Its behavior in dental tissues was evaluated through an energy dispersive X-ray spectroscopy (EDS) analysis, using a scanning electron microscope (SEM). The characterization of Ag-NPs in terms of shape, size, and polydispersity was performed through spectrophotometry of ultraviolet-visible light analysis (UV-vis), as well as by transmission electron microscopy. Isolation and culture of strains *S. mutans* and *L. casei* were done to perform the microbiological analysis.

In Petri dishes, paper discs containing different concentrations of Ag-NPs (synthesized by *Hi*, and by *Cs*) were deposited and tested along with paper discs containing CHX. Their antibacterial effect against both bacteria was evaluated by the inhibition zones test. By means of UV-Vis and TEM analysis, it was possible to observe that *Heterotheca inuloides* produced smaller and more stable nanoparticles, also in greater quantities (17.5 nm), when compared to *Camellia sinensis*. EDS analysis through SEM showed a 6.25 average absorption of silver in dental tissues. The microbiological analysis revealed a greater zone of inhibition when the test bacteria were in contact with 20 μl of Ag-NPs, synthesized by Hi, being statistically significant ($p < 0.05$), compared to the growth inhibition zones produced by Cs, and CHX against both strains. We can conclude that eco-friendly methods produced Ag-NPs with an important antibacterial effect in both strains.

Keywords: silver nanoparticles, chlorhexidine, *Streptococcus mutans*, *lactobacillus casei*, eco-friendly chemistry

1. Introduction

While *Streptococcus mutans* plays an important role in the initiation of dental caries, *Lactobacillus casei*, on the other hand, is considered an important secondary invader; both microorganisms are actively involved in the process of tooth decay [1–5]. Dental practitioners recognize that chlorhexidine has been the gold standard for more than 3 decades [6–8]; it is considered a potent agent against *S. mutans.* Nevertheless, *L. casei,* which dominates among oral Lactobacilli, is relatively resistant [9]. The main concern about its use is its limited period of substantivity (which is the ability of chlorhexidine to bind to tissues and release slowly for a longer time), and some reported cytotoxicity cases [10, 11].

Therefore, we consider it important to find substances with a potent antibacterial effect but with a minor impact on human health and the environment [12].

In recent years, nanotechnology has become an important discipline in the field of biology [13]. A considerable achievement is the ability to form atoms and molecules to further form new structures (*id est*., one-billion times smaller than what can be observed with the naked eye). Therefore, the new materials and devices can be developed with high atomic precision. Nanoscience involves the use of nanoparticles in a range between 1 and 100 nm to obtain unique and improved properties [14–20]. Nanomedicine is an extremely useful tool because most of the body's natural processes occur at an almost imperceptible level [21, 22].

Due to the aforementioned reasons, the interest in the study and synthesis of nanoparticles has grown recently. Silver nanoparticles (Ag-NP) are broad spectrum microbicide agents widely used in health sciences [23]; they are nanostructured materials based on silver salts. Silver is currently being used to inhibit bacterial growth in a variety of applications, including dentistry [17, 24]. Efforts have been made to explore the properties of Ag-NPs, as an efficient way to provide stability and improve antibacterial effect is the reduction in size [25, 26]. It is known that Ag-NPs exert an antimicrobial effect on Gram+ and Gram− producing lysis in peptides of the membrane of microorganisms [27].

"Eco-friendly" chemistry seeks to reduce waste, and eliminate pollution and environmental damage; it promotes the creation of products that are environmentally and economically sustainable [12]. Different forms of syntheses have been sought, in which natural and renewable reducing agents are used during the chemical processes. The principles of green chemistry are oriented to the search for new ways of synthesizing substances, not only minimizing the costs but also the damage to human health and reducing environmental pollution, while taking advantage of the benefits and properties of plants such as *Heterotheca inuloides* (Hi) and *Camellia sinensis* (Cs), which have shown antimicrobial and inhibitory activity, as well as antioxidant and cytotoxic properties against oral bacteria [28, 29].

http://dx.doi.org/10.5772/intechopen.76183

Mexican medicinal plants have enormous potential [30]. *Heterotheca inuloides* (Arnica) is a Mexican plant widely used due to its medicinal properties; it has shown anti-inflammatory and analgesic effect [31]. The plant grows abundantly in the Mexican region and has been used as part of folk medicine for the topical treatment of contusions, bruises as well as for the treatment of skin wounds and injures [28, 32].

This medicinal herb has been reported to exhibit antimicrobial activity, cytotoxic, and antioxidative properties [33], which has led the World Health Organization (WHO) to recognize its use in medicine [34].

Several constituents of *H. inuloides* have been identified, mainly, flavonoids, sesquiterpenoids, triterpenoids, and sterols. The composition of the essential oil has also been described. Recently, four sesquiterpenoids of *H. inuloides* were identified as antimicrobial agents [35].

The dried flowers of *H. inuloides* have been used for the treatment of postoperative thrombophlebitis, and externally for acne, bruises, and muscle aches in Mexico. Previously, sesquiterpenoids, 7-hydroxy-3,4-dihydrocadalin and 7-hydroxycadalin, were characterized as antibacterial agents from the dried flower of *H. inuloides*. The flavonoids, quercetin, kaempferol, and their glycosides were also isolated from the same source and showed tyrosinase inhibitory activity [36].

2. Experimental details

2.1. Synthesis of silver nanoparticles

Ag-NPs were synthesized from silver nitrate salts with the use of sodium borohydride ($NaBH_4$), a conventional chemical reducing agent. Pursuing the same purpose, two ecofriendly agents, were separately used as green reducers: *Heterotheca inuloides* and *Camellia sinensis*.

For chemical synthesis, $NaBH_4$ (in a concentration of 1×10^{-2}) was weighed on an analytical balance (Explorer Pro, model EP213C, OHAUS, USA), and then dissolved in a flask with distilled water.

A 10 mM silver nitrate solution ($AgNO_3$, Sigma-Aldrich) was prepared and mixed along with the $NaBH_4$ solution, in a 1:2.5 ratio to generate Ag-NPs.

The resulting solution was placed in a beaker on a heating grate (Thermo Scientific Cimarec). Using a magnetic stirrer, the incorporation of powder was achieved. The mixture was centrifuged with filter paper, allowing obtaining the smallest particles (i.e., nanoscale).

Water (H_2O) and alcohol (ETOH) were separately used as diluents.

The ecofriendly synthesis was performed by collecting dried flowers of Hi and Cs.

The leaves were mashed to a powder and mixed to obtain a homogeneous sample (both powders were used separately for the synthesis). One gram of each powder was immersed in

100 mL of distilled water; it then underwent a boiling process. Afterward, the solution was filtered through a filter paper.

2.2. Characterization of Ag-NPs

Following Ag-NPs formation, UV-vis analysis was carried out every hour, for the next 6 hours. UV-vis spectra measurements were recorded on a Cary 5000 UV-vis scanning spectrophotometer using quartz cells. The wavelength ranges from 300 to 600 nm.

To observe the size and shape of solutions, transmission electron microscopy (TEM) analysis was also carried out with a JEOL JEM-2100-Tokyo, Japan Microscope.

Scanning electron microscope (SEM) analysis was performed in a JSM-6510-LV microscope (JEOL) at 20 kV of acceleration, using secondary electrons.

The two eco-friendly substances were deposited in 20 deciduous teeth to analyze, through EDS (energy dispersive spectroscopy), the behavior of silver in dental tissues.

2.3. Microbiological analysis

Strains of *S. mutans* and *L. Casei* were isolated and cultivated in specific mediums for their growth (Gold *mitis salivarius* and Rogosa). Discs embedded with Ag-NPs synthesized by the two eco-friendly reducing agents, at different concentrations (10, 20, and 30 μl), were placed in Petri dishes. Some discs were used as blank control, and others were embedded with 2% CHX (Consepsis, Ultradent products Inc). Petri dishes were incubated at 37°C for 48 hours. The inhibitory halos of each substance were measured in millimeters to compare the antibacterial effect at different doses.

3. Results

The synthesis with H_2O provided more stable Ag-NPs because the chemical polarity of a molecule of water is greater than that of ETOH, and through the boiling process (applying heat to the mixture), the active ingredients are extracted from the infusions. UV-vis analysis determined, through the formation of the plasmon (maximum peak where light is absorbed), that Ag-NPs synthesized by Hi showed more stable and smaller nanoparticles in greater quantities compared to Cs but bigger than $NaBH_4$, because this is a more drastic reducing agent (**Figure 1**).

UV-vis shows that the plasmon wavelength lies between 440 and 456 nm in Ag-NPs synthesized by *Heterotheca inuloides* **(Figure 1A)**. While the plasmon wavelength lies between 355 and 448 nm in Ag-NPs synthesized by *Camellia sinensis* **(Figure 1B)**; which, unambiguously, indicates the presence of silver nanoparticles under the specific conditions of each synthesis.

http://dx.doi.org/10.5772/intechopen.76183

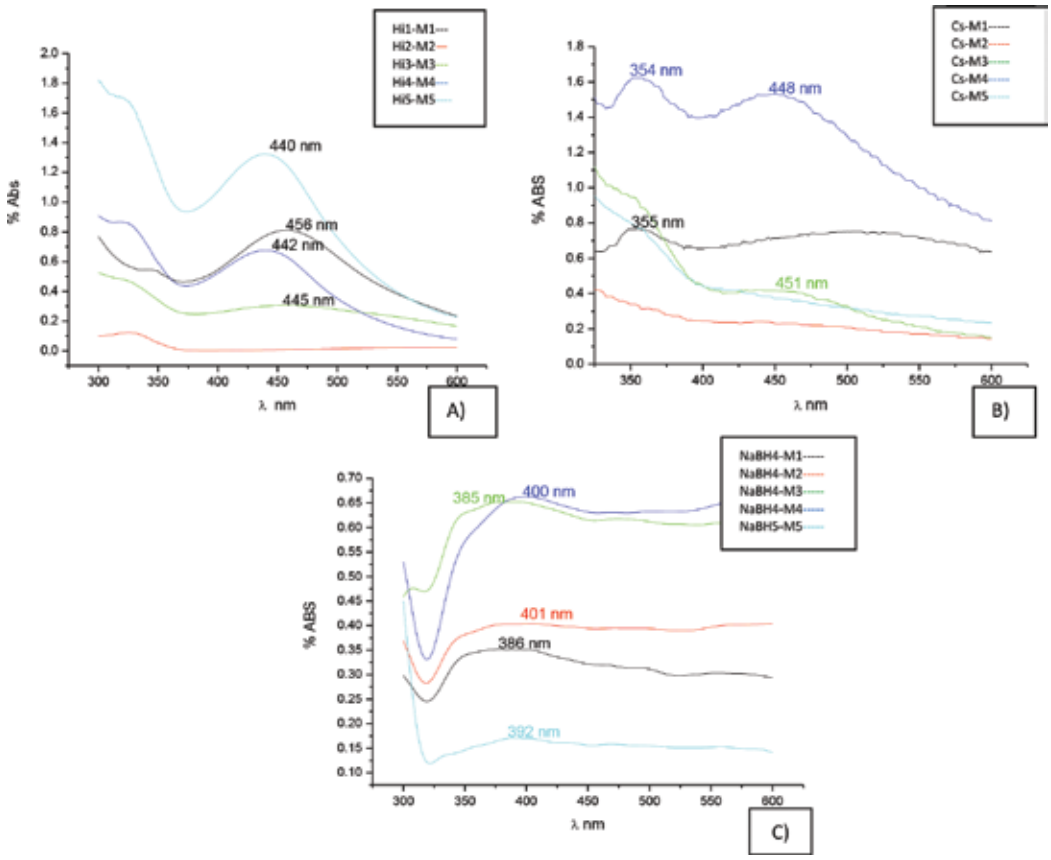

Figure 1. UV-visible spectroscopy analysis of Ag-Np synthesized by (A) *Heterotheca inuloides*, (B) *Camellia sinensis*, and (C) sodium borohydride.

The plasmon wavelength lies between 385 and 401 nm in Ag-Np synthesized by sodium borohydride because this is a more drastic reducing agent **(Figure 1C)**.

TEM allowed us to see that Hi showed smaller nanoparticles than *Camellia sinensis* while sodium borohydride were smaller (**Figure 2**).

3.1. Characterization of Ag-Np

Assessment of Ag-NPs impregnated teeth was performed through EDS (energy dispersive spectroscopy) analysis. A 6.26 weight percent mean absorption of silver to dental tissues was found among the total percent, meaning that Ag-NPs are compatible with deciduous teeth. A statistical analysis at a confidence level of 95% was set (**Figure 3A** and **B**).

Elemental chemical analysis through EDS by SEM.

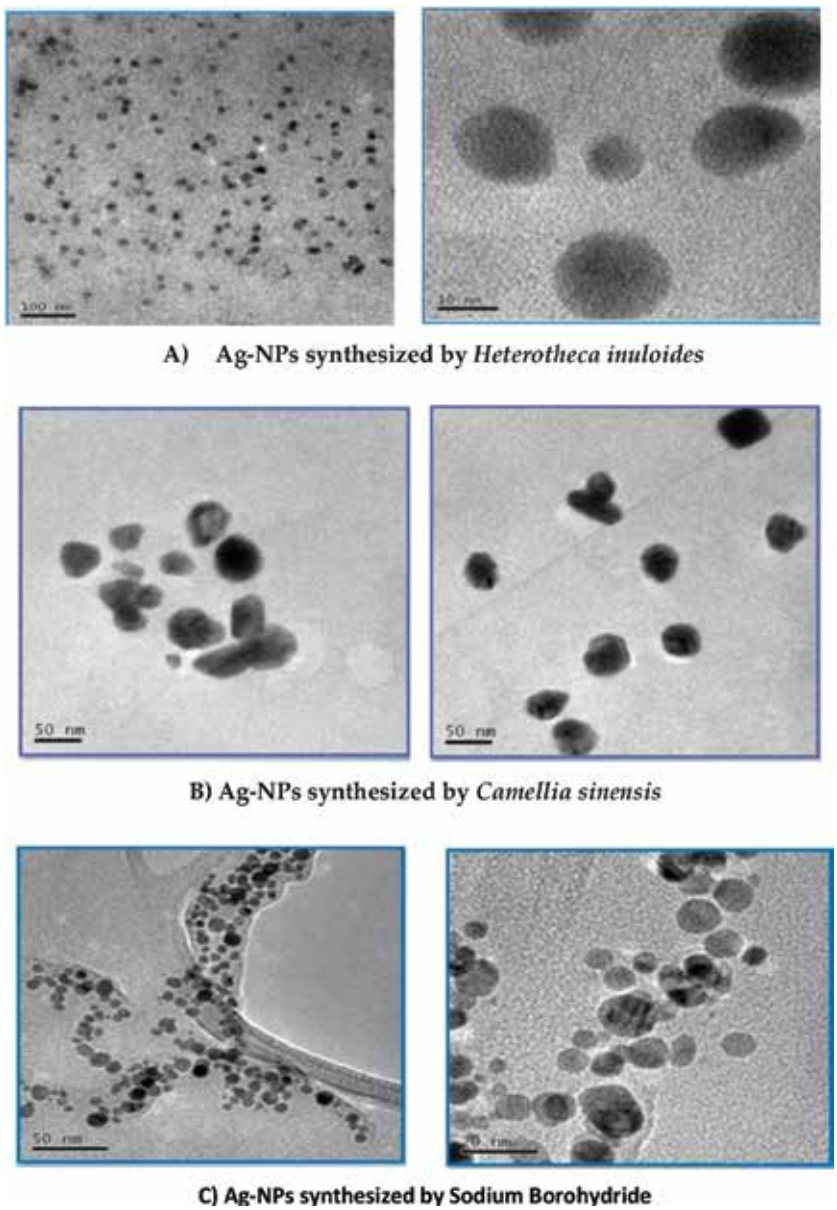

Figure 2. The size of silver nanoparticles synthesized by two eco-friendly reducing agents *Heterotheca inuloides* (17.5 nm) and *Camellia sinensis* (48.2 nm), and sodium borohydride (8 nm).

Student t test for unknown variances was used to establish the average inhibition of bacterial growth. A higher antibacterial effect of Ag-NPs synthesized with Hi, followed by Cs was observed, compared with CHX, particularly at the dose of 20µl. The effect on both bacteria was similar. The results were statistically significant to a confidence level of 95% (**Figure 4** and **Table 1**).

http://dx.doi.org/10.5772/intechopen.76183

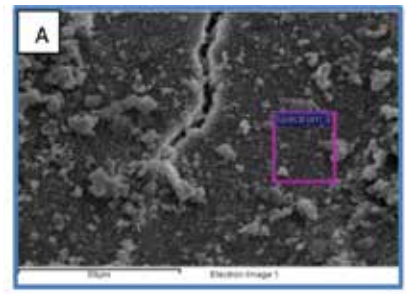

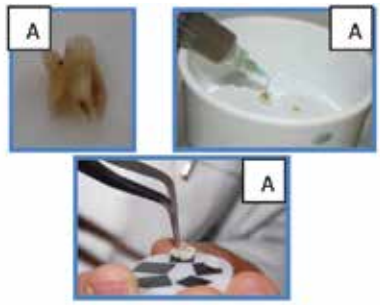

A) Lower deciduous molar through SEM

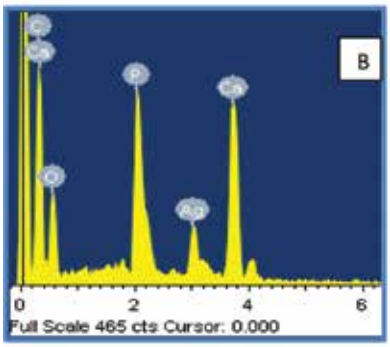

Lower Deciduous Molar	Weight percent	Atomic percent
C	43.70	59.11
O	30.99	31.47
P	6.76	3.54
Ca	12.09	4.90
Ag	6.47	0.97
TOTAL	100	100

B

B) Absorption of Silver to teeth through EDS

Figure 3. Weight percent of elements on deciduous teeth showing the absorption of silver. (A) Lower deciduous molar through SEM. (B) Absorption of silver to teeth through EDS.

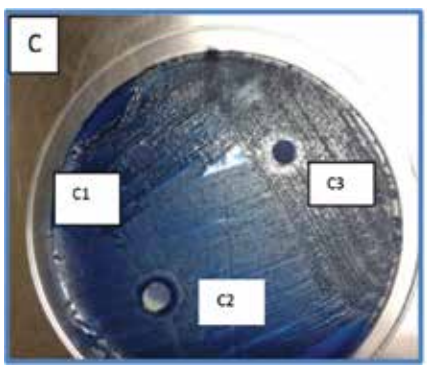

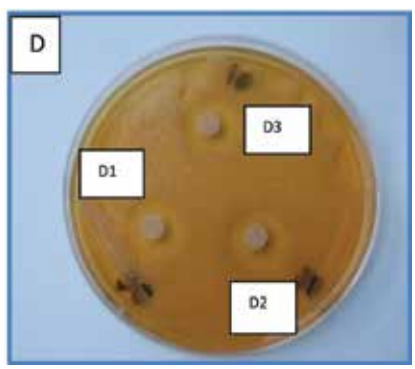

Figure 4. Petri dishes showing inhibitory halos of the discs rinsed with Ag-NPs by two reducing agents (Hi and Cs) *versus* chlorhexidine against *S. mutans* and *L. casei.* C1. Blank disc; C2. Disk containing chlorhexidine; C3. Disk containing Ag-NPs synthesized by *Heterotheca inuloides versus S. mutans.* D1. Disk containing 30 µl of Ag-NPs synthesized by *Heterotheca inuloides***;** D2. Disk containing 20 µl; D3. Disk containing 10 µl *versus L. casei*. Values of inhibitory halos of Ag-NPs with two eco-friendly reducing agents and chlorhexidine ₸.

	Against S. mutans				Against L. casei			
Doses	Mean	S.D	Minimum value	Maximun value	Mean	S.D	Minimun value	Maximum value
10 microliters								
Ag-Np reduced by Camellia sinensis	6.20	0.264	5.9	6.4	6.26	0.404	5.8	6.5
Ag-Np reduced by Heterotheca inuloides	5.43	0.404	5.0	5.8	5.43	0.153	5.3	5.6
Chlorhexidine	5.60	0.264	5.3	5.8	5.56	0.493	5.0	5.9
20 microliters								
Ag-Np reduced by Camellia sinensis	6.38	0.252	6.6	7.1	7.00	0.264	6.8	7.3
Ag-Np reduced by Heterotheca inuloides	6.93	0.416	6.6	7.4	6.93	0.231	6.8	7.2
Ag-Np reduced by Chlorhexidine	6.06	0.305	5.8	6.4	5.83	0.568	5.2	6.3
30 micloliters								
Ag-Np reduced by Camellia sinensis	6.03	0.252	5.8	6.3	6.30	0.458	5.8	6.7
Ag-Np reduced by Heterotheca inuloides	6.56	0.737	6.0	7.4	6.50	0.781	6.0	7.4
Chlorhexidine	5.83	0.252	5.6	6.1	5.70	0.700	5.0	6.4

Table 1. As can be seen from the experimental data, with the agents used at different concentrations, the inhibitory halos' size ranged from 5.0 to 7.4 mm. The highest growth inhibition means were observed at doses of 20 μl. The greatest variability in the size of halos was observed with Ag-NPs synthesized with *Heterotheca inuloides*. Ŧ en mm. SD. Standard deviation.

4. Discussion

We consider it important that dental science search for treatment alternatives incorporating products of natural origin, such as green plants. Mexico's varied vegetation allows the implementation of traditional medicine, as an alternative treatment for various diseases, including dental caries. Eco-friendly chemistry may propose a dental practice that is environmentally and economically sustainable. Nanotechnology has moved rapidly toward the improvement of health. The incorporation of silver salts in dental materials allows the dentist to ensure a longer lasting effect against pathogenic microorganisms.

As it is known, the size of bacteria is measured in microns, three orders of magnitude greater than the nanoparticles obtained by any of the three methods used. Therefore, the probability that nanoparticles come into contact with bacteria is higher when the size of Ag-NPs is smaller; hence, Hi turns out to be the best eco-friendly reducing agent.

L. casei has shown some resistance to chlorhexidine [9]. In this study, it is shown that green Ag-NPs inhibited both *L. casei* and *S. mutans*. Ag-NPs at a concentration of 1×10^{-2} showed acceptable antibacterial effect when compared to 2% CHX (containing 20 mg of chlorhexidine gluconate). The concentration used in Ag-NPs is minimal (nm) compared with the various concentrations shown in different presentations of CHX [6, 7, 37–41].

The knowledge of nanoscience and the emergence of new technologies in medical practice can transform the traditional way of attending a patient and promote a new paradigm based not only on clinical experience, but on the use of technological tools [42].

Having not found in our country, a study where Ag-NPs were in contact with deciduous teeth, in order to observe their behavior, the authors would like to propose deeper research in this matter.

The study of tissues from a nanoscale perspective, at molecular and cellular levels, leads to a better understanding of the structure-function-physiological relationship of oral structures, making it possible that diseases can be better understood and thereby prevented.

Ag-NPs have demonstrated efficacy in inhibiting the main microorganisms causing tooth decay. So the authors consider it relevant to continue research in this area. Ag-NPs can be used in various fields of treatment as an effective antibacterial agent; as an example, we can mention, the area of periodontology, where its action as a mouthwash agent can reduce gingival conditions. It is also possible to prepare toothpastes combining the antibacterial effect of silver and the benefits of green plants. In other areas of dental practice, Ag-NPs can be added to traditional dental cements or surgical materials and thereby diminish the risk of a possible postoperative infection.

From the visionary talk "There's Plenty of Room at the Bottom," given by physicist Richard Feynman in the American Physical Society meeting at Caltech in the late 1950s, from the "nanorobots" used in medicine, nanodentistry can really improve dental practice and treat common problems, such as dental hypersensitivity and implant placement; it can provide more durable and biocompatible restorations and more precise orthodontic treatments and reduce the appearance of gum and bone diseases.

5. Conclusions

Interpretation of the UV-vis spectra and images obtained through TEM showed that the formation of silver nanoparticles is more effective when the active ingredients are extracted from the bioreducers in the boiling process. This shows that the polarity of the active ingredients is similar to that of water, and that temperature plays an important role by increasing solubility and antibacterial effect. It is also concluded that nanoparticles obtained by Hi have a very good size (17 nm), in sufficient quantity, and with a narrow particle size distribution.

Ag-NPs can be an alternative for treatment, not only against dental caries, but also to prevent the formation of pathogenic bacteria affecting the balance of the oral cavity. They may be an option to reduce the harmful effect of the major pathogens, to diminish postoperative infectious processes, while also representing an attractive option as part of the eco-friendly substances, which would result not only in less costly drugs, but also in substances with a minor risk to human health and the environment.

Conflict of interest

The authors declare that they have not conflict of interest.

Author details

Raul Alberto Morales Luckie[1]*, Rafael Lopez Casatañares[1], Rogelio Schougall[2], Sarai Carmina Guadarrama Reyes[2] and Víctor Sanchez Mendieta[1]

*Address all correspondence to: ramoralesl@uaemex.mx

1 Joint Center for Research in Sustainable Chemistry (CCIQS), Autonomous University of the State of Mexico, Toluca, State of Mexico, Mexico

2 School of Dentistry, Autonomous University of the State of Mexico, Toluca, State of Mexico, Mexico

References

[1] Allah A, Ibrahium M, Al-atrouny A. Effect of black tea on some cariogenic bacteria. World Applied Sciences Journal. 2011;**12**(4):552-558

[2] Loesche WJ. Role of Streptococcus mutans in human dental decay. Microbiology Reviews. 1986;**50**(4):353-380

[3] Li M, Lai G, Wang J. The prevalence of virulent clonal strains of mutans streptococci in vivo and co-culture sucession of the strains in vitro. Journal of Stomatology. 2011;**1**:18-24

[4] Loesche W, Rowan J, Straffon L, Loops P. Association of Streptococcus mutans with human dental decay. Infection and Immunity. 1975;**11**:1252-1259

[5] Yonglin D, Wei W, Meng F, Zhongchun T, Rong K, WenKai J, Longxing N. Antimicrobial and anti-biofilm effect of Bac8c on major bacteria associated with dental caries and Streptococcus mutans biofilms. Peptides. 2014;**52**:61-67

[6] Macias J, Arreguin V, Munoz J, Alvarez JA, Mosqueda JL, Macias AE. Chlorhexidine is a better antiseptic than povidone iodine and sodium hypochlorite because of its substantive effect. American Journal of Infection Control. 2013;**41**:634-637

[7] Mathur S, Mathur T, Srivasta R, Khatri R. Chlorhexidine: The gold standard in chemical plaque control. National Journal of Phisiolgy, Pharmacy and Pharmacology. 2011; **1**(2):45-50

[8] Jones C. Chlorhexidine: Is it still the gold standard? Periodontology 2000. 1997;**15**:55-62

[9] Emilson C. Potential efficacy of chlorhexidine against MutansStrepctocci and human dental caries. Journal of Dental Research. 1999;**73**(4):682-691

[10] Li Y-C, Kuan Y-H, Lee T-H, Huang F-M, Chang Y-C. Assessment of the cytotoxicity of chlorhexidine by employing an in vitro mammalian test system. Journal of Dental Sciences. 2014;**9**:130-135

[11] Lee T-H, Hu C-C, Lee S-S, Chou M-Y, Chang Y-C. Cytotoxicity of chlorhexidine on human osteoblastic cells is related to intracellular glutathione levels. International Endodontic Journal. DOI: 10.1111/j.1365-2591.2010.01700.x

[12] Anastas P, Autor J. Green Chemistry: Theory and Practice. Oxford: Oxford University Press; 2000. pp. 1-135

[13] Poole C, Owens F. Introduction to Nanotechnology. New York: Wiley Ed; 2003. pp. 1-387

[14] Sahoo S, Parveen S, Panda J. The present and future of nanotechnology. Nanomedicine: Nanotechnology, Biology and Medicine. 2007;**3**:20-31

[15] Cobo L, Akyildiz I. Bacteria-based communication in nanonetworks. Nanocomunication Network. 2010;**1**:244-256

[16] Editorial. The future of nanotechnologies. Technovation. 2012;**32**:157-160

[17] García-Contreras R, Argueta-Figueroa L, Mejía-Rubalcava C, Jiménez-Martínez R, Cuevas-Guajardo S, Sánchez-Reyna P, Mendieta-Zerón H. Perspectives for the use of silver nanoparticles in dental practice. International Dental Journal. 2011;**61**:297-301

[18] Sánchez F, Sobolev K. Nanotechnology in concrete – A review. Construction and Building Materials. 2010;**24**:2060-2071

[19] Beer C, Foldbjerg R, Hayashi Y, Sutherland D, Autrup H. Toxocity of silver nanoparticles-nanoparticle or silver ion? Toxicology Letters. 2012;**208**:286-292

[20] Siddhartha S, Tanmay B, Arnab R, Gajendra S, Ramachandrarao P, Debabrata D. Characterization of enhanced antibacterial effects of novel silver nanoparticles. IOP Nanotechnology. 2007;**18**(22):1-9

[21] Sung J, Kuk E, Yu K, Kim J, Park A, Lee H, Kim S, Park Y, Hwang C, Kim Y, Lee Y, Jeong D, Cho M. Antimicrobial effects of silver nanoparticles. Nanomedicine: Nanotechnology, Biology and Medicine. 2007;**3**:95-101

[22] Caruthers S, Wickline S, Lanza G. Nanotechnological applications in medicine. Current Opinion in Biotechnology. 2007;**18**:26-30

[23] Parveen S, Misra R, Sahoo SK. Nanoparticles: A boon to drug delivery, therapeutics, diagnostics and imaging. Nanomedicine: Nanotechnology, Biology, and Medicine. 2012;**8**: 147-166

[24] Guzmán M, Dille J, Godet S. Synthesis and antibacterial activity of silver nanoparticles against gram-positive and gram-negative bacteria. Nanomedicine: Nanotechnology, Biology and Medicine. 2012;**8**:37-45

[25] Wu Q, Cao H, Luan Q, Zhang J, Wang Z, Warner J, Watt A. Biomolecule-assisted synthesis of water-soluble silver nanoparticles and their biomedical applications. Inorganic Chemistry. 2008;**47**:5882-5888

[26] Rajan S, Acharya S, Saraswhaty V. Nanodentistry. Indian Journal of Scientific Research. 2013;**4**(2):233-238

[27] Fayaz AM, Balaji K, Girilal M, Yadav R, Kalaichelvan PT, Venketesan R. Biogenic synthesis of silver nanoparticles and their synergistic effect with antibiotics: A study against gram-positive and gram-negative bacteria. Nanomedicine: Nanotechnology, Biology and Medicine. 2010;**6**(1):103-109

[28] Delgado G, Olivares M, Chávez M, Ramírez T, Linares E, Robert B, Espinosa-García F. Antiinflammatory constituents from Heterothecainuloides. Journal of Natural Products. 2000;**64**:861-864

[29] Jalayer N, Niakan M, Kharazi F, Zardi S. Antibacterial activity of Iranian green and black tea on Streptococcus mutans: An in vitro study. Journal of Dentistry. 2011;**8**(2):55-59

[30] Rosas-Piñóna Y, Mejíaa A, Díaz-Ruizb G, Aguilara MI, Sánchez-Nietoc S, Fausto Rivero-Cruza J. Ethnobotanical survey and antibacterial activity of plants used in the Altiplane region of Mexico for the treatment of oral cavity infections. Journal of Ethnopharmacology. 2012;**141**:860-865

[31] Coballase-Urrutia E, Pedraza-Chaverric J, Camacho-Carranza R, Cárdenas-Rodríguez N, Huerta-Gertrudis B, Medina-Campos ON, Mendoza-Cruz M, Delgado-Lamas G, Javier Espinosa-Aguirre J. Antioxidant activity of Heterothecainuloides extracts and of some of its metabolites. Toxicology. 2010;**276**:41-48

[32] Coballase-Urrutia E, Pedraza-Chaverr J´, Cardenas-Rodrıguez N, Huerta-Gertrudis B, recedes, Garcıa-Cruz E, Ramırez-Morales A, Sanchez-Gonzalez DJ, Martınez-Martınez CM, Camacho-Carranza R, Espinosa-Aguirre JJ. Hepatoprotective effect of acetonic and methanolic extracts of Heterotheca inuloides against CCl4-induced toxicity in rats. Experimental andToxicologic Pathology. 2011;**63**:363-370

[33] Hiroyuki H, Harumi I, Yolanda S, Tetsuya O, Yumi K, Isao K. Antioxidative constituents in Heterothecainuloides. Bioorganic and Medicinal Chemistry. 1997;**5**(5):865-871

[34] World Health Organization. General guidelines for methodologies on research and evaluation of traditional medicine. 2000

[35] Gene R, Segura L, Adzet T, Marin E, Iglesias J. Heterothecainuloides: Anti-inflammatory and analgesic effect. Journal of Ethnopharmacology. 1998;**60**:157-162

[36] Haraguchi H, Ishikawa H, Sanchez Y, Ogura T, Kubo Y, Kubo I. Antioxidative constituents in Heterothecainuloides. Bioorganic & Medicinal Chemistly. 1997;**5**(5):865-871. Elsevier Science Ltd All rights reserved. Printed in Great Britain PII: S0968-0896(97)00029-1 0968-0896/97

[37] Komorowski R, Grad H, Yu Wu X, Friedman S. Antimicrobial Substantivity of chlorhexidine-treated bovine root dentin. Journal of Endodontics. 2000;**26**(6):315-317

[38] Mc Coy L, Wehler C, Rich S, García R, Miller D, Jones J. Adverse events associated with chlorhexidine use: Results from the Department of Veterans Affairs Dental Diabetes study. Journal of the American Dental Association (Chicago, IL). 2008;**139**(2):178-183

[39] Singh H, Kapoor P, Meshram G, Warhadpande M. Evaluation ossubstantivity of chlorhexidine to human dentin and its application in adhesive dentistry-an in vitro analysis. Indian Journal of Dentistry. 2011;**2**:8-10

[40] Zanatta F, Antoniazzi R, Rosing C. The effect of 0.12% chlorhexidine gluconate rinsing on previously plaque-free and plaque-covered surfaces: A randomized, controlled clinical trial. Journal of Periodontology. 2007;**78**(11):2127-2134

[41] Saliba CF, Oliveira HF, Breder J, Dario R, Córtes ME. Evaluation of the substantivity of clorhexidine in association with sodium fluoride in vitro. PesquiOdontol Bras. 2003;**17**(1):78-81

[42] Preeti-Satheesh Kumar, Satheesh-Kumar, Ravindra S, Jins J. Nanodentistry: A paradigm shift-from fiction to reality. Journal of Indian Prosthodontic Society. Mar 2011;**11**(1):1-6. DOI: 10.1007/s13191-011-0062-0

Chapter 7

Biological Activity of Silver Nanoparticles and Their Applications in Anticancer Therapy

Magdalena Skonieczna and Dorota Hudy

Additional information is available at the end of the chapter

http://dx.doi.org/10.5772/intechopen.77075

Abstract

Nanotechnology delivers materials and nanoparticles (NPs) with high biological potential, useful in bioengineering, nanomedicine, and human health protection. Silver nanoparticles (NPs), because of their wide spectrum of activities and physical and chemical properties, are nowadays extensively researched. However, careful studies on living organism should be performed, with strong attention to biocompatibility. Multiple cellular effects, displayed after AgNP treatments, show interesting potential of metal-based NPs, not only in bio-nanotechnology but also in molecular medicine and anticancer therapy. AgNPs are promising anticancer agents, influencing the cell cycle, inhibiting cancer proliferation, and inducing oxidative stress and propagation of programmed cellular death (apoptosis). Additionally, they protect against bacterial, fungal, and viral infections. During chemo- and radio-therapies, such antimicrobial protection will be desirable because of the decreased immunological resistance of cancer patients. In conclusion, AgNPs often present in the human environment should be studied for novel findings and better characteristic. This article discusses advantages of AgNP's "eco-friendly" production, followed by green synthesis, with particular consideration of antimicrobial and anticancer properties. Cellular processes, induced after AgNP treatments, are focused on antiproliferative, pro-oxidative, and pro-apoptotic activities of NPs.

Keywords: silver nanoparticles (AgNPs), nanotechnology, anticancer therapies, microbiological activity, nanoparticles (NPs), cancer cell lines

1. Introduction

Nanotechnology has developed a wide spectrum of engineered materials, composites, and particles, which in size are defined as nanoscale (below 100 nm) [1]. Comprised of different

compounds, nanocomposites have opened possibilities for applications in fields of bioengineering for agriculture [2], green technology [3], antifungal plant protection [4], and different strategies for human and animal health care—from tissue remodeling and scaffold production in regenerative medicine [5] or antiviral [6], antimicrobial [6, 7], and anticancer therapies [7, 8], in conventional/unconventional medical and veterinary science (**Figure 1**) [10, 11].

Among engineered materials various compounds are used including metals: silver (Ag) [12, 13], gold (Au) [13, 14], copper (Cu) [14], zinc (Zn) [15, 16], gallium (Al) [17], metal oxides [16], and many others [1, 18, 19]. Based on the physical and chemical approaches of metal-based nanoparticles, numerous features can be used in their applications, including shape recognition, paramagnetic properties, biocompatibility, fluorescence, and optical density [19]. Some NPs are suitable in diagnostic techniques, because of their paramagnetic behavior, unique optical properties, and quantum size effect used in bio-imaging (**Figure 2**) [18]. NPs can be used separately, as spheres 10 nm [12] or 18 nm in diameter as reported by Zielinska et al. [20] diluted in aqueous citrate buffer. Colloidal solutions of AgNPs were for that reason applied at different concentrations of particles per ml of solvent. In combination with different active compounds such as antibiotics, AGNP complexes, with improved size of their active surfaces, improved cytotoxicity against bacteria [9]. Because of their antibacterial properties and biocompatibility with human cells, many of active commercially designed Ag-based compounds are used for nanomaterial production, including by the coaxial electrospinning process [5].

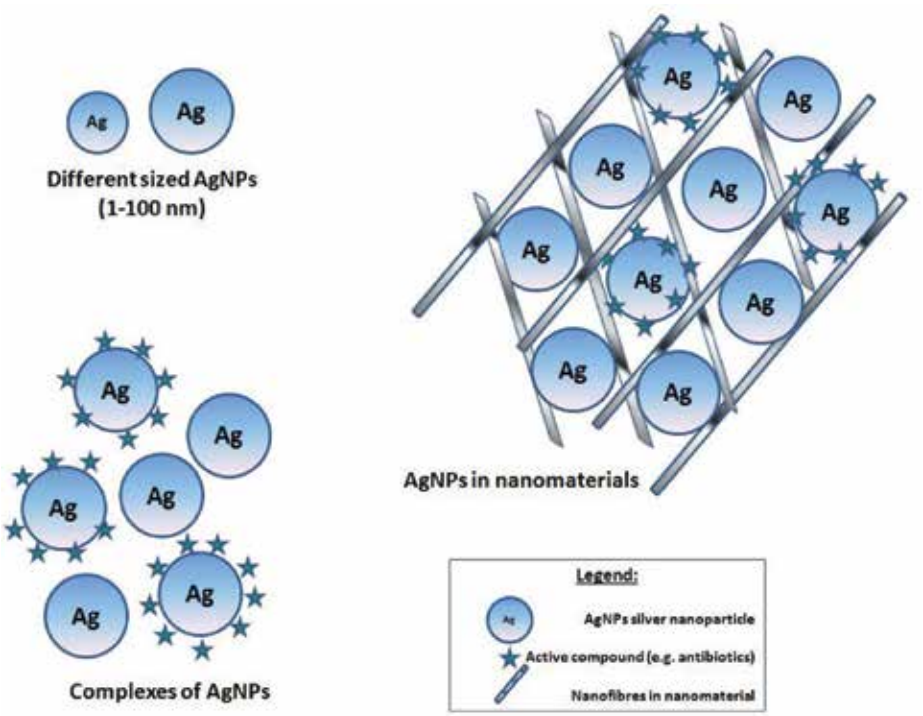

Figure 1. Types of applications for AgNPs as different-sized single particles in self-organized complexes with active compounds (e.g., antibiotics) or in nanofabricated materials (based on [5, 9]).

http://dx.doi.org/10.5772/intechopen.77075

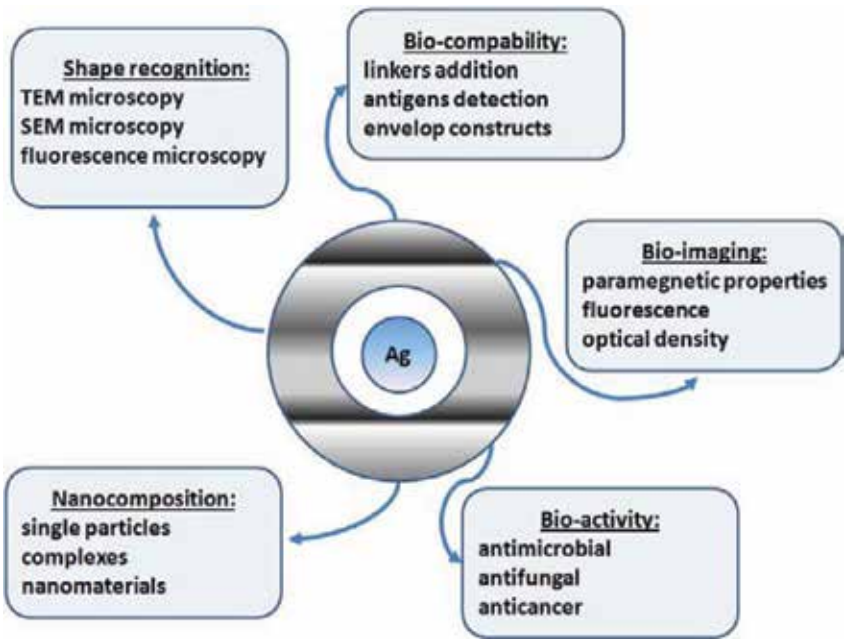

Figure 2. Physical and chemical properties of AgNPs implicated in their applications (based on [18]).

2. Characteristics of silver nanoparticles

Silver nanoparticles (AgNPs) are well known because of their wide spectrum of applications in diverse fields of research; this review will focus on their biological activities. For such reason size-dependent physical and chemical properties of AgNPs are discussed [18]. Living organisms are one-cell or multicellular structures with typically 10 μm across for a single cell, so the much smaller nanoparticles (NPs) (1–100 nm) can interact with cell surfaces (plasma membranes, plant cellulose walls, bacterial and fungal cell walls, and membranes). NPs or their active nano-complexes can penetrate and pass through the organism's external envelopes. The plasma membrane's permeability for small-sized AgNPs allows for accumulation of them in internal compartments of cells. Physical properties of Ag are used for tracking and visualization of NPs in living organisms and cells using, for example, TEM micrography or X-ray absorption spectroscopy [21]. The uptake mechanisms of NPs in eukaryotic cells were observed to be phagocytosis, endocytosis, or micropinocytosis [22] and were rather dose-dependent with diverse protection or cytotoxicity effects [21]. NPs must be well characterized before addition to cells and their physical and chemical properties well defined. These properties result mainly from different protocols of AgNP synthesis, and only nontoxic ones should be preferred in bioassays using living organisms.

2.1. Synthesis of AgNPs

Different strategies of AgNP synthesis should be focused on novel methods for ecological fabrication, allowing toxic chemical discrimination. Some so-called eco-friendly methods were

developed using ethanol extracts from many plant species, for example, ethanolic extract of *Rosa indica* petals [7]. Other procedures followed by encapsulation, microemulsions, or dispersion in polymeric solutions, based generally on plants or algae, also bacteria [23], and fungi organism. Intra- or externalization of NPs into one-cell organisms resulted with protein tagging, for example, AgNPs covered with proteins from the fungus *Coriolus versicolor* [24]. Protein-conjugated NPs could play a role of mimetic envelopes constructed from cellular proteins during inter- or externalization processes in living one-cell organisms. Bio-AgNP coverings stabilize NPs and extend the possibilities of their application in living tissues [24]. During simple aqueous synthesis, temperature elevation of a starch solution for 20 h above room temperature, with addition of silver nitrate and glucose is sufficient to produce eco-starched AgNPs [23]. It was reported also that virus particles also seem to be useful in NP production (**Figure 3**) [23].

2.2. Antimicrobial activity

2.2.1. Antibacterial properties

Among the biological activities of AgNPs, an antimicrobial action is already well characterized [7–9, 25]. The most effective is an antiproliferative impact where in a minimum inhibition concentration (MIC) assay, inhibition of bacterial growth on plate cultures is observed. Typically, the tests are made both Gram-negative and Gram-positive bacteria, with plate agar, liquid LB medium (lysogeny broth, named also Luria-Bertani medium), or a migration assay. It was reported, in MIC assays against different bacterial strains and human pathogenic bacteria such as *Streptococcus* mutants (MTCC-896), *Enterococcus faecalis* (MTCC-439) (Gram-positive), *E. coli*

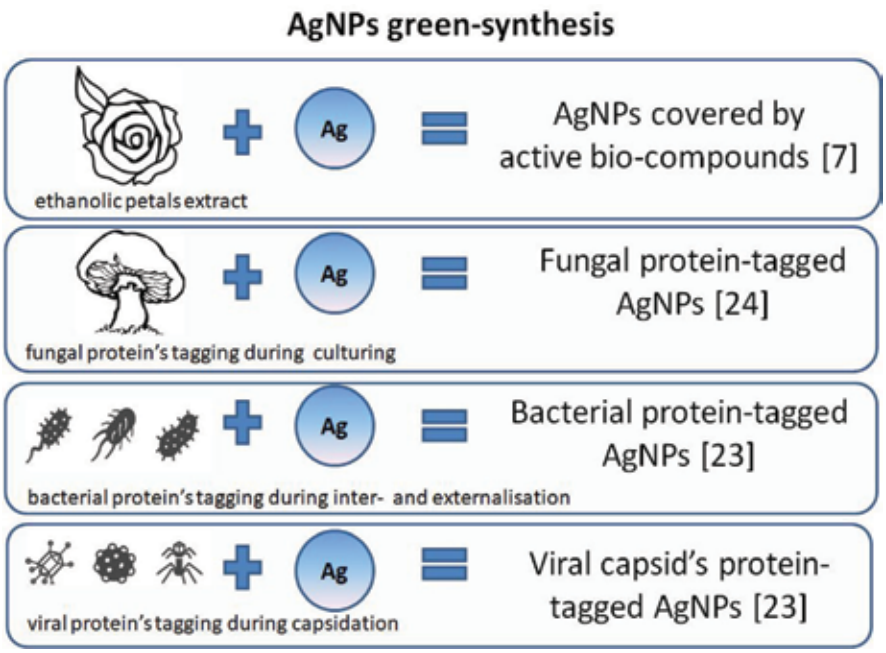

Figure 3. Scheme of green-synthesized "eco-friendly" AgNPs (based on [7, 23, 24]).

(MTCC-40), and *Klebsiella pneumonia* (MTCC-740) (Gram-negative), it was reported that addition of ethanolic petal extract of *Rosa indica* or $AgNO_3$ solutions (each 30 μl) reduced significant microbial proliferation significantly [7]. The mechanism of action that resulted in proliferative potential reduction during MIC assays was explained by the good permeability of AgNPs through the bacterial wall and plasma membranes [7]. The cytotoxic effect was improved when biologically synthesized nanoparticles were used together with $AgNO_3$ solutions [7]. On the other hand, addition of Ag^+ ions to the culture media resulted in reduction of biofilm formation by bacteria during growth. Anti-biofilm formation effects of AgNPs were observed against Gram-positive (*Enterococcus faecalis* and *Staphylococcus aureus*) and Gram-negative (*Shigella sonnei* and *Pseudomonas aeruginosa*) bacteria in biological assays [6]. Other pathogens, strains of *Escherichia coli*, *Staphylococcus aurous*, *Pseudomonas aeruginosa*, *Klebsiella pneumoniae*, and *Haemophilus influenzae*, were inhibited by AgNPs synthesized with leaf extract of *Artemisia vulgaris* [3]. The inhibitory effect was discussed there in terms of plasma membrane interaction of AgNPs and release of Ag^+ ions into the cytoplasm that eventually resulted in disruption of respiratory mechanisms located in in the bacterial membrane and mesosomes, and also of ion exchange processes, and blockade of synthesis of sulfur-containing proteins on ribosomes [3]. All of those schemes of action demonstrate the antimicrobial properties of AgNPs and implicate their usage as anti-pathogenic agents reducing the proliferative potential of microbes.

2.2.2. Antifungal properties

The unicellular *fungi*, and mostly multicellular *fungi*, are responsible within plant agricultures for plant diseases. They are cost-risky and noneconomic for vegetables and fruit farms, also during long-term production, storage, and transportation procedures. AgNP addition during plant growth could play a role of environmentally safe anti-fungicides [4, 26, 27]. AgNPs, added at different concentrations to agar plates, were very effective against plant phytopathogenic fungi in studies of 18 different fungal species [4]. In vitro studies showed a hypothetical molecular mechanism of action for AgNPs, where released Ag^+ ions into the cytoplasmic compartment of fungal cells disrupt respiratory system and have an impact on DNA replication process and on expression of genes implicated in replication [4, 28, 29]. Multifunctional bio-applications of AgNPs 20 nm in size were studied for protection against pathogenically species of fungi, strains of *Trichophyton mentagrophytes* and *Candida* species, in immunosuppressed patients [30]. Similar effects, with reduction of proliferation, were observed on agar plate assays against species potentially pathogenic for plants and humans: *Penicillium brevicompactum*, *Chaetomium globosum*, *Cladosporium cladosporioides*, *Mortierella alpina*, *Stachybotrys chartarum*, and *Aspergillus fumigatus* [30].

2.2.3. Antiviral properties

Anti-pathogenic activity of AgNPs is wide, and the spectrum of their action has been reported against viral infections in plants, animals, and humans [6, 31]. The most effective prevention against diseases caused by different viruses is an antiviral vaccine. Although effective vaccines have not been discovered against every viral infection, antiviral agents are still being developed, and AgNPs are also in this potential group [31]. Human viral diseases such as influenza, human immunodeficiency virus, hepatitis, chickenpox, infectious mononucleo-

sis, herpes keratitis, or viral encephalitis are still studied with novel therapeutics, because of their high mortality risk in the human population, together with increases of virus resistance against already used pharmaceuticals [31]. The interaction of AgNPs, synthesized by a biological method using fungi, was tested against herpes simplex virus types 1 and 2 (HSV-1 and HSV-2, respectively) and human parainfluenza virus type 3 (HPIV-3) [31]. In these reports the particular mechanism of prevention against viral infection in Vero cells *in vitro* was explained as a physical barrier, built by NPs [31]. Monolayer culture of Vero cells were preincubated with AgNPs for 1 h at 37°C and then infected with HSV-1, HSV-2, or HPIV-3 and in the next 2 days, the monolayers were fixed and stained with X-gal (HSV-1 and HSV-2) or crystal violet (HPIV-3), and plaque numbers were scored [31]. The final results showed a lower infectiveness of viruses for cells pretreated with AgNPs in comparison to untreated cells without NPs [31]. Size-dependent mechanical protection against Monkeypox virus infection was also previously reported in vitro, in tests with 10 nm AgNPs a, with significant inhibition of disease [32]. In human cells the addition of AgNPs could inhibit enzymes responsible for DNA replication, a crucial process for further viral infection [31]. Pure AgNPs, synthesized by the electrochemical method were tested against poliovirus by adding different concentrations of AgNPs were added to human rhabdomyosarcoma (RD) monolayer cells before viral infection [33]. The results confirm silver protection against poliovirus infection, with the cell viability up to 98% at 48 h postinfection [33]. For the food industry it is important to avoid viral infections within a big farm where the animals are cultured and are crowded. Food production in India could be endangered by infectious bursal disease (IBD) virus [34] and therefore alternative technology against IBD virus using AgNPs started to be developed. This strategy is based on two schemes, inoculation of viral particles first for 2 h with active AgNP solutions and then injection of such mixtures into embryonated chicken eggs, whereas the second method is first infection of embryonated chicken eggs with virus and then the AgNP injection. In both strategies the viral infection was reduced [34].

Antiviral activity of silver nanoparticles (AgNPs) is still unknown and needs to be studied, because of its usefulness for human applications. However, not only direct action on virus particles is important in developing novel strategies against viral infections. In many cases an intermediate carrier/host is required in the replication cycle of a virus, and a strategy was developed against such a vector using AgNPs fabricated with *Pedalium murex*, an ancient Indian medicinal plant's seed extract, for inducing mortality in mosquito's larvae stage [6]. Zika virus needs the vector *Aedes aegypti* for a complete replication cycle and spreading the disease. AgNPs fabricated with *P. murex* extract tested on fourth instar mosquito larvae reduced the viability of Zika vector after 24 h [6]. This promising finding showed a wide spectrum of applications of different fabricated AgNPs alone against different viral infections and diseases. The mode of action could be direct or indirect.

2.3. Anticancer activity

Combined cancer therapy allows limitation of the side effects of chemotherapy, decreasing effective doses or inducing cellular self-protection against damaging agents [35]. For many aspects of conventional therapies, combinations of novel drugs and NPs together with already well known compounds, is still tested. Searching for more effective protocols for drug

administration leads to the modification of already existing procedures and combining pharmacological agents with natural, unconventional molecules. Metal-based AgNPs, known as pro-oxidative in different cancer cell lines [36] including breast MCF-7 and lung A549 cells [37] and squamous carcinoma SCC-25 cells [12], have shown novel applications in photodynamic therapy [37, 38]. The alkaloid berberine was tested on squamous carcinoma cells as an antiproliferative and pro-apoptotic agent alone [22, 39–41] or in combination with AgNPs that improved its anticancer properties [12]. The antimicrobial activity of AgNPs as aseptic or preservative agents has been known since decades, and they also serve for synthesis of novel nanomaterials with potential applications in regenerative medicine [5]. For many applications, compounds such as metal NPs should be carefully examined, especially when they are easily applied by living organisms.

2.3.1. Antiproliferative activity

Use of AgNPs in the food industry, as antimicrobial preservatives, has an impact on the human digestive tract. Interactions of AgNPs with healthy cells (epithelial cells, mucous membrane cells, etc.) and cancer cells (squamous, liver, or colon cells) through the gastrointestinal tract has implicated diverse actions of NPs as anti- or pro-oncogenic factors. Knowledge about processes of carcinogenesis are still unclear; however, applications of AgNPs as anticancer agents is nowadays strongly developed. The most widely used AgNPs disrupt the proliferative system and cell cycle of cancer cells, with finally inhibition of proliferation. Tested on squamous carcinoma SCC-25 cells, colloidal solutions of 10-nm-diameter NPs at a dose of 10 ng/ml arrested the cell cycle in the sub-G1 or G0/G1 phase after 24 and 48 h, respectively [12]. The cells responded with a failure of mitosis, and in the treated population there were not as many bi-nucleated and doublet cells as in controls. DNA synthesis was also stopped, probably because of DNA damage (single- and double-stranded breaks, sSBs and dSBs) and because of the presence of AgNP's inside the cell nuclei. This suggestion was confirmed by measuring production of reactive oxygen species (ROS) in parallel cytometric assays, which damage DN, influence the S-phase of the cell cycle, and inhibit replication [12]. Additionally, cell proliferation was monitored by colorimetric MTT assays, where absorbance measured at 570 nm is proportional to the amount of cells in each well on a plate. This simple assay showed that after AgNP treatment, viability and proliferation of SCC-25 cells decreased in dose-dependent manner with increased concentration of AgNPs [12]. Larger 20 nm diameter AgNPs also displayed antiproliferative effects at higher concentrations (up to 20 μg/ml) in two cancer cell lines, HepG2 (liver) and Caco-2 (colon) when cytotoxicity was estimated fluorometrically by the resazurin (Alamar Blue) reduction assay [42] in which nonfluorescent Alamar Blue is taken up by viable cells and reduced by mitochondria to the fluorescent product resorufin. Fluorescence is proportional to the viability of the cells and corresponds to the cell number [42]. After 24 h of incubation with AgNPs, viability and proliferation of HepG2 cells were more reduced than those of Caco-2 cells; however, in both cell lines they were significantly lower than untreated controls [42]. Tests on different human cell line models showed tissue-dependent sensitivity and the importance for applied doses potentially used in anticancer therapies of NPs. The same research group, working again with HepG2 and Caco-2 cells, discussed the genotoxic potential of AgNPs as a result of chromosome damage

during mitosis, where chromosomal abnormalities occurred as seen by micronucleus formation (Mn assay) [43]. The nanosilver genotoxicity resulted in viability reduction in a dose-dependent manner and was explained by cytokinesis blockade [43], which could be a result of abnormal formation of histone H2A, that disrupts cellular division and proper chromatin (chromosome) formation [44]. AgNPs act also as epigenetic factors and influence genetic profiles in treated cells [45]. It was reported that several genes could be impacted by AgNPs, especially those related to the cell cycle, where they could be upregulated or downregulated. The most important findings were connected with genes coding for cell cycle checkpoint proteins and also for DNA repair pathways during the S-phase [45–47]. All of these molecular disruptions resulted in the antiproliferative action of AgNPs in living cells, especially in cancer and cancer stem cells [44].

2.3.2. Pro-oxidative activity

Most of the findings about toxically effects of AgNPs in antimicrobial and anticancer defense, based on the mitochondrial activation and reactive oxygen species overproduction, are interpreted as pro-oxidative properties. AgNPs possess the ability to induce mitochondrial chain and complex disruption that leads to superoxide anion leakage [12, 22, 48]. After AgNP internalization, into cytoplasm compartments, typically Ag^+ ions are released which influence mitochondrial enzymes and also interact with –SH groups of proteins and glutathione (GSH). In such situation the ROS scavenging potential of GSH decreased and oxidative stress occurred [44]. DNA damage changed gene expression, and cellular death could be manifested as programmed death (apoptosis) [44]. In photodynamic therapy (PDT), AgNPs caused tumor cell sensitization via intracellular ROS overproduction [19, 37, 38]. Ag ions are captured by free electrons, which affect mitochondrial membrane potential (Ψ) and leads to an increase in mitochondrial membrane permeability [45]. The production of intracellular ROS is amplified by the next generation of oxidizing agents and lowered production of ATP by mitochondria in tumor cells [45]. The ROS production and damages resulting from oxidative stress are AgNP size-dependent; smaller NPs cause greater ROS overproduction [1]. Those observations result from the ability of AgNPs to interact with cellular components and to penetrate to organelles (mitochondria, nuclei, liposomes, endoplasmic reticulum, etc.) and to release free Ag^+ ions there (**Figure 4**) [1].

2.3.3. Pro-apoptotic activity

After AgNP internalization into cancer cells, a cascade of processes starts with loss of inner homeostasis and redox state destabilization. A series of free radical waves damages mitochondrial and nuclear membranes and propagates oxidative stress. Additionally, in S-phase (DNA replication) of the cell cycle, damaged DNA is not repaired effectively because repair enzymes are blocked by Ag+ ions and replication stops [12, 49]. Because of uncoupling in mitochondria and effects on mitochondrial membrane potential, the ROS level increases to propagate the canonical apoptotic pathway (**Figure 4**). The mitochondria-dependent apoptosis pathway was studied in SCC-25 cells at the transcriptional level, where expression of the genes Bax and Bcl-2 was assayed [12, 50]. The pro-apoptotic Bcl-2 gene was upregulated after 24 h of treatment with AgNPs [12]. ROS production in Caco-2 cells was manifested also by an inflammatory state that resulted in cellular death due to release of the pro-inflammatory

cytokine interleukin(IL)-8 after 24 h of AgNP exposure [49]. This state was also propagated between cells by external pro-apoptotic signals. Use of AgNPs as good pro-apoptotic agents in cancer therapy seems to be reasonable. Toxicity of AgNPs is shown through the intrinsic ROS-mediated mitochondrial apoptotic pathway [49]. AgNPs could propagate a free radical wave, with further lysosomal rupture and free radical accumulation. Lysosomal damage leads to cathepsin release into the cytoplasm, which is a signal for lysosome-mediated apoptosis [1, 51]. Any of these disruptions have been described as cytotoxic effects of AgNPs of different origins; however, the most desirable one is the lethal apoptotic effect on cancer cells.

2.4. Applications of AgNPs

The numerous physical and chemical properties of AgNPs implicate possible applications in the human environment: in agriculture, food industry, cosmetology and finally in human health protection and medicine [1, 2, 13, 19]. Metal-based particles, because of their paramagnetic property and optical density (**Figure 2**), are widely used in bio-imaging as well as in electron microscopy, in magnetic resonance, in computed tomography for visualization, and in molecular diagnostics [19, 21, 50]. AgNPs, as cellular sensitizers with pro-oxidative and pro-apoptotic potential, also serve as therapeutic agents in photodynamic therapy against cancer cells [37, 38]. In future applications some possible controversies must be resolved: dosage for different tissues, because of tissue-specific biocompatibility and side effects during therapy or microbial resistance against NPs. Some effects of AgNPs appear to be dual

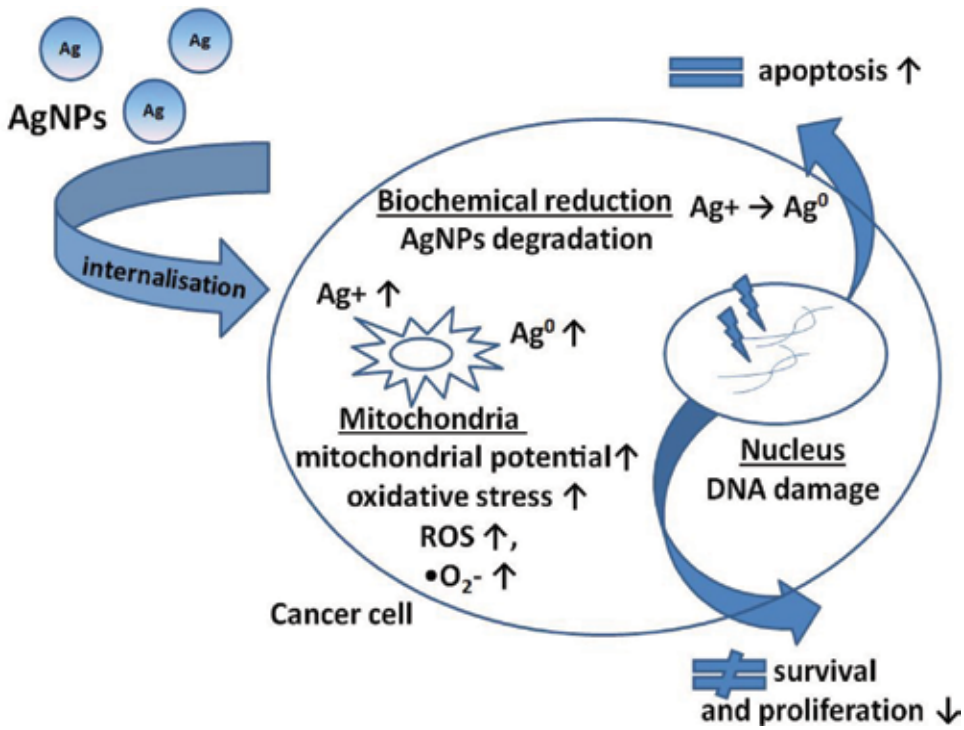

Figure 4. Pro-oxidative activities of AgNPs in cancer cells.

and even opposite in different situations, such as anti- or pro-oxidative, anti- or pro-apoptotic, biosensing, or bioresisting-activity depending on the type of organism or cells [30]. Nanotechnology allows for technical applications of AgNPs, for example for fabrication in material technology [5]. Size-dependent activities and the ability to form different complexes with natural or pharmaceutical compounds have opened further applications for AgNPs, especially in biomaterials, health care, cancer therapy, environment protection, agriculture, and chemical synthesis [5, 9, 52]. Biomedical applications, particularly in nanomedicine, are nowadays the most desirable.

3. Conclusions

Silver nanoparticles, because of their wide spectrum of activities and physical and chemical properties, are nowadays studied extensively. However, careful studies on living organisms should be performed, with strong attention to biocompatibility. Multiple effects displayed after AgNP treatment show an interesting potential of metal-based NPs, not only in bionanotechnology but also in molecular medicine and anticancer therapy. AgNPs are promising anticancer agents: they influence the cell cycle, inhibit cancer cell proliferation, induce oxidative stress, and propagate programmed cellular death (apoptosis). Additionally, they protect against bacterial, fungal, and viral infections. During chemo- and radio-therapies, such antimicrobial protection is desirable, because of the decreased immunological resistance of cancer patients. In conclusion, more studies on AgNPs should be carried out for novel findings and better characteristic of silver NPs.

Acknowledgements

Magdalena Skonieczna received financial support from the Association for the Support of Cancer Research in Gliwice, Poland.

Conflict of interest

The authors declared no potential conflicts of interest with respect to the research, authorship, and/or publication of this article.

Author contributions

Magdalena Skonieczna conceived the idea of this review, participated in writing of the manuscript, and performed all literature surveys. Dorota Hudy prepared the figures and reviewed the literature. Both authors were involved in revising the paper's important content, read, and approved the final manuscript.

Author details

Magdalena Skonieczna[1,2]* and Dorota Hudy[1,2]

*Address all correspondence to: magdalena.skonieczna@polsl.pl

1 Biosystems Group, Silesian University of Technology, Institute of Automatic Control, Gliwice, Poland

2 Biotechnology Centre, Silesian University of Technology, Gliwice, Poland

References

[1] Riaz Ahmed KB, Nagy AM, Brown RP, Zhang Q, Malghan SG, Goering PL. Silver nanoparticles: Significance of physicochemical properties and assay interference on the interpretation of in vitro cytotoxicity studies. Toxicology in Vitro. 2017;**38**:179-192. DOI: 10.1016/j.tiv.2016.10.012

[2] Bouwmeester H, Dekkers S, Noordam MY, et al. Review of health safety aspects of nanotechnologies in food production. Regulatory Toxicology and Pharmacology. 2009;**53**(1): 52-62. DOI: 10.1016/j.yrtph.2008.10.008

[3] Rasheed T, Bilal M, Iqbal HMN, Li C. Green biosynthesis of silver nanoparticles using leaves extract of Artemisia vulgaris and their potential biomedical applications. Colloids and Surfaces. B, Biointerfaces. 2017;**158**:408-415. DOI: 10.1016/j.colsurfb.2017.07.020

[4] Kim SW, Jung JH, Lamsal K, Kim YS, Min JS, Lee YS. Antifungal effects of silver nanoparticles (AgNPs) against various plant pathogenic fungi. Mycobiology. 2012;**40**(1):53-58. DOI: 10.5941/MYCO.2012.40.1.053

[5] Hudecki A, Gola J, Ghavami S, et al. Structure and properties of slow-resorbing nanofibers obtained by (co-axial) electrospinning as tissue scaffolds in regenerative medicine. PeerJ. 2017;**5**:e4125. DOI: 10.7717/peerj.4125

[6] Ishwarya R, Vaseeharan B, Anuradha R, et al. Eco-friendly fabrication of Ag nanostructures using the seed extract of Pedalium murex, an ancient Indian medicinal plant: Histopathological effects on the Zika virus vector Aedes aegypti and inhibition of biofilm-forming pathogenic bacteria. Journal of Photochemistry and Photobiology B: Biology. 2017;**174**(July):133-143. DOI: 10.1016/j.jphotobiol.2017.07.026

[7] Baghbani-Arani F, Movagharnia R, Sharifian A, et al. Biosynthesis of silver nanoparticles using ethanolic petals extract of Rosa indica and characterization of its antibacterial, anticancer and anti-inflammatory activities. Journal of Photochemistry and Photobiology B: Biology. 2017;**138**(July):640-649. DOI: 10.1016/j.jphotobiol.2017.07.026

[8] Baghbani-Arani F, Movagharnia R, Sharifian A, Salehi S, Shandiz SAS. Photo-catalytic, anti-bacterial, and anti-cancer properties of phyto-mediated synthesis of silver nanoparticles

from Artemisia tournefortiana Rchb extract. Journal of Photochemistry and Photobiology B: Biology. 2017;**173**(July):640-649. DOI: 10.1016/j.jphotobiol.2017.07.003

[9] Deng H, McShan D, Zhang Y, et al. Mechanistic study of the synergistic antibacterial activity of combined silver nanoparticles and common antibiotics. Environmental Science & Technology. 2016;**50**(16):8840-8848. DOI: 10.1021/acs.est.6b00998

[10] Hill EK, Li J. Current and future prospects for nanotechnology in animal production. Journal of Animal Science and Biotechnology. 2017;**8**(1):1-13. DOI: 10.1186/s40104-017-0157-5

[11] Singla R, Guliani A, Kumari A, Yadav SK. Metallic nanoparticles, toxicity issues and applications in medicine. Chapter 3. In: Yadav SK, editor. Nanoscale Materials in Targeted Drug Delivery, Theragnosis and Tissue Regeneration. Singapore: © Springer Science+Business Media; 2016:41-80. DOI: 10.1007/978-981-10-0818-4

[12] Dziedzic A, Kubina R, Buldak RJ, et al. Silver nanoparticles exhibit the dose-dependent anti-proliferative effect against human squamous carcinoma cells attenuated in the presence of berberine. Molecules. 2016;**21**(3). DOI: 10.3390/molecules21030365

[13] Aueviriyavit S, Phummiratch D, Maniratanachote R. Mechanistic study on the biological effects of silver and gold nanoparticles in Caco-2 cells—Induction of the Nrf2/HO-1 pathway by high concentrations of silver nanoparticles. Toxicology Letters. 2014;**224**(1):73-83. DOI: 10.1016/j.toxlet.2013.09.020

[14] Czerwińska K, Golec M, Skonieczna M, et al. Cytotoxic gold(III) complexes incorporating a 2,2′:6′,2″-terpyridine ligand framework—The impact of the substituent in the 4′-position of a terpy ring. Dalton Transactions. 2017;**46**(10):3381-3392. DOI: 10.1039/C6DT04584G

[15] Maduray K, Karsten A, Odhav B, Nyokong T. In vitro toxicity testing of zinc tetrasulfophthalocyanines in fibroblast and keratinocyte cells for the treatment of melanoma cancer by photodynamic therapy. Journal of Photochemistry and Photobiology B: Biology. 2011;**103**(2):98-104. DOI: 10.1016/j.jphotobiol.2011.01.020

[16] Mishra PK, Mishra H, Ekielski A, Talegaonkar S, Vaidya B. Zinc oxide nanoparticles: A promising nanomaterial for biomedical applications. Drug Discovery Today. 2017; **22**(12):1825-1834. DOI: 10.1016/j.drudis.2017.08.006

[17] Maduray K, Odhav B, Nyokong T. In vitro photodynamic effect of aluminum tetrasulfophthalocyanines on melanoma skin cancer and healthy normal skin cells. Photodiagnosis and Photodynamic Therapy. 2012;**9**(1):32-39. DOI: 10.1016/j.pdpdt.2011.07.001

[18] Salata OV. Applications of nanoparticles in biology and medicine. Journal of Nanobiotechnology. 2004;**6**(3):1-6. DOI: 10.1186/1477-3155-2-12

[19] Rai M, Ingle AP, Birla S, Yadav A, Santos CA Dos. Strategic role of selected noble metal nanoparticles in medicine. Critical Reviews in Microbiology 2016;42(5):696-719. DOI: 10.3109/1040841X.2015.1018131

[20] Zielinska E, Zauszkiewicz-Pawlak A, Wojcik M, Inkielewicz-Stepniak I. Silver nanoparticles of different sizes induce a mixed type of programmed cell death in human pancreatic ductal adenocarcinoma. Oncotarget. 2017 Nov 20;**9**(4):4675-4697. DOI: 10.18632/oncotarget.22563

[21] Veronesi G, Deniaud A, Gallon T, et al. Visualization, quantification and coordination of Ag^+ ions released from silver nanoparticles in hepatocytes. Nanoscale. 2016;**8**(38):17012-17021. DOI: 10.1039/C6NR04381J

[22] Foldbjerg R, Jiang X, Miclăuş T, Chen C, Autrup H, Beer C. Silver nanoparticles—Wolves in sheep's clothing? Toxicology Research. 2015;**4**:563-575. DOI: 10.1039/C4TX00110A

[23] Raveendran P, Fu J, Wallen SL, Am J. Completely "green" synthesis and stabilization of metal nanoparticles. Journal of the American Chemical Society. 2003;**125**(46):13940-13941. DOI: 10.1021/ja029267j

[24] Sanghi R, Verma P. Biomimetic synthesis and characterisation of protein capped silver nanoparticles. Bioresource Technology. 2009;**100**(1):501-504. DOI: 10.1016/j.biortech.2008.05.048

[25] Bello-Vieda N, Pastrana H, Garavito M, Ávila A, Celis A, Muñoz-Castro A, et al. Antibacterial activities of azole complexes combined with silver nanoparticles. Molecules. 2018;**23**(2):361. DOI: 10.3390/molecules23020361

[26] Jo YK, Kim BH, Jung G. Antifungal activity of silver ions and nanoparticles on phytopathogenic fungi. Plant Disease. 2009;**93**:1037-1043. DOI: 10.1094/PDIS-93-10-1037

[27] Park HJ, Kim SH, Kim HJ, Choi SH. A new composition of nanosized silica-silver for control of various plant diseases. Plant Pathology Journal. 2006;**22**:295-302. DOI: 10.5423/PPJ.2006.22.3.295

[28] Kim SW, Kim KS, Lamsal K, Kim YJ, Kim SB, Jung M, Sim SJ, Kim HS, Chang SJ, Kim JK, et al. An *in vitro* study of the antifungal effect of silver nanoparticles on oak wilt pathogen *Raffaelea sp*. Journal of Microbiology and Biotechnology. 2009;**19**:760-764. DOI: 10.4014/jmb.0812.649

[29] Min JS, Kim KS, Kim SW, Jung JH, Lamsal K, Kim SB, Jung M, Lee YS. Effects of colloidal silver nanoparticles on sclerotium-forming phytopathogenic fungi. Plant Pathology Journal. 2009;**25**:376-380. DOI: 10.5423/PPJ.2009.25.4.376

[30] Zhang X-F, Liu Z-G, Shen W, Gurunathan S. Silver nanoparticles: Synthesis, characterization, properties, applications, and therapeutic approaches. International Journal of Molecular Sciences. 2016;**17**(9):1534. DOI: 10.3390/ijms17091534

[31] Gaikwad S, Ingle A, Gade A, Rai M, Falanga A, Incoronato N, et al. Antiviral activity of mycosynthesized silver nanoparticles against herpes simplex virus and human parainfluenzavirus type 3. International Journal of Nanomedicine. 2013;**8**:4303-4314. DOI: 10.2147/IJN.S50070

[32] Speshock JL, Murdock RC, Braydich-Stolle LK, Schrand AM, Hussain SM. Interaction of silver nanoparticles with Tacaribe virus. Journal of Nanbiotechnology. 2010;**8**:19. DOI: 10.1186/1477-3155-8-19

[33] Huy TQ, Hien Thanh NT, Thuy NT, Chung PV, Hung PN, Le AT, Hong Hanh NT. Cytotoxicity and antiviral activity of electrochemical-synthesized silver nanoparticles against poliovirus. Journal of Virological Methods. 2017 Mar;**241**:52-57. DOI: 10.1016/j.jviromet.2016.12.015. Epub 2016 Dec 28

[34] Pangestika R, Ernawati R, Suwarno. Antiviral activity effect of silver nanoparticles (AgNPs) solution against the growth of infectious bursal disease virus on embryonated chicken eggs with ELISA test. KnE Life Sciences. 2017;**3**(6):536-548. DOI: 10.18502/kls.v3i6.1181

[35] Khuda-Bukhsh AR, Mondal J, Panigrahi AK. Conventional chemotherapy: Problems and scope for combined therapies with certain herbal products and dietary supplements. Austin Journal of Molecular and Cellular Biology. 2014;**1**(1):1-10

[36] Dayem AA, Hossain MK, Lee S, et al. The role of reactive oxygen species (ROS) in the biological activities of metallic nanoparticles. International Journal of Molecular Sciences. 2017;**18**(1):E120. DOI: 10.3390/ijms18010120

[37] Mfouo-Tynga I, El-Hussein A. Photodynamic ability of silver nanoparticles in inducing cytotoxic effects in breast and lung cancer cell lines. International Journal of Nanomedicine. 2014;**9**:3771-3780. DOI: 10.2147/IJN.S63371

[38] El-Hussein A, Hamblin MR. ROS generation and DNA damage with photo-inactivation mediated by silver nanoparticles in lung cancer cell line. IET Nanobiotechnology. 2017; **11**(2):173-178. DOI: 10.1049/iet-nbt.2015.0083

[39] Ho YT, Lu CC, Yang JS, et al. Berberine induced apoptosis via promoting the expression of caspase-8, −9 and −3, apoptosis-inducing factor and endonuclease G in SCC-4 human tongue squamous carcinoma cancer cells. Anticancer Research. 2009;**29**:4063-4070. DOI: 10.1002/mnfr.200900265

[40] Ho YT, Yang JS, Li TC, et al. Berberine suppresses *in vitro* migration and invasion of human SCC-4 tongue squamous cancer cells through the inhibitions of FAK, IKK, NF-kappaB, u-PA and MMP-2 and -9. Cancer Letters. 2009;**279**:155-162. DOI: 10.1016/j.canlet.2009.01.033 Epub 2009 Feb 28

[41] Seo YS, Yim MJ, Kim BH, et al. Berberine-induced anticancer activities in FaDu head and neck squamous cell carcinoma cells. Oncology Reports. 2015;**25**:3025-3034. DOI: 10.3892/or.2015.4312

[42] Sahu SC, Zheng J, Graham L, et al. Comparative cytotoxicity of nanosilver in human liver HepG2 and colon Caco2 cells in culture. Journal of Applied Toxicology. 2014;**34**(11):1155-1166. DOI: 10.1002/jat.2994

[43] Sahu SC, Roy S, Zheng J, Ihrie J. Contribution of ionic silver to genotoxic potential of nanosilver in human liver HepG2 and colon Caco2 cells evaluated by the cytokinesis-block micronucleus assay. Journal of Applied Toxicology. 2016;**36**(4):532-542. DOI: 10.1002/jat.3279

[44] Braydich-Stolle LK, Lucas B, Schrand A, Murdock RC, Lee T, Schlager JJ, et al. Silver nanoparticles disrupt GDNF/Fyn kinase signaling in spermatogonial stem cells. Toxicological Sciences. 2010;**116**:577. DOI: 10.1093/toxsci/kfq148. Epub 2010 May 20

[45] Dubey P, Matai I, Kumar SU, Sachdev A, Bhushan B, Gopinath P. Perturbation of cellular mechanistic system by silver nanoparticle toxicity: Cytotoxic, genotoxic and epigenetic potentials. Advances in Colloid and Interface Science. 2015;**221**:4-21. DOI: 10.1016/j.cis.2015.02.007

[46] Foldbjerg R, Irving ES, Hayashi Y, Sutherland DS, Thorsen K, Autrup H, et al. Global gene expression profiling of human lung epithelial cells after exposure to nanosilver. Toxicological Sciences. 2012;**130**:145. DOI: 10.1093/toxsci/kfs225. Epub 2012 Jul 24

[47] AshaRani PV, Mun LKG, Hande MP, Valiyaveettil S. Cytotoxicity and genotoxicity of silver nanoparticles in human cells. ACS Nano. 2009;**3**:279. DOI: 10.1021/nn800596w

[48] Skonieczna M, Cielar-Pobuda A, Saenko Y, et al. The impact of dids-induced inhibition of voltage-dependent anion channels (VDAC) on cellular response of lymphoblastoid cells to ionizing radiation. Medical Chemistry (Los Angeles). 2017;**13**(5):477-483. DOI: 10.2174/1573406413666170421102353

[49] Chen N, Song Z-M, Tang H, et al. Toxicological effects of Caco-2 cells following short-term and long-term exposure to Ag nanoparticles. International Journal of Molecular Sciences. 2016;**17**(6):974. DOI: 10.3390/ijms17060974

[50] Liu Y, Li X, Bao S, Lu Z, Li Q, Li CM. Plastic protein microarray to investigate the molecular pathways of magnetic nanoparticle-induced nanotoxicity. Nanotechnology. 2013;**24**:175501. DOI: 10.1088/0957-4484/24/17/175501. Epub 2013 Apr 4

[51] Haase A, Rott S, Mantion A, Graf P, Plendl J, Thünemann AF, Meier WP, Taubert A, Luch A, Reiser G. Effects of silver nanoparticles on primary mixed neural cell cultures: Uptake, oxidative stress and acute calcium responses. Toxicological Sciences. 2012;**126**:457-468. DOI: 10.1093/toxsci/kfs003

[52] Calderón-Jiménez B, Johnson ME, Montoro Bustos AR, Murphy KE, Winchester MR, Vega Baudrit JR. Silver nanoparticles: Technological advances, societal impacts, and metrological challenges. Frontiers in Chemistry. 2017;**5**(February):1-26. DOI: 10.3389/fchem.2017.00006

Chapter 8

Silver Nanoparticles and PDMS Hybrid Nanostructure for Medical Applications

Solano-Umaña Victor and
Vega-Baudrit José Roberto

Additional information is available at the end of the chapter

http://dx.doi.org/10.5772/intechopen.74372

Abstract

For many years, people have known about silver's antibacterial qualities. Silver nanoparticles are widely used in consumer products, biomedical equipment, textile products and in other applications. Having a larger surface area to coat or spread over another surface, offers a greater contact area, therefore, increases antimicrobial properties. Also, these nanoparticles can be incorporated into polydimethylsiloxane (PDMS) implants as immobilized or occluded particles to improve their performance in the body. PDMS is commonly used for biomedical applications, including components for microfluidics, catheters, implants, valves, punctual plugs, orthopedics and micro gaskets. It can be manufactured easily in different forms such as fibers, fabrics, films, blocks and porous surfaces. The use of silver nanoparticles for their antimicrobial qualities improves PDMS biocompatibility, because it inhibits microbial growth, thereby making it more attractive for biomedical applications. The presence of metal nanoparticles also helps to reduce the hydrophobic nature of PDMS. This property of PDMS does not encourage cell adhesion, which is a very critical requirement for medical implants. Silver nanoparticles improve the silicone's wettability. The exceptional properties of silver nanoparticles combined with the PDMS have made this hybrid nanostructure applicable to different medical uses.

Keywords: silver, nanoparticles, polydimethylsiloxane, hydrophobicity, hydrophilicity

1. Introduction

Polydimethylsiloxane (PDMS) is a biocompatible material approved by the US Food and Drug Administration in the Biocompatibility Guidelines for Medical Products (Code of

Federal Regulations, 2013). PDMS is odorless, flavorless and resistant to both temperature and chemicals, including acids, oxidants, ammonia and alcohol.

All of these properties are advantages for using this polymer in human body implants. In addition, it can be manufactured easily in different forms. The PDMS is a hybrid compound with a chemical formula $(R_2SiO)_n$, where R is an organic group, such as methyl, ethyl or phenyl, attached to an inorganic chain of silicon and oxygen (**Figure 1**).

This kind of compound can be synthesized with a wide variety of properties and compositions, allowing the consistency to vary from liquid to gel, or rubber to hard plastic.

PDMS is a good elastomer, because the bonds between the silicon atom and the two oxygen atoms are highly flexible and very strong at the same time, so the angle formed by these links can be opened and closed [1], **Figure 2**.

The substrate elasticity of PDMS plays an important role in cell adhesion, proliferation and differentiation, thus improving implant integration in the human body.

The porosity, roughness, and surface energy are dominant factors for the material's wettability. These factors are especially valuable in biological environments.

The use of porous materials can be a very practical approach to reaching several goals in current medical applications such as surgical implants. Some chemical compounds, such as sugar or salts with water solubility, can play an important role in the synthesis of porous matrices because these compounds can be removed with water to empty the pores. The pore size, pore connection, and pore density are directly proportional to the crystals size of the chemical compounds and their quantity [2]. Pore size window and accessible void space are critical factors for medical applications [3].

Therefore, optimal pore size and specific surface area are important factors determining migration and cell attachment [4]. Small pores limit the cells' access within the porous matrix, and the diffusion of nutrients and removal of waste products, that can produce necrotic

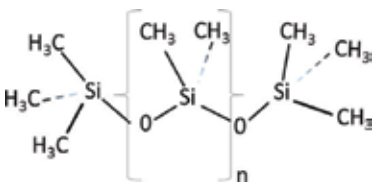

Figure 1. PDMS molecular structure.

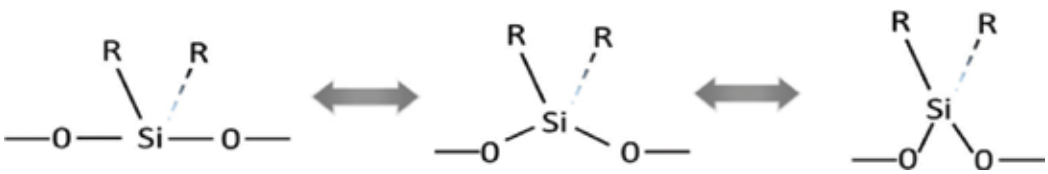

Figure 2. PDMS flexibility and elasticity.

effects in the end. Large pores limit cell attachment in a porous matrix. Composite scaffolds with preserved morphology and microstructure at micrometer scale are promising for tissue engineering. Pore size distribution from 164 ± 52 μm can support the cells' attachment to the porous material for medical applications [5].

Material technologies are critically important for tissue engineering in designing scaffolds or implants, and control of certain properties, such as porosity and pore size distribution, key factors on medical applications [6, 7]. Cell adhesion and growth on a scaffold or implant is controlled by the size and structure of the pore matrix [8, 9].

Sugar or sodium chloride can be used as pore-forming agents. For example, sieved sodium chloride salt (99% purity), with a controlled crystal size can be mixed with polymers to prepare a slurry, then the polymer is cured and the salt removed with water to obtain a porous material with a controlled pore size distribution [10, 11].

The pore structures typically consist of irregularly shaped voids and connecting channels that can be difficult to define. This is due to merging of adjacent cavities in the void walls. Pore size and interconnectivity play key roles in cell interaction with scaffolds and implants [12], see **Figure 3**.

Adding to the benefits of porous biomaterials, micro, meso and macro channels can be covered with metallic nanoparticles, to further improve their biocompatibility properties. Recent research has been focused on providing porous materials with interconnected channels and walls. The growing surface functionality is centered primarily on silica-based materials, where their composition arrangement can add different functional groups that interact with metals [13]. Porous materials can be prepared with organic compounds used as templates or pore-forming agents that are later removed with a solvent to empty the pores. Compounds such as sucrose, fructose, d-glucose, d-maltose, dibenzoyl-L-tartaric acid, ascorbic acid, citric acid, etc., can be used as pore-forming agents, then removed these with a solvent extraction process [14]. These pore-forming agents can control the growth of biopolymers into various sizes and shapes to obtain porous matrices for medical applications. Biomaterials of different

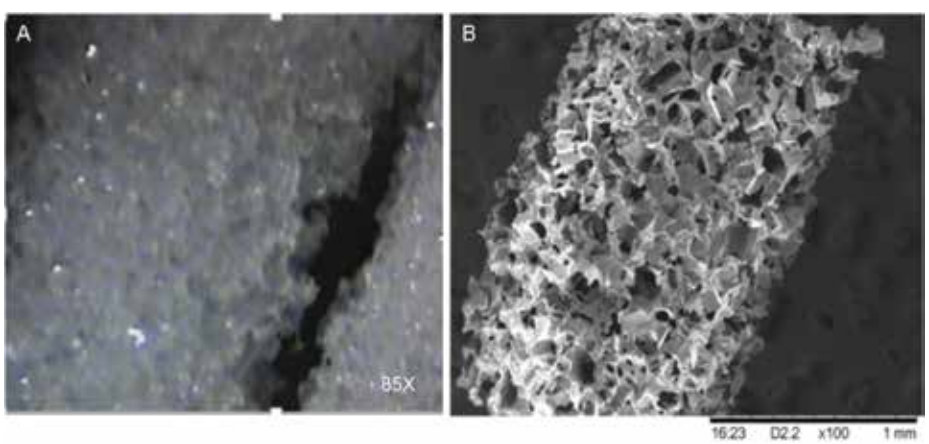

Figure 3. Porous PDMS matrix synthesized with sieved sugar as an agent to form pores: (A) optical micrograph and (B) SEM micrograph.

composition and structures (nanoparticles, nanowires, nanotubes, and nanoporous) can be synthesized through simple wet chemistry [15].

Biocompatible materials (scaffolds and implants) allow the human body to recover biological and mechanical functions, thereby increasing the quality of life. Based on the application or use, the implant must support mechanical loads, and promote long-term biological interaction with the body tissue. Current characteristics from bulk material give the load-bearing capacities for implant applications where this characteristic is required. The interaction with the adjacent tissue is dependent on the scaffold or implant surface [16, 17]. However, the biomaterials, which have micro, meso and macro-porous, show special characteristics, based on pore size, roughness, porosity, and surface energy, that can induce tissue development. The porous matrices with functionalized surfaces can be hosted and allow to leave specific biological molecules that encourage cells to grow inside and over the porous matrix. The hosting and releasing of peptides and proteins is an important key factor, because it opens new design ways for surgical scaffolds and implants. Biomaterials can improve bone rebuilding. In general, organ regeneration, as well as cell and tissue growth where required [18]. Silica porous materials have been used extensively for different medical applications, such as bone regeneration. Ceramic's characteristics, such as large surface area, porosity, and easy functionalization, allow the design biomaterial to enclose active molecules (drugs, peptides, proteins, etc.) [19].

The combination of porous materials with inorganic materials is a developing research area. These products are actually based on the outstanding properties for specific applications of this combination. Direct substitution of component elements in original porous materials, while maintaining structural regularity, provides novel properties that could be applied to surgical implants [20].

A porous PDMS matrix can incorporate silver nanoparticles, and immobilize these particles without affecting pore size distribution or producing a cytotoxic effect [21].

The ability of silver particles to kill microbes by airway blockage or breaking the outer walls of the bacteria has become one of the most important properties or factors for the development of these technologies at nanoparticle level. Application of nanoparticles in medical devices is currently important because some of them have bactericidal and disinfectant effects. The use of biomaterials in implants or scaffolds for medical application is limited by bacterial contamination that introduces infection or disease. Silver nanoparticle coatings or nanoparticle immobilization are currently used as antibacterial additive in poly-methylmethacrylate, the polymer used to manufacture bone implants (prosthetic knees, hips, etc.) [22].

The constantly expanding field of silver nanocomposites has gained significant importance, mainly due to proven antimicrobial properties offering great potential as antimicrobial coatings and agents. Many experimental methods have been proposed, but all of these have advantages as well as drawbacks. In general, identifying the method that allows the preparation of composites with biocompatible, biodegradable, and nontoxic materials (minimize toxic effects after production) is an objective for creating outstanding medical products [23, 24].

Currently, bacterial resistance to antibiotics that have been customarily used poses a challenge. A possible solution is turning to silver nanoparticles, because of their special properties. Antimicrobial uniform or non-uniform films, such as silver nanoparticles immobilized on a biomaterial, may be a viable solution to help in this critical issue [25, 26].

http://dx.doi.org/10.5772/intechopen.74372

This new research field is not only investigating nanoparticles but also focuses in nanostructures, nanocompounds, nanofilms, and so on. This is a new technology, nanotechnology that has gained widespread acceptance.

2. Experiment

The experimental method used synthetized porous PDMS matrices with pore sizes from 100 to 300 μm and PDMS film, described in previous papers. Silver nanoparticle immobilization was addressed in two different ways:

- Surface silver nanoparticles immobilization
- Occluded silver nanoparticles inside the polymer

The PDMS film is prepared from a solution (30% PDMS, 70% heptane, mass/volume). This solution was applied over a piece of glass, evaporating the heptane for 25 min at room temperature and curing the PDMS film at a temperature of 100°C.

2.1. Chemicals

Poly-dimethylsiloxane (PDMS) Nusil Silicone technology's product (MED-4860), silver nitrate (99.99%, Sigma-Aldrich), disodium ethylenediaminetetra-acetate (EDTA-2Na) ACS reagent (99.4%, powder from Sigma-Aldrich), d-glucose monohydrate (USP grade, Sigma-Aldrich), sodium hydroxide (ACS reagent, ≥97.0%, pellets, Sigma-Aldrich), ammonia water solution (ACS reagent, 28.0–30.0%, Sigma-Aldrich), anhydrous heptane (99%, Sigma-Aldrich), and anhydrous sodium sulfite (≥98%, Sigma-Aldrich).

2.2. Nano-film coating

Silver nitrate ($AgNO_3$) was dissolved in a minimum amount of DI-water, later ammonia water solution was added, and the chemical mixture produced a silver ammoniacal complex. The silver concentration was adjusted to 0.0135 M. Next, ethylenediaminetetraacetic disodium salt solution was prepared, and this solution was added to the silver solution, molar ratio 1:1 respect to $AgNO_3$.

Next the porous silicone matrices or PDMS film was combined with the silver solution, and mixed. Then, d-glucose solution was prepared and added to the mixture, and heated to reach at a temperature of 50°C for 1 h. The molar ratio from silver nitrate to d-glucose monohydrate was 1:5, final pH = 9.0.

For more details on preparation of a porous PDMS matrix, silver immobilization, and PDMS's film see previous papers.

2.3. Occluded silver nanoparticles inside the polymer

The $AgNO_3$ was dissolved in DI-water, added to the PDMS solution (30% PDMS, 70% heptane) mass/volume, placed in a magnetic mixer hot plate, mixed and heated from 35 to 45°C. Heptane was added to maintain the volume.

Later the solution was applied over a piece of glass, the heptane was evaporated for 25 min at room temperature and the PDMS film was cured at a temperature of 100°C.

2.4. Characterization method

2.4.1. Optical inspection

An optical microscope, Smart Scope Flash 200, model CNC200, serial SVW2003849 was used to perform a visual inspection. Smart Scope Flash is an automatic dimensional piece of equipment, with a measurement system, and optical metrology.

2.4.2. Scanning electron microscope (SEM)

SEM images were obtained, using a JEOL JSM-6390LV Scanning Electron Microscope, pores and particle size were verified.

2.4.3. Wettability test

A contact angle goniometer was used to measure PDMS's wettability, some film samples with and without silver immobilized nanoparticles were used to measure the wettability. The silicone film was mixed with the silver solution as described in Section 2.3. Then the contact angle was measured.

2.4.4. Transmission electron microscopy (TEM)

Transmission electron microscopy (TEM) is a microscopy technique in which a beam of electrons is transmitted through a specimen to form an image and observe small components such as metallic nanoparticles.

2.4.5. Fourier transform infrared (FTIR)

FTIR was used to show some changes in the functional groups on the silicone surface.

3. Results

The PDMS can be oxidized to produce silanol. Silanol is a functional group with the bond Si—O—H, as the functional group (C—O—H) found in alcohols.

Silanol compounds are more acidic than corresponding organic alcohols. This behavior contrasts with its electronegative property. Silicone is less electronegative than carbon (1.90 vs. 2.55), Et_3SiOH's pKa is 13.6 vs. 19 for tert-butyl alcohol. Because of their greater acidity, silanol can be fully deprotonated in an aqueous solution [27]. Also this group Si—O—H gives a little polar characteristic to the polymer that contributes to the surface energy and improves the wettability.

Poly-dimethylsiloxane (PDMS) product, from Nusil Silicone technology (MED-4860), can be oxidized with hydrochloric acid and sodium hydroxide solution treatment (etching).

Figure 4 shows PDMS ATR FTIR spectrum from the elastomer without treatment and **Figure 5** shows PDMS ATR FTIR spectrum after the etching process and silver immobilization.

PDMS spectrums, **Figures 4** and **5** show the symmetric and asymmetric stretching peaks of the methyl groups at 2963 and 2906 cm^{-1}, along with the deformation vibration peak of this group, too, at 1412 and 1258 cm^{-1}. Also, the Si—O—Si asymmetric stretching peaks are present, between 930 and 1200 cm^{-1}, and the Si—C vibrations and methyl rocking peak at around 800 cm^{-1}.

Comparing **Figure 4** to **Figure 5**, a weak broad peak approximately from 3200 to 3700 cm^{-1} is present only in **Figure 5**, and it corresponds to the —OH functional group present on the PDMS surface representing Si—OH bonding after the oxidation process (etching). Also, the characteristic peaks shown by the presence of methyl (—CH_3) functional group in **Figure 5** show a gradual decrease in intensity.

The different and bright colors observed on the porous PDMS matrices after silver immobilization are produced by the nanoparticles' plasmon effect (the quantum of plasma oscillation produced by the vibration of noble metals, such as silver and gold, and free electrons that is the consequence of the formation of a dipole in the material due to exposition of electromagnetic

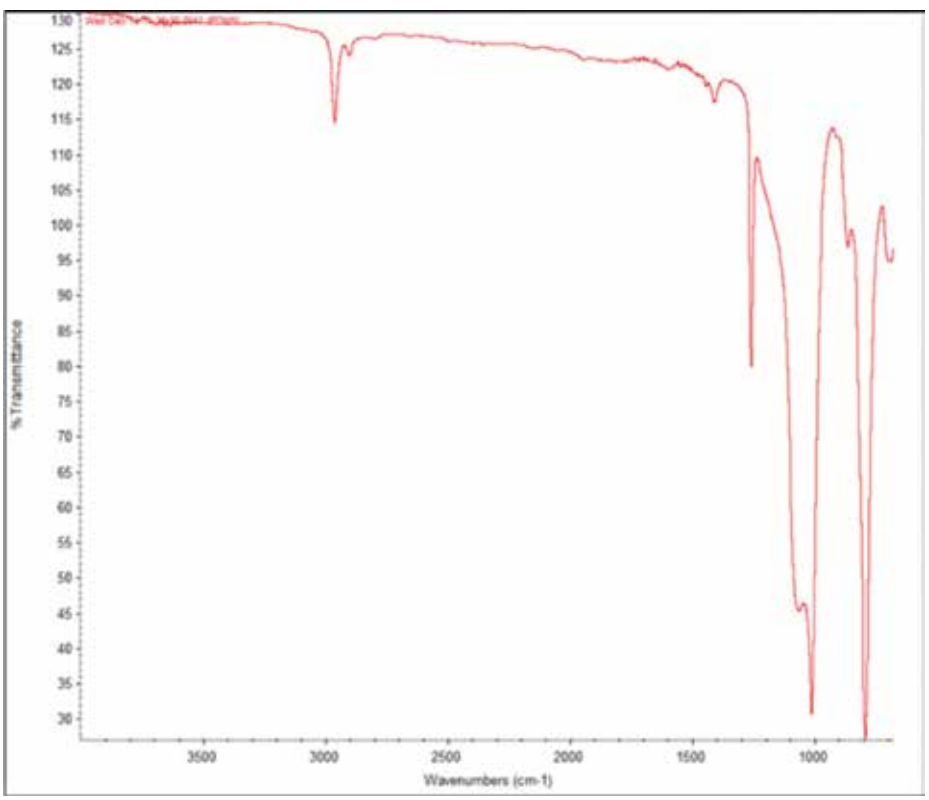

Figure 4. PDMS, ATR FTIR spectrum, sample without treatment.

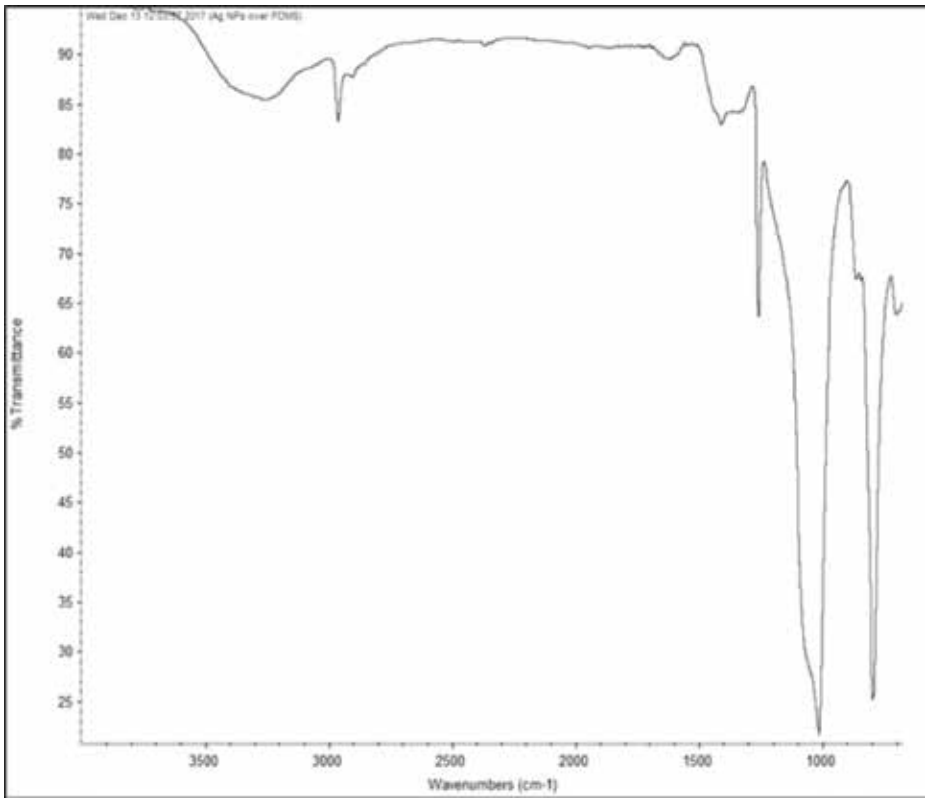

Figure 5. PDMS, ATR FTIR spectrum from a sample after the etching treatment and silver nanoparticle immobilization.

waves). Generally metallic silver nanocrystals show typical optical absorption due to their surface plasmon resonance, showing a bright color (**Figure 6**).

The silver nanoparticles' immobilization on PDMS has an important medical application improving the PDMS surface properties. Therefore, these particles potentially have antimicrobial activity toward many microbes. Along with this antimicrobial activity, silver nanoparticles show unacceptable toxic effects on human health. In addition, chronic exposure to silver causes adverse effects such as permanent bluish-gray discoloration of the skin (argyria) and eyes (argyrosis). Exposure to soluble silver compounds may produce other toxic effects. Some of these effects are liver and kidney damage, eyes, skin, respiratory and intestinal tracts irritation, and changes to blood cells [28].

Despite the toxicity data, silver nanoparticles have many medical applications. During recent years outbreaks of re-emerging and emerging infectious diseases have been a significant burden on the global economy and public health. Population and urbanization growth, poor water quality and lack of environmental hygiene are the main reasons for increased outbreak of infectious pathogens. Comprehensive treatments using advanced disinfectant nanomaterials have been proposed for prevention of such outbreaks. Among these nanomaterials, silver nanoparticles (Ag-NPs) with unique properties of high antimicrobial activity have attracted much interest from scientists and technologists for the development of nanosilver-based products [29].

http://dx.doi.org/10.5772/intechopen.74372

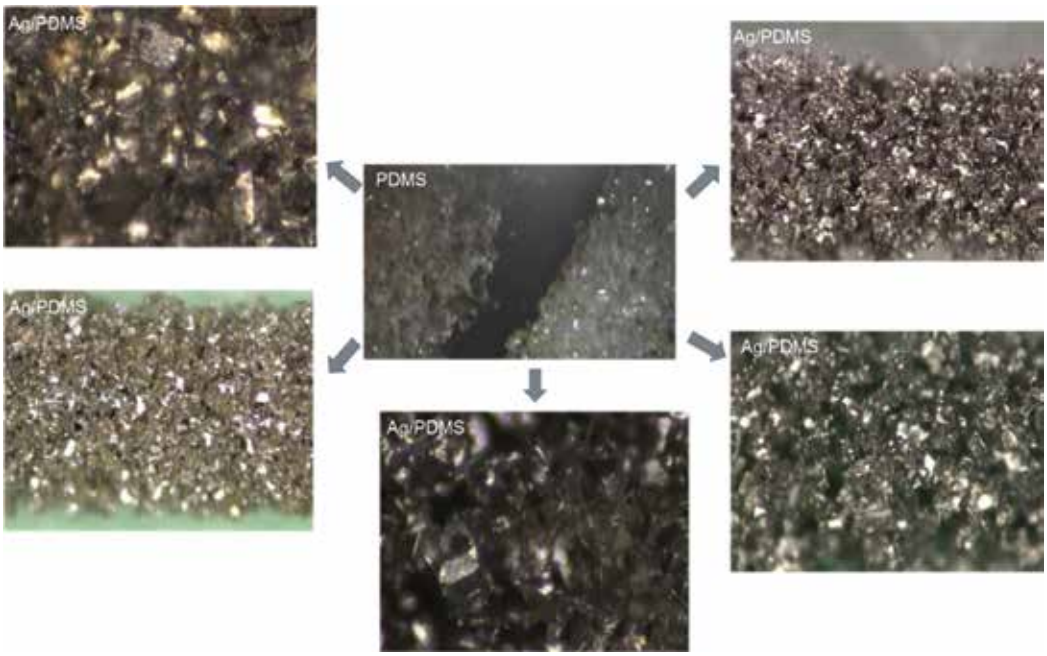

Figure 6. PDMS before and after silver nanoparticle immobilization, optical micrograph from different positions.

Silver nanoparticles have been demonstrated to be an effective biocide with a broad-spectrum, including Gran-negative and Gram-positive bacteria, in which there are many highly pathogenic bacterial strains [30, 31].

Silver nanoparticles biocide activity is based on three mechanisms:

1. Nanoparticles can attach to the surface of the cell membrane and drastically disturb its proper functions, such as permeability and respiration.
2. Nanoparticles are able to penetrate inside the bacteria and cause further damage by interacting with sulfur and phosphorus containing compounds.
3. Silver nanoparticles release silver ions. Silver ions are predominantly responsible of silver nanoparticles' bactericidal activity. Silver ions can kill bacteria cells [32].

Silver nanoparticles' toxic responses are related to their chemical characteristics and their aggregation; their toxicity depends on their composition [33]. There are mechanisms devised to nullify any toxicity caused by silver nanoparticles to humans and the environment so that their unique properties can be used to increase human quality of life without any negative effects [34].

Antimicrobial materials with immobilized or occluded silver nanoparticles are of considerable interest because those applications avoid all issues associated with the negative impact from the nanoparticles' toxicity. There is a significant debate on the mode of bactericidal action of silver nanoparticles. Both contact killing and/or ion-mediated killing have been proposed. Contact killing is the predominant bactericidal mechanism when silver nanoparticles are immobilized in or on a substrate, and these show great efficacy. Silver–silica-based hybrid

nanostructures are becoming more and more common as silica surface satisfies different functionalities for silver nanoparticles' immobilization, which makes possible the nanostructure surface modification. The silica's surface terminates in siloxane groups (—Si—O—Si—) with oxygen atoms on its surface as silanol groups (—Si—OH) that make the silver nanoparticles' immobilization possible. The antibacterial surface was found to be extremely stable in an aqueous medium; no significant leaching was observed. Thus, immobilization of silver nanoparticles on a silica surface may promote reuse, reduce environmental risks associated with leaching of AgNPs and also enhance cost-effectiveness [35].

PDMS as was mentioned has (—Si—O—Si—) too and it can perform a chemical reaction with different compounds to produce (—Si—OH) groups, the same functional group used on the silver nanoparticle immobilization over silica. The research consists of silver nanoparticle immobilization in PDMS. In this application, silver ion release decreases because silver nanoparticles are not free, and their big surface area is not totally exposed based on the silver's interaction with the oxygen groups (silver immobilization over PDMS surface). This effect is reflected by the non-toxicity of this nanostructure as reported in previous papers.

As shown in **Figure 7**, silver nanoparticles were immobilized over the PDMS surface and some of them formed clusters near to the pores. Also, the EDX spectrum shows the presence of silver, **Figure 8**.

When silver nitrate solution is mixed with the PDMS solution, the silver ions are reduced to silver nanoparticles and the PDMS is oxidized to silanol. This reaction is illustrated by the color change in the mixture, **Figure 9**. Later the solvent evaporated, and the silver nanoparticles were occluded inside the polymer structure, **Figure 10**.

Figure 11, as in **Figures 4** and **5**, demonstrates strong characteristic peaks from the PDMS, the methyl symmetric and asymmetric stretching respectively, and the deformation vibration of the same group, the Si—O—Si asymmetric stretching, Si—C vibrations and methyl rocking. Also, as in **Figure 5**, the spectrum shows a weak broad flat peak ranging from approximately 3200 to 3700 cm^{-1} that correlates to Si—OH bonding after the redox chemical reaction between the silver ions and the PDMS. On this spectrum (**Figure 7**) the characteristic peaks from methyl (—CH_3) functional groups also show a decrease in intensity.

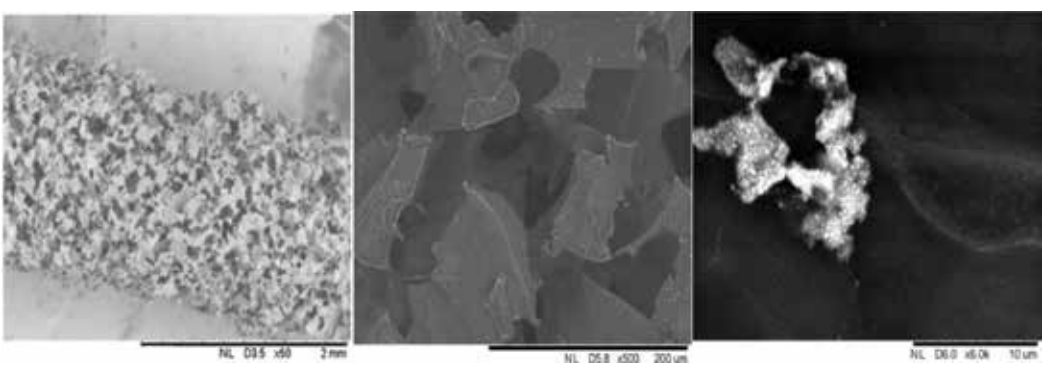

Figure 7. Silver nanoparticles immobilized on PDMS, SEM micrograph. (A) ×50, (B) ×500, (C) ×6000.

http://dx.doi.org/10.5772/intechopen.74372

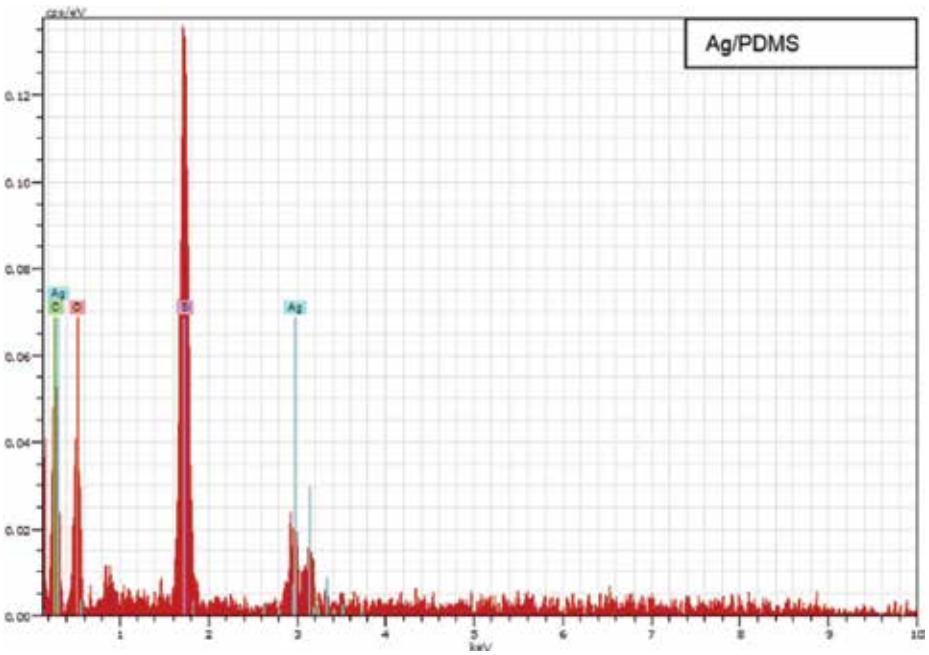

Figure 8. Silver nanoparticles immobilized on PDMS, Energy-dispersive X-ray spectroscopy (EDS) spectrum.

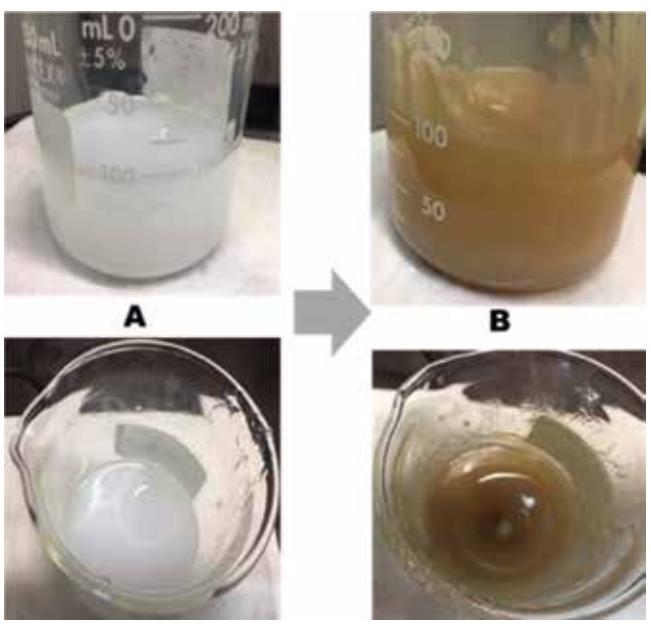

Figure 9. Silver nanoparticles synthetized inside PDMS' dispersion: (A) PDMS heptane solution and (B) PDMS heptane solution and silver nanoparticles synthetize inside.

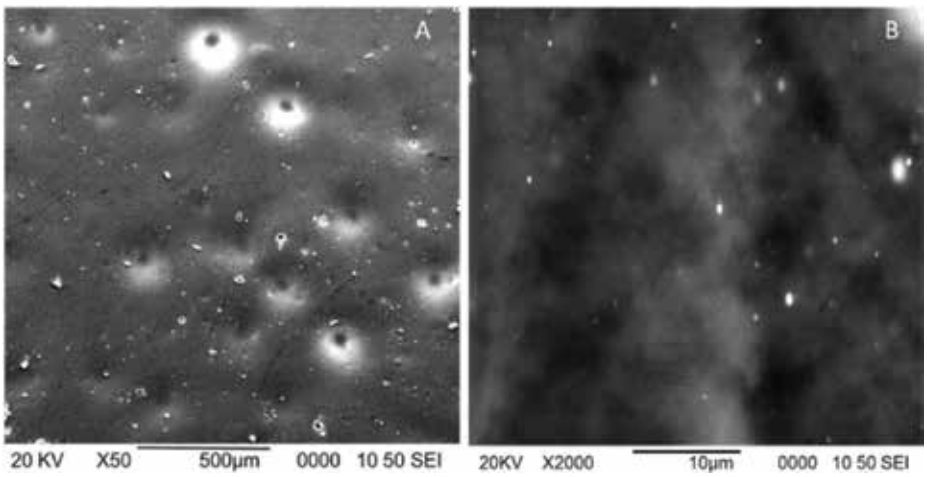

Figure 10. Silver nanoparticles occluded inside PDMS' film, SEM micrograph: (A) ×50 and (B) ×2000.

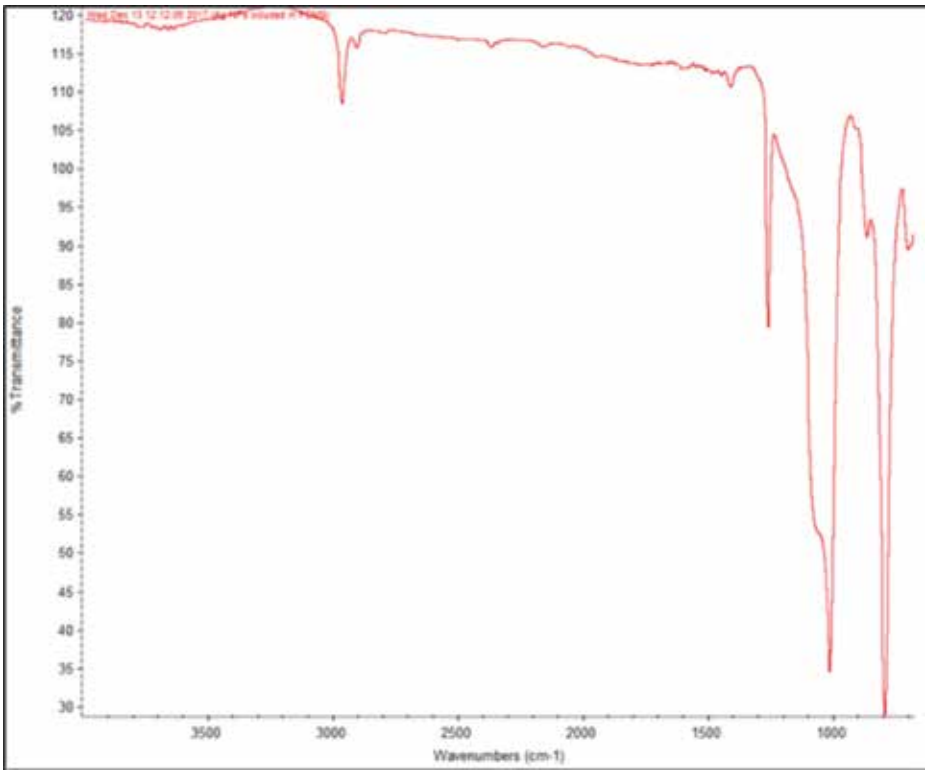

Figure 11. PDMS, ATR FTIR spectrum from a sample with occluded silver nanoparticles.

PDMS material in general comprises of repeated units of —O—Si$(CH_3)_2$–, which on exposure to oxygen plasma or corona treatment develops silanol groups (—OH) at the expense of methyl groups (—CH_3). The surface oxidation layer increases the concentration of hydroxyl groups. As the

hydroxyl groups are polar, they turn the hydrophobic exposed PDMS surface to a hydrophilic surface [36]. This effect can be shown by the contact angle change of deionized water or the changes in ATR FTIR spectrum peaks; the OH peak appears and the methyl peaks' intensity is reduced.

The mix of strong acids like H_2SO_4 and HNO_3 in an H_2O solution can induce the PDMS oxidation. Wet surface chemical oxidation produces a rough oxidase surface [37]. A different wet surface chemical oxidation (etching) used to treat the PDMS is piranha solution, followed by a dip in KOH solution. The piranha solution has hydrogen peroxide (H_2O_2) and sulfuric acid (H_2SO_4) in 1:1 ratio. The above-mentioned PDMS surface activation processes involve cleavage of the nonpolar hydrophobic methyl (—CH_3) group of the siloxane polymer chain and oxidation of the cleaved sites to polar hydrophilic silanol (Si—OH). The result is the increase of the polymer surface energy, thereby rendering it wettable [38].

The silver nanoparticles immobilized over the surface or occluded on PDMS film (**Figures 10** and **12**) were visualized with a SEM and TEM micrograph. The TEM micrograph shows an agglomerated or cluster when the nanoparticles are immobilized over the surface, **Figure 12A**. When these nanoparticles are occluded, these are more spread out, **Figure 12B**.

PDMS film samples with immobilized and occluded silver nanoparticles were tested to check their wettability and compare them with pure PDMS film, see **Figure 13**.

The obtained results are:

- Water drop contact angle measured of the pure PDMS sample 107°
- PDMS with immobilized silver nanoparticles over their surface 61°
- PDMS with occluded silver nanoparticles 76°

The data obtained reflect the different wettability (surface energy) between the samples. Pure PDMS' wettability is lower than occluded silver nanoparticles in PDMS' wettability, but silver

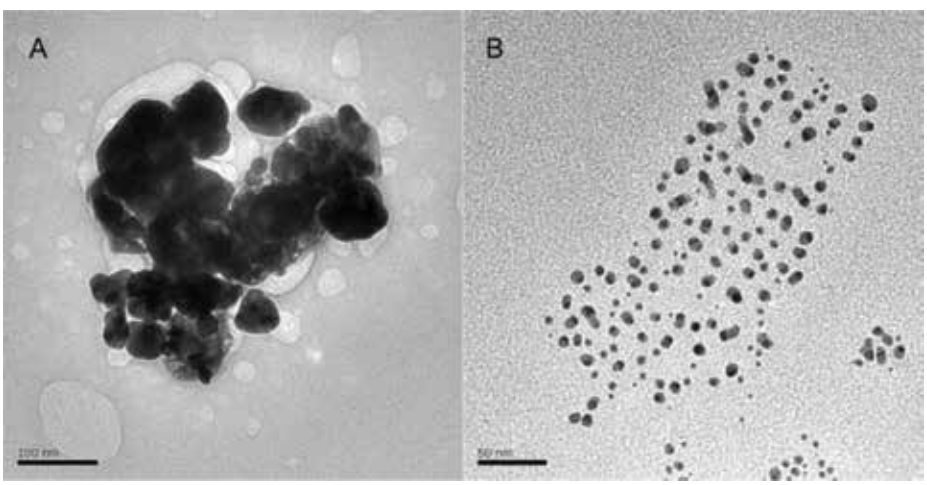

Figure 12. TEM micrograph, silver nanoparticles on PDMS. (A) Immobilized over the surface and (B) occluded.

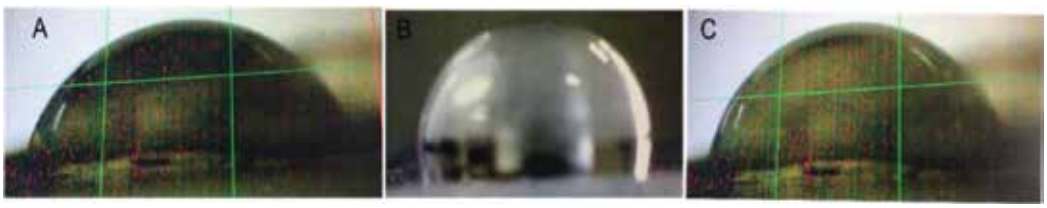

Figure 13. Water drop placed on different PDMS hybrid structures. (A) Silver nanoparticles immobilized over PDMS surface, (B) pure PDMS, and (C) occluded silver nanoparticles inside PDMS.

nanoparticles immobilized over PDMS surface's wettability is stronger than occluded silver nanoparticles in PDMS' wettability. These data demonstrate how the silver nanoparticles turn the hydrophobic PDMS surface into a hydrophilic surface. Also the decrease in the water drop contact angle coincides with the results obtained in **Figures 4**, **5** and **7**. **Figure 5** shows stronger Si—OH peak than **Figure 11**. Si—OH peak intensity is related to wettability properties, because silanol groups contribute to the wettability too, just as the silver nanoparticles.

4. Conclusion

The PDMS chain, although it has oxygen groups (Si—O—Si) on its structure, is hydrophobic, because the methyl groups (—CH_3) bond to the chain are non-polar compounds with hydrophobic properties.

PDMS oxidation can turn a hydrophobic surface into a hydrophilic surface, because in this process the methyl group is changed by the hydroxyl group. The hydroxyl group is polar and gives hydrophilic characteristics to the surface, so then surface energy increases.

Hydrophilic PDMS can be addressed with a special treatment such as plasma, corona or other treatments, but it can also be done with wet chemical treatment (etching). In this process the strong acids following the alkaline solution produce the PDMS oxidation, as is shown in these research data. This etching process permits the silver nanoparticle immobilization on a PDMS surface, and wettability increases. Also, the silver nitrate can react directly with a PDMS/heptane solution to produce a PDMS nanostructure with occluded silver nanoparticles. During the process a little PDMS oxidation is produced and it improves PDMS wettability, too.

Production of PDMS' matrices with silver nanoparticles to form hybrid nanostructures, in addition to giving bactericidal properties to the surface, fosters cellular growing, associated with wettability.

Author details

Solano-Umaña Victor[1]* and Vega-Baudrit José Roberto[2]

*Address all correspondence to: victor.solno@yahoo.com

1 Hologic Surgical Products, Alajuela, Costa Rica

2 National Laboratory of Nanotechnology (LANOTEC-CeNAT-CONARE), San José, Costa Rica

References

[1] Mark J, Curro J. A non-Gaussian theory of rubberlike elasticity based on rotational isomeric state simulations of network chain configurations. Polyethylene and polydimethylsiloxane short-chain unimodal networks. Journal of Chemical Physics. 1998;**79**(11):5698. DOI: 10.1063/1.445656

[2] Solano-Umaña V, Vega-Baudrit J. Micro, Meso and macro porous materials on medicine. Journal of Biomaterials and Nanobiotechnology. 2015;**6**:247-256. DOI: 10.4236/jbnb.2015.64023

[3] Solano-Umaña V, Vega-Baudrit J. Gold and silver nanotechnology on medicine. Journal of Chemistry and Biochemistry. 2015;**3**(1):21-33. DOI: 10.15640/jcb.v3n1a2

[4] Nayak S, Kundu S. Mint: Sericin–carboxymethyl cellulose porous matrices as cellular wound dressing material. Journal of Biomedical Materials Research. 2014;**102A**:1928-1940. DOI: 10.1002/jbm.a.34865

[5] Qian J, Xu W, Yong X, Jin X, Zhang W. Fabrication and in vitro biocompatibility of biomorphic PLGA/nHA composite scaffolds for bone tissue engineering. Materials Science and Engineering. 2014;**36**:95-101. DOI: 10.1016/j.msec.2013.11.047

[6] Zadegan S, Hosainalipour M, Rezaie H, Ghassai H, Shokrgozar M. Synthesis and biocompatibility evaluation of cellulose/hydroxyapatite nanocomposite scaffold in 1-n-allyl-3-methylimidazolium chloride. Materials Science and Engineering. 2011;**3**:954-961. DOI: 10.1016/j.msec.2011.02.021

[7] Wu L, Zhu F, Tao G. In vitro biocompatibility evaluation of collagen-hyaluronic acid? Bioactive glass nanocomposite scaffold. Journal of Macromolecular Science. 2013;**50**:1121-1125. DOI: 10.1080/10601325.2013.829360

[8] Zhijiang C, Chengwei H, Guang YM. Poly(3-hydroxubutyrate-co-4-hydroxubutyrate)/bacterial cellulose composite porous scaffold: Preparation, characterization and biocompatibility evaluation. Carbohydrate Polymers. 2012;**87**:1073-1080. DOI: 10.1016/j.carbpol.2011.08.037

[9] Machado J, Santos L. Evaluation and biocompatibility of a new type of scaffold for tissue growth based on calcium phosphate cement. Key Engineering Materials. 2009;**396-398**: 667-670. DOI: 10.4028/www.scientific.net/KEM.396-398.667

[10] Tran R, Thevenof T, Zhang Y, Gywali D, Tang L, Yang J. Scaffold sheet design strategy for soft tissue engineering. Materials. 2010;**3**:1375-1389. DOI: 10.3390/ma3021375

[11] Yoshimura K, Nakano K, Okamoto K, Miyake T. Mechanical and electrical properties in porous structure of Ketjenblack/silicone–rubber composites. Sensors and Actuators A: Physical. 2012;**180**:55-62. DOI: 10.1016/j.sna.2012.04.006

[12] Chang H, Wang Y. Cell responses to surface and architecture of tissue engineering scaffolds. In Eberli D, editor. Regenerative Medicine and Tissue Engineering—Cells and Biomaterials. 2011. p. 569-588. ISBN: 978-953-307-663-8. DOI: 10.5772/21983

[13] Ozin G, Arsenault A, Cademartiri L. Nanochemistry a chemical approach to nanomaterials. Royal Society of Chemistry. 2005;**2009**:396-417. DOI: 10.1002/cjoc.20000180507

[14] Pang J, Qiu K, Wei Y. Synthesis of mesoporous silica materials with ascorbic acid as template via sol-gel process. Chinese Journal of Chemistry. 2000;**18**:693-697. DOI: 10.1002/cjoc.20000180507

[15] Ryoo R. Tricontinuous mesoporous system. Nature Chemistry. 2009;**1**:105-106. DOI: 10.1038/nchem.190

[16] Boyan B, Hummert T, Dean D, Schwartz Z. Role of material surfaces in regulating bone and cartilage cell response. Biomaterials. 1996;**17**(2):137-146. DOI: 10.1016/0142-9612(96)85758-9

[17] Kretlow J, Mikos A. From material to tissue: Biomaterial development, scaffold fabrication, and tissue engineering. AICHE Journal. 2008;**54**:3048-3067. DOI: 10.1002/aic.11610

[18] Balas F, Manzano M, Colilla M, Vallet-Regi M. L-Trp adsorption into silica mesoporous materials to promote bone formation. Acta Biomaterilia. 2007;**4**(3):514-522. DOI: 10.1016/j.actbio.2007.11.009

[19] Izquierdo-Barba I, Sánchez-Salcedo S, Colilla M, Feito M, Ramírez-Santillán C, Portolés M, Vallet-Regí M. Inhibition of bacterial adhesion on biocompatible Zwitterionic SBA-15 mesoporous materials. Acta Biomaterialia. 2011;**7**(7):2977-2985. DOI: 10.1016/j.actbio.2011.03.005

[20] Vinu A, Mori T, Ariga K. New families of mesoporous materials. Science and Technology of Advanced Materials. 2006;**7**:753-771. DOI: 10.1016/j.stam.2006.10.007

[21] Solano-Umaña V, Vega-Baudrit J. Gold, silver, copper and silicone hybrid nanostructure cytotoxicity. International Journal of Recent Scientific Research. 2017;**8**(2):15478-15486

[22] Rai M, Yadav A, Gade A. Silver nanoparticles as a new generation of antimicrobials. Biotechnology Advance. 2009;**27**(1):76-83. DOI: 10.1016/j.biotechadv.2008.09.002

[23] Dallas P, Sharma V, Zboril R. Silver polymeric nanocomposites as advanced antimicrobial agents: Classification, synthetic paths, applications, and perspectives. Advance Colloid Interface Science. 2011;**166**(1-2):119-135. DOI: 10.1016/j.cis.2011.05.008166(1-2)

[24] Lok C, Ho C, Chen R, He Q, Yu W, Sun H, Tam P, Chiu J, Che C. Silver nanoparticles: Partial oxidation and antibacterial activities. Journal of Biological Inorganic Chemistry. 2007;**12**(4):527-534. DOI: 10.1007/s00775-007-0208-z

[25] Prucek R, Tuček J, Kilianová M, Panáček A, Kvítek L, Filip J, Kolář M, Tománková K, Zbořil R. The targeted antibacterial and antifungal properties of magnetic nanocomposite of iron oxide and silver nanoparticles. Biomaterials. 2012;**32**(21):4704-4713. DOI: 10.1016/j.biomaterials.2011.03.039

[26] Solano-Umaña V, Vega-Baudr J. Controlled deposition of gold and silver on a porous silicone matrix. Jacobs Journal of Nanomedicine and Nanotechnology. 2016;**2**(1):006

[27] Lickiss P. The synthesis and structure of organosilanols. Advances in Inorganic Chemistry. 1995;**42**:147-262. DOI: 10.1016/S0898-8838(08)60053-7

[28] Panyala N, Pena-Mendez E, Havel J. Silver or silver nanoparticles: A hazardous threat to the environment and human health. Journal of Applied Biomedicine. 2008;**6**:117-129. ISSN 1214-0287

[29] Tran Q, Nguyen N, Le A. Silver nanoparticles: Synthesis, properties, toxicology, applications and perspectives. Advances in Natural Science: Nanoscience and Nanotechnology. 2013;**4**:1-20. DOI: 10.1088/2043-6262/4/3/033001

[30] Ibrahim H. Green synthesis and characterization of silver nanoparticles using banana peel extract and their antimicrobial activity against representative microorganisms. Journal of Radiation Research and Applied Sciences. 2015;**8**(3):265-275. DOI: 10.1016/j.jrras.2015.01.007

[31] Ropisah M, Mohd W, Laily B, Azizan A, Nazlina I, Siti N. Synthesis of silver nanoparticles with antibacterial activity using the lichen *Parmotrema praesorediosum*. International Journal of Nanomedicine. 2014;**9**:121-127. DOI: 10.2147/IJN.S52306

[32] Marambio-Jones C, Hoek E. A review of the antibacterial effects of silver nanomaterials and potential implications for human health and the environment. Journal of Nanoparticle Research. 2010;**12**(5):1531-1551. DOI: 10.1007/s11051-010-9900-y

[33] Asghari S, Johari S, Lee J, Kim Y, Jeon Y, Choi H, Moon M, Yu J. Toxicity of various silver nanoparticles compared to silver ions in *Daphnia magna*. Journal of Nanobiotechnology. 2012;**10**(14):1-11. DOI: 10.1186/1477-3155-10-14.10(14)

[34] Prabhu S, Poulose E. Silver nanoparticles: Mechanism of antimicrobial action, synthesis, medical applications, and toxicity effects. International Nano Letters. 2012;**2**(32):1-10. DOI: 10.1186/2228-5326-2-3

[35] Agnihotri S, Mukherji S, Mukherji S. Immobilized silver nanoparticles enhance contact killing and show highest efficacy: Elucidation of the mechanism of bactericidal action of silver. Nanoscale. 2013;**5**(16):7328-7340. DOI: 10.1039/c3nr00024a

[36] Bhattacharya S, Datta A, Berg J, Gangopadhyay S. Studies on surface wettability of poly(dimethyl) siloxane (PDMS) and glass under oxygen-plasma treatment and correlation with bond strength. Journal of Microelectromechanical Systems. 2005;**14**(3):590-597. DOI: 10.1109/JMEMS.2005.844746

[37] Yin J, Han X, Cao Y, Lu C. Surface wrinkling on polydimethylsiloxane microspheres via wet surface chemical oxidation. Scientific Reports. 2014;**4**(5710):1-8. DOI: 10.1038/srep05710

[38] Maji D, Lahirib S, Dasa S. Study of hydrophilicity and stability of chemically modified PDMS surface using piranha and KOH solution. Surface and Interface Analysis. 2012; **44**:62-69. DOI: 10.1002/sia.3770

Chapter 9

Exploring the Effect of Operational Factors and Characterization Imperative to the Synthesis of Silver Nanoparticles

Adewumi O. Dada, Folahan A. Adekola,
Oluyomi S. Adeyemi, Oluwasesan M. Bello,
Adetunji C. Oluwaseun, Oluwakemi J. Awakan and
Femi-Adepoju A. Grace

Additional information is available at the end of the chapter

http://dx.doi.org/10.5772/intechopen.76947

Abstract

The synthesis and application of silver nanoparticles are increasingly becoming attractive. Hence, a critical examination of the various factors needed for the synthesis of silver nanoparticles as well as the characterization is imperative. In light of this, we addressed in this chapter, the nitty-gritty on the operational parameters (factors) and characterization relevant to synthesis of silver nanoparticle. The following characterization protocols were discussed in the context of silver nanoparticle synthesis. These protocols include spectroscopic techniques such as ultraviolet visible spectroscopy (UV–Vis), Fourier transform infrared spectroscopy (FTIR), scanning electron microscopy (SEM), transmission electron microscopy (TEM), energy-dispersive X-ray spectroscopy (EDX), X-ray fluorescence (XRF), X-ray diffraction (XRD), thermogravimetric analysis (TGA) and X-ray photoelectron spectroscopy (XPS).

Keywords: silver nanoparticles, characterization, morphology, operational factors

1. Introduction

The field of nanotechnology is gaining more attention daily from different researchers based on the vast applications and its efficacy. Silver nanoparticle is a metallic nanoparticle with the size of 1–100 nm existing either as zerovalent silver (Ag^o) or silver oxide due to their large ratio

of surface-to-bulk silver atoms. Of all the metallic nanoparticles, silver nanoparticles is exceptional and it is the most explored by researchers globally because of its various versatility, simplicity of synthesis, adaptability, morphology and its extreme surface area that paves way for the coordination of a vast number of ligands [1–9]. The following methods have been identified for synthesis of silver nanoparticles: Wet chemistry, Ion implantation, Biological synthesis and product functionalization. Wet chemistry involves nucleation of the nanoparticles within the solution by the action of a reducing agent on the silver ion complex forming colloidal silver. A number of wet chemistry methods, including the use of reducing sugars, citrate reduction, reduction via sodium borohydride, the silver mirror reaction, the polyol process seed-mediated growth and light-mediated growth have been identified [10–14]. However, reduction by borohydride is gradually facing out because of its toxicity thus the major reason why biological method of synthesis has been more preferable. Biological method of synthesizing silver nanoparticles may involve the use of bacteria, fungi and plant extract using green synthesis route. This method is ecofriendly, low cost and silver nanoparticles formed are stable and well dispersed with limited aggregation and good size control [15, 16]. There are different applications of silver nanoparticles ranging from its function as catalyst [5, 17], water treatment [6], antimicrobial properties [8], chemotherapeutic agent and drug delivery [18], Optical sensor [19], food packaging [20], and adsorption [21]. Although, there have been reports on the synthetic routes and applications of silver nanoparticle, however, nitty-gritty on the operational parameters imperative to the synthesis have not been so reported and the cogent considerable factors in characterization have not been majorly explored by researchers. Therefore, this book chapter aimed at taking a review survey of the operational parameters (factors) and the characterization imperative to synthesis of silver nanoparticles.

2. Operational parameters for synthesis of silver nanoparticles

The synthesis of silver nanoparticles depends on some important operational parameters. Irrespective of the technique used for the synthesis of silver nanoparticles, certain operational factors such as the concentration and volume ratio of reacting substances, reaction time, temperature and pH influence the synthesis rate, size and shape of the nanoparticles. These parameters could be varied to control its size, shape and general morphology, efficiency and applicability. A survey of these operational parameters are examined in this section.

2.1. Effects of concentration

The silver ion concentration majorly affects the synthesis of silver nanoparticles. This parameter was investigated to identify the amount of silver ion most suitable for the generation of silver nanostructure. To investigate the effect of initial silver ion concentration, range of concentrations were prepared while other parameters was kept constant. The common practice is to vary the concentration of Ag^{+} ion from 10^{-3} to 10^{-2} M. Report from the literature have established and approved 10^{-3} M as the most appropriate and suitable concentration where better surface plasmon resonance was obtained. In most wet chemistry and biological synthetic

methods, increase in silver ion intensity increases the rate at which the surface plasmon resonance will be attained. Silver nanoparticle is formed within the wavelength range of 400–490 nm with the formation of the ideal bell shape which is characteristic for the formation of Ag^0 nanoparticles [19].

Studies have shown that a variation in the concentration of metal salt used in the synthesis of nanoparticles influences the product of synthesis. Ibrahim [21] synthesized silver nanoparticle using silver nitrate as metallic salt and banana peel extract as reductant and capping agent, and reported a variation in color tending from yellowish brown to light reddish brown and darker shades of reddish brown with increasing silver nitrate concentration. Surface plasmon resonance (SPR) also attained distinctiveness with increasing concentrations of silver nitrate. These findings were also corroborated by reports from literature [22, 23]. Typical result of effect of concentration is shown in **Figure 1A**.

2.2. Effect of volume ratio

The volume ratio of silver ion solution to the extract which is serving as the reducing and stabilizing or sodium borohydride plays a substantive in the synthesis of silver nanoparticles. Report from different literature showed that in biological method/green synthesis route, excess silver ion is needed for better formation of the silver nanoparticles. In some instances, ratio 9:1 (Silver ion solution: plant extract/broth) were used while in some other reports, ratio of 4:1 was

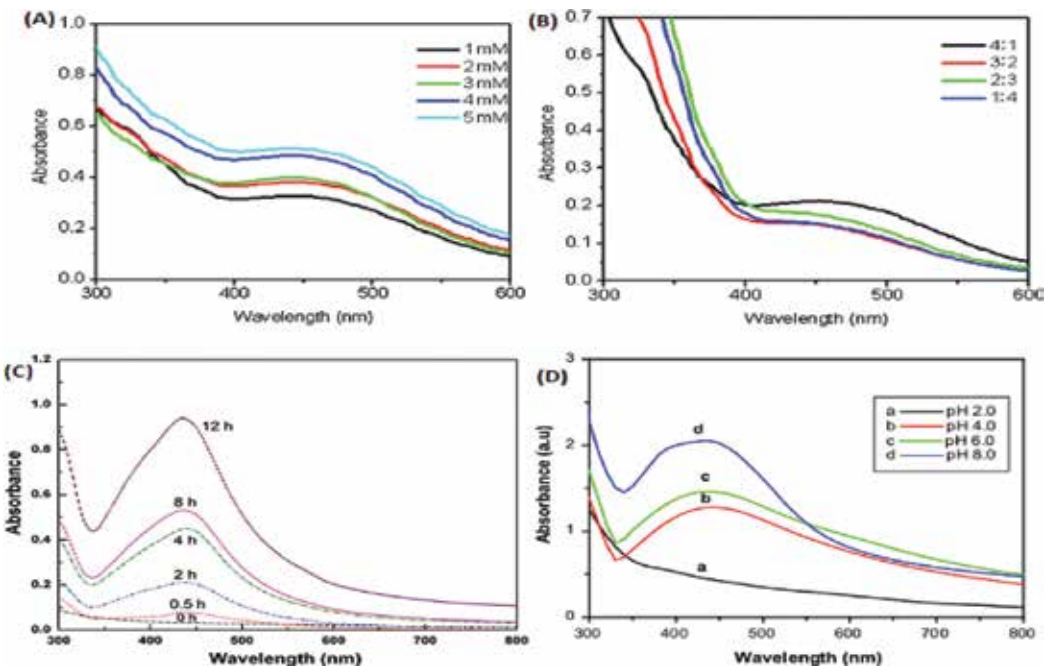

Figure 1. (A-D): (A) effect of variation of concentrations of Ag + solution (B) effect of volume ratio (C) effect of contact time (D) effect of change in pH carried out by different researchers [22–24].

used. Typical instances is seen in the synthesis of silver nanoparticle using *T. peruviana* (**Figure 1B**). Oluwaniyi et al., (2016) [22] investigated the influence of change in volume of silver nitrate to *T. peruviana* aqueous leaf extract other parameters were kept constant. Different volume ratios ranging from 4:1, 3:2, 2:3 and 1:4 of 1 mM silver nitrate to *T. peruviana* aqueous leaf extract, respectively, were used. Excellent surface plasmon resonance (SPR) was recorded on the UV–Vis at ratio 4:1. At 4 parts of 1 mM silver nitrate solution to 1 part of *T. peruviana* aqueous leaf extract (4,1), the leaf extract bioreduced and stabilized the nanoparticles with the plasmon resonance at 460 nm. Other volume ratios, 3:2, 2:3 and 1:4 of 1 mM silver nitrate to *T. peruviana* aqueous leaf extract did not give distinct characteristics SPR for silver nanoparticles at the visible region of the UV–Vis. However, the in case of wet chemistry method using sodium borohydride ($NaBH_4$) as the reducing agent, excess volume of borohydride is needed for better formation of silver nanoparticle for better dispersion and low agglomeration. Typical, the ratio of $NaBH_4$ to silver ion solution is 4:1 or 5:1 [25, 26].

2.3. Effect of contact time and temperature

Another important factor influencing the growth of silver nanoparticles is the contact time which is also known as reaction time (**Figure 1C**). This was done by varying the time taken for the formation of silver nanoparticle. Generally, the change in color to yellow or brown is an evidence of the growth of silver nanoparticle. This is monitored with use of UV–Vis spectrophotometer until the maximum absorption wavelength is reached with excellent surface plasmon resonance (SPR). The intensity of the peak is function of the contact time therefore it increases with increase in time. Contact time is one of the parameters that controls the size of silver nanoparticles because of the blue shift of the adsorption peaks. It can be inferred that at between 0 and 20 minutes (at the early stage), the SPR band is broadened because of the slow conversion of silver ion (Ag^+) to zerovalent silver (Ag^0) nanoparticles. Increasing the contact time enhances excellent plasmon band formation because large amount of Ag^+ has been converted to Ag^0. However, further increase in the contact time leads to noticeable decrease in the absorption intensity and wavelength which is an indication of some aggregation of silver nanoparticles leading to decrease in particle size [17, 19–23, 25, 26].

Temperature is another essential factor that should be considered in the synthesis of silver nanoparticles because it controls the reaction kinetics of the synthetic process. Increase in temperature is known to increase the rate of reaction because there will be an increase in the effective collision and the frequency factor of the reacting species. From the literature reports, studies showed that increase in temperature leads to increase in the intensity of the plasmon band as a result of bathochromic shift resulting in a decrease in the mean diameter of silver nanoparticle. At the beginning of the reaction, the synthesis of AgNPs may be rapid but this does not connote optimum temperature of the system because low temperature readily underscores the ability of reducing and stabilizing agent [27, 28].

2.4. Effect of pH

There are so many factors that influence the reduction of silver ion to AgNP. Effect of pH as one of the operational parameters plays a major role because it influences the chemistry of the

silver nanoparticle synthesis (**Figure 1D**). This is carried out by pH adjustment using phosphoric acid or hydrochloric acid and sodium hydroxide. In practice, during green synthesis, the extract pH is adjusted from pH 2 to 11 and it reduction process monitored by UV–Vis spectrophotometer. This change in the chemical nature of the extract affects its performance as well as the rate of reduction. In the study carried out by Heydari and Rashidipour on the green synthesis of silver nanoparticles using extract of Oak fruit hull, the result showed that the rate of AgNPs synthesis increases with increasing pH up to pH = 9 and then decrease [29]. More so, investigation carried out by Kokila et al., on biosynthesis of silver nanoparticles from Cavendish banana peel extract and its antibacterial and free radical scavenging assay showed that formation of AgNPs depends mostly on the pH of the reaction medium. The result confirmed that formation of silver nanoparticles is favorable in the basic medium than in acidic medium because the absorbance values increase with increase in pH. This could be accredited to the ionization of the functional groups at higher pH and the slow rate of reduction observed in the acidic medium could be attributed to electrostatic repulsion of anions present in the reaction mixture. This was in accordance with the findings in the literature [30–34].

3. Characterization

One of the main problems confronting scientists is understanding the properties a novel material displayed. This can only be achieved by knowing and determining the structure of this new material by characterization. Presently, there is an established and well accepted concept that structures are driven by properties. This is acknowledged in chemistry and in all fields where chemistry plays a primary character such as biochemistry, biology, environmental science, engineering, medicine, polymer science and nutrition. The make-up or property of a nano/biomaterial is placed into three groups i.e. chemical (e.g., equilibrium position, reaction rates, etc.), physical (e.g., melting/boiling points, solubility, spectra, symmetry, etc.) and biological (e.g., color, drug action, odor, taste, toxicity, etc.). This property gives rise to structural features which affect intensely the macroscopic character of the material. Since this is a structure driven properties concept, the structure of the novel material mostly signifies its composition at each level of complexity. However, this varies from the simple molecule formula (giving the ratio that the elements present bears to each other) and the exact positions and locations of all atoms in the molecules of this novel material referring to the three (3) dimensional electronic density distribution [35]. This section of book chapter therefore, excellently and succinctly state the relevant of various characterization techniques relevant to the synthesis of silver nanoparticles.

3.1. UV: Vis spectroscopy

Ultraviolet visible spectroscopy (UV–Vis Spec) remains the most useful characterization relevant to the synthesis of silver nanoparticles [2–23, 25–28]. In principle, the absorption of light occurs in the visible region of the electromagnetic spectrum where atoms and molecules undergo electronic transition of π-π^*, n-π^*, σ-σ^*, and n-σ^*. Absorption of energy in the form

of ultraviolet or visible light is by molecules containing π-electrons or non-bonding electrons (n-electrons) to excite these electrons to higher anti-bonding molecular orbitals. The length of wave depends on the excitation of the electrons, the more easily excited the electrons the longer the wavelength of light it can absorb. The absorption in the visible range directly affects the perceived color of the chemicals involved. UV–Vis in silver nanoparticle synthesis provides vivid information on the surface plasmon resonance (SPR) at the absorption maximum wavelength. The surface plasmon resonance comes from the free electron arising from the conduction and valence bands lying close to each other in metal nanoparticles. It is as a result of the collective oscillation of free electron of silver nanoparticles in resonance with the light wave in silver nanoparticle synthesis [36, 37]. All the experimental operational parameters vis-à-vis effect of initial concentration, contact time, temperature, pH, and volume ratio are monitored using the UV–Vis spectrophotometric technique. Information obtained from the absorption spectrum as a result of SPR surface, gives a clue on the type of shape of the silver nanoparticles. It is important that the interpretation from the UV–Vis measurement corroborates with TEM measurement [38]. **Figures 1(A-D)** portray different UV–Vis spectra at various operational factors influencing the synthesis in the studies carried by researchers.

3.2. Fourier transform infrared spectroscopy (FTIR)

The nature, structure and physicochemical properties of silver nanoparticles (AgNPs) are imperative to their activity, behavior, bio-distribution and safety. Therefore, characterization of AgNPs is essential and important for the assessment of the functional features and characteristics of the synthesized nanoparticles.

FTIR measurements is usually carried out to identify the possible biomolecules which are involved in the synthesis of nanoparticles and to find out their functions in reduction and stabilizing the nanoparticles. This spectroscopy method is employ to detect and distinguish small absorption bands (changes on the order of 10^{-3}) of functional group covalently grafted onto silver or functionally active points that is characteristics to AgNPs. This method has the ability to give precision, it is easily reproducible and also a favorable signal-to-noise ratio [39–41]. One of the major advantage of FTIR spectrometers to other methods of characterization of AgNPs is that, it is a non-invasive technique, data are collected rapidly data, signals are strong and bold, large signal-to-noise ratio, and very little sample is heat-up [42].

Lately, attenuated total reflection (ATR)-FTIR spectroscopy which is more advance in measurement than the conventional FTIR method has been discovered [43]. Using ATR-FTIR, we can easily know and establish the chemical properties on the polymer surface, nanoparticle surfaces and nature, its sample preparation is very simple when compared to conventional FTIR [44]. Therefore, FTIR as a method is appropriate, indispensable, non-invasive, affordable, easy and hands-on technique to know the function of biological molecules in the reduction of silver nitrate to silver.

Identification of the functional groups or biomolecules which are responsible for the reduction of silver ions in silver nanoparticles could be achieved by the Fourier transform infrared (FTIR) spectroscopy. This is achieved by comparing the intense bands with standard values. The

proportionate shift in band revealed after treatment with silver nitrate is a likely indication of participation of the functional groups in the process of nanoparticle synthesis [45].

3.3. Scanning electron microscopy (SEM) and transmission electron microscopy (TEM)

The significance attributes of synthesized silver nanoparticles have been documented to have a greater consequence on their behavior and toxicity encompasses of particle size, shape, surface properties, aggregation state, solubility, structure and chemical make-up. The characterization of silver nanoparticle is necessary for proper insight into the formation, synthesis and their utilization in various fields including agriculture, medical, industries, and environment [46, 47]. The validation and confirmation of synthesized nanoparticle have been carried out using various techniques however transmission electron microscopy (TEM) and scanning electron microscopy (SEM) is important methods for the cases. The significant of Microscopic techniques in the characterization of silver nanoparticles cannot be overemphasized because they give a more clear insight from the obtained data on the size, size distribution, and other quantifiable properties. The significant of electron microscopy in the analysis the synthesized silver premised on their ability to show the real structure of the particle between some ranges of nanometers (nm) conventional bright field images and the intermediate resolution darkfield techniques, to the high-resolution atomic images [48].

3.3.1. Scanning electron microscopy (SEM)

The SEM works by producing images whenever the electron beams scanning probe the peripheral surface of the given sample in order to confirm its structure as well as the topographical and elemental composition present in the materials [48]. During SEM analysis the electrons possess large amount of kinetic energy that is distributed and eventually leads to the generation numerous signals during the analysis of samples during whenever they interacts with the surface of the atom in the sample. The generated signal are secondary electrons, backscattered electrons, characteristics X rays, cathodoluminescence, specimen current and transmitted electrons which can generate a high-resolution magnified descriptions of a synthesized silver nanoparticle, illuminating facts with sizes that varies from 1 to 5 nm in size. Appropriate signals are collected depending upon the mode of operation of the instrument. The numerous field observed in SEM could be linked to the facts that it produced a large depth of field. Many researchers have utilized SEM for the determination of various synthesized silver nanoparticles including, polyhedral [49], flake flower [50], hexagonal [51], isotropic [52], irregular [53], triangular [54], anisotropic [55] and rod like structures [56], pentagonal [57].

3.3.2. Transmission electron microscopy (TEM)

The TEM works based on the application of a very high resolution microscopy method to generate an image as well as a diffraction patterns of the atomic size as well as shape of material by focusing the electron beam that can penetrate through the given material as well as interact with the sample of microstructure of materials. The major difference between TEM and SEM is that TEM can detect the following in the synthesized silver nanoparticles in a microstructure: crystallographic defects, line defects and planar defects. Another major difference

is that TEM could determine the available elemental composition at nano level [58, 59]. There are different forms of TEM including high-resolution transmission electron microscopy (HRTEM), scanning transmission electron microscopy (STEM) and analytical transmission electron microscopy (ATEM). TEM also shows a better image, diffraction properties, and the chemical analysis competences when compared to SEM. TEM can also detect a small size up to 0.2 nm when compared to SEM. Also, TEM produced a better resolution image because it utilized a low wavelength electron when compared to SEM. Finally, TEM can shift from diffraction to imaging by shifting the excitation of the lenses following the objective lens. TEM can be utilized to capture silver synthesized particle image in the plane of the fluorescent screen as well as the diffraction pattern from the particles. The nanoparticle size and particle size distribution of the synthesized nanoparticle could be determined and evaluated by transmission electron microscopy (TEM) and high-resolution microscopy. Moreover, the application of image J software for the plotting of histogram by measuring the size of different nanoparticles could be explored. Some of the demerits of using TEM entails required high vacuum, thin sample section, time consuming for the sample preparation [60]. Further insight and details about the morphology of AgNPs are provided by TEM. The most common size of the silver nanoparticles from various TEM image is spherical [61].

3.4. Energy-dispersive X-ray spectroscopy (EDX) and X-ray fluorescence (XRF)

The elemental constituents and composition of nano-materials could be determined by EDX and XRF. This section explores the principle and relevance of these analytical techniques in nano-research and most especially, silver nanoparticles studies.

3.4.1. Energy-dispersive X-ray spectroscopy (EDX)

Energy-dispersive X-ray spectroscopy (EDX) is an analytical technique that gives information on the surface atomic distribution and the chemical elemental composition [62–65]. In most cases, the EDX is always coupled with SEM. The EDX is used in the elemental determination of composition of the silver nanoparticles.

In Practice, it relies on an interaction of some source of X-ray excitation and a sample. Its characterization capabilities are due in large part to the fundamental principle that each element has a unique atomic structure allowing a unique set of peaks on its electromagnetic emission spectrum. In order to determine the peak of an element, a high energy beam of electron or beam of X-ray is targeted toward the sample to analyze. Excitation of electrons in the inner shell (lower energy level) occurs via the incident beam creating an electron holes which electron from the outer shell (higher energy level) fills. The difference between the higher and lower energy levels is released in form of an X-ray. The number and energy of the X-rays emitted from the silver nanoparticle can be measured by an energy-dispersive spectrometer. Electron beam excitation is used in electron microscopes, scanning electron microscopes (SEM) and scanning transmission electron microscopes (STEM). X-ray beam excitation is used in X-ray fluorescence (XRF) spectrometers. A detector is used to convert X-ray energy into voltage signals; this information is sent to a pulse processor, which measures the signals and passes them onto an analyzer for data display and analysis [66, 67]. Most researchers

utilize EDX for characterization of silver nanoparticles than XRF. Report from the literature vividly revealed that AgNPs signal is detected at 3.0 keV [19, 22, 23, 61, 68–70].

3.4.2. X-ray fluorescence (XRF)

This is the emission of characteristic "secondary" (or fluorescent) X-rays from a material that has been excited by bombarding with high energy x-rays or gamma rays. XRF technology provides one of the simplest, most accurate and most economic analytical methods for the determination of the chemical composition of many types of materials, particularly in the investigation of metals, glass, ceramics and building materials, and for research in geochemistry, forensic science and archeology. It is non-destructive and reliable, requires no, or very little, sample preparation and is suitable for solid, liquid and powdered samples It can be used for wide range of elements and provide detection limits at the sub-ppm level; it can also measure concentrations of up to 100% easily and simultaneously [71].

In principle, an inner shell electron is excited by an incident photon in the X-ray region. During the de-excitation process, an electron is moving from a higher energy level to fill the vacancy. The energy difference between the two shells appears as an X-ray, emitted by the atom. The X-ray spectrum acquired during the above process reveals a number of characteristic peaks. The energy of the peaks leads to the identification of the elements present in the sample (qualitative analysis), while the peak intensity provides the relevant or absolute elemental concentration (semi-quantitative or quantitative analysis) [72]. A typical XRF spectroscopy arrangement includes a source of primary radiation (usually a radioisotope or an X-ray tube) and equipment for detecting the secondary X-rays. When materials are exposed to short wavelength x-rays or to gamma rays, ionization of their component atoms may take place. If an X-ray beam is used to excite atoms in a sample, electrons near the nucleus emit secondary fluorescent x-rays on reversion to their original states [73].

In silver nanoparticle studies, XRF could be employed for elemental determination of the composition of nanoparticles although this is not frequently used compared to EDX. The X-ray fluorescence technique is of special interest for the analysis of silver nanoparticles because the technique is not only fast, sensitive and capable of simultaneous multi-element analysis, but also ensures that the sample can be quantitatively analyzed without damage. Therefore, it is mostly used to identify determining the presence of silver and other element in the compound. Specifically, silver nanoparticle is detected at 3.0 keV which is the characteristic peak reported by different researchers [74].

3.5. X-ray diffraction (XRD)

X-ray diffraction (XRD) (among others, such as FT-IR, UV, TEM, SEM, EDX) is a widely used technique for structural characterization which participate (a main part) in identifying the structure of a (nano/bio)-material or particle. Hence, XRD is a widely held analytical technique, which has been employed in the analysis of both molecular and crystal structures, qualitative detection of elements and their compounds, quantitative resolution of chemical species, quantifying the degree/measure of crystallinity, isomorphous substitutions, stacking faults, polymorphisms, particle sizes, *in situ* studies at process temperatures and in reactive atmospheres, phase identification and quantification etc. [75, 76].

XRD technique is a handy popular technique for characterizing silver nanoparticles and has grown into a common characterization method for evaluating these nanoparticles. Some of the main structural uniqueness are related with these i.e., measuring degree of crystallinity, phase identification, super-lattice generation, impurities detection, material's vacancy characterization and also novel materials development [77]. The crystalline structure or nature of bio-synthesized silver nanoparticles is determined by XRD analysis and patterns; this also use to confirm the structural information. Many authors reported a similar diffraction profile for most Ag-NPs with XRD peaks at 2θ of 38.18°, 44.25°, 64.72°, and 77.40° which are indexed to the 111, 200, 220, and 311 crystallographic planes of Bragg's reflections of the face-centered cubic structure of silver crystals, which suitably matched the standard diffraction data with those reported for silver by joint committee on powder diffraction standards. The average crystalline size of the silver nanoparticles was estimated using (Eq. 1), the Debye-Scherrer's equation [45, 78]:

$$D = {}^{0.9\lambda}/_{\beta \cos \theta} \tag{1}$$

where d is the particle size, λ is the wavelength of X-ray radiation (1.5406 Å), β is the full-width at half-maximum (FWHM) of the height (in radians) and 2θ is the Bragg angle. The precision, significance, sensitivity and easy use of XRD increases its importance in AgNPs. However, there are some limitations that one might face using this analysis. It can only analyze and identify an unknown material that is homogeneous and single phase. There should be a standard reference file for compounds especially inorganic ones (d-spacings, *hkl*s), peaks overlay mostly happened in XRD and worsen for high angle' reflections, to determine unit cell using XRD, indexing of patterns for non-isometric crystal systems is complicated.

3.6. Thermogravimetric analysis (TGA) and X-ray photoelectron spectroscopy (XPS)

The advancement of nanotechnology is rapidly evolving and holds potential to completely redefine applications of material science in the nearest future. In order to maximize the prospects of nanotechnology for diverse applications, the characterization of nanomaterials and/or nanoparticles have become imperative. Among the several techniques available for the characterization of nanomaterials are thermogravimetric analysis (TGA) and X-ray photoelectron spectroscopy (XPS).

3.6.1. Thermogravimetric analysis

Thermogravimetric analysis (TGA) is an analytical technique for measuring changes in the mass of a material that occur in response to programmed temperature changes [79]. TGA represents a branch of thermal analysis examining the mass changes of a sample as a function off temperature (in the scanning mode) or as a function of time (in the isothermal mode). In TGA changes in physical and chemical properties of materials are measured as a function of increasing temperature (with constant heating rate), or as a function of time (with constant temperature and/or constant mass loss). The changes in the mass of a sample due to various thermal events (desorption, absorption, sublimation, vaporization, oxidation, reduction and decomposition) can be studied while the sample is subjected to a program of change in temperature. TGA has found applications in the analysis of volatile products, gaseous

products lost during the reaction in thermoplastics, thermosets, elastomers, composites, films, fibers, coatings, paints among others. Further practical applications, are determining composition and thermal stability of materials, evaluating the kinetics of thermally stimulated processes, predicting lifetimes, and studying reactions of materials with gases. There are different types of TGA ranging from isothermal to dynamic TGA.

3.6.1.1. Thermal properties of silver nanoparticles

In a recent investigation, thermal behavior of silver nanoparticles was monitored by TGA Khan et al. [80], authors reported dominant weight loss in silver nanoparticles occurred in temperature region between 200 and 300°C. There was almost no weight loss below 200°C and above 300°C. The weight loss was attributed to the evaporation of water and organic components. Overall, TGA results show a loss of 14.58% up to 300°C. In the same study, the differential thermal analysis (DTA) plot displayed an intense exothermic peak between 200 and 300°C which mainly could be attributed to crystallization of silver nanoparticles. DTA profiles suggest that complete thermal decomposition and crystallization of the sample occur simultaneously. Taken together, the TGA/DTA study shows that the dominant weight loss occurs between 200 and 300°C; and the reaction is of exothermic type [80].

In a separate study, the low-temperature sintering behavior of Ag nanoparticles was investigated. The silver nanoparticles were shown to exhibit obvious sintering behavior at significantly lower temperatures (~150°C) than the T_m (960°C) of silver while coalescence of the silver nanoparticles was observed by sintering the particles at 150, 200, and 250°C. The thermal profile of the nanoparticles was examined by a differential scanning calorimeter (DSC) and a thermogravimetric analyzer (TGA). Shrinkage of the silver nanoparticle compacts during the sintering process was observed by thermomechanical analysis (TMA). Sintering of the nanoparticle pellet led to a significant increase in density and electrical conductivity. The size of the sintered particles and the crystallite size of the particles increased with increasing sintering temperature [81].

3.6.2. X-ray photoelectron spectroscopy (XPS)

As the demand for high performance materials increases, so does the importance of surface engineering. Typically, the surface of a material represents the platform of interaction with the external environment and other materials. In the case of nanotechnology, surface chemistry of nanomaterials and/or nanoparticles is key to exploring the prospects of these particles for diverse applications. Surface modification can be used to alter or improve the properties of nanomaterials and/or nanoparticles, and so surface analysis becomes a technique for probing the surface chemistry of these particles. More so, nanotechnology approaches include surface modification of nanomaterials in order to suit specific purposes. Therefore, it becomes expedient to understand the physical and chemical interactions occurring at the surface, or at the interfaces of the nanomaterial's layers.

X-ray photoelectron spectroscopy (XPS) also known as electron spectroscopy for chemical analysis (ESCA) is a widely accepted technique for surface analysis. This probably may be because XPS can be applied to a broad range of materials and provides valuable quantitative and chemical state information from the surface of the material being studied. The average depth of analysis for an XPS measurement is approximately 5 nm. XPS measurement involves

irradiating the surface of sample materials with monochromatic Al–K-α x-rays. This leads to excitation thereby causing photoelectrons to be emitted from the sample surface. Then an electron energy analyzer is used to measure the energy of the emitted photoelectrons. From the binding energy and intensity of a photoelectron peak, the elemental identity, chemical state, and quantity of a detected element can be determined.

3.6.2.1. X-ray photoelectron spectroscopy (XPS) of silver nanoparticles

Several investigations have reported the use XPS technique to characterize the surface chemistry of silver nanoparticles. Larrude et al. [82] characterized silver-multiwalled carbon nanotubes (Ag-MWCNTs) nanocomposite using the XPS technique. Their report showed spectrum revealing the dominance of silver and carbon, with small amounts of sodium and sulfur in the sample. According to the author of the investigation, presence of Na and S was attributable to the use of sodium dodecyl sulfate (SDS) for the MWCNTs dispersion. Also, the study demonstrated increased oxygen content compared to a pure MWCNTs sample. However, there was no evident relationship between the oxygen and the silver contents because the O/Carbon atomic rate did not change significantly between the different silver concentrations. Furthermore, the spectrum of the Ag 3d core level of the Ag-decorated MWCNTs, confirmed the presence of metallic silver because the 3d5/2 component occurred at a binding energy of 368.3 eV, which is characteristic of the metallic Ag (0) oxidation state [82].

In a separate study involving a surface chemical characterization of silver nanoparticles thin film using XPS instrument equipped with monochromatic Al–K-α X-ray source [83]; the XPS spectrum and the high-resolution XPS window of the core level atoms comprising the silver nanoparticles capped with carboxylate/1-dodecylamine revealed the presence of Ag, C, O, and N atoms according to their binding energies. The most prominent signal in the XPS spectrum was the Ag 3 s consisting of two spin-orbit components at 368.8 ($Ag3d_{5/2}$) and 374.8 ($Ag3d_{3/2}$) eV and separated by 6.0 eV. Moreover, the deconvolution of Ag (3d) doublet revealed asymmetric peak shape. These two characteristics indicated the existence of the Ag in metallic form.

Furthermore, another investigation reported consistence of the XPS analysis of silver behenate was with the theoretical C: O: Ag atomic composition. The report noted that brown discoloration of silver behenate powder within a few seconds of exposure to monochromatic X-rays and that this increased significantly with time. Further, noticeable changes to the XPS spectra and the observed surface composition begin to occur after about 30 minutes of X-ray exposure, while prolonged exposure to monochromatic X-rays resulted in significant changes in the C 1s, O 1s, and Ag 3d peak shapes and positions. Changes in the XPS spectra indicated that exposure to Al Kα X-rays resulted in the formation of silver metal particles and decomposition of the carboxylic acid portion of the molecule to hydrocarbon species. Thermal reduction of silver behenate powder produced similar changes in the XPS spectra [84].

4. Conclusion

This chapter has examined the operational parameters which are imperative to the synthesis of silver nanoparticles. Effect of concentration, volume ratio, contact time, temperature and pH

affect the synthesis of silver nanoparticles. Conditions attached to each of these have been identified. Chief among these factors is the effect of pH which affect the chemistry of the silver nanoparticle synthesis. However, irrespective of the synthetic route and conditions, characterization Techniques which are germane to the studies of silver nanoparticles have also been critically examined. The UV–Vis spectroscopy helps in determining the surface plasmon resonance absorption band and this is vital in nanoparticle studies. The functional groups are determined by FTIR, morphology and sizes by SEM and TEM, atomic distributions and relative abundances were revealed by EDX and XRF respectively. The crystallinity can be determined by XRD, surface chemical characterization by X-ray photoelectron spectroscopy (XPS) and silver content by thermogravimetric analysis (TGA). It can be concluded that relevant research in nanoparticle studies rely on both the operational conditions and excellent characterization.

Acknowledgements

The authors appreciate the management of Landmark University for providing enabling environment for research.

Conflict of interest

The authors declare that there is no conflict of interest.

Author details

Adewumi O. Dada[1]*, Folahan A. Adekola[2], Oluyomi S. Adeyemi[3], Oluwasesan M. Bello[4], Adetunji C. Oluwaseun[5], Oluwakemi J. Awakan[3] and Femi-Adepoju A. Grace[6]

*Address all correspondence to: dada.oluwasogo@lmu.edu.ng

1 Industrial Chemistry Programme, Nanotechnology Laboratory, Department of Physical Chemistry, Landmark University, Omu-Aran, Nigeria

2 Department of Industrial Chemistry, University of Ilorin, Nigeria

3 Medicinal Biochemistry and Toxicology Laboratory, Department of Biological Sciences, Landmark University, Omu-Aran, Nigeria

4 Department of Applied Chemistry, Federal University Dutsin-Ma, Katsina State, Nigeria

5 Department of Biological Sciences, Applied Microbiology, Biotechnology and Nanotechnology Laboratory, Landmark University, Omu Aran, Kwara State, Nigeria

6 Department of Plant and Environmental Biology, Kwara State University, Malete, Kwara State, Nigeria

References

[1] Christina G, Vossen DLJ, Arnout I, Alfon VB. General method to coat colloidal particles with silica. Langmuir. 2013;**19**(17):6693-6700. DOI: 10.1021/la0347859

[2] Benn TM, Westerhoff P. Nanoparticle silver released into water from commercially available sock fabrics. Environmental Science & Technology. 2008;**42**:4133-4139

[3] Shi J, Xu B, Sun X, Ma C, Yu C, Zhang H. Light induced toxicity reduction of silver nanoparticles to *Tetrahymena pyriformis*: Effect of particle size. Aquatic Toxicology. 2010. DOI: 10.1016/j.aquatox.2013.02.001

[4] Chen E, Su H, Zhang W, Tan T. A novel shape-controlled synthesis of dispersed silver nanoparticles by combined bioaffinity adsorption and TiO_2 photocatalysis. Powder Technology. 2011;**212**:166-172

[5] Edison TJI, Sethuraman MG. Biogenic robust synthesis of silver nanoparticles using *Punica granatum* peel and its application as a green catalyst for the reduction of an anthropogenic pollutant 4-nitrophenol. Spectrochimica Acta Part A: Molecular and Biomolecular Spectroscopy. **104**:262-264

[6] Dankovich TA, Gray DG. Bactericidal paper Impregnated with silver nanoparticles for point-of-use water treatment. Environmental Science & Technology. 2011;**45**:1992-1998

[7] Hendi A. Silver nanoparticles mediate differential responses in some of liver and kidney functions during skin wound healing. Journal of King Saud University (Science). 2011;**23**:47-52

[8] An J, Wang D, Luo Q, Yuan X. Antimicrobial active silver nanoparticles and silver/polystyrene core-shell nanoparticles prepared in room-temperature ionic liquid. Materials Science and Engineering C. 2009;**29**:1984-1989

[9] Mohanty S, Mishra S, Jena P, Jacob B, Sarkar B, Sonawane A. An investigation on the antibacterial, cytotoxic, and antibiofilm efficacy of starch-stabilize d silver nanoparticles. Nanomedicine: Nanotechnology, Biology, and Medicine. 2012;**8**:916-924

[10] Dong X, Ji X, Jing J, Li M, Li J, Yang W. Synthesis of triangular silver nanoprisms by stepwise reduction of sodium borohydride and trisodium citrate. Journal of Physical Chemistry C. 2010;**114**(5):2070-2074. DOI: 10.1021/jp909964k

[11] Shan Z, Wu J, Xu F, Huang F-Q, Ding H. Highly effective silver/semiconductor photocatalytic composites prepared by a silver mirror reaction. Journal of Physical Chemistry C. 2008; **112**(39):15423-15428. DOI: 10.1021/jp804482k

[12] Wiley B, Sun Y, Xia Y. Synthesis of silver nanostructures with controlled shapes and properties. Accounts of Chemical Research. 2007;**40**:1067-1076

[13] Pietrobon B, Mceachran M, Kitaev V. Synthesis of size-controlled faceted pentagonal silver nanorods *with* tunable plasmonic properties and self-assembly of these nanorods. ACS Nano. 2009;**3**:21-26. DOI: 10.1021/nn800591y

[14] Tanimoto H, Ohmura S, Maeda Y. Size-selective formation of hexagonal silver nanoprisms in silver citrate solution by monochromatic-visible-light irradiation. Journal of Physical Chemistry C. 2012, 2012;**116**(29):15819-15825. DOI: 10.1021/jp304504c

[15] Yong SJ, Kim SKB. Rapid biological synthesis of silver nanoparticles using plant leaf extracts. Bioprocess and Biosystems Engineering. 2008;**32**(1):79-84. DOI: 10.1007/s00449-008-0224-6 PMID 18438688

[16] Shiv SS, Absar A, Murali S. Geranium leaf assisted biosynthesis of silver nanoparticles. Biotechnology Progress. 2003;**19**(6):1627-1631. DOI: 10.1021/bp034070w. PMID 14656132

[17] Wen C, Shao M, Zhuo S, Lin Z, Kang Z. Silver/graphene nanocomposite: thermal decomposition prep catalytic performance. Materials Chemistry and Physics. 2012;**135**:780-785

[18] Dan P, Jeffrey MP, Seungpyo H, Omid CF, Rimona M, Robert L. Nanocarriers as an emerging platform for cancer therapy. Nature Nanotechnology. 2007;**2**(12):751-760. Bibcode:2007NatNa…2..751P. DOI: 10.1038/nnano.2007.387

[19] Pandey S, Goswami GK, Nanda KK. Green synthesis of biopolymer–silver nanoparticle nanocomposite: An optical sensor for ammonia detection. International Journal of Biological Macromolecules. 2012;**51**:583-589

[20] de MMR, Mattoso LHC, Zucolotto V. Development of cellulose-based bactericidal nanocomposites containing silver nanoparticles and their use as active food packaging. Journal of Food Engineering. 2012;**109**:520-524

[21] Ibrahim HMM. Green synthesis and characterization of silver nanoparticles using banana peel extract and their antimicrobial activity against representative microorganisms. Journal of Radiation Research and Applied Sciences. 2015;**8**:265-275

[22] Oluwaniyi OO, Adegoke HI, Adesuji ET, Alabi AB, Bodede SO, Labulo AH, Oseghale CO. Biosynthesis of silver nanoparticles using aqueous leaf extract of Thevetia peruviana Juss and its antimicrobial activities. Applied Nanoscience. 2015. DOI: 10.1007/s13204-015-0505-8

[23] Kokila T, Ramesh PS, Geetha D. Biosynthesis of silver nanoparticles from Cavendish banana peel extract and its antibacterial and free radical scavenging assay: A novel biological approach. Applied Nanoscience. 2015;**5**:911-920

[24] Vinod VTP, Saravanan P, Sreedhar B, Devi KD, Sashidhar RB. A facile synthesis and characterization of Ag, Au and Pt nanoparticles using a natural hydrocolloid gum kondagogu (Cochlospermum gossypium). Colloids and Surfaces B: Biointerfaces. 2011; **83**:291-298

[25] Ravindran A, Chandran P, Khan SS. Biofunctionalized silver nanoparticles: Advances and prospects. Colloids and Surfaces B: Biointerfaces. 2013;**105**:342-352

[26] Lü X, Cui S. Wool keratin-stabilized silver nanoparticles. Bioresource Technology. 2010; **101**:4703-4707

[27] Bindhu MR, Umadevi M. Silver and gold nanoparticles sensor and antibacterial applications. Spectrochim Acta Part A Molecular and Biomolecular Spectroscopy. 2014;**128**:37-45

[28] Maidul Islam AKM, Mukherjee M. Effect of temperature in synthesis of silver nanoparticles in triblock copolymer micellar solution. Journal of Experimental Nanoscience. 2011;**6**(6):596-611. DOI: 10.1080/17458080.2010.506518

[29] Heydari R, Rashidipour M: Green synthesis of silver nanoparticles using extract of oak fruit hull (Jaft): Synthesis and in vitro cytotoxic effect on MCF-7 cells. International Journal of Breast Cancer Volume 2015, Article ID 846743, 6 pages. http://dx.doi.org/10.1155/2015/846743

[30] Sun L, Wang L, Yonghai S, Guo C, Sun Y, Peng C. Aggregation- based growth of silver nanowires at room temperature. Applied Surface Science. 2008;**254**:2581-2587

[31] Martinez-Castanon GA, Nino-Martinez N, Martinez-Gutierrez F, Martinez- Mendoza JR. Synthesis and antibacterial activity of silver nanoparticles with different sizes. Journal of Nanoparticle Research. 2008;**10**:1343-1348

[32] Velgosová O, Mražíková A, Marcinčáková R. Influence of pH on green synthesis of Ag nanoparticles. Materials Letters. http://dx.doi.org/10.1016/j.matlet.2016.04.045

[33] Alqadi MK, Noqtah OAA, Alzoubi FY, Alzouby J, Aljarrah K. pH effect on the aggregation of silver nanoparticles synthesized by chemical reduction. Materials Science-Poland. 2014;**32**(1):107-111

[34] Baranova OA, Khizhnyak SD, Pakhomov PM. Effect of the pH value on the synthesis of silver nanoparticles in an aqueous cysteine–silver solution. Journal of Structural Chemistry. 2016;**57**(6):1203-1208

[35] Giannini C, Ladisa M, Altamura D, Siliqi D, Sibillano T, De Caro L. X-ray diffraction: A powerful technique for the multiple-length-scale structural analysis of nanomaterials. Crystals. 2016;**6**:87. DOI: 10.3390/cryst6080087

[36] Skoog DA, Holler FJ; Crouch SR: Principles of Instrumental Analysis (6th ed.). Belmont, CA: Thomson Brooks/Cole. 2007; pp. 169-173. ISBN: 9780495012016

[37] Das R, Nath SS, Chakdar D, Gope G, Bhattacharjee R. Preparation of silver nanoparticles and their characterization. Journal of Materials Science. 2009:1-9. DOI: 10.2240/azojono0129

[38] Van Dong P, Ha CH, Binh LT, Kasbohm J. Chemical synthesis and antibacterial activity of novel-shaped silver nanoparticles. International Nano Letters. 2012;**2**(9):1-9

[39] Jung C. Insight into protein structure and protein-ligand recognition by Fourier transform infrared spectroscopy. Journal of Molecular Recognition. 2000;**13**:325-351. DOI: 10.1002/1099-1352(200011/12)13:6<325::AID-JMR507>3.0.CO;2-C

[40] Kim S, Barry BA. Reaction-induced FT-IR spectroscopic studies of biological energy conversion in oxygenic photosynthesis and transport. The Journal of Physical Chemistry. B. 2001;**105**:4072-4083. DOI: 10.1021/jp0042516

[41] Vogel R, Siebert F. Vibrational spectroscopy as a tool for probing protein function. Current Opinion in Chemical Biology. 2000;**4**:518-523. DOI: 10.1016/S1367-5931(00)00125-3

[42] Kumar S, Barth A. Following enzyme activity with infrared spectroscopy. Sensors. 2010; **10**:2626-2637. DOI: 10.3390/s100402626

[43] Hind AR, Bhargava SK, McKinnon A. At the solid/liquid interface: FTIR/ATR—The tool of choice. Advances in Colloid and Interface Science. 2001;**93**:91-114. DOI: 10.1016/S0001-8686(00)00079-8

[44] Liu H, Webster TJ. Nanomedicine for implants: A review of studies and necessary experimental tools. Biomaterials. 2007;**28**:354-369. DOI: 10.1016/j.biomaterials.2006.08.049

[45] Bankar A, Joshi B, Kumar AR, Zinjarde S. Banana peel extract mediated novel route for the synthesis of silver nanoparticles. Colloids and Surfaces A-Physicochemical and Engineering Aspects. 2010;**368**:58-63

[46] Adetunji CO, Sarin NB. Impacts of biogenic nanoparticle on the biological control of plant pathogens. Advances in Biotechnology & Microbiology. 2017;**7**(3):555711. DOI: 10.19080/AIBM.2017.07.555711

[47] Adetunji CO, Phazang P, Sarin NB. Biosensors: A Fast-Growing Technology for Pathogen Detection in Agriculture and Food Sector. InTechOpen; 2018

[48] Wang ZL. Transmission electron microscopy of shape-controlled nanocrystals and their assemblies. The Journal of Physical Chemistry. B. 2000;**104**:1153-1175

[49] Ortega-Arroyo L, Martin-Martinez ES, Aguilar-Mendez MA, Cruz-Orea A, Hernandez-Perez I, Glorieux C. Green synthesis method of silver nanoparticles using starch as capping agent applied the methodology of surface response. Starch-Starke. 2013;**65**:814-821. http://dx.doi.org/10.1002/star.201200255

[50] Sreekanth TVM, Nagajyothi PC, Lee KD. *Dioscorea batatas* rhizome-assisted rapid biogenic synthesis of silver and gold nanoparticles. Synthesis and Reactivity in Inorganic, Metal-Organic, and Nano-Metal Chemistry. 2012;**42**:567-572. http://dx.doi.org/10.1080/15533174.2011.613886

[51] Vigneswaran N, Ashtaputre NM, Varadarajan PV, Nachane RP, Paralikar KM, Balasubramanya RH. Biological synthesis of silver nanoparticles using the fungus *Aspergillus flavus*. Materials Letters. 2007;**61**:1413-1418. http://dx.doi.org/10.1016/j.matlet.2006.07.042

[52] Vigneshwaran N, Kathe AA, Varadarajan PV, Nachane RP, Balasubramanya RH. Biomimetics of silver nanoparticles by white rot fungus. Colloids and Surfaces B: Biointerfaces. 2006;**53**:55-59. http://dx.doi.org/10.1016/j.colsurfb.2006.07.014

[53] Jagtap UB, Bapat VA. Green synthesis of silver nanoparticles using *Artocarpus heterophyllus* lam. Seed extract and its antibacterial activity. Industrial Crops and Products. 2013;**46**:132-137. http://dx.doi.org/10.1016/j.indcrop.2013.01.019

[54] Vijayaraghavan K, Nalini SPK, Prakash NU, Madhankumar D. One step green synthesis of silver nano/micro particles using extracts of *Trachyspermum ammi* and *Papaver somniferum*. Colloids and Surfaces B: Biointerfaces. 2012;**94**:114-117. http://dx.doi.org/10.1016/j.colsurfb.2012.01.026

[55] Sant DG, Gujarathi TR, Harne SR, Ghosh S, Kitture R, Kale S, Chopade BA, Pardesi KR. *Adiantum philippense* L. Frond assisted rapid green synthesis of gold and silver nanoparticles. Journal of Nanoparticles. 2013 Article ID: 182320

[56] Satishkumar G, Gobinath G, Karpagam K, Hemamalini V, Premkumar K, Sivaramakrishna S. Phyto-synthesis of silver nanoscale particles using *Morinda citrifolia* L. and its inhibitory action against human pathogens. Colloids and Surfaces B: Biointerfaces. 2012;**95**:235-240. http://dx.doi.org/10.1016/j.colsurfb.2012.03.001

[57] Rajakumar G, Rahuman AA. Larvicidal activity of synthesized silver nanoparticles using *Eclipta prostrata* leaf extract against Filariasis and malaria vectors. Acta Tropica. 2011;**118**: 196-203. http://dx.doi.org/10.1016/j.actatropica.2011.03.003

[58] Joshi M, Bhattacharyya A. Characterization techniques for nanotechnology applications in textiles. Indian Journal of Fiber Textiles Research. 2008;**33**:304-317

[59] Williams DB, Carter CB. The Transmission Electron Microscope. New York, NY, USA: Springer Verlag; 2009

[60] Lin PC, Lin S, Wang PC, Sridhar R. Techniques for physicochemical characterization of nanomaterials. Biotechnology Advances. 2014;**32**:711-726

[61] Jyoti K, Baunthiyal M, Singh A. Characterization of silver nanoparticles synthesized using Urtica dioica Linn. leaves and their synergistic effects with antibiotics. Journal of Radiation Research and Applied Sciences. 2016;**9**:217-227

[62] Dada AO, Adekola FA, Odebunmi EO. Liquid phase scavenging of Cd (II) and Cu (II) ions onto novel nanoscale zerovalent manganese (nZVMn): Equilibrium, kinetic and thermodynamic studies. Environmental Nanotechnology, Monitoring & Management. 2017;**8**:63-72. http://dx.doi.org/10.1016/j.enmm.2017.05.001

[63] Dada AO, Adekola FA, Odebunmi EO (2017). Kinetics, mechanism, isotherm and thermodynamic studies of liquid phase adsorption of Pb2+ onto wood activated carbon supported zerovalent iron (WAC-ZVI) nanocomposite. Cogent Chemistry Journal. 3: 1351653, pg 1–20. DOI: http://doi.org/10.1080/23312009.2017.1351653

[64] Dada AO, Adekola FA, Odebunmi EO. Novel zerovalent manganese for removal of copper ions: Synthesis, characterization and adsorption studies. Applied Water Science. 2017;**7**:1409-1427. DOI: 10.1007/s13201-015-0360-5

[65] Dada AO, Adekola FA, Odebunmi EO. Kinetics and equilibrium models for sorption of cu (II) onto a novel manganese nano-adsorbent. Journal of Dispersion Science and Technology. 2015;**37**(1):119-133. DOI: 10.1080/01932691.2015.103461

[66] Corbari L, Cambon-Bonavita MA, Long GJ, Grandjean F, Zbinden M, Gaill F, Compere P. Iron oxide deposits associated with the ectosymbiotic bacteria in the hydrothermal vent shrimp *Rimicaris exoculata*. Biogeosciences. 2008;**5**(5):1295-1310. DOI: 10.5194/bg-5-1295-2008

[67] Goldstein J. Scanning Electron Microscopy and X-Ray Microanalysis. 2003. Springer. ISBN: 978-0-306-47292-3. Retrieved 26 May 2012

[68] Anandalakshmi K, Venugobal J, Ramasamy V. Characterization of silver nanoparticles by green synthesis method using Pedalium murex leaf extract and their antibacterial activity. Applied Nanoscience. 2016;**6**:399-408. DOI: 10.1007/s13204-015-0449-z

[69] Torrent L, Iglesias M, Hidalgo M, Margu E. Determination of silver nanoparticles in complex aqueous matrices by total reflection X-ray fluorescence spectrometry combined with cloud point extraction. Journal of Analytical Atomic Spectrometry. 2018. DOI: 10.1039/c7ja00335h

[70] Sasikala A, Rao ML, Savithramma N, Prasad TNVKV. Synthesis of silver nanoparticles from stem bark of Cochlospermum religiosum (L.) Alston: An important medicinal plant and evaluation of their antimicrobial efficacy. Applied Nanoscience. 2015;**5**:827-835. DOI: 10.1007/s13204-014-0380-8

[71] John A, Alexanda S, Larry A. Approaching a universal sample preparation method for XRF analysis of powder materials. International center for diffraction data. Advances in X-Ray Analysis. 2001;**44**:368-370

[72] Loupilov A, Sokolov A, Gostilo V. X – Ray Peltier cooled detectors for X – Ray. Radiation Physics and Chemistry. 2001;**61**(3–6):463-464

[73] De Viguerie L, Sole VA, Walter P. Multilayer quantitative X-ray fluorescence analysis applied to easel paintings. Analytical and Bioanalytical Chemistry. 2009 Dec;**395**(7):2015-2020. DOI: 10.1007/s00216-009-2997-0

[74] Fierascu RC, Bunghez IR, SOMOGHI R, Fierascu I, Ion RM. Characterization of silver nanoparticles obtained by using *Rosmarinus officinalis* extract and their antioxidant activity. Revue Roumaine de Chimie. 2014;**59**(3–4):213-218

[75] Ivanisevic I, McClurg RB, Schields PJ. In: Uses of X-ray powder diffraction in the pharmaceutical industry, ed. by S.C. Gad, Pharmaceutical Sciences Encyclopedia: Drug Discovery, Development, and Manufacturing (John Wiley & Sons, Inc., New Jersey). 2010. p. 1

[76] Pecharsky V, Zavalij P. Fundamentals of Powder Diffraction and Structural Characterization of Materials. 2nd ed. Springer; 2009

[77] Das R, Ali ME. Abd Hamid nan SB: Current applications of X-ray powder. Reviews on Advanced Material Science. 2014;**38**:95-109

[78] Ajitha B, Reddy YAK, Reddy PS. Biogenic nano-scale silver particles by *Tephrosia purpurea* leaf extract and their inborn antimicrobial activity. Spectrochim Acta Part A. 2014;**121**:164-172

[79] Vyazovkin S. Thermogravimetric analysis. Characterization of Materials. 2012:1-12

[80] Khan MAM, Kumar S, Ahamed M, Alrokaya SA, Alsalhi MS. Structural and thermal studies of silver nanoparticles and electrical transport study of their thin films. Nanoscale Research Letters. 2011;**6**(434):2011

[81] Moon KS, Dong H, Maric R, et al. Thermal behavior of silver nanoparticles for low-temperature interconnect applications. Journal of Electronic Materials. 2005;**34**(2):168-175. DOI: https://doi.org/10.1007/s11664-005-0229-8

[82] Larrude DG, Maia da Costa MEH, Freire FL Jr. Synthesis and characterization of silver nanoparticle-multiwalled carbon nanotube composites. Journal of Nanomaterials. 2014; **2014**:7 Article ID 654068. DOI: 10.1155/2014/654068

[83] Uznanski P, Zakrzewska J, Favier F, Kazmierski S, Bryszewska E. Synthesis and characterization of silver nanoparticles from (bis)alkylamine silver carboxylate precursors. Journal of Nanoparticle Research. 2017;**19**(3):121. DOI: 10.1007/s11051-017-3827-5

[84] Strohmeier BR, Bunker KL, Lopano CL, Marquis JP, Piasecki JD, Bennethum KE, White RG, Nunney T, Lee RJ. XPS and SEM/STEM characterization of silver nanoparticles formed from the X-ray-induced and thermal reduction of silver behenate. Microscopy and Microanalysis. 2009;**15**:1298-1299

Chapter 10

Assessment of Nano-toxicity and Safety Profiles of Silver Nanoparticles

Yasemin Budama-Kilinc, Rabia Cakir-Koc,
Tolga Zorlu, Burak Ozdemir, Zeynep Karavelioglu,
Abdurrahim Can Egil and Serda Kecel-Gunduz

Additional information is available at the end of the chapter

http://dx.doi.org/10.5772/intechopen.75645

Abstract

Nanotoxicology, which is related with toxic potentials of nanoparticles (NPs) and their adverse effects on living organisms and environment, is a sub-branch of toxicology discipline. Nano-toxicity of NPs depends on their doses, unique chemical, and physical properties. Nowadays, silver (Ag) NPs are used in many consumer and scientific applications such as antimicrobial and pharmaceutical applications, water purification systems, textile industry, and food packaging processes. However, the information that about their nano-toxic potentials is still not complete, and it is considered that several parameters of Ag NPs such as size, shape, surface, and stability affect the toxic potential in different ways. Nano-toxic potentials of Ag NPs were mentioned as *in vivo*, *in vitro*, and *in silico* the studies. In this chapter, it was evaluated the common unique properties of NPs are related with nanotoxicology such as size, surface area and modifications, shape, agglomeration status, and dose.

Keywords: *in vivo*, *in vitro*, *in silico*, nanoparticles, nano-toxicity, silver

1. Introduction

Toxicology is a discipline that investigates the adverse effects of chemical substances and the interaction mechanisms of these substances on the living organisms. Toxicology is derived from a combination of Greek words which are "toxicos" and "logos" these mean "poisonous" and "subject". Nowadays, modern toxicology concerns with the sources of the poisons, physical, chemical, and biological properties of toxic materials, the alteration of these substances

within organism, and the mechanisms of the actions. At the same time, this concept involves the isolation of the poisons, the analysis of toxic materials as quantitative and qualitative besides that risk analyses, optimization processes, and treatments of poisons [1].

Nanotoxicology is a part of bio-nanoscience, which studies on toxicity of nanoparticles (NPs). The changes in structural and physicochemical characteristics of a material in nano-size compared to micro-size, would lead to number of changes in toxicological impacts [2]. The toxicological potential of a material can be investigated in two subdivisions as health and environmental hazard. The main goal of nanotoxicological studies is the determination of which properties of NPs become a threat for the organisms and environment.

There are several ways of taking NPs from organism, such as dermal, inhalation, oral, intravenous and subcutaneous [3–7]. The skin, lung and digestive tract get contacted with the environment. It is clear that lung and digestive tract are more vulnerable than skin since the skin is forceful barrier against foreign substances in general. On the other hand, injections and implants are the other possible routes for intake of NPs [8, 9]. Due to their ultra-small sizes, NPs can reach tissues and organs through circulatory and lymphatic systems. Thus, they may cause some adverse effects on organism that lead to various problems.

Gold (Au), silver (Ag) and iron oxides (Fe_2O_3 or Fe_3O_4) are extensive metals to be used as a nano-sized form, since they have excellent physicochemical properties such as optical, magnetic activity, high thermal and electrical conductivity as well as their great surface area to volume ratio [10–12]. Among these metals, Ag NPs are more prominent than the others due to their antibacterial, antiviral and antifungal effects [13–15]. Therefore, Ag NPs have become a popular topic among the scientific community. **Figure 1** shows that the number of published research articles in this field within last 8 years [16]. According to graphic, the studies which were carried out with Ag NPs, have been increasing continuously.

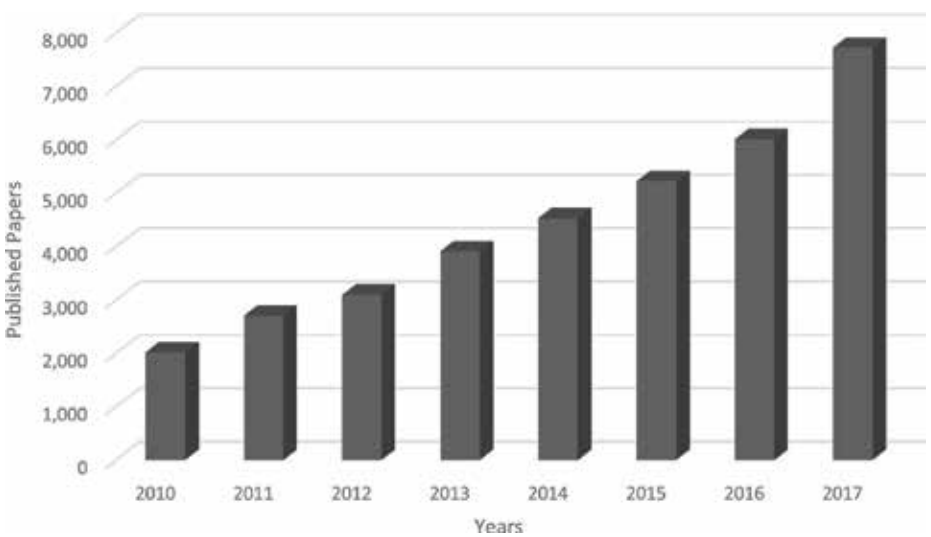

Figure 1. Trend in published research articles on the topic of Ag NPs.

The nano-toxic effects of Ag NPs should be investigated properly because the numerous usage areas of these NPs such as pharmaceutical applications [17], water purification systems [18], textile industry [19] and food packaging processes [20] make them as an outstanding material for humankind and for environment. A comprehensive investigation about toxicity of Ag NPs will provide useful information in risk management for present and future issues.

In this chapter, nano-toxic potentials and common unique properties of Ag NPs related with toxicology such as size, surface area and modifications, shape, agglomeration status and dose were evaluated.

2. The properties affect the nanotoxicology

The physicochemical properties which are related with nanotoxicology can be classified as size-dependent [21], surface-dependent [22], shape-dependent [23], aggregation or agglomeration-dependent [24] and dose-dependent [25]. These properties may change the nano-toxic potentials of NPs in different ways as indicated below.

2.1. Size-dependent toxicity

NPs are defined as materials which are at least one-dimensional and range in 1–100 nm. According to studies, the size of NPs may alter toxicological effects on organism [26].

Toxicological properties of NPs may be induced when the particle surface interacts with cellular components [27]. Therefore, surface area of NPs is depended on their diameters [28] and is enlarged exponentially when the diameter drops off [29]. This situation means that NPs may have several levels of toxicity based on their particle sizes and surface reactivates even if they have same compounds and crystalline structure [30]. Moreover, sizes of NPs increase significantly cellular uptake mechanisms and distribution in the body [31].

Some studies showed that NPs need to migrate across the epithelial barriers to cause toxicity and inflammatory response in animal models [32, 33]. NPs can diffuse into the lung parenchyma when they are inhaled [34, 35]. Different sizes of NPs indicate the special dispersion patterns in the respiratory tract. Stokes number and Reynolds number affect the dispersions of NPs. At the beginning, dispersion of NPs is highly stable in the gas phase. However, their dispersion stabilities may be changed in liquid phase of respiratory fluids depending on the numbers that was mentioned above [36, 37]. Thus, dispersion patterns of NPs are a crucial consideration to determine nano-toxicity [38]. It was reported that kidneys cannot excrete the NPs which were bigger than 6 nm and accumulate some specific organs such as liver and spleen till the clearance of this accumulation by mononuclear phagocyte system [39]. Many NPs cause important adverse effects by accumulation in the liver and spleen [40].

At cellular level, uptake mechanisms and efficiency of NPs are important factors which affect toxicity. NPs penetrate the cell through several ways such as phagocytosis and pinocytosis depending on their particle size and surface properties [41, 42]. The range of 10–500 nm is suitable size for uptake by cells and 5 mm is upper limit for this. The bigger NPs are swallowed

with the help of macro-pinocytosis. The size of vesicle of clathrin-mediated endocytosis is about 100 nm, meanwhile the size of vesicle of caveolae-mediated endocytosis is about 60–80 nm [27].

The size of Ag NPs not only changes with the uptake mechanism but also with the cytotoxicity potential of them [36]. In one study, researchers suggested that Ag NPs have an adverse effect, dependent on size, on lactate dehydrogenase (LDH) activity, cell viability and reactive oxygen species (ROS) generation in different cell lines [36]. In another study, Carlson et al. investigated that 55 and 15 nm of hydrocarbon coated Ag NPs for generating ROS in macrophage cell line. The results showed that the generation of ROS levels with 15 nm of Ag NPs was higher than 55 nm Ag NPs [43]. Wang et al. reported that 20 nm of citrate-coated Ag NPs had more toxicity potential than 110 nm of Ag NPs and 20 nm of citrate-coated Ag NPs have more capacity for generating acute neutrophilic inflammation in the lungs of mice when compare with 110 nm of Ag NPs [44]. However, Kaba et al. showed that smaller Ag NPs do not have a crucial role in the viability of tumor cells [45].

2.2. Surface-dependent toxicity

Surface area and charge of NPs have also important role in biological toxicity. Some studies were reported that a large surface area causes alterations in band gap, decreased melting points and higher reactivities which have critical adverse effects including inflammation, toxicity and cytotoxicity [46–48]. The NPs that have bigger surface area can interact with the other particles which are nearby, and may cause the higher reactivity. Thus, NPs with higher reactivity induces harmful effects in cosmetic products and drug carrier components when used as fillers [49]. From this point of view, it can be inferred that when size of NPs are decreased, biological activity of them are increased, substantially [50].

Some researchers investigated that effect of different surface areas and specific reactivities of NPs in lung for understanding connection between surface area of NPs and their potential toxicities [51]. The result of a research shown that the nano-toxicity which depends on different sizes were not occurred significantly, however, it was suggested that total surface area had an important role to consist of lung inflammation [52, 53]. Particle surface reactivity can be easily determined by single particle aggregate [54–56].

The surface charge of NPs can affect the distribution stability in aqueous solutions and for this reason; it may cause dramatic effects on biological systems and organisms. The surface charge may represent the surface of native NPs and adsorption capacity of ions and biomolecules at their interface [57]. In one study, researchers investigated the bacterial activity of Ag NPs positively and negatively charged. In the result of this study, it showed that positively charged Ag NPs have higher bactericidal activity than negatively charged ones. In either case, bactericidal activity against both Gram-positive and Gram-negative bacteria can change according to the surface charge [58]. Cytotoxic properties of NPs can also be affected by different functional groups on the particle surface and they are associated with protein charges. These different functional groups have important role in forming the NP-protein corona [59].

2.3. Shape-dependent toxicity

There are several chemical and physical synthesis methods of Ag NPs. These differences about synthesis method cause different types of Ag NPs such as spherical, triangular, square, cubic, rectangular, rod, oval and flower. It is still unclear that which critical factors of Ag NPs are playing a role in the formation of particles for toxicity and how they are affecting the biological systems. This situation may occur based on multiple factor. In one study, researchers investigated effect of different shapes of Ag NPs on alveolar epithelial cells (A549) and it was reported that agglomeration of Ag^{+} ions occurred in the cytoplasm in the result of the study [60]. In another study, shape of NPs affects cellular uptakes. Gratton et al. showed that nano-rods has the highest uptake potential and nano-spheres, -ylinders and -cubes are followed it, respectively [39, 61]. In the other study, the researchers used NPs which were smaller than 100 nm. In the result of this research, nano-spheres had a significant advantage over rods. The study also showed that total cell uptake of nano-rods decreased when the aspect ratio of them increased [62, 63].

2.4. Aggregation or agglomeration-dependent toxicity

Aggregation or agglomeration potentials of NPs are very high in solution and air. The parameters such as diffusion, gravitation and convection forces can affect the interaction between NPs and the cells [64, 65]. The agglomeration can increase or decrease association with pH, electrolyte or salt content, and protein composition in the culture medium [66]. Some studies reported that binding capacity of NPs with protein can be changed depending on both composition of NPs and protein [67–69].

It is also known that preparation methods influence the agglomeration status of Ag NPs in medium. Lankoff et al. investigated that the aggregation ranges of Ag NPs using Ag NPs at 20 and 200 nm sizes in culture medium. The results showed that range of aggregation changed based on the culture medium preparation. The hydrodynamic diameter of Ag NPs could also change based on the culture medium preparation and it could be larger than nominal size of NPs. In conclusion, more aggregated particles have lower nano-toxic effect on the cells [70]. Ag NPs may show a high agglomeration tendency in culture medium because Ag NPs have high surface area. Occasionally, aggregation may play a vital role in the several types of intracellular response. Therefore, in terms of toxicological interest, agglomeration or aggregation states of NPs are very crucial for understanding different effects of biological responses [71].

2.5. Dose-dependent toxicity

The dose of NPs is one of the critical factors affecting toxicity. To determine the minimum dose of NPs which is induces toxicity, dose is very important. In one study, 0.2 ppm of Ag NPs decreased cell viability by 20%, meantime 1.6 ppm reduced Ag NPs viability by 40% [72]. Similarly, in human Chang liver cell, cell viability was reduced based on concentration and dose. In another study, researchers investigated toxicity potential of dose range of between 1 and 25 ppm. Result of this study showed that 25 ppm of Ag NPs was the most toxic dose [73].

There is still a problem about dose-dependent issues, which is crucial for understanding and comparing toxicological data. In many studies, which are carried out *in vitro*, doses of NPs are given as mass per volume (μg/ml) due to different experimental setup of studies [74]. Mass per surface area or particle number per surface area is alternative units which were given in some studies. Additionally, there are some differences between nominal dose and theoretical mass which is applied, delivered dose and targeted dose, cellular dose and internalized mass. For example, the deliver dose is related to the stability of NPs in the biological ambient and the viscosity of the dispersion medium [75].

3. *In vivo* toxicological information and experiments about silver NPs

In vivo toxicological studies are carried out with animals. Especially, mammalians such as mice, rat and rabbit are preferred by the researchers because they have the similar biological structure as humans. Over the last decade, the number of *in vivo* studies that examined the toxic effects of NPs has increased. This is due to the presence of NPs in many consumer products. However, the limitations of *in vivo* nanotoxicological studies which are carried out with these products still make it impossible to understand full toxicity profiles of Ag NPs.

Ag NPs naturally use three exposure ways into the body: (1) dermal, (2) inhalation and (3) oral route [76, 77]. In this regard, Ag NPs can make transition to circulatory system and may accumulate in various tissues and organs such as spleen, liver and brain. In recent years, use of Ag NPs in topical antibacterial formulations has caused skin interaction as a primary exposure route [78]. Skin, which constitutes 10% of the total body mass, exhibits a barrier property against external threats and maintains the special feature with various physical, immunological and metabolic activities. In this way, it can also resist particulate factors, especially various microorganisms, and keep the factors out of the body. The role of Ag NPs in the healing of skin wounds by dissociating into Ag^+ ions has made these materials as one of the most successful topical application materials [79]. However, their nano-toxic potentials that exhibit during topical application remains a question mark. From this point of view, *in vivo* animal models are confronting and helping us to test the nano-toxic activities of Ag NPs on the skin. For this purpose, porcine skin is an ideal *in vivo* model for acute nano-toxicity studies. This model is preferred due to its similarity to human skin in terms of either thickness or absorption rate [80]. Rats are also used further as *in vivo* skin nanotoxicology models. However, nanotoxicology studies which are carried out with both models have shown that Ag NPs have not toxic effects on the skin, surprisingly [81]. This may indicate that Ag NPs are using the skin as a transit route, not as a point where can exhibit their toxic abilities [3]. Extra small dimensions of Ag NPs are the biggest factor in achieve this passing.

Oral route is the one of the most important ways for nano-toxic effects of Ag NPs in the physiological systems. According to the Center for Food Safety (CFS), it has been reported that Ag NPs are included in various food additives, baby products and kitchen utensils [82] and this enhances the oral intake of Ag NPs. Since Ag NPs does not have any vital effect on human physiology as an essential metal, the intake into the body is also an undesirable situation [83].

Nonetheless, the studies have reported that the amount of Ag NPs from 0.4 to 27 μg per day can be taken orally by the human body [84–86]. It is known that the microparticulate sizes of silver cause argyria disease, which triggers pigment changing on the skin [87, 88]. However, it is not known whether Ag NPs provoke such a disease. It was shown that 10 nm of citrate-stabilized Ag NPs accumulation leads to oxidative stress in brain [89]. This suggests that Ag NPs may pass through the blood-brain barrier (BBB). BBB is the one of the most important physiological barriers that prevents the passage of various chemical agents and toxic substances into the brain. However, localization of Ag NPs in brain by passing the barrier and, moreover, having the nano-toxic potential to cause loss of function are highly thought provoking. Another *in vivo* study which was carried out by rats showed that it is also sufficient to localize 50–100 nm of Ag NPs in the brain by subcutaneous administration [90]. Intake of Ag NPs by oral administration may cause not only accumulation in brain but also in spleen, liver, kidney, stomach, salivary gland, skin and heart [91–94]. Although the inhalation route does not directly induce the nano-toxic effect, it causes Ag NP accumulation in various tissues and organs via the circulatory system, and indirectly supports to emerge of nano-toxic effects when compared to the other two main exposure routes.

Inhalation exposure is another key route for intake of Ag NPs. Since Ag NPs participate in the construction of various hygiene sprays, it is not difficult for the body to intake by inhalation route [95]. Therefore, it is useful to examine the nano-toxic potentials of Ag NPs on respiratory system. An acute inhalation nano-toxicity study, which was carried out with Ag NPs indicates that the NPs have diameters of 18–20 nm, generated nano-toxic effects at higher doses greater than 3.1×10^6 particles/cm^3 [96]. However, another study using Ag NPs have 12–15 nm indicates that nano-toxic effects did not occur even at higher doses than 1.32×10^6 particles/cm^3 [97]. A fundamental question arises here because these studies were acute and chronic inhalation toxicity studies, respectively. The differences between acute and chronic toxicity studies may help to determine the nano-toxic potentials of Ag NPs. It was observed that Ag NPs accumulated in two major organs such as lung and liver. Changing of lung function was occurred after 90 days in the sub-chronic inhalation nano-toxicity studies that were carried out with *in vivo* rat models [98, 99]. The dose-dependent nano-toxicity is another factor that affects the accumulations of Ag NPs in various tissues and organs. Kim et al. (2011) reported that there was not a significant weight gain of Ag NPs in the organs such as brain, stomach, liver, lungs and kidneys of both male and female rats at the end of 90 days in the lower doses, while the higher doses was effective to accumulating in these organs [100]. This situation can be explained as inhalation exposure leads to a rapid Ag NPs transition to the circulatory system and causes to accumulate of the NPs in various organs. The accumulations can induce to uptake of Ag NPs due to their size, stability, shape and surface activity to the cells which is building blocks of the higher organisms, and cause to loss of function of vital biochemical structures such as DNA and RNA [36, 101–103].

An *in vivo* sub-acute immunotoxicity study which was carried out with rainbow trout showed that approximately 12 nm of Ag NPs caused immunosuppression and inflammation-inducing effects on the fish after 96 hours [104]. In another *in vivo* study using 20–100 nm of Ag NPs, it was observed that Ag NPs almost completely suppressed natural killer (NK) cell activity and decreased the production of interferon-γ, interleukin (IL)-10 and IL-6 at the end of the 28 days in rats [105].

The adverse effects of Ag NPs on the cardiovascular system are still debated [106–108]. It is also possible to use different exposure routes to investigate the nano-toxic potentials of Ag NPs on the cardiovascular system [109]. Tang et al. (2009) reported that Ag NPs could transit directly to the cardiovascular system and cause adverse effects by accumulating in various organs [110]. Researchers also investigated the nano-toxic potentials of Ag NPs on heart in *in vivo* study which carried out with rats and it showed that approximately 20 nm of Ag NPs localized in the myocardium and caused to disorders in cardiac physiology by generating oxidative stress [111, 112]. Another *in vivo* study which used rainbow trout suggested that 50–60 nm of Ag NPs could produce cardiotoxicity in the fish [113].

Nano-toxic effects of Ag NPs on development and reproduction in animal models are another problem. An *in vivo* acute toxicity study that was carried out with male rabbits showed that 45 nm of Ag NPs were detected in acrosome and semen axonemal after intravenous injection [114]. Another study which was conducted with male rats revealed that 60 nm of Ag NPs occurred sperm abnormalities after 23–55 days [115]. The situation is the same for the female individuals. The study which was carried out with female rats showed that intake of 15 nm of Ag NPs orally induced decrease in body weight and increase in the number of atretic and degenerated follicles [116]. Another study also reported that 20 nm of Ag NPs influenced many gene sets including the genes which control the circadian clock regulation and photoreception in zebrafish [117].

4. *In vitro* toxicological information and experiments about silver NPs

The physicochemical and structural features of Ag NPs have an important role in their associations with cells. These different features can bring about different toxicity effects. For this reason, the physicochemical properties of Ag NPs are fundamental parameters in risk assessments and health studies. The assays which are used for predicting of nano-toxic potential of Ag NPs, their toxicity mechanisms and *in vitro* effects of Ag NPs were mentioned below.

4.1. *In vitro* assays for determining of nano-cytotoxicity and -genotoxicity

Cell viability test is the most commonly used method which evaluates the toxicity of Ag NPs. Typically, the percentage of dead cells is directly commeasurable to the toxicity of Ag NPs. Generally, cell viability tests are comprised of chemicals and they are based on differential inclusion, exclusion or transformation of dye or dye precursor which can only be enzymatically converted to detectible dye in living cells. In addition, the toxicity of Ag NPs can be identified by taking into consideration of morphological alterations in cells, cell viability, metabolic activity and oxidative stress. In the present case, nano-toxicity potential of Ag NPs can be evaluated by some assays such as MTT (3-[4,5-dimethylthiazol-2-yl]-2,5 diphenyl tetrazolium bromide), 96AQueous One (96AQ), alamarBlue, LDH, live/dead and neutral red. Due to ability of Ag NPs to adsorb the chemicals onto their surface area, they may interact with dyes or assay reagents, and this situation may lead to incorrect results. Thus, wrong results may occur [118].

As a one of the most used method, the main goal of MTT assay is to measure cell viability in 96 well plates without the necessity of exhaustive cell counting. In brief, the principle of MTT assay is based on mitochondrial activity of viable cells, since decrease or increase of living cell number is directly related with mitochondrial activity. The mitochondrial activity of cells is reflected by the transformation of the tetrazolium salt into formazan crystals which should be dissolved for homogenous evaluation. In this way, any increase or decrease of viable cell number can be determined by measuring formazan concentration reflected in optical density utilizing a plate reader at 540 and 720 nm [119].

The neutral red assay is another cytotoxicity test which is used for measuring cell viability. According to this assay, viable cells are capable of binding the supravital dye neutral red in the lysosomes. This assay may be applied successfully for most of the primary cells and different cell lines. This weakly cationic dye penetrates cell membranes by non-ionic passive diffusion and concentrates in the lysosomes, where it binds by electrostatic hydrophobic bonds to anionic and/or phosphate groups of the lysosomal matrix [120–122]. Then, the absorbance of the solubilized dye which is extracted from the viable cells using an acidified ethanol solution, is quantified using a spectrophotometer.

On the other hand, alamar blue assay is a fluorometric method to determine metabolic activity of cells. The method depends on reduction of resazurin to resorufin via mitochondrial enzymes which carry diaphorase activity, like NADPH dehydrogenase [123]. Resazurin is blue and optical, it has poor fluorescent property. Via cells, resazurin is incrementally converted into the resorufin which is red and highly fluorescent. Fluorescence of resazurin and resorufin can be observed at 530–560 nm stimulation wave length, in addition emission wave length and oxidized form does not fluoresce much at 590 nm. Absorbance value can be observed at 570 and 600 nm, respectively, for the oxidized and reduced forms [124].

In addition to these, genotoxicity tests are also important for evaluating of nano-toxic potential of Ag NPs. These tests are implemented to determine potential genotoxic carcinogens and germ cell mutagens. Ames test (*Salmonella*/Microsome test) is known as the most exact and frequently used step to determine genotoxic carcinogens which cause base pair substitution mutation and small frameshift mutation [125]. The Ames test can be utilized as an indicator of the carcinogenic potential in mammals and it utilizes bacterial strains of *Salmonella typhimurium.* Because of the existence of mutations in the histidine operon, *these strains* are auxotrophic for histidine (*his*$^-$) (i.e., it cannot grow in a minimal culture medium without histidine). Base pair substitutions, frameshift types and gene mutations can be detected via these strains [126]. Although Ames test is generally preferred as first method to determine genotoxicity, there are a lot of studies suggesting that Ames assay is not a proper test method to evaluate the genotoxicity of NPs because Ames assay is mainly negative on NPs. Contrastingly, although many NPs are negative in the Ames assay, they generate positive genotoxic response in comet assay and micronucleus (MN) assay which are two of the *in vitro* mammalian cell test systems [125].

Comet assay is a quick and sensitive test which can determine the DNA damage at the level of individual eukaryotic cell. To perform this test, the cells are fixed in agarose gel on microscope slides and lysed under mild alkaline conditions to discard the cellular proteins. Then, slides are exposed to alkaline conditions to induce the DNA to unwind and electrophoresis.

During the electrophoresis, the migration of the undamaged super coiled DNA is slow, and it is close to the nucleoid, however, the migration of broken DNA fragments and relaxed chromatin is faster and further away from the nucleoid toward the anode. Thus the appearance of a "comet tail" is occurred. The DNA is marked with a fluorescent dye, so the DNA damage can be determined under a fluorescence microscope by visual scoring or via computerized image analysis [127]. In addition, this assay is the one of the most commonly used tests for determining the genotoxicity of NPs and also this test gives the most positive outcomes [125]. Genotoxicity of Ag NPs was evaluated by alkaline comet assay in human peripheral blood cells [128]. After exposure for 3 hours, the results demonstrated that Ag NPs (50 and 100 g/ml) lead to DNA damage. Besides, a short exposure of 5 minutes also demonstrated DNA damage too. To sum up, the study has demonstrated that the synthesized Ag NPs induced DNA damage in human peripheral blood cells and it was detected by the alkaline comet assay. Moreover, results showed that there was no inducing of any DNA damage in the presence of hydrogen peroxide, when the cells were exposed to Ag NP's.

In vitro micronucleus (MN) assay swiftly determines small membrane-bound DNA fragments which are located in cytoplasm of interphase cells [125]. This assay detects the genotoxic damage in interphase cells and it is also an alternative to chromosome aberration test. The evaluation of micronuclei can be counted faster, thanks to the ability of the assay to investigate cells during interphase. Micronuclei may be the result of aneugenic and clastogenic (chromosome breakage or whole chromosome) damage [129]. Li et al. [130] used 5 nm of Ag NPs to determine their genotoxicity via *in vitro* micronucleus assay. Frequency of micronucleus was increased by the Ag NP exposure and increase of micronucleus is dependent on dose of Ag NPs. At the concentration rate of 30 μg/ml (with 45.4% relative population doubling), Ag NPs induced a significant 3.17-fold increase with a net increase of 1.60% in micronucleus frequency over the vehicle control, a weak positive response by criteria of the study. These results showed that 5 nm of Ag NP are genotoxic on TK6 cells.

4.2. Nano-toxicity mechanism and *in vitro* toxic effects of Ag NPs

There are various types of nano-toxicity mechanisms which are suggested for Ag NPs. However, toxicity of this material is fundamentally associated with reactions such as the surface oxidation, Ag ion release and interaction between biological macromolecules and Ag NPs [131]. AshaRani et al. (2008) suggested that deformation of the mitochondrial respiratory chain via Ag NPs raised ROS generation, and interruption of ATP synthesis [101]. Thus, DNA was damaged due to this situation. Ag NPs can interact with membrane proteins and activate signaling pathways. Hence, they lead to inhibition of cell proliferation. It is also suggested that Ag NPs can uptake the cell via diffusion or endocytosis, and they may cause some disorders such as mitochondrial function disorder, generation of ROS, damaging of the proteins and nucleic acids and inhibition of cell proliferation [101]. Hsin et al. (2008) were studied about nano-toxicity mechanisms of Ag NPs in NIH3T3 fibroblast cells [132]. They have discovered that exposing Ag NPs induced the releasing of cytochrome C into the cytosol and increasing of translocation of Bax to the mitochondria. It is the fact that Ag NPs may induce apoptosis via the mitochondrial pathway while acting through ROS and C-Jun N-terminal kinase. In addition to this situation, interaction of Ag NPs with DNA can cause cell cycle

arrest at the G2/M phase [132, 133]. The antibacterial property of Ag NPs makes them lethal to bacteria, besides it makes nano-toxic effects on human cells. For instance, lethal concentration (LC) of Ag NPs for bacteria is also lethal for keratinocytes and fibroblasts [133]. AshaRani et al. (2009) have investigated the antiproliferative activity of Ag NPs and they proposed a mechanism of toxicity as shown in **Figure 2** [134]. Ag NPs can cause cell proliferation interacting with membrane proteins and activating signaling pathways [135]. Besides, the Ag NPs can enter into the cell via different ways such as diffusion and endocytosis. After entering into the cell, mitochondrial dysfunction and generation of ROS are occurred, proteins and nucleic acids inside the cell are damaged and finally, it results inhibition of cell proliferation [131].

Traditionally, easily ionized nanoparticles such as silver nanoparticles induce toxicity by a Trojan-horse type mechanism [72, 95]. Phagocytosis of Ag NPs stimulates inflammatory signaling via the generation of ROS in macrophage cells, following that the activated macrophage cells induced secretion of TNF-α. The increasing level of TNF-α leads to damage of cell membrane and apoptosis. All these results seemed to be caused by ionization of Ag NPs in cells which is expressed by a Trojan-horse type mechanism.

As a rule, the change of cell shape or morphology in a monolayer culture is the first and easily perceptible effect after exposing of toxic materials with cells. According to the microscopic observations, exposed cells with Ag NPs showed that significant morphological alterations which are hints of unhealthy cells, whereas control appear normal. In comparison to control group, the cells which were exposed with Ag NPs appeared to be clustered with a few cellular extensions and cell spreading patterns were limited. Those can be examined by deformations in cytoskeletal functions which are result of Ag NPs exposure [101].

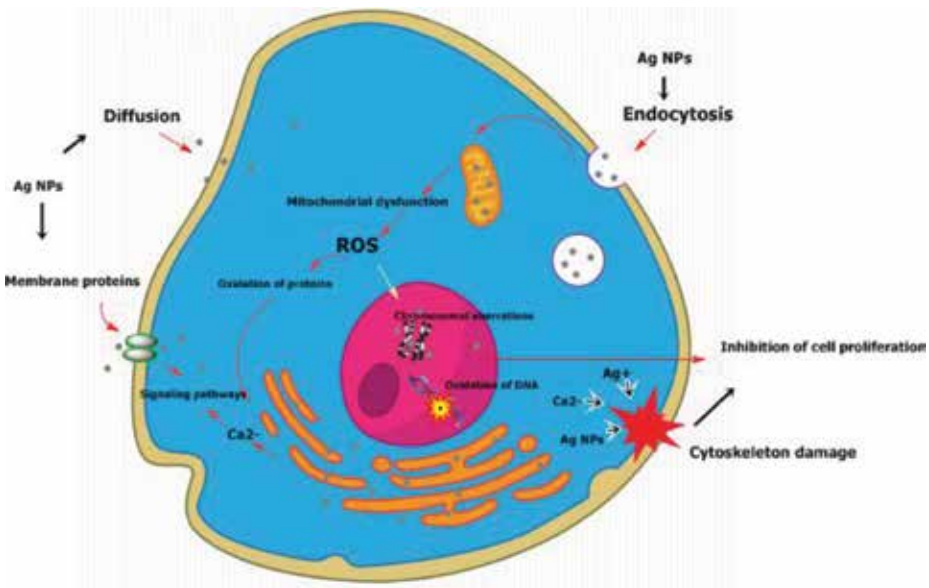

Figure 2. Proposed antiproliferative activity and nano-toxicity mechanism of Ag NPs.

Size effect of the Ag NPs is the one of the most important parameters which affects nano-toxicity. In a study using Ag NPs with different sizes (10, 40 and 100 nm), it was reported that all types of Ag NPs showed powerful cytotoxic activity at lower concentrations and they lead to overproduction of ROS at concentrations, which are lower than cytotoxic ones. Ag NPs, which are smaller than 10 nm, are the most toxic ones. According to this study, the nano-cytotoxicity of Ag NPs is related to production of ROS [136]. Another study suggested that the nano-toxicity potentials of Ag NPs which were coated similarly and had different sizes including 10, 20, 40, 60 and 80 nm were investigated on bacteria, yeast, algae, crustaceans and mammalian cells *in vitro*. According to the study, cells of *Daphnia magna* were the most sensitive cells to Ag NPs. *Pseudokirchneriella subcapitata, Escherichia coli*, *Pseudomonas fluorescens, Saccharomyces cerevisiae* and lastly mammalian fibroblast cells followed them, respectively. Also, researchers reported that as the size of particles is decreased, their toxic effect is increased. In addition, the toxic effect difference between 10 and 80 nm of Ag NPs was the biggest for *D. magna* and the smallest for mammalian fibroblast cells [137].

The shape of the Ag NPs is also another important parameter which affects nano-toxicity potentials of Ag NPs. In a study, differences between toxicity of Ag nano-spheres (30 nm) and nano-wires (length: 1.5–25 μm; diameter 100–160 nm) were investigated by using alveolar epithelial cells. In conclusion, the nano-wires had powerful impact on the alveolar epithelial cells, while the nano-spheres had no specific effect [60]. In another study, nano-toxic differences of Ag NPs which had nano-spheres (diameter 40–80 and 120–180 nm; two different samples), nano-platelets (20–60 nm), nano-cubes (140–180 nm) and nano-rods (diameter 80–120 nm, length > 1000 nm) were investigated. As the result of study, all NPs which exposed to human mesenchymal stem cells were cytotoxic at concentrations greater than 12.5 mg/ml. However, particle shape had no distinct cytotoxic effect toward the cells. On the other hand, the nano-toxicity against *Staphylococcus aureus* is increased by a higher dissolution rate and this situation was suggested that dissolved Ag ions were one of the toxic species against the bacteria. The particles, which had higher specific surface area, were more toxic against the bacteria in comparison to particles, which had lower specific surface area. The differences in the solution rate may be utilized to practice Ag NPs with a comparatively higher bacterial effect with a lower cytotoxic effect toward tissue [138].

Coating is another factor which affects nano-toxicity to the cells. Samberg et al. (2010) determined the nano-toxicity of Ag NPs using human epidermal keratinocytes *in vivo* and *in vitro* [81]. The cells were exposed to varied concentrations of uncoated and carbon coated NPs, individually. Viability of the cells which were exposed to uncoated Ag NPs decreased due to the doses. On the other hand, there was no toxic effect was observed in the cells treated with carbon coated Ag NPs [139]. In an *in vitro* study on yeast cells and lung cells (A549) showed that Ag NPs, which were coated with positively charged bPEI, were more toxic toward yeast cells in comparison to Ag NPs, which were coated with negatively charged citrate. Besides, the researchers determined that positively charged Ag nanoparticles (10 and 80 nm) adsorbed onto the surface of the yeast cell. In the lung cells, 10 nm of Ag NPs, which were coated with positively charged bPEI, were more toxic than Ag NPs, which were coated with negatively

http://dx.doi.org/10.5772/intechopen.75645

charged citrate. In addition, positively and negatively charged Ag NPs were adsorbed onto the cell surface of the lung epithelial cells [140].

5. *In silico* toxicological information and experiments about silver NPs

Determination of the toxicity of chemicals used as active substance in medicine is very important for the detection of harmful effects on people, animals, plants or environment. Although the animal models for toxicity determination have been used for a very long time but the long duration of these experiments, ethical issues, financial burden and animal damage make these models unfavorable. For this reason, computerized calculation methods have begun to gain attention for toxicological studies. *In silico* toxicology is a type of toxicity assessment method used to estimate the toxicity of chemicals, and through these computational method toxicities of chemicals are modeled, analyzed and identified. The computational methods, which are also complementary to *in vivo* and *in vitro* toxicity tests, aim to minimize the need for animal testing with the reliability of toxicity determination and reduce the cost and time. Another advantage of computational methods is that they can predict the toxicity of chemicals before further synthesis takes place [141].

The relationship between structure and toxicity has led to the creation of a new model called quantitative nanostructure-toxicity relationship (QNTR), which provides us with NPs and their toxic properties. In this model, the mathematical objects, which are called descriptors, are described. These descriptors must be computable sizes and they are related with some properties of NPs such as the chemical and structural properties, particle shape, size, surface area, ionization potential, formation heat, zeta potential and physicochemical properties of molecules that was attached to NPs surfaces. Subsequently, a subset of the identifiers associated with most biological properties (e.g. cell apoptosis, metabolism or signaling pathway modulation) is selected and modeled using mathematical techniques. In statistical modeling, neural networks are often used and a mathematical model that links the biologic activity and the identifiers is created. Finally, the robustness and adequacy of models are assessed and interpreted using statistical cross-validation techniques without anticipating the properties of new materials [142]. Although the determination of the *in vivo* effects of NPs via experiments is very laborious and difficult, it is possible to create fingerprints of NPs on the organisms, while estimating with obtained from the QNTR models. Use of molecular descriptors and *in vitro* assay results of NPs is also an effective method for the prediction *in vivo* toxicities of these materials [143]. Quantitative structure-activity relationship (QSAR) is a model that is used to estimate the toxicity of chemicals. QSAR modeling tools include statistical methods such as multiple linear regression, polynomial and kernel regression, as well as machine learning methods such as artificial neural networks and clustering methods like random forest and decision trees [144–146]. These methods have revealed that there is a mathematical relationship between the physicochemical or molecular properties of NPs and their biological activities. These associations are often very complex. However, thanks to the QSAR and QNTR methods, toxicity can be predicted for drugs, which is used on humans and animals, or chemicals, which is used in industry [147]. The obstacles that make it difficult to implement QSAR methods; insufficiency

of modeling the biological properties of NPs and experimental data on the bio-corona composition, and unpredictability of *in vivo* effects of NPs compared with *in vitro* studies.

Nano-QSAR is a QSAR method that is used as the descriptor of NPs such as size, surface area, solubility, protein corona, zeta potential, bio-distribution and shape. There are not so many researches about nano-QSAR method that was carried out with Ag NPs in the literature. Therefore, it can be helpful to look up the study which was conducted by Silva et al. [148]. In this research, nano-QSAR method was used for predicting the organo-coated Ag NPs such as citrate-coated, polyvinylpyrrolidone-coated and branched polyethyleneimine-coated. These NPs were applied to two model organisms, *E. coli* and *D. magna*, and nano-toxic potentials of Ag NPs were predicted. However, it is the fact that there is more study about computational predicting of nano-toxic effects of Ag NPs needed.

6. Conclusion

NPs are commonly used in many different areas such as technology, health, transportation, construction, information and communication. Ag NPs, which have antibacterial, antiviral and antimicrobial properties are used in many area and highly preferred compared to other NPs due to their physical properties, such as high biocompatibilities, unique electronic and catalytic properties. However, Ag NPs may appear to be potential risk to the environment. Size, shape, surface area and dose are the most important factors which affect the toxic potential. Toxicity of Ag NPs can be determined via *in vivo* and *in vitro* assays, and *in silico* models. *In vitro* toxicity assays are more sensitive and rapid than *in vivo* assays. However, *in vitro* toxicity assays can be contaminated by external factors such as microorganisms and different particulate matters. On the other hand, *in vivo* toxicity assays show more realistic results, but they take a long time. Besides, different doses unit such as ppm, mass per volume or mass per unit of NPs may be altered the result of toxicity assays. Therefore, *in silico* methods can be replaced to other methods in the future because of *in silico* methods are rapid and they predict the adverse effects of NPs, correctly as well as *in vivo* and *in vitro* assays. One of the main goals of the nanotoxicological studies is preventing animal sacrificing. Thus, *in silico* models can overcome this issue. However, it is disadvantage that use of computational methods for predicting to determine the toxic potentials of NPs is relatively new and their usage is quite restricted. Evaluation of complete toxicological profile of Ag NPs depends on the development of combined and strong nanotoxicological assays.

Author details

Yasemin Budama-Kilinc[1]*, Rabia Cakir-Koc[1], Tolga Zorlu[1], Burak Ozdemir[1], Zeynep Karavelioglu[1], Abdurrahim Can Egil[1] and Serda Kecel-Gunduz[2]

*Address all correspondence to: yaseminbudama@gmail.com

1 Yildiz Technical University, Bioengineering Department, Esenler, Istanbul, Turkey

2 Istanbul University, Physics Department, Vezneciler, Istanbul, Turkey

References

[1] Casarett LJ, Klaassen CD. Casarett and Doull's Toxicology: The Basic Science of Poisons. USA: McGraw-Hill; 2001

[2] Gatoo MA et al. Physicochemical properties of nanomaterials: Implication in associated toxic manifestations. BioMed Research International. 2014;**2014**:1-8

[3] Schneider M et al. Nanoparticles and their interactions with the dermal barrier. Dermato-Endocrinology. 2009;**1**(4):197-206

[4] Fröhlich E, Salar-Behzadi S. Toxicological assessment of inhaled nanoparticles: Role of in vivo, ex vivo, in vitro, and in silico studies. International Journal of Molecular Sciences. 2014;**15**(3):4795-4822

[5] Date AA, Hanes J, Ensign LM. Nanoparticles for oral delivery: Design, evaluation and state-of-the-art. Journal of Controlled Release. 2016;**240**:504-526

[6] Guo H et al. Intravenous administration of silver nanoparticles causes organ toxicity through intracellular ROS-related loss of inter-endothelial junction. Particle and Fibre Toxicology. 2015;**13**(1):21

[7] Jogala S, Rachamalla SS, Aukunuru J. Development of subcutaneous sustained release nanoparticles encapsulating low molecular weight heparin. Journal of Advanced Pharmaceutical Technology & Research. 2015;**6**(2):58

[8] Nichols JW, Bae YH. Odyssey of a cancer nanoparticle: From injection site to site of action. Nano Today. 2012;**7**(6):606-618

[9] Parnia F et al. Overview of nanoparticle coating of dental implants for enhanced osseointegration and antimicrobial purposes. Journal of Pharmacy & Pharmaceutical Sciences. 2017;**20**:148-160

[10] Takeuchi I et al. Biodistribution and excretion of colloidal gold nanoparticles after intravenous injection: Effects of particle size. Bio-medical Materials and Engineering. 2017;**28**(3):315-323

[11] Rai M et al. Recent advances in use of silver nanoparticles as antimalarial agents. International Journal of Pharmaceutics. 2017;**526**(1-2):254-270

[12] Schneider MGM, Lassalle VL. Magnetic iron oxide nanoparticles as novel and efficient tools for atherosclerosis diagnosis. Biomedicine & Pharmacotherapy. 2017;**93**:1098-1115

[13] Jalali SAH et al. An antibacterial study of a new magnetite silver nanocomposite. Journal of Environmental Chemical Engineering. 2017;**5**(6):5786-5792

[14] Huy TQ et al. Cytotoxicity and antiviral activity of electrochemical–synthesized silver nanoparticles against poliovirus. Journal of Virological Methods. 2017;**241**:52-57

[15] Xia Z-K et al. The antifungal effect of silver nanoparticles on *Trichosporon asahii*. Journal of Microbiology, Immunology and Infection. 2016;**49**(2):182-188

[16] Available from: http://www.sciencedirect.com/search?qs=silver%20nanoparticles&origin=home&zone=qSearch&years=2010%2C2011%2C2012&lastSelectedFacet=years [Accessed: Dec 11, 2017]

[17] Prusty K, Swain SK. Nano silver decorated polyacrylamide/dextran nanohydrogels hybrid composites for drug delivery applications. Materials Science and Engineering: C. 2017;**85**:130-141

[18] Thakare SR. And S.M. Ramteke, fast and regenerative photocatalyst material for the disinfection of *E. coli* from water: Silver nano particle anchor on MOF-5. Catalysis Communications. 2017;**102**:21-25

[19] Lorenz C et al. Characterization of silver release from commercially available functional (nano) textiles. Chemosphere. 2012;**89**(7):817-824

[20] Li L et al. Effect of stable antimicrobial nano-silver packaging on inhibiting mildew and in storage of rice. Food Chemistry. 2017;**215**:477-482

[21] Karlsson HL et al. Size-dependent toxicity of metal oxide particles—A comparison between nano-and micrometer size. Toxicology Letters. 2009;**188**(2):112-118

[22] Zhao X et al. Exploring the diameter and surface dependent conformational changes in carbon nanotube-protein corona and the related cytotoxicity. Journal of Hazardous Materials. 2015;**292**:98-107

[23] Oh WK et al. Shape-dependent cytotoxicity and proinflammatory response of poly (3,4-ethylenedioxythiophene) nanomaterials. Small. 2010;**6**(7):872-879

[24] Abdelmonem AM et al. Charge and agglomeration dependent in vitro uptake and cytotoxicity of zinc oxide nanoparticles. Journal of Inorganic Biochemistry. 2015;**153**:334-338

[25] Tiwari DK, Jin T, Behari J. Dose-dependent in-vivo toxicity assessment of silver nanoparticle in Wistar rats. Toxicology Mechanisms and Methods. 2011;**21**(1):13-24

[26] Buzea C, Pacheco II, Robbie K. Nanomaterials and nanoparticles: Sources and toxicity. Biointerphases. 2007;**2**(4):MR17-MR71

[27] Shin SW, Song IH, Um SH. Role of physicochemical properties in nanoparticle toxicity. Nanomaterials. 2015;**5**(3):1351-1365

[28] Warheit DB et al. Pulmonary instillation studies with nanoscale TiO_2 rods and dots in rats: Toxicity is not dependent upon particle size and surface area. Toxicological Sciences. 2006;**91**(1):227-236

[29] Tihanyi K, Vastag M. Solubility, Delivery and ADME Problems of Drugs and Drug-Candidates. Belgium: Bentham Science Publishers; 2011:33-51

[30] Howland MA et al. Goldfrank's Toxicologic Emergencies. 10th ed. USA: McGraw-Hill Education; 2014

[31] Gustafson HH et al. Nanoparticle uptake: The phagocyte problem. Nano Today. 2015; **10**(4):487-510

[32] Lefebvre DE et al. Utility of models of the gastrointestinal tract for assessment of the digestion and absorption of engineered nanomaterials released from food matrices. Nanotoxicology. 2015;**9**(4):523-542

[33] Bellmann S et al. Mammalian gastrointestinal tract parameters modulating the integrity, surface properties, and absorption of food-relevant nanomaterials. Wiley Interdisciplinary Reviews: Nanomedicine and Nanobiotechnology. 2015;**7**(5):609-622

[34] Geiser M, Kreyling WG. Deposition and biokinetics of inhaled nanoparticles. Particle and Fibre Toxicology. 2010;**7**(1):2

[35] Miller MR et al. Inhaled nanoparticles accumulate at sites of vascular disease. ACS Nano. 2017;**11**(5):4542-4552

[36] Gliga AR et al. Size-dependent cytotoxicity of silver nanoparticles in human lung cells: The role of cellular uptake, agglomeration and Ag release. Particle and Fibre Toxicology. 2014;**11**(1):11

[37] Qiao H et al. The transport and deposition of nanoparticles in respiratory system by inhalation. Journal of Nanomaterials. 2015;**2015**:2

[38] Varna M et al. In vivo distribution of inorganic nanoparticles in preclinical models. Journal of Biomaterials and Nanobiotechnology. 2012;**3**(02):269

[39] Albanese A, Tang PS, Chan WC. The effect of nanoparticle size, shape, and surface chemistry on biological systems. Annual Review of Biomedical Engineering. 2012;**14**:1-16

[40] Ballou B et al. Noninvasive imaging of quantum dots in mice. Bioconjugate Chemistry. 2004;**15**(1):79-86

[41] Zhao F et al. Cellular uptake, intracellular trafficking, and cytotoxicity of nanomaterials. Small. 2011;**7**(10):1322-1337

[42] Kou L et al. The endocytosis and intracellular fate of nanomedicines: Implication for rational design. Asian Journal of Pharmaceutical Sciences. 2013;**8**(1):1-10

[43] Carlson C et al. Unique cellular interaction of silver nanoparticles: Size-dependent generation of reactive oxygen species. The Journal of Physical Chemistry. B. 2008;**112**(43): 13608-13619

[44] Wang X et al. Use of coated silver nanoparticles to understand the relationship of particle dissolution and bioavailability to cell and lung toxicological potential. Small. 2014;**10**(2):385-398

[45] Kaba SI, Egorova EM. In vitro studies of the toxic effects of silver nanoparticles on HeLa and U937 cells. Nanotechnology, Science and Applications. 2015;**8**:19

[46] Klabunde KJ et al. Nanocrystals as stoichiometric reagents with unique surface chemistry. The Journal of Physical Chemistry. 1996;**100**(30):12142-12153

[47] Campbell CT, Parker SC, Starr DE. The effect of size-dependent nanoparticle energetics on catalyst sintering. Science. 2002;**298**(5594):811-814

[48] Suttiponparnit K et al. Role of surface area, primary particle size, and crystal phase on titanium dioxide nanoparticle dispersion properties. Nanoscale Research Letters. 2011;**6**(1):27

[49] Nel A et al. Toxic potential of materials at the nanolevel. Science. 2006;**311**(5761):622-627

[50] Oberdörster G et al. Principles for characterizing the potential human health effects from exposure to nanomaterials: Elements of a screening strategy. Particle and Fibre Toxicology. 2005;**2**(1):8

[51] Duffin R et al. The importance of surface area and specific reactivity in the acute pulmonary inflammatory response to particles. Annals of Occupational Hygiene. 2002;**46**(suppl_1):242-245

[52] Stoeger T et al. Instillation of six different ultrafine carbon particles indicates a surface area threshold dose for acute lung inflammation in mice. Environmental Health Perspectives. 2006;**114**(3):328

[53] Sager TM, Kommineni C, Castranova V. Pulmonary response to intratracheal instillation of ultrafine versus fine titanium dioxide: Role of particle surface area. Particle and Fibre Toxicology. 2008;**5**(1):17

[54] Warheit DB, Reed KL, Sayes CM. A role for nanoparticle surface reactivity in facilitating pulmonary toxicity and development of a base set of hazard assays as a component of nanoparticle risk management. Inhalation Toxicology. 2009;**21**(suppl 1):61-67

[55] Monteiller C et al. The pro-inflammatory effects of low-toxicity low-solubility particles, nanoparticles and fine particles, on epithelial cells in vitro: The role of surface area. Occupational and Environmental Medicine. 2007;**64**(9):609-615

[56] Rabolli V et al. The cytotoxic activity of amorphous silica nanoparticles is mainly influenced by surface area and not by aggregation. Toxicology Letters. 2011;**206**(2):197-203

[57] Mu Q et al. Chemical basis of interactions between engineered nanoparticles and biological systems. Chemical Reviews. 2014;**114**(15):7740-7781

[58] Abbaszadegan A et al. The effect of charge at the surface of silver nanoparticles on antimicrobial activity against gram-positive and gram-negative bacteria: A preliminary study. Journal of Nanomaterials. 2015;**16**(1):53

[59] Caracciolo G, Farokhzad OC, Mahmoudi M. Biological identity of nanoparticles in vivo: Clinical implications of the protein corona. Trends in Biotechnology. 2017;**35**(3):257-264

[60] Stoehr LC et al. Shape matters: Effects of silver nanospheres and wires on human alveolar epithelial cells. Particle and Fibre Toxicology. 2011;**8**(1):36

[61] Gratton SE et al. The effect of particle design on cellular internalization pathways. Proceedings of the National Academy of Sciences. 2008;**105**(33):11613-11618

[62] Qiu Y et al. Surface chemistry and aspect ratio mediated cellular uptake of Au nanorods. Biomaterials. 2010;**31**(30):7606-7619

[63] Chithrani BD, Ghazani AA, Chan WC. Determining the size and shape dependence of gold nanoparticle uptake into mammalian cells. Nano Letters. 2006;**6**(4):662-668

[64] Teeguarden JG et al. Particokinetics in vitro: Dosimetry considerations for in vitro nanoparticle toxicity assessments. Toxicological Sciences. 2006;**95**(2):300-312

[65] Lison D et al. Nominal and effective dosimetry of silica nanoparticles in cytotoxicity assays. Toxicological Sciences. 2008;**104**(1):155-162

[66] Vippola M et al. Preparation of nanoparticle dispersions for in-vitro toxicity testing. Human & Experimental Toxicology. 2009;**28**(6-7):377-385

[67] Lundqvist M et al. Nanoparticle size and surface properties determine the protein corona with possible implications for biological impacts. Proceedings of the National Academy of Sciences. 2008;**105**(38):14265-14270

[68] Ehrenberg MS et al. The influence of protein adsorption on nanoparticle association with cultured endothelial cells. Biomaterials. 2009;**30**(4):603-610

[69] Kittler S et al. The influence of proteins on the dispersability and cell-biological activity of silver nanoparticles. Journal of Materials Chemistry. 2010;**20**(3):512-518

[70] Lankoff A et al. The effect of agglomeration state of silver and titanium dioxide nanoparticles on cellular response of HepG2, A549 and THP-1 cells. Toxicology Letters. 2012;**208**(3):197-213

[71] Bae E et al. Effect of agglomeration of silver nanoparticle on nanotoxicity depression. Korean Journal of Chemical Engineering. 2013:**30**(2):1-5

[72] Park E-J et al. Silver nanoparticles induce cytotoxicity by a Trojan-horse type mechanism. Toxicology In Vitro. 2010;**24**(3):872-878

[73] Piao MJ et al. Silver nanoparticles induce oxidative cell damage in human liver cells through inhibition of reduced glutathione and induction of mitochondria-involved apoptosis. Toxicology Letters. 2011;**201**(1):92-100

[74] Hussain SM et al. At the crossroads of nanotoxicology in vitro: Past achievements and current challenges. Toxicological Sciences. 2015;**147**(1):5-16

[75] Kong B et al. Experimental considerations on the cytotoxicity of nanoparticles. Nanomedicine. 2011;**6**(5):929-941

[76] Lankveld DP et al. The kinetics of the tissue distribution of silver nanoparticles of different sizes. Biomaterials. 2010;**31**(32):8350-8361

[77] Chen X, Schluesener H. Nanosilver: A nanoproduct in medical application. Toxicology Letters. 2008;**176**(1):1-12

[78] Tian J et al. Topical delivery of silver nanoparticles promotes wound healing. ChemMedChem. 2007;**2**(1):129-136

[79] Prow TW et al. Nanoparticles and microparticles for skin drug delivery. Advanced Drug Delivery Reviews. 2011;**63**(6):470-491

[80] Monteiro-Riviere NA, Riviere J. The pig as a model for cutaneous pharmacology and toxicology research. In: Advances in Swine in Biomedical Research. USA: Springer; 1996. pp. 425-458

[81] Samberg ME, Oldenburg SJ, Monteiro-Riviere NA. Evaluation of silver nanoparticle toxicity in skin in vivo and keratinocytes in vitro. Environmental Health Perspectives. 2010;**118**(3):407

[82] Anonymus. Nano-Silver in Food and Food Contact Products. 2017. Available from: https://www.centerforfoodsafety.org/files/nano-silver_product_inventory-in-food-12514_66028.pdf [Accessed: Dec 11, 2017]

[83] Lansdown A. Critical observations on the neurotoxicity of silver. Critical Reviews in Toxicology. 2007;**37**(3):237-250

[84] Clemente G, Rossi L, Santaroni G. Trace element intake and excretion in the Italian population. Journal of Radioanalytical and Nuclear Chemistry. 1977;**37**(2):549-558

[85] Gibson RS, Scythes CA. Chromium, selenium, and other trace element intakes of a selected sample of Canadian premenopausal women. Biological Trace Element Research. 1984;**6**(2):105-116

[86] Hamilton E, Minski M. Abundance of the chemical elements in man's diet and possible relations with environmental factors. Science of the Total Environment. 1973;**1**(4):375-394

[87] Berger P et al. Localized argyria caused by metallic silver aortic grafts: A unique adverse effect. European Journal of Vascular and Endovascular Surgery. 2013;**46**(5):565-568

[88] Rodriguez V, Romaguera RL, Heidecker B. Silver-containing wound cream leading to Argyria—Always ask about alternative health products. The American Journal of Medicine. 2017;**130**(4):e145-e146

[89] Skalska J, Dąbrowska-Bouta B, Strużyńska L. Oxidative stress in rat brain but not in liver following oral administration of a low dose of nanoparticulate silver. Food and Chemical Toxicology. 2016;**97**:307-315

[90] Tang J et al. Influence of silver nanoparticles on neurons and blood-brain barrier via subcutaneous injection in rats. Applied Surface Science. 2008;**255**(2):502-504

[91] Goebel HH, Muller J. Ultrastructural observations on silver deposition in the choroid plexus of a patient with argyria. Acta Neuropathologica. 1973;**26**(3):247-251

[92] Loeschner K et al. Distribution of silver in rats following 28 days of repeated oral exposure to silver nanoparticles or silver acetate. Particle and Fibre Toxicology. 2011;**8**(1):18

[93] van der Zande M et al. Distribution, elimination, and toxicity of silver nanoparticles and silver ions in rats after 28-day oral exposure. ACS Nano. 2012;**6**(8):7427-7442

[94] Hadrup N, Lam HR. Oral toxicity of silver ions, silver nanoparticles and colloidal silver – A review. Regulatory Toxicology and Pharmacology. 2014;**68**(1):1-7

[95] Luoma SN. Silver nanotechnologies and the environment. The Project on Emerging Nanotechnologies Report. 2008;**15**:12-13

[96] Sung JH et al. Acute inhalation toxicity of silver nanoparticles. Toxicology and Industrial Health. 2011;**27**(2):149-154

[97] Ji JH et al. Twenty-eight-day inhalation toxicity study of silver nanoparticles in Sprague-Dawley rats. Inhalation Toxicology. 2007;**19**(10):857-871

[98] Sung JH et al. Subchronic inhalation toxicity of silver nanoparticles. Toxicological Sciences. 2008;**108**(2):452-461

[99] Sung JH et al. Lung function changes in Sprague-Dawley rats after prolonged inhalation exposure to silver nanoparticles. Inhalation Toxicology. 2008;**20**(6):567-574

[100] Kim JS et al. In vivo genotoxicity of silver nanoparticles after 90-day silver nanoparticle inhalation exposure. Safety and Health at work. 2011;**2**(1):34-38

[101] AshaRani P et al. Cytotoxicity and genotoxicity of silver nanoparticles in human cells. ACS Nano. 2008;**3**(2):279-290

[102] Meyer JN et al. Intracellular uptake and associated toxicity of silver nanoparticles in *Caenorhabditis elegans*. Aquatic Toxicology. 2010;**100**(2):140-150

[103] Greulich C et al. Uptake and intracellular distribution of silver nanoparticles in human mesenchymal stem cells. Acta Biomaterialia. 2011;**7**(1):347-354

[104] Bruneau A et al. Fate of silver nanoparticles in wastewater and immunotoxic effects on rainbow trout. Aquatic Toxicology. 2016;**174**:70-81

[105] De Jong WH et al. Systemic and immunotoxicity of silver nanoparticles in an intravenous 28 days repeated dose toxicity study in rats. Biomaterials. 2013;**34**(33):8333-8343

[106] Grosse S, Evje L, Syversen T. Silver nanoparticle-induced cytotoxicity in rat brain endothelial cell culture. Toxicology In Vitro. 2013;**27**(1):305-313

[107] Haase A et al. A novel type of silver nanoparticles and their advantages in toxicity testing in cell culture systems. Archives of Toxicology. 2012;**86**(7):1089-1098

[108] Kang K et al. Vascular tube formation and angiogenesis induced by polyvinylpyrrolidone-coated silver nanoparticles. Toxicology Letters. 2011;**205**(3):227-234

[109] Gonzalez C et al. Role of silver nanoparticles (AgNPs) on the cardiovascular system. Archives of Toxicology. 2016;**90**(3):493-511

[110] Tang J et al. Distribution, translocation and accumulation of silver nanoparticles in rats. Journal of Nanoscience and Nanotechnology. 2009;**9**(8):4924-4932

[111] Ramirez-Lee MA et al. Effect of silver nanoparticles upon the myocardial and coronary vascular function in isolated and perfused diabetic rat hearts. Nanomedicine: Nanotechnology, Biology and Medicine. 2017;**13**(8):2587-2596

[112] Manuel AR-L et al. Evaluation of vascular tone and cardiac contractility in response to silver nanoparticles, using Langendorff rat heart preparation. Nanomedicine: Nanotechnology, Biology and Medicine. 2017;**13**(4):1507-1518

[113] Callaghan NI et al. Nanoparticulate-specific effects of silver on teleost cardiac contractility. Environmental Pollution. 2017:1-10

[114] Castellini C et al. Long-term effects of silver nanoparticles on reproductive activity of rabbit buck. Systems Biology in Reproductive Medicine. 2014;**60**(3):143-150

[115] Mathias FT et al. Daily exposure to silver nanoparticles during prepubertal development decreases adult sperm and reproductive parameters. Nanotoxicology. 2015;**9**(1):64-70

[116] Elnoury MAH et al. Study of the effects of silver nanoparticles exposure on the ovary of rats. Life Science Journal. 2013;**10**(2):1887-1894

[117] Cambier S et al. Fate and effects of silver nanoparticles on early life-stage development of zebrafish (Danio rerio) in comparison to silver nitrate. Science of the Total Environment. 2018;**610**:972-982

[118] Deyhle H, Schulz G, Müller B. Imaging Human Body Down to Molecular Level, in Encyclopedia of Nanotechnology. Springer. 2012. pp. 1049-1056

[119] van Meerloo J, Kaspers GJ, Cloos J. Cell sensitivity assays: The MTT assay. Cancer Cell Culture: Methods and Protocols. 2011:**731**:237-245

[120] Winckler J. Vital staining of lysosomes and other cell organelles of the rat with neutral red (author's transl). Progress in Histochemistry and Cytochemistry. 1974;**6**(3):1

[121] Nemes Z et al. The pharmacological relevance of vital staining with neutral red. Experientia. 1979;**35**(11):1475-1476

[122] Repetto G, Del Peso A, Zurita JL. Neutral red uptake assay for the estimation of cell viability/cytotoxicity. Nature Protocols. 2008;**3**(7):1125-1131

[123] O'brien J et al. Investigation of the Alamar Blue (resazurin) fluorescent dye for the assessment of mammalian cell cytotoxicity. The FEBS Journal. 2000;**267**(17):5421-5426

[124] Zachari MA et al. Evaluation of the alamarblue assay for adherent cell irradiation experiments. Dose-Response. 2014;**12**(2):246-258

[125] Kim HR et al. Appropriate in vitro methods for genotoxicity testing of silver nanoparticles. Environmental Health and Toxicology. 2013;**28**:1-8

[126] Oliveira N d MS et al. In vitro mutagenicity assay (Ames test) and phytochemical characterization of seeds oil of *Helianthus annuus* Linné (sunflower). Toxicology Reports. 2016;**3**:733-739

[127] Žegura B, Filipič M. Application of In Vitro Comet Assay for Genotoxicity Testing. In: Optimization in Drug Discovery: In Vitro Methods. USA: Springer; 2004. pp. 301-313

[128] Flower NA et al. Characterization of synthesized silver nanoparticles and assessment of its genotoxicity potentials using the alkaline comet assay. Mutation Research/Genetic Toxicology and Environmental Mutagenesis. 2012;**742**(1):61-65

[129] Doherty AT. The in vitro micronucleus assay. Genetic Toxicology: Principles and Methods. 2012;**817**:121-141

[130] Li Y et al. Genotoxicity of silver nanoparticles evaluated using the Ames test and in vitro micronucleus assay. Mutation Research/Genetic Toxicology and Environmental Mutagenesis. 2012;**745**(1):4-10

[131] McShan D, Ray PC, Yu H. Molecular toxicity mechanism of nanosilver. Journal of Food and Drug Analysis. 2014;**22**(1):116-127

[132] Hsin Y-H et al. The apoptotic effect of nanosilver is mediated by a ROS-and JNK-dependent mechanism involving the mitochondrial pathway in NIH3T3 cells. Toxicology Letters. 2008;**179**(3):130-139

[133] Singh SP et al. Silver nanoparticles: Biomedical applications, toxicity, and safety issues. International Journal of Research in Pharmacy and Pharmaceutical Sciences. 2017; **4**(2):01-10

[134] Asharani P, Hande MP, Valiyaveettil S. Anti-proliferative activity of silver nanoparticles. BMC Cell Biology. 2009;**10**(1):65

[135] Roh J-Y, Eom H-J, Choi J. Involvement of *Caenohabditis elegans* MAPK signaling pathways in oxidative stress response induced by silver nanoparticles exposure. Toxicological Research. 2012;**28**(1):19

[136] Zapór L. Effects of silver nanoparticles of different sizes on cytotoxicity and oxygen metabolism disorders in both reproductive and respiratory system cells. Archives of Environmental Protection. 2016;**42**(4):32-47

[137] Ivask A et al. Size-dependent toxicity of silver nanoparticles to bacteria, yeast, algae, crustaceans and mammalian cells in vitro. PLoS One. 2014;**9**(7):e102108

[138] Helmlinger J et al. Silver nanoparticles with different size and shape: Equal cytotoxicity, but different antibacterial effects. RSC Advances. 2016;**6**(22):18490-18501

[139] Pandiarajan J et al. Synthesis and toxicity of silver nanoparticles. In: Nanoscience in Food and Agriculture. Vol. 3. Switzerland: Springer; 2016. pp. 73-98

[140] Kasemets K et al. Charge and size-dependent toxicity of silver nanoparticles to yeast cells. In: Eurotox. 2014;**229**:S194-S195

[141] Raies AB, Bajic VB. In silico toxicology: Computational methods for the prediction of chemical toxicity. Wiley Interdisciplinary Reviews: Computational Molecular Science. 2016;**6**(2):147-172

[142] Bondarenko O et al. Toxicity of Ag, CuO and ZnO nanoparticles to selected environmentally relevant test organisms and mammalian cells in vitro: A critical review. Archives of Toxicology. 2013;**87**(7):1181-1200

[143] Lee S et al. Importance of structural information in predicting human acute toxicity from in vitro cytotoxicity data. Toxicology and Applied Pharmacology. 2010;**246**(1):38-48

[144] Burden FR, Winkler DA. Robust QSAR models using Bayesian regularized neural networks. Journal of Medicinal Chemistry. 1999;**42**(16):3183-3187

[145] Fourches D et al. Quantitative nanostructure − Activity relationship modeling. ACS Nano. 2010;**4**(10):5703-5712

[146] Katritzky AR et al. Quantitative correlation of physical and chemical properties with chemical structure: Utility for prediction. Chemical Reviews. 2010;**110**(10):5714-5789

[147] Lessigiarska I et al. Quantitative structure-activity-activity and quantitative structure-activity investigations of human and rodent toxicity. Chemosphere. 2006;**65**(10): 1878-1887

[148] Silva T et al. Particle size, surface charge and concentration dependent ecotoxicity of three organo-coated silver nanoparticles: Comparison between general linear model-predicted and observed toxicity. Science of the Total Environment. 2014;**468**:968-976

Chapter 11

Use of Silver Nanoparticles as Tougheners of Alumina Ceramics

Enrique Rocha-Rangel, Azucena Pérez-de la Fuente,
José A. Rodríguez-García,
Eddie N. Armendáriz-Mireles and
Carlos A. Calles-Arriaga

Additional information is available at the end of the chapter

http://dx.doi.org/10.5772/intechopen.76949

Abstract

In this work, alumina/silver composites were produced through powder techniques, which involve the combination of high energy mechanical milling combined with sintering in the presence of a liquid phase and with the idea of having ceramics with good toughness values. From mechanical characterizations, it was found that increases of the silver content in the alumina origins decrease the elastic's modulus and flexural strength of the final composite. The fracture toughness of alumina increases from 4.2 $MPam^{-0.5}$ for monolithic alumina to 10 $MPam^{-0.5}$ for alumina with 2 wt% silver additions. It was determined that the reinforcement mechanism of these materials is due to the deflection of cracks owing to metallic bridges formed by the silver used as toughener material.

Keywords: silver reinforcements, fracture toughness, alumina, silver nanoparticles, ceramic composites

1. Introduction

Manufacturing, in its broadest sense, is the process of converting raw material into a finished product. It includes the design of the product, the selection of the raw material and the sequence of processes and operations through which it will be manufactured [1]. This method exists since approximately 5000–4000BC. The manufacture of products for various uses began with the production of articles made of wood, ceramics, stone, and metal. The materials and

processes that were first used to form products through smelting and forging have been developed gradually over the centuries, using in the actuality new materials and more complex operations, at increasing production rates and higher levels of quality [1].

In the modern sense, manufacturing involves the manufacture of products from raw materials through various processes, machinery, and operations, through a well-organized plan for each required activity [1]. Each approach is suitable only for producing just a particular component and material, and it cannot be used to do all types of products. In reality, the sequence of the manufacturing process is designed according to the requirements of the component to be manufactured.

The metallurgy of powders has been used since 300 BC when massively large iron objects were manufactured [2]. In 1829, new developments were achieved in this area when an English engineer applied cold pressure and sintered platinum powder to produce ductile platinum. Later, in 1870, osmium filaments were made using the powder metallurgy method. In 1916 a commercial tungsten cable manufactured employing this method was also produced. After all these developments in the field of powder metallurgy, a wide variety of components are currently manufactured, such as tungsten carbide cutting tools, refractory parts, and electronic components, among many others [2].

Until now the techniques of processing of powders involve working with very fine powders with sizes of the order of microns, where materials with excellent physical and chemical properties have been obtained. However, with the advance of science, researchers have observed that it is possible to get materials with much better properties working with powders finer than microns. These studies at nanometric levels are what have given way to the nanotechnology and the development of the nanostructured materials. Nanotechnology is a current issue that involves several branches of science, so it is difficult to define it. However, it could be said that it is the design, manufacture, and application of nanostructures or nanomaterials, and the knowledge of the relationships between physical properties or phenomena and the dimensions of the material [3].

The search for new nanostructured functional materials has focused on nanometric scale manipulation, which leads to the improvement of properties at the macro scale [4].

Nanomaterials are a new class of materials (whether they are ceramic, metals, semiconductors, polymers, or a combination of these) in which at least one of their dimensions is between 1 and 100 nm; represent a transition between molecules and atoms and a material with solid volumetric dimensions [5, 6].

At the end of the previous century, there is a classification of these advanced materials called functional materials with a gradient [7]. The functional materials with gradient represent those advanced materials that comprise a particular gradient in structure composition, or both, and adapted for a specific application or function [8]. Ceramic materials in recent years have been developed as advanced materials, and above all, as functional materials with a gradient, due to the favorable properties that they possess and the many ways in which they can be processed [9–14]. They are compounds formed by metallic and non-metallic elements; with general properties that characterize them, it can be pointed out that they are hard, fragile, and resistant to compression; some are transparent, others translucent. Regarding the conductivity

of heat and electricity, some are insulators, others have low conductivity, although this is subject to several factors; they are mostly resistant to corrosion at room temperature and others also at high temperatures [15].

However, the ceramic materials in general present great fragility, in the particular case of the materials made of alumina (Al_2O_3) are not the exception. Alumina is a very useful and widely used industrial ceramic material. Its applications include cutting tools, dental implants, prostheses, electrical and thermal insulations, and wear resistant. Its utility is attributed to its high hardness, high resistance to compression, and high properties of electrical and thermal insulation. However, despite its desirable and potential characteristics, its use as a structural material has been considerably hindered due to its low resistance to fracture (as is typical of ceramics) [9]. Ceramic materials can be made more robust by incorporating fine metal particles into their matrix. This development has been successfully used before in different systems [9, 16–19].

Researchers have used numerous methods aimed at improving fracture toughness and other mechanical properties of alumina processing. In these studies, different systems have been prepared with an alumina-based ceramic matrix reinforced with the incorporation of metallic particles presenting the following results: Yao [20] has applied spark plasma sintering for the preparation of Al_2O_3/Ni nanocomposite and has reported a fracture toughness of 3.84 $MPam^{-0.5}$. Sekino [21] has prepared an Al_2O_3/Ni nanocomposite by hot pressing of an Al_2O_3/NiO mixture at a pressure of 30 MPa and temperature of 1450°C, reporting a resistance of more than 1 GPa, but the fracture toughness was only 3.5 $MPam^{-0.5}$ for 5% by volume of Ni content. So from this investigation, it was concluded that the Ni increases only nominally the fracture toughness, even though the nickel is appreciably ductile. The lack of coincidence of the coefficient of thermal expansion between nickel and alumina could be responsible for the reduction of gain in fracture toughness. Guichard [22] has reported the production of Al_2O_3/Cr composites with fracture toughness values between 4 and 7.2 $MPam^{-0.5}$ by varying only the chromium content. The densification of these composites was carried out by sintering without pressure, and hot pressing at temperatures between 1400 and 1600°C. The samples of the hot pressing proposed work were much denser and with higher hardness than those sintered without pressure. Ji and Yeomans [23] have manufactured an Al_2O_3/Cr nanocomposite containing 5% by volume of chromium, registering a strength and fracture toughness of 736 MPa and 4.72$MPam^{-0.5}$, respectively. Therefore, they concluded from this study that a relatively high chromium content is necessary for the improvement of fracture toughness. In his research, Prielipp [24] has used Al_2O_3/Al and the gas pressure infiltration for the porous alumina reinforcement. He has obtained a resistance of 810 MPa and a fracture toughness of 10.5 $MPam^{-0.5}$, this result was registered in a composite with 35% aluminum volume. These values are remarkable in comparison with the values corresponding to the non-reinforced monolithic alumina. Another notable feature of this compound is that both fracture strength and fracture toughness were significantly improved without compensation. Although 35% by volume of aluminum was concluded in this work, it is a significantly high amount for reinforcement, since the fact that aluminum is of a density much lower than alumina making this percentage of values comfortable [25]. In different studies, authors comment that the reinforcement models indicate that the size of the metal inclusion and the homogeneous distribution of it in the ceramic matrix are critical to ensure obtaining a composite material with favorable tenacity properties [9].

In general, to get the best microstructures and properties, a ceramic based compound must be carefully prepared since the powder synthesis stage. Ceramic/metal composite materials have typically been prepared by hot pressing powder mixtures prepared by chemical routes [26–30]. However, there have been problems in the reproduction of their very peculiar properties and their routine use in practical applications of this type of compounds, due to the contamination of the powders during the milling operation, the complexity of the chemical solutions and the costs of producing large quantities of materials by hot pressing. From the review made so far, the Al_2O_3 ceramics have not been reinforced with silver, despite the excellent ductility of silver, in such a way that it would be very interesting to determine the effect of silver on fracture toughness of Al_2O_3-based ceramics. In this way the objective of this study is; to fabricate alumina-based ceramic materials (Al_2O_3) reinforced with Ag (silver) nanoparticles through mechanical grinding and pressureless sintering and to determine the effect of silver on the fracture toughness of alumina.

2. Experimental

This chapter describes the experimentation carried out detailing each of the working conditions in each stage of the process, for obtaining the alumina-based composites with silver nanoparticles and the characterizations made in the obtained materials to determine their mechanical properties, mainly fracture toughness.

2.1. Powders

The starting materials were alumina (Al_2O_3) powder (Sigma-Aldrich, 5 μm size and 99.9% purity), silver (Ag) powder (Mayer, 1 μm size and 99.9% purity).

2.2. Milling

The final contents of silver in the alumina-silver composites were: 0.0, 0.5, 1, 2, and 3% weight. The grinding and mixing of the powders were carried out in a planetary type mill (Retsch, PM100 German), in dry for 3 h with turning intervals every 3 min, at a rotation speed of 250 rpm. It was used a 250 ml stainless steel container with ZrO_2 zirconia grinding elements (0.3 cm diameter), the ratio between the weight of the balls and the powder weight was 12:1.

2.3. Powder granulometry

After the grinding stage for each of the samples, a granulometric analysis of the powder was carried out (Malvern Instruments, Masterziser 2000, England); this equipment uses the laser diffraction technique to measure the size of the particles suspended in an aqueous solution.

2.4. Compaction

With the powders obtained from the milling, and with the help of a steel die tool grade they were manufactured cylindrical samples. The dimensions were of 2 cm diameter by 0.3 cm thickness with an approximate weight of 2 grams; the compaction of said samples was carried out at room temperature, by uniaxial pressing using 350 MPa in a hydraulic press (Montequipo, LAB-30-T, Mexico).

2.5. Density of samples in green

The measurements of the densities of green samples (before sintering) were obtained through direct measurements taking the diameter and the thickness in millimeters with a digital calibrator (Mitutoyo, D6CS, Japan) to register their volume. The weight in grams was obtained through a digital balance (A&D, HR-120, Japan). Once these measurements were made, the real green density was calculated using a ratio of mass to volume, taking the following formulas:

$$V_s = \pi r^2 h \tag{1}$$

$$\rho_r = \frac{W_s}{V_s} \tag{2}$$

where V_s is the sample's volume (cm^3), r is the sample's radius (cm), h is sample's height (cm), ρ_r is the sample's real density (gcm^{-3}), and W_s is the sample's weight (g). In the same way, theoretical density of each composition was calculated by the rule of mixtures according to the following formula:

$$\rho_t = (\rho_t Al_2O_3)(X\,Al_2O_3) + (\rho_t Ag)(X\,Ag) \tag{3}$$

where $\rho_t Al_2O_3$ is the theoretical density of alumina (3.98 gcm^{-3}), $\rho_t Ag$ is the theoretical density of silver (10.5 gcm^{-3}), $X\,Al_2O_3$ is the molar fraction of alumina and $X\,Ag$ is the molar fraction of silver. Finally, we proceed to calculate the relative density of each sample with the following formula:

$$\rho_{rel} = \frac{\rho_r}{\rho_t} \times 100 \tag{4}$$

2.6. Sintering

The pressed samples were subjected to different sintering cycles, using temperatures of 1400, 1500, and 1600°C, during sintering times of 1, 2, and 3 h. For this, an electric furnace was used (Carbolite, RHF17/3E, England) with super Kanthal resistances, a heating rate of 5°$Cmin^{-1}$ was used in all cycles, in each sintering cycle, an argon gas flow of 10 $cm^3\,min^{-1}$ was injected into the furnace chamber to inhibit the oxidation of silver. The cooling of the pellets was carried out inside the furnace by turning off this once the sintering cycle was completed. The choice of sintering conditions is due to the fact that at temperatures below 1400°C the alumina is not sintered. While, at temperatures above 1600°C, besides there would be an excessive growth of grain, there is a risk that the silver evaporates. Conducting studies at intermediate temperatures between 1400 and 1600°C would not seem to give a different behavior. Something similar happens with the sintering times; at low times there would not be an adequate sintering of the alumina, while longer times would cause grain growth, deteriorating with these the mechanical properties of the final material.

2.7. Density of sintered samples

Once the samples were sintered, the density of each of them was measured using the Archimedes method by placing water in a plastic container, which was placed on a balance and the weight of samples was recorded. Immediately, the temperature of the water was measured with a thermocouple (National Instruments, NI USB-TC01, USA), the time the sample

was submerged in the water was 10 min, this in order that the water was introduced into the porosity and removed the air contained in the sample. Following this procedure and with the water weight readings recorded, the real density of the sintered samples was calculated using the following formula:

$$\rho_r = \frac{(W_s H_2 O)(\rho_{H_2O})}{W_s} \times 100 \quad (5)$$

where $W_s H_2 O$ is the sample's weight in H_2O (g), and ρ_{H2O} is the density of water at the experimental temperature (gcm^{-3}).

2.8. Contraction percentage

Before and after sintering the samples, their diameter was measured with the help of a digital calibrator (Mitutoyo, CD6CS, Japan). With this data, the contraction percentage of each sample was calculated applying the following formula:

$$C_s = 1 - \frac{D_s}{D_v} \times 100 \quad (6)$$

where C_s is the sample's contraction (%), D_s is the diameter of sample heat treated (cm), and D_v is the diameter of sample in green (cm).

2.9. Microstructure

2.9.1. Optical microscopy (OM)

Microstructure observations of each sample were made by optical microscopy, using an optical microscope (Nikon Eclipse, Ma200, Japan). The images were taken at different magnifications and using different light filters, in different parts to observe better details of the microstructure, such as grain growth, the homogeneity of the distribution of silver, and the shape and size of the grain.

2.9.2. Scanning electron microscopy (SEM)

Microstructure observations of each sample were also made by scanning electron microscopy, which allows obtaining better details of the microstructure. Before being analyzed the samples were coated with a layer of graphite to make them conductive, to carry out the observations, 15Kv of acceleration voltage was used in an electron microscope (JEOL, JSM 6300, Japan).

2.9.3. Analysis by energy dispersive of X-rays (EDX)

For this study, it was used a Hitachi equipment (SU9000 UHR FE-SEM, Japan) and the Image plus S-75 software. With which punctual analyzes were made in different areas of the samples, to verify the existing chemical elements in each phase present in the microstructure.

2.10. X-ray diffraction (XRD)

This study was carried out with the help of a Siemens diffractometer (D-5000, German), here it was corroborated the existence of the crystalline phases in the composites.

2.11. Mechanical properties

2.11.1. Elastic modulus

The sintered samples were cut to a rectangular shape and placed on a pair of polyester supports (to avoid absorption of vibration). Then they are hit with a metal hammer, this activity emits a sound which travels through the sample at a certain speed, and this resonance is captured using an ultrasonic sensor (GrindoSonic, A-360, Japan). Subsequently, the equipment has software to which data such as the size of the sample and its density are entered, which calculates the elastic module according to the following expression:

$$E = \rho_r v^{0.5} \tag{7}$$

where E is the sample's elastic modulus (GPa), and v is the sound velocity in the sample (cms^{-1}).

2.11.2. Flexural strength

To measure the flexural strength, it was necessary to cut the samples in a rectangular shape using a diamond disc cutter. For the test, the sample was placed on a pair of supports located at a distance from each other and applying the load just in the center of the sample. During the test, no preload was applied, after this, a head moved at a speed of 0.05 $mmmin^{-1}$ with a cell with a load of 10 GPa to perform the test, the machine that was used to measure the resistance to bending is from the Instron brand with a mobile head.

2.11.3. Microhardness

For the microhardness test, 20 measurements were made in different places of the sample; this was done with a micro durometer (Wilson Instruments, S400, Japan). In each test a force of 9.8 N was applied during 10s, once the indentation was finished, it was preceded to determine the measure of the diagonals d_1 and d_2 of the print (**Figure 1**) and depending on the results and dimensions of this print it can be determined the hardness of the material.

2.11.4. Fracture toughness

To measure the fracture toughness, the same 12 tests of the measurement of microhardness are used, with the measurements of the cracks generated in the vertices of the indentation print and with the dimensions of diagonal of the print; the fracture toughness can be evaluated in agreement with the next equation [31]:

$$K_{1c} = \frac{0.16}{(c/a)^{1.5}} \times (H a^{0.5}) \tag{8}$$

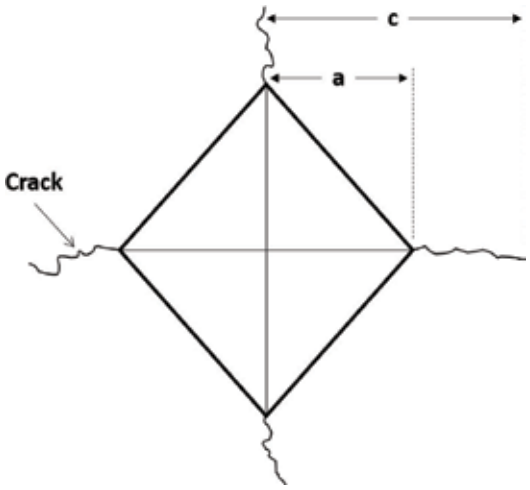

Figure 1. Image showing the cracks generated in the vertices of the indentation print.

where K_{IC} is the critical stress intensity factor in load mode I, H is the Vickers hardness (GPa), c is the average length of the cracks obtained from the tips of the Vickers (μm), and a is the average length of the half of the diagonal of the Vickers (μm).

3. Results

3.1. Morphology and powder size

Figure 2 shows micrographs of mixtures of alumina powders with different percentages of silver. In this figure, there can be visualized very fine particles with nanometric sizes. There can be observed few spherical particles. However, the particles are mostly irregular and dendritic, in the same way in the majority of the samples particle; they have formed agglomerates with sizes greater than 2 microns. Having this homogeneity in the sizes and shapes of the powders will undoubtedly benefit the compaction of the samples and the resulting densification of the same. The observation of the silver particles is difficult due to their nanometric size; however, in the pictures, they observe very small white dots at intergranular positions, and these small dots correspond to silver.

In the graphs of **Figure 3** are shown the results obtained from the granulometric analysis. Based on them, it can be determined that approximately 45% of the powder has particle sizes between 0.1 and 1 microns (nanometer size), about 30% of the powder presents particles between 1 and 10 microns, and about 25% of the particles powders have sizes greater than 10 microns. In some cases, particle sizes are close to 100 microns, and due to the presence in the mixtures of very fine powders with nanometric sizes, surely these large particles are the result of the agglomeration of small powders. In any case, a proper distribution of particle sizes is present in the powder mixtures, with nanometric powders, which must mean large surface areas and therefore many contact points that will favor atomic diffusion during the sintering stage.

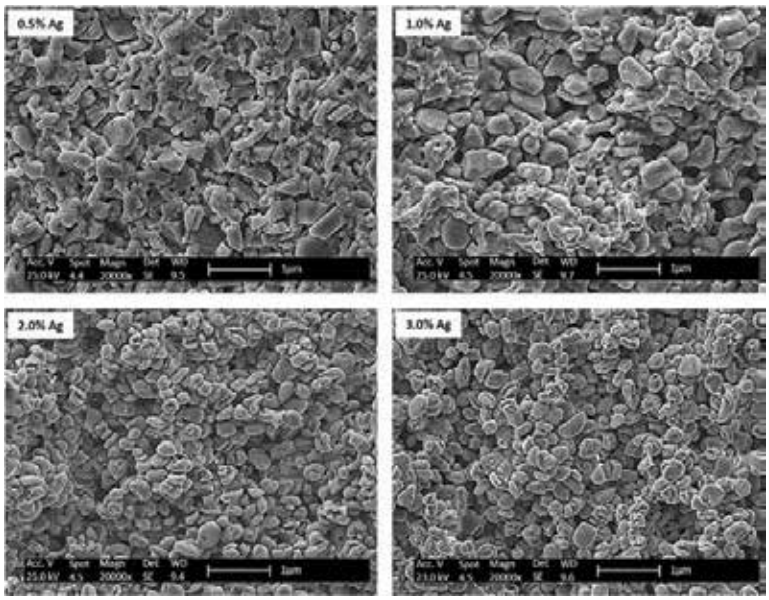

Figure 2. Micrographs of alumina powders with different silver percentages.

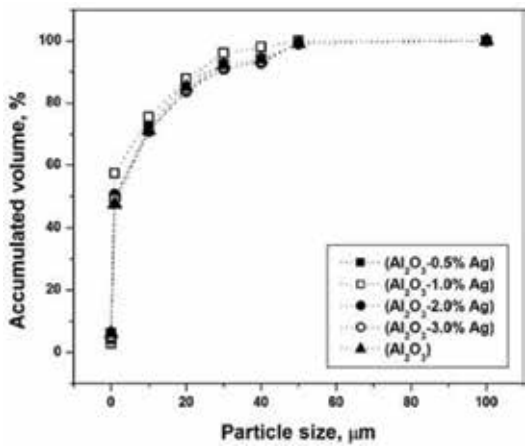

Figure 3. Graphs showing the granulometry of alumina powders reinforced with silver nanoparticles.

3.2. Density

In **Figure 4** are presented the comparison of the results obtained from the densities in green and the densities of the sintered samples for each studied composition. In this figure, it is observed that the density of the sintered samples compared with the samples in green increased considerably. This increase occurred because during the sintering stage the porosity in the samples was reduced due to the homogeneity, shape, and size of the particles. Final density reached by the samples are close to 100%, this means thoroughly densified bodies were obtained after sintering.

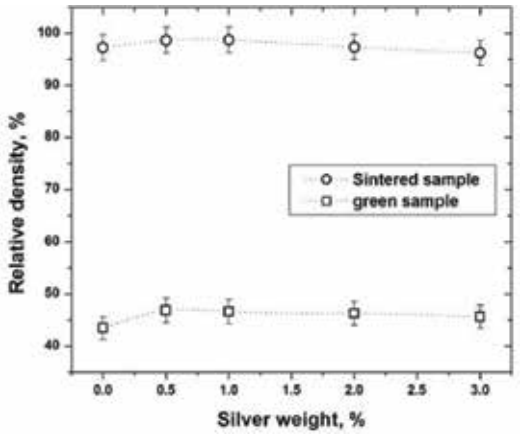

Figure 4. Comparison between green density and sintered density, as a function of silver content in the composite.

3.3. Contraction percentage

In the graph of **Figure 5**, it can be observed the contraction percentages obtained in the samples sintered at 1500°C for 2 h, where the results of previous discussions are reinforced, the samples with inclusions of 0.5–1.0 wt% of Ag obtained a higher percentage of contraction. This means that the more the sample is contracted, the volume decreases due to the elimination of porosity and its density increases. The sample with 0.0% of Ag presents a minimum contraction percentage, well below the other samples, with respect to the samples with inclusions of 2.0–3.0% of Ag; the tendency to decrease with the higher amount of Ag is presented again in these results. Therefore, in agreement with the results, it has that silver present in the composite favor contraction, and therefore, densification of composites. In other words, composites with low porosity were manufactured, which means that there are fewer sites for the initiation and propagation of cracks.

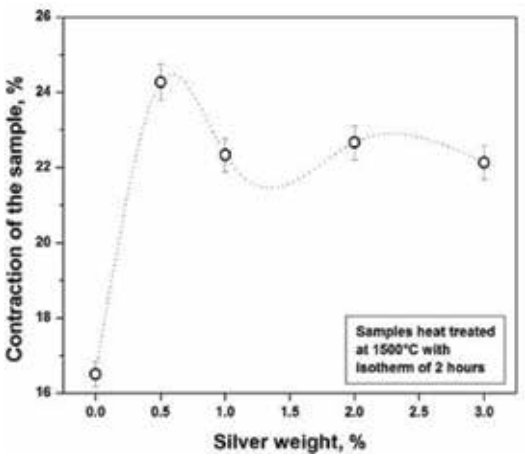

Figure 5. Contraction percentage of the sintered samples at 1500°C, during 2 h.

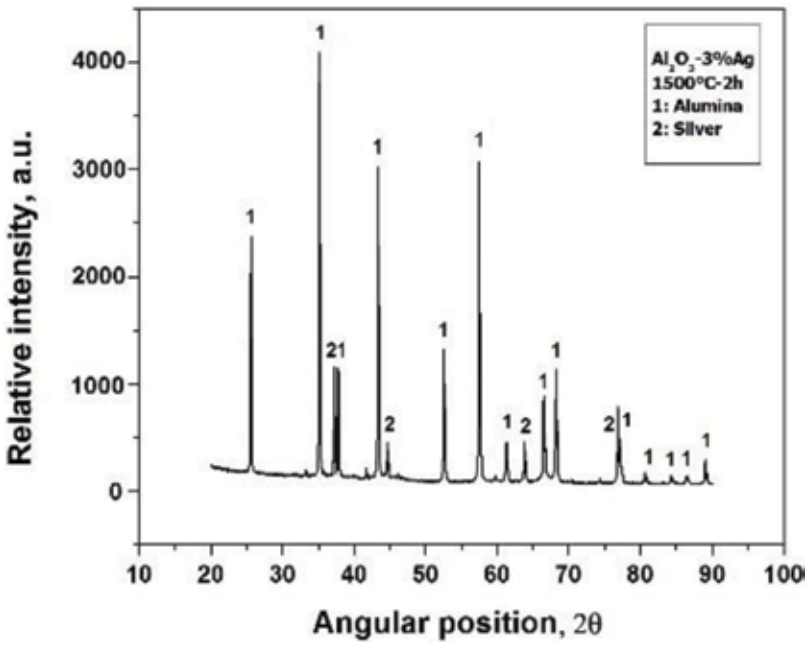

Figure 6. XRD pattern of composite with 3 wt% silver, sintered at 1500°C during 2 h.

3.4. X-ray diffraction of sintered samples

Figure 6 shows the results of the diffraction of x-rays made to the reinforced sample with 3.0 wt% silver. In this figure it can be observed the existence of two phases: The number 1 indicates the presence of alumina and the number 2 indicates the presence of silver, thus obtaining samples without the presence of any possible silver oxide, and this thanks to the argon gas used to protect the atmosphere of the furnace.

By means of the diffraction spectra of **Figure 6**, the particle size for the sample was calculated using the Debye-Scherrer equation [32]:

$$D = \frac{0.9\,\lambda_{k\alpha}}{B_{2\theta}\cos\theta} \tag{9}$$

where D is the particle size, 0.9 is the shape factors for spherical particles, λ is the radiation wavelength (1.5406 Å), $B_{2\theta}$ is the full width at half maximum, and θ is the angle at maximum intensity of the Al_2O_3 (110) and Ag (111). The value for the particle size of Al_2O_3 was 733.87 nm, while the Ag has a particle size of 24.9 nm.

3.5. Microstructure

3.5.1. Optical microscopy (OM)

In the micrographs of **Figure 7** that were obtained with the help of an optical microscope, they are observed the samples with silver inclusions in their different percentages 0.5, 1.0, 2.0, and 3.0% in

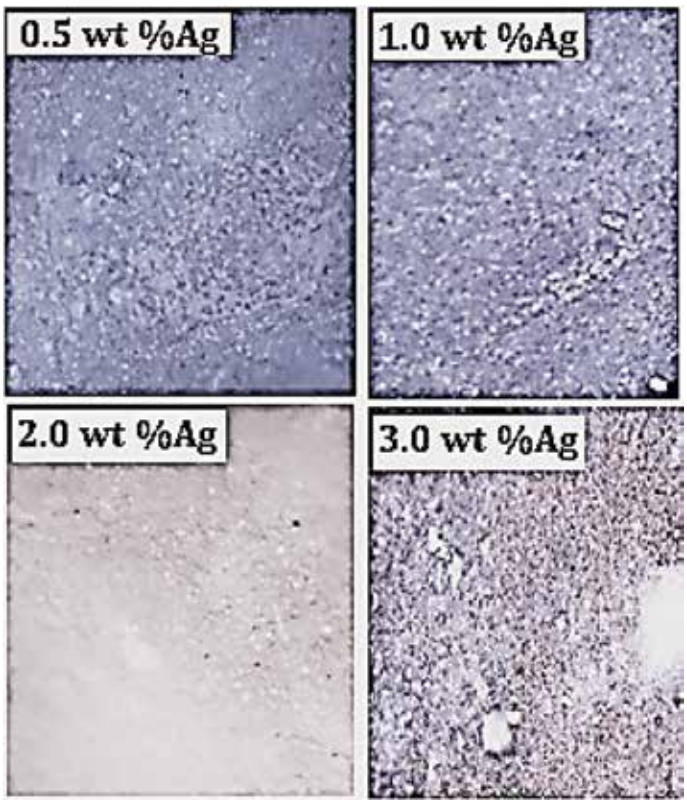

Figure 7. Micrographs of the samples sintered at 1500°C, during 2 h.

weight; these samples were sintered at 1500°C during 2 h. In the 0.5–1.0 wt% samples, they have visualized very fine microstructures with small grain size and evenly distributed. For the samples with 2.0–3.0 wt% silver a minimum grain growth is observed with respect to the previously mentioned samples, the grain size is observed small and uniform in most of the sample. This uniformity and control in grain growth are since the alumina was sintered in the presence of a liquid phase (molten silver), which allowed a filtration throughout the sample and the energy generated during the sintering was absorbed more evenly and due to this control in the grain growth.

3.5.2. Scanning electron microscopy (SEM)

Figure 8 shows the micrographs taken with the scanning electron microscope of the samples with inclusions of 0.0, 0.5, 1.0, 2.0 and 3.0% weight silver sintered at 1500°C during 2 h. In this figure it is possible to observe in all samples the presence of a very homogeneous microstructure with the presence of the matrix with a very fine second phase, the latter is well distributed in the matrix. No porosity is observed in any sample. This confirms previous density results, in where densities close to 100% of the relative density were reached. So the presence of the silver helps significantly consolidation of composites, and at the same time inhibits grain growth of the matrix. The microstructure with the characteristics obtained in these samples, combined with the grade of densification reached, suggests that composites with suitable mechanical properties will be obtained.

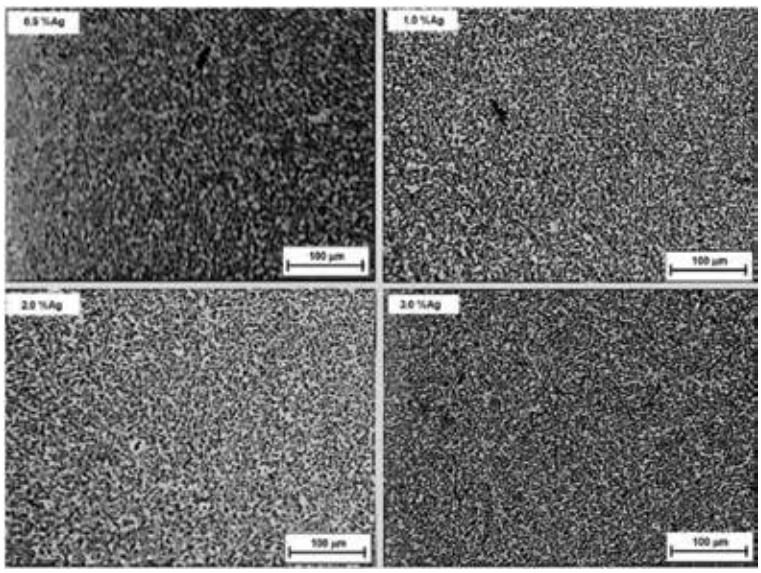

Figure 8. Micrographs of samples with different silver contents, sintered at 1500°C during 2 h.

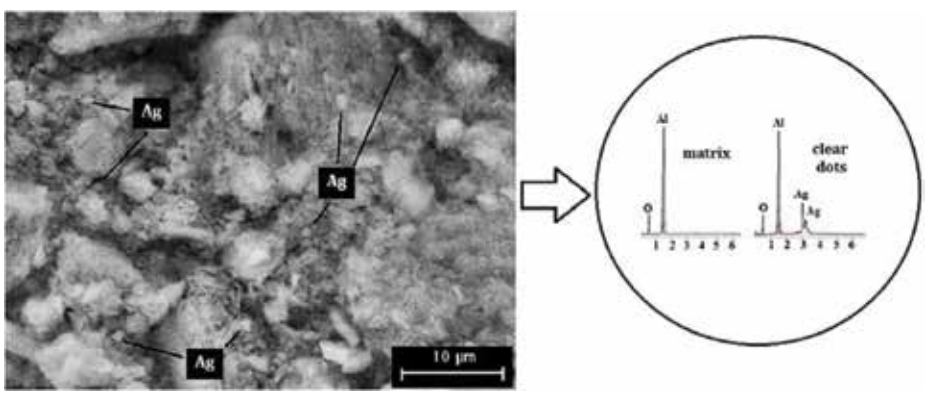

Figure 9. EDX microanalysis of sample with 2 wt% Ag sintered at 1500°C during 2 h.

3.5.3. Analysis by energy dispersive of X-rays (EDX)

Figure 9 presents the results of the analysis made by energy dispersive of X-rays performed in a punctual manner in the two phases (light and dark) that are observed in the microstructure of the samples with the different inclusions of silver. In spectra, the chemical elements present in each phase can be identified, the dark phase belongs to the matrix, and the elements found in this phase were oxygen and aluminum, indicating that this phase corresponds to alumina. The bright phase belongs to the inclusion present in the matrix, here the elements aluminum, oxygen, and silver were found, which means that the 2nd phase present in the microstructure is the silver added to the ceramic matrix as the reinforcement material.

3.6. Mechanical properties

3.6.1. Elastic modulus

Figure 10 shows the result of the measurements of the elastic modulus of the samples with different inclusions of silver. The value reported with its respective standard deviation is the average of 20 measurements made for each sample. The graph shows a decrease in the modulus of elasticity as the number of silver particles increases specifically for 1.0, 2.0, and 3.0 wt% silver with respect to the average value of the monolithic alumina. These results present a tendency similar to that shown in the density results of sintered samples; this means that samples with higher densification have less porosity. Consequently, they present more rigid bodies, the reason why a greater load is required to deform them. The elastic modulus is a measure of the stiffness of materials, in such a way that more rigid and fragile bodies have a higher value of elastic's modulus, that is why the high value of elastic's module in the sample of 0.5 wt% silver, does not have enough material to be less rigid. On the other hand, a ductile material such as metals in this case silver has lower elastic's modulus than alumina. Concerning the sample without inclusions of silver 0.0 wt%, a result is observed slightly below the monolithic alumina and slightly higher than the samples with 1.0, 2.0, and 3.0 wt% silver.

3.6.2. Flexural strength

In the same **Figure 10**, it can be observed the results obtained of flexural strength made to the samples with inclusions of 0.0, 0.5, 1.0, 2.0, and 3.0 wt% silver. The reported result is the average of 10 measurements made to each of the samples; the three-point bending test was used to obtain these results. The graph of **Figure 10** shows a similar behavior to that obtained in the density of the sintered samples as in the elastic's modulus, because the sample with 0.5 wt% silver reached the highest value, in this case, flexural strength, and above the average value of monolithic alumina. It is also observed that when silver increases in the composite there is

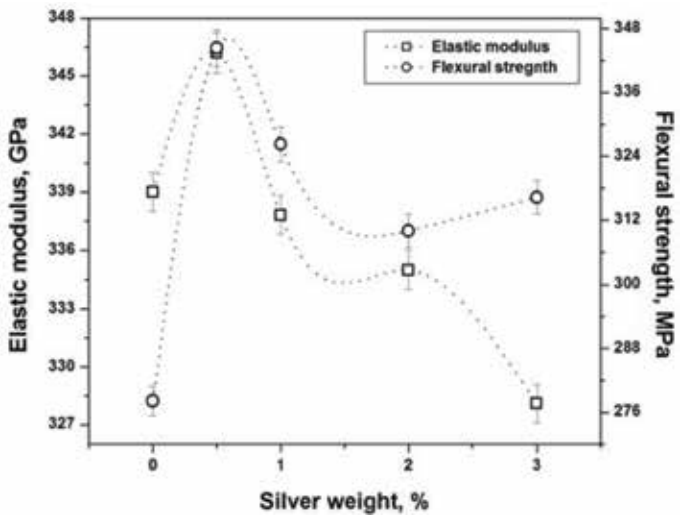

Figure 10. Elastic's modulus and flexural strength of the samples sintered at 1500°C during 2 h.

a downward trend. With respect to the sample with 0.0 wt% silver, a well below value was obtained in comparison with the samples with silver inclusions, as well as the value of monolithic alumina reported in the literature. With these results, it is determined that the inclusion of silver does not affect the flexural strength due to the good distribution of the particles during milling and to the sintering which helped to avoid the formation of defects in the sample.

3.6.3. Microhardness

Figure 11 reports the average and its standard deviation result of 20 measurements of the microhardness made in the samples sintered at a temperature of 1500°C during 2 h with different inclusions of silver. In **Figure 11** it is possible to observe that in the samples with higher silver inclusions the hardness values tend to increase slightly as the amount of silver increases. In these results, the positive effect of the silver particles is observed. With respect to the sample with 0.0 wt% silver, it was obtained a much lower value of microhardness than that obtained in the samples reinforced with silver, as well as that of the monolithic alumina reported in the literature. This result is due to the uncontrolled growth of the grains during sintering.

3.6.4. Fracture toughness

In the same **Figure 11** are shown the fracture toughness results obtained by the indentation fracture method in the sintered samples at a temperature of 1500°C during 2 h. The fracture toughness results reported are the average of 20 tests performed on each sample.

One of the most important observations in this figure is that in the samples with silver inclusions, values obtained are well above the average of the monolithic alumina. This improvement in fracture toughness is more significant in samples with 2.0–3.0 wt% silver. In the late sample, the improvement of fracture toughness reaches 450% more than the value of monolithic alumina. In agreement with the density results and the microstructure presented by the samples, these enhances in fracture toughness is due to the having a sample with very small grain sizes and

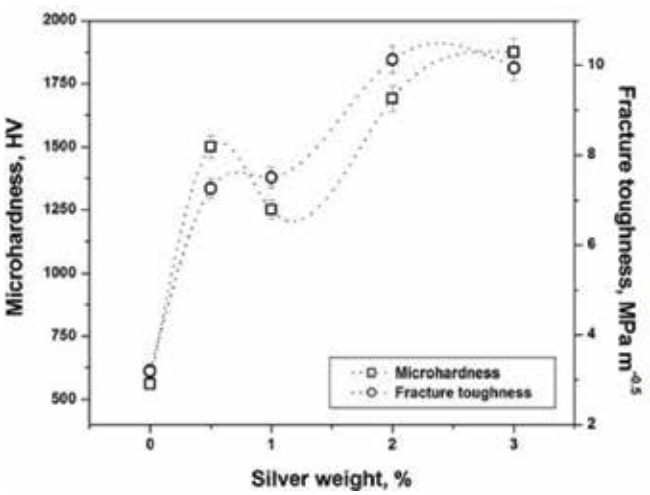

Figure 11. Microhardness and fracture toughness of the samples sintered at 1500°C for 2 h.

with a homogeneous distribution of the reinforcements in the matrix. For this reason, when in the ceramic matrix a cracking is generated, and it tries to propagate, there is a high possibility that the crack will meet or collide with some of the silver particles which act as metal bridges. This effect causes the crack to stop due to the ductility of the metal, or try to dodge it. Hence, the high values of tenacity obtained. With respect to the sample without silver inclusions, a result is observed that is much lower than that obtained in the samples reinforced with silver, as well as the average of the monolithic alumina due mainly to the disordered growth of the grains during sintering, as well as to the absence of a metallic agent or bridge that contributes to avoiding the propagation of cracks.

3.6.5. Indentation prints and fracture mechanism

Some authors have determined that the improvements in the properties of ceramics reinforced with metallic particles are due to the mechanical properties of the metal [5]. Then it can be said that ductility of silver is a factor that influences the improvement of the tenacity in the alumina. The silver particles which are distributed in a homogeneous way as shown in **Figures 7** and **8**, with their plastic deformation form bridges of fissures that absorb the energy of a crack when it is generated. These bridges cause the crack to stop or seek to avoid the metallic bridge, in such a way that it requires more energy to keep growing, slowing down and even being able to stop the advance of the same. **Figure 12** shows a crack in the sample reinforced with 0.5 wt% silver, that when it encounters a particle of ductile silver, it stops or diverts its trajectory, requiring more energy to continue advancing. In this way, it is proved that the mechanism of reinforcement of alumina by silver is due to the deflection of cracks. With this, we can comment that the overall silver objective which was at the beginning of this work was reached: Obtaining alumina-based ceramic materials (Al_2O_3) reinforced with Ag nanoparticles with high fracture toughness, through powder techniques.

A second study was performed only for samples with silver inclusions of 0.0 and 0.5 wt% under the same grinding settings. However, there were considered other sintering conditions such as time of 2 h varying the sintering temperature at 1400, 1500, and 1600°C. Besides, a sintering temperature of 1500°C varying the sintering time to 1, 2, and 3 h, heating speed of 5°Cmin^{-1}, as

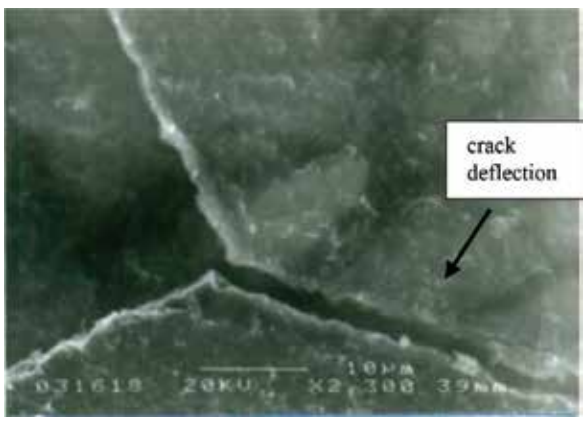

Figure 12. Crack deflection by a silver particle present in the sample with 2.0 wt% Ag.

well as the argon gas flow of 10 cm^3min^{-1}. It should be noted that these samples were selected because they presented the highest fracture toughness values. For the characterization of the samples, only the relative density tests of sintered samples, contraction of the samples, analysis of the microstructure by MO, microhardness, and fracture toughness were considered.

3.7. Density

Figure 13 shows the results of the relative density of the samples of both pure alumina and alumina reinforced with 0.5 wt% silver, which was sintered at a temperature of 1500°C during 1, 2 and 3 h. In the monolithic alumina samples, it is observed in the densification an increase with linear tendency with increments of sintering time. While, in the samples of 0.5 wt% silver it is observed a minimum increase in the densification when increasing the time from 1 to 2 h, but a considerable increase is reached at 3 h sintering time. Hence, an effect can be determined by improving results in silver when the samples are densified during 3 h at 1500°C. In the same **Figure 13** are observed the results of the relative density of the samples with inclusions of 0.0–0.5 wt% silver sintered during 2 h at 1400, 1500, and 1600°C. In pure alumina samples, an increase in densification is observed when the sintering temperature is increased, obtaining a greater densification when samples were sintered at 1600°C. Whereas, in the samples reinforced with 0.5 wt% silver, a considerable increase in the densification is observed in the sintered samples at 1600°C compared with the sintered samples at 1400–1500°C. Therefore, it can be determined that the temperature of 1600°C is the ideal for obtaining a greater densification in the composites.

3.8. Contraction

Figure 14 shows the results of the contraction of the samples with 0.0 and 0.5 wt% silver, which were sintered at 1500°C during 1, 2, and 3 h. It can be seen that the contraction in the

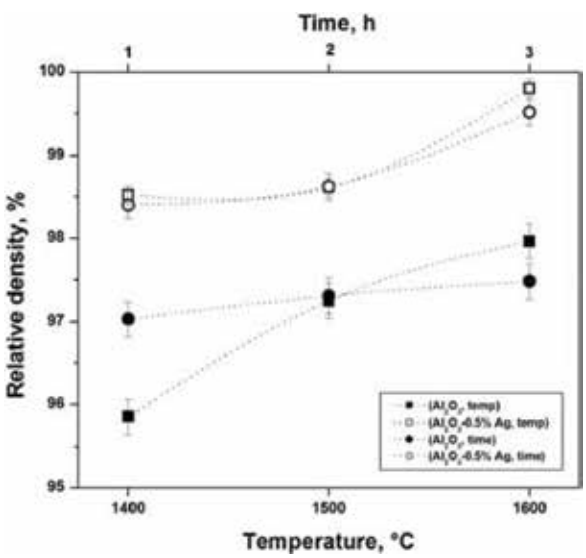

Figure 13. Relative density of the samples as a function of time and sintering temperature.

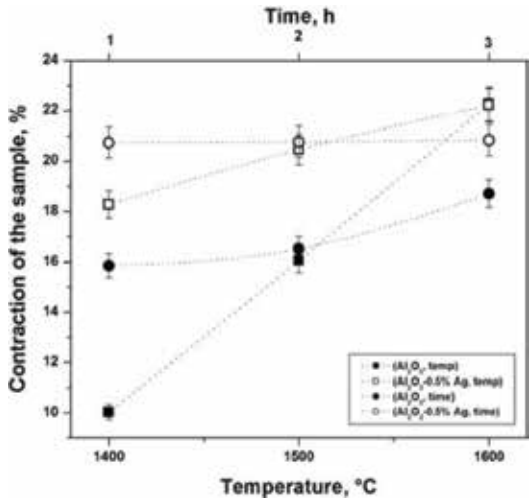

Figure 14. Contraction of the samples as a function of time and sintering temperature.

samples with silver does not present a significant variation. While, in samples of alumina without silver a different trend can be observed, and with an increasing tendency as the sintering time increases. However, it is significant the greater contraction in the samples with silver compared to the samples without silver. This behavior is due to the good thermal conductivity of the silver that favors the sintering phenomena. In the same **Figure 14** the results of the contraction of the samples are observed, when they were sintered during 2 h at 1400, 1500, and 1600°C. It can be observed that in the samples without silver, the contraction is more significant every time the sintering temperature tends to increase. In samples with silver inclusions, it is observed an increase in less drastic shrinkage. From the interpretation of the results it can be determined that the silver inclusions allow obtaining samples with a greater contraction during the sintering stage, and therefore, obtain more densified samples.

3.9. Microstructure by optical microscopy (OM)

Figure 15a shows the micrographs obtained from the optical microscope of the samples reinforced with 0.5 wt% silver sintered during 2 h at 1400, 1500, and 1600°C. They display very fine microstructures with small grain size and uniformly distributed. Minimal grain growth is observed although the temperature has varied. This uniformity and control in grain growth are because that most of the silver particles were sintered in the presence of a liquid phase, which allowed a filtration throughout the sample and the energy generated during the sintering was absorbed more uniformly, and due to this, there is the control on grain growth. In the **Figure 15b** the micrographs of the samples with 0.0 wt% silver sintered for 2 h are observed varying the temperature 1400, 1500, and 1600°C. In the images, it can see a microstructure very different from the one obtained in the samples with 0.5 wt% silver, in these figures it is difficult to determine and appreciate the distribution of the sizes of the grains. However, the importance of the addition of metallic particles in the matrix can be mentioned and emphasized to control the growth, distribution of the grains and consequently improvement in the mechanical properties.

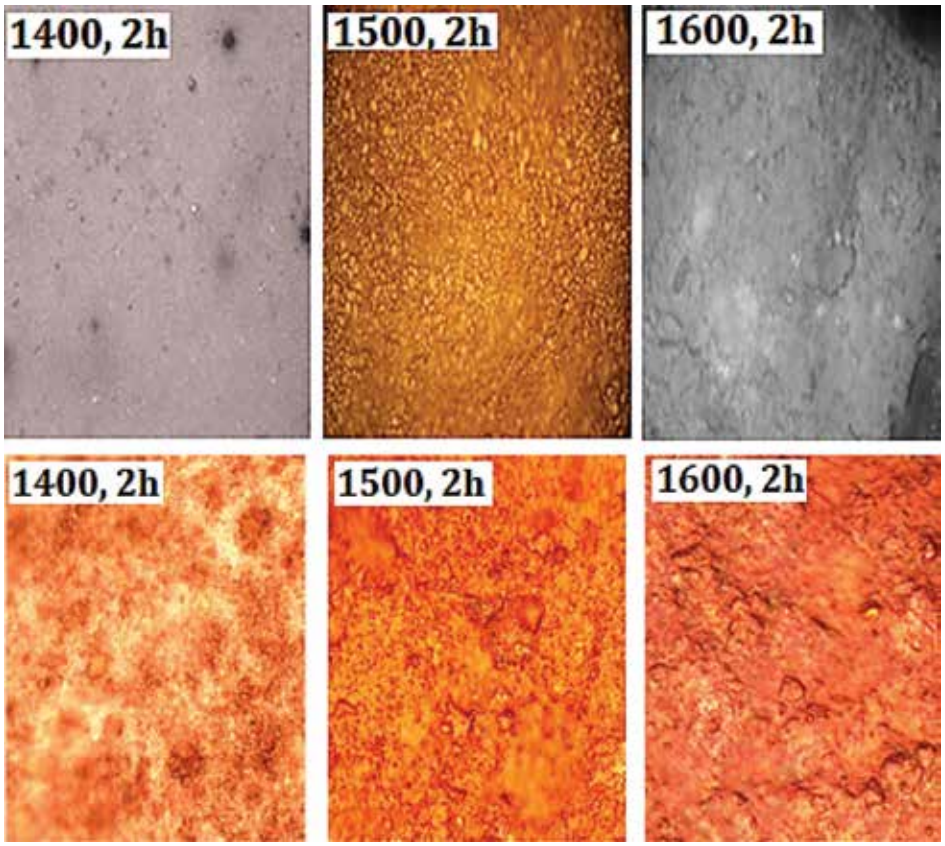

Figure 15. (a) Samples with 0.5 wt% Ag varying the sintering temperature. (b) Samples with 0.0 wt% Ag varying the sintering temperature.

3.10. Microhardness

Figure 16 shows the microhardness results of the samples with inclusions of 0.0 and 0.5 wt% silver sintered at a temperature of 1500°C with time variation of 1, 2, and 3 h. For the sample with 0.5 wt% Ag it can be seen in the graph that the sample sintered for 1 h obtained values below the monolithic alumina.

For the sample sintered during 2 and 3 h, it can be observed that with the inclusion of silver the value is very similar to that of the monolithic alumina. In this **Figure 16** also are observed the values of the samples of alumina with 0.0 wt% silver sintered with somewhat similar conditions. For the samples sintered for 1 and 2 h, a very similar value was obtained while, for a sample sintered for 3 h, the result was improved. However, it is well below the average of monolithic alumina. In the same **Figure 16** are observed the results of the samples with inclusions of 0.0 and 0.5 wt% silver sintered at different temperatures 1400, 1500, and 1600°C. For the sample with 0.5 wt% Ag it is observed in this figure that the sample sintered at 1400°C obtained a value well below the average of the monolithic alumina for the samples sintered at 1500 and 1600°C the results increased significantly. In the case of the

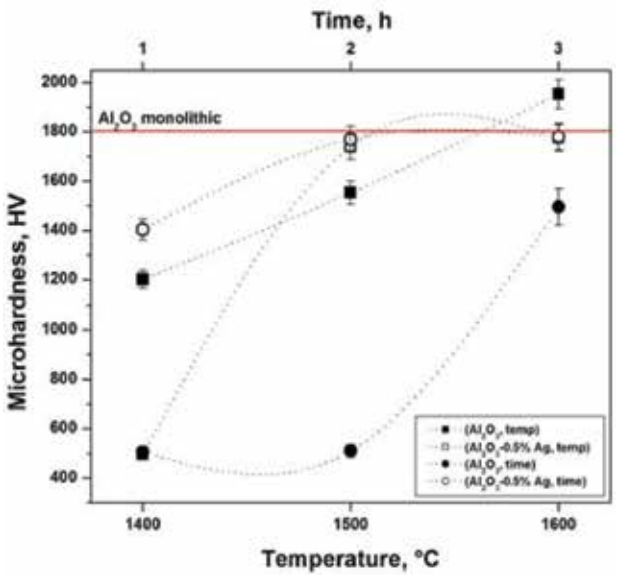

Figure 16. Microhardness of the samples as a function of time and sintering temperature.

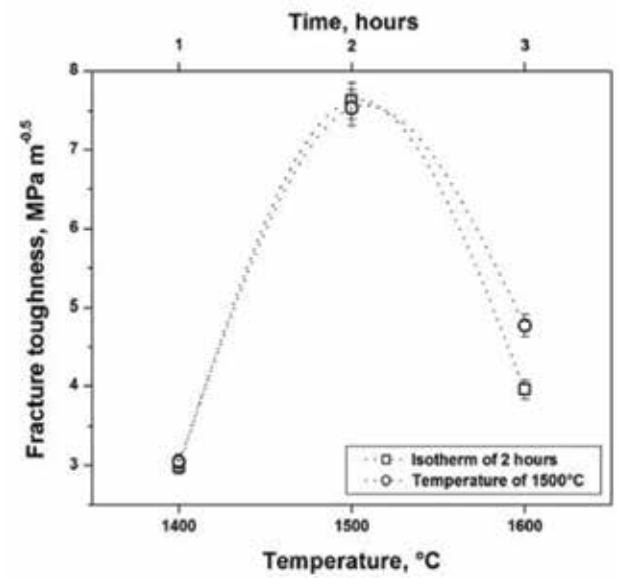

Figure 17. Fracture toughness results as a function of both sintering time and sintering temperature.

sintered sample at 1600°C it obtained a value very similar to that of the monolithic alumina, and in the case of the sample sintered 1500°C the value reached in the previous results was reduced a little. Regarding the samples without silver inclusions, a considerable increase is observed as the sintering temperature is increased. The hardness values of the samples sintered at 1400 and 1500°C were well below the average value of the monolithic alumina, but the sample sintered at 1600°C obtained a value slightly above the average value.

3.11. Fracture toughness

The results of the fracture toughness of the sintered samples varying the temperature and time are presented in **Figure 17**, in which a very similar behavior of the results can be observed. The samples with 0.5 wt% silver at 2 h at a temperature of 1500°C have values above the average of the monolithic alumina, showing a tendency opposite to previous results since as it increases the temperature and the time the value tends to decrease. In both cases, results are presented with an increasing tendency, and the importance of the sintering temperature in obtaining less fragile ceramics is demonstrated.

4. Conclusions

- Through the processing methodology proposed, dense alumina-based composites toughened with Ag nanoparticles were obtained.
- Grinding conditions used in this work were effective, as they managed to obtain particles with nanometric sizes.
- The fracture toughness of the Al_2O_3 was improved up to 450% with the reinforcement of the same by means of Ag nanoparticles homogeneously distributed in the ceramic matrix.
- Probably toughening mechanism of Al_2O_3 is owing to metallic bridges formed by the presence of ductile silver particles in the ceramic matrix.

Acknowledgements

The laboratories facility and the economic support given by UPV are appreciated. In addition, ERR is grateful to CONACyT for the funding given to carry out this work through Project 270294.

Conflict of interest

Compliance with ethics guidelines the authors declare that they have no conflict of interest or financial conflicts to disclose.

Author details

Enrique Rocha-Rangel*, Azucena Pérez-de la Fuente, José A. Rodríguez-García, Eddie N. Armendáriz-Mireles and Carlos A. Calles-Arriaga

*Address all correspondence to: erochar@upv.edu.mx

Victoria Polytechnic University, Ciudad Victoria, Tamaulipas, México

References

[1] Serope K, Steven R. Manufactura, Ingeniería y Tecnología. México: Pearson Educación; 2002. 1p

[2] Bawa HS. Procesos de Manufactura. México: Editorial Mc Graw Hill; 2007. 1p

[3] Leyva AG. Síntesis y caracterizacion de nano-estructuras de óxidos de metales de transición, Tesis doctoral. República Argentina: Universidad Nacional de General San Martín; 2007

[4] Singh DK. Fundamentals of Manufacturing Engineering. Florida: CRS Press; 2008. 1p

[5] Bansal NP, Boccaccini AR. Ceramics and Composites Processing Methods. New Jesey: John Wiley and Sons; 2012. 1p

[6] Wei WCJ, Wang SC, Cheng FH. Characterization of Al_2O_3 composites with fine Mo particulates, I. Microstructural development. Nanostructured Materials. 1998;**10**:965-981

[7] Freitag D. Progress and opportunities in the development and application of advanced ceramics. In: 14th International Conference on Ultra-High Temperature Materials; 2000

[8] Szafran M, Konopka K, Bobryk E, Kurzydłowski KJ. Ceramic matrix composites with gradient concentration of metal particles. Journal of the European Ceramic Society. 2007;**27**:651-654

[9] Ighodaro OL, Okoli OI. Fracture toughness enhancement for alumina systems: A review. International Journal of Applied Ceramic Technology. 2008;**5**:313-323

[10] Singh JP, Bansal NP, Goto T, Lamon J, Choi SR, Mahmound MM, Link G, editors. Processing and Properties of Advanced Ceramics and Composites IV. Ceramic Transactions. Vol. 234. New Jersey: John Wiley and Sons; 2012. 1p

[11] Narayan R, Bose S, Bandyopadhyay A, editors. Biomaterials Science: Processing Properties and Applications II. Ceramic Transactions. Vol. 237. New Jersey: John Wiley and Sons; 2012. 1p

[12] Singh JP, Bansal NP, Ko SW, Castro RH, Pickrell G, Manjooran J, Nair KM, Singh G, editors. Processing and Properties of Advanced Ceramics and Composites V. Ceramic Transactions. Vol. 240. New Jersey: John Wiley and Sons; 2013. 1p

[13] Singh JP, Bansal NP, Bhalia AS, Mahmound MM, Manjooran N, Singh G, Lamon J, Choi SR, Pickrell G, Lu K, Brennecka G, Goto T, editors. Processing and Properties of Advanced Ceramics and Composites VI. Ceramic Transactions. Vol. 249. New Jersey: John Wiley and Sons; 2014. 1p

[14] Basu B, Balani K. Advanced Structural Ceramics. New Jersey: John Wiley and Sons; 2011. 1p

[15] Chung YW. Introduction to Materials Science and Engineering. Florida: CRC Press; 2006. 1p

[16] Daguano JKMF, Santos C, Souza RC, Balestra RM, Strecker K, Elias CN. Properties of ZrO_2-Al_2O_3 composite as a function of isothermal holding time. International Journal of Refractory Metals and Hard Materials. 2007;**25**:374-379

[17] Liu C, Zhang J, Sun J, Zhang X. Addition of Al-Ti-B master alloys to improve the performances of alumina matrix ceramic materials. Ceramics International. 2007;**33**:1319-1324

[18] Ko SJ, Min KH, Kim YD. A study on the fabrication of Al_2O_3/cu nanocomposite and its mechanical propertie. Journal of Ceramic Processing Research. 2002;**3**:192-194

[19] Rocha-Rangel E, Moreno-Guerrero MS, Velásquez-Naranjo A, Refugio-García E. Synthesis of Al_2O_3-Ni_3Al cermets by room-temperature ball milling of Al, Ni and Al_2O_3 mixtures. Materials Science Forum, "Advanced Structural Materials II". 2006;**509**:205-210

[20] Yao X, Huanga Z, Chena L, Jianga D, Tana S, Michel DI, Wang G, Mazerolles L, Pastol J. Alumina–nickel composites densified by spark plasma sintering. Materials Letters. 2005; **59**:2314-2318

[21] Sekino T, Nakajima T, Niihara K. Mechanical and magnetic properties of nickel dispersed alumina-based nanocomposite. Materials Letters. 1996;**29**:165-169

[22] Guichard JL, Tillement O, Mocellin A. Alumina-chromium cermets by hot-pressing of nanocomposite powders. Journal of the European Ceramic Society. 1998;**8**:1143-1152

[23] Ji Y, Yeomans JA. Processing and mechanical properties of Al_2O_3-5 vol.% Cr nanocomposites. Journal of the European Ceramic Society. 2002;**22**:1927-1936

[24] Prielipp H, Knechtel M, Claussen N, Streiffer S, Miillejans H, Ruhle M, Rodel J. Strength and fracture toughness of aluminum/alumina composites with interpenetrating networks. Materials Science and Engineering. 1995;**A197**:19-30

[25] Konopka K, Szafran M. Fabrication of Al_2O_3-Al composites by infiltration method and their characteristics. The Journal of Materials Processing Technology. 2006;**175**:266-270

[26] Shackelford JF, Alexander W. Materials Science and Engineering Handbook. Florida: CRS Press; 2001. 1p

[27] Vlack LM. Physical Ceramics for Engineering. Massachusetts: Addison Wesley Publishing Company; 1964. 1p

[28] Auerkari P. Mechanical and Physical Properties of Engineering Alumina Ceramics. Espoo: Technical Research Centre of Finland; 1996. pp. 3-36

[29] Rahaman MN. Ceramic Processing and Sintering. New York: Marcel Dekker Inc.; 2003. 1p

[30] Baudin C, Moya JS. Sinterización en estado sólido. Boletín de la Sociedad Española de Cerámica y Vidrio. 2007;**22**:133-142

[31] Evans AG, Charles EA. Fracture toughness determinations by indentation. The Journal of the American Ceramic Society. 1976;**59**:371-372

[32] Holzwarth U, Gibson N. The Scherrer equation versus the 'Debye-Scherrer equation. Nature Nanotechnology. 2011;**6**:534-539

Chapter 12

Modification of Electrical Properties of Silver Nanoparticle

Markus Diantoro, Thathit Suprayogi,
Ulwiyatus Sa'adah, Nandang Mufti, Abdulloh Fuad,
Arif Hidayat and Hadi Nur

Additional information is available at the end of the chapter

http://dx.doi.org/10.5772/intechopen.75682

Abstract

This chapter focuses on the synthesis of silver nanoparticles (AgNPs), AgNP composites, and its role in the structure and electrical properties modification. The research and its various applications of nanoparticles are interesting among others. Silver nanoparticles (AgNPs) are now becoming to take an essential role in the diverse field of application. Establishing the simple and inexpensive of AgNPs is greatly required, since it will also influence it used. Many different methods to obtain AgNPs have been reported. The inducing AgNPs on a various number of other materials has been investigating. We report a brief review of simple AgNP fabrication method at different MSA, PEG, and ultrasonic irradiations regarding its structure and conductivity. We also report the influence of AgNPs on the electrical conductivity of conducting polymers, i.e., PANI, flavonoids of *Jatropha multifida* L. (JML) and *Pterocarpus indicus* W. (PIW). It is found that in general, the increase of AgNP concentration gives rise to increase of its electrical conductivity. The conductivity of the AgNPs doped of polymers does not directly reflect by its crystallinity or crystal size. Some exciting aspect of crystal structure and its conductivity are discussed.

Keywords: silver nanoparticles, mercaptosuccinic acid, *Pterocarpus indicus* W., *Jatropha multifida* L., polyaniline, conductivity

1. Introduction

The silver nanoparticle research continues to grow, drawing the attention of researchers. It is known that silver has very high electrical conductivity [1, 2]. Silver has been widely used as a

conductor wire in circuits that require low dissipation, and high conductivity [3, 4]. Silver paste has also been widely used as a paste conductor [5–7]. The use of silver paste has been extensively utilized mainly in the bulk conductivity characterization of bulk semiconductor materials or four-point probe method films. In the field of superconductors, silver has a dominant role as a sheath [8–12]. Silver has also been used in various industries and health fields. Silver is known to have antibacterial properties [13–16], as a catalyst [17–20], and it shows stable to the environment [21] and has been utilized as a significant component of water treatment.

Various methods of synthesis have been developed to produce silver in the order of nanometers. Synthesis of silver nanoparticle is commonly known to control the shape and size. Among these methods are ball milling method [22], precipitation [23], polyol method [24], and several other methods to produce silver nanoparticle [3, 25–28].

Nanostructure engineering has been performed to produce the expected properties. Nanofluid Ag-ZnO has been successfully synthesized to determine the behavior of thermal conductivity at various fractions [29]. Silver nanoparticles dotted on the external walls of multi-walled carbon nanotubes (MWCNTs) were prepared by an aldehyde reduction process in supercritical carbon dioxide ($SCCO_2$) fluid. The friction reduced about 30% [30]. Modification of nanostructure Ag into nanowire also improves physical performance such as electrical conductivity and power transfer [31]. Further engineering in the form of silver nanocage has reported. The nanocages exhibited unique and attractive characteristics for metal catalytic systems, thus offering the scope for new development as heterogeneous catalysts [32]. The aqueous persistence performance of Ag nanocolloids particles has been studied in depth in various environments [33]. Silver nanoparticles capped with Oleylamine (AgNPs/OLA) and its application in conductive ink for the electroanalytical application has been reported in [34].

Some of those examples show that silver nanoscale research and application are of concern to researchers. Due to the broad scope of the study of silver nanoparticles, we have limited this article to the synthesis of nanoparticles by simple methods, particle nanoparticle effects on structures, and electrical properties in polymers such as polyaniline, and some organic polymers such as *Pterocarpus indicus* Willd (PIW) and *Jatropha multifida* Linn (JML).

2. Materials and method

2.1. Synthesis of silver nanoparticle with various MSA

Basic of experimental method used in the current work was a chemical reduction from the silver nitrate salt of $AgNO_3$. The silver nitrate ($AgNO_3$) dissolves into a positive ion (Ag^+) and negative ion (NO_3^-). From the process, we could obtain solid silver grain due to the ions experience a reduction process by accepting electrons from a donor. After forming the silver nucleus, a crystal growth continues at the relatively short time. By this way, a crystal of nanosize obtained. This nanoparticle fabrication and other similar synthesize are known as bottom-up technic.

The raw materials used are silver nitrate $AgNO_3$, sodium borohydride $NaBH_4$ as a reductor, and mercaptosuccinic acid (MSA) as a stabilizer. Conventional solvents which normally used

are aquades and methanol. A series of MSA, namely 0.03, 0.06, 0.12, and 0.15 M, was dissolved in methanol of 400 mL, then stirred rigorously using magnetic stirrer in an ice bath. Into the solution, add the second solution, i.e., silver nitrate about 340 mg to 6.792 mL aquades. While the mixture of both solutions is being stirred, sodium borohydride of 756.6 mg in 100 mL aquades drops small wisely. After adding the second solvent, the clear MSA solution changed into an amber one. Further, by adding the third solution, the mixture solution transforms into black-brownish. The final solution has then employed a stirring for 30 min at 500 rpm and maintained at a temperature of 5–10°C. The obtained particles then rinse using methanol on Whatman filter. The latter step was conducted several times to ensure the only silver particle remains. The collected material was then exposed to 80°C yielding silver nanopowder.

2.2. Synthesis of PANI-AgNP film

Two series of silver-doped PANI-AgNPs/Ni and ultrasonic irradiation time films have been prepared using spin-coating method. Each series was provided five samples. The basic configuration of PANI-EB and PANI-ES were synthesized following the procedure of previous report [7]. The solutions of PANI-Ag had been prepared with synthesizing PANI-EB from aniline using the chemical oxidizing method. About 1.82 mL aniline (0.1 M) was dissolved into 50 mL HCl (0.2 M) liquid for about 1 h. Along with this, a solution of 5.71 g $(NH_4)_2S_2O_8$ (0.1 M) in 50 mL aquadest was also prepared at the same time. After 1 h, those two solutions were mixed and stirred a while, then exposed at room temperature for about 24 h for polymerization. The precipitated material was filtered using Whatman filter paper, then washed using deionized water and aquades until clear liquids are observed. The obtained precipitated materials are then mixed and homogenized using magnetic stirrer in NH_4OH (0.5 M) for 4 h, and then let them rest for about 24 h and washed using aquades to obtain a blue PANI-EB. The powder of PANI-EB can be obtained after annealing the material for 5 h at 80°C. PANI-EB then mixed with camphor sulfonic acid (CSA) and then mixed with $AgNO_3$ solution in chloroform and employing ultrasonic irradiation for various irradiation times. The obtained solution was filtered to obtain a PANI-Ag solution for deposition on nickel substrate using spin-coating method. A different series of various $AgNO_3$ PANI doped of 0.1, 0.2, 0.3, 0.4, and 0.5 M was also prepared in the same manner. The films have been deposited onto 1 × 1 cm^2 Ni substrate using spin-coating method at 1000 rpm for 1 min. The obtained films were then annealed at 100°C for 1 min.

2.3. Synthesis of flavonoids' JML-AgNP and PIW-AgNP films

Samples were prepared in several stages. The initial step was the extraction of *Pterocarpus indicus* Willd (PIW) by preparing 800 g of *Pterocarpus indicus* Willd leaf powder mixed with 3 L methanol p.a. in a large bottle, and then the mixture was shaken and awaited for 1 week. After that, it was filtered using a Buckner funnel under pressure with Whatman's filter paper 01. The obtained slurry materials were evaporated using a rotary evaporator to get a rough methanol extract. About 25 g of methanol extract was introduced into the separating funnel, in which the mixture was manually shaken with 50 mL of n-hexane solvent for 30 min. Once separated, the two steps of this process are repeated using 50 mL n-hexane. The hexane phase in the treatment is separated, and the sum of the second procedure is combined and evaporated to obtain a crude hexane extract. The general process is applied to obtain extracts of

chloroform (100 mL), ethyl acetate (100 mL), and butanol (100 mL), respectively. In this way, flavonoid type quercetin can be achieved.

A similar way was performed to obtain a flavonoid extract of *Jatropha multifida* L. (JML) with a little more straightforward. The first step is extracting flavonoid using the wet method. Five grams of the liquid latex of JML, which was taken from wounded stem, was first heated on a glass plate to remove water. The water-free condensed latex was then solved into 10 mL of 80% methanol and homogenized for 30 min using magnetic stirrer while heating. In addition, it was also implemented to ultrasonic irradiation for 60 min, and let them to precipitate for 24 h. The mixture was then separated using a Whatman filter paper and dried up to evaporate the solvent to obtain flavonoid extract powder. The flavonoids of PIW can be prepared in a similar way using the extracted latex of the wounded stem.

To fabricate a thin film of AgNP-doped flavonoid, the mixture should be transformed into the liquid phase. In this case, two solutions were first prepared separately. The first solution was obtained from 0.1 M $AgNO_3$, which was dissolved in acetone. A relatively fine-ground camphor sulfonic acid (CSA) was mixed with the flavonoid extract PIW. The two solutions were then incorporated into a glass beaker and then stirred. The process proceeds until a homogenous mixture was obtained. To promote smaller size of silver ion as well as flavonoid incorporation in the homogenous mixture, we employed ultrasonic irradiation for 60 min. To achieve different AgNP-doped flavonoids/Ni films, the process has been repeated with a different $AgNO_3$ concentration of solutions. By following the preparation of JML-AgNP/Ni films, the flavonoid's PIW-AgNP/Ni films were also prepared in five different molar ratios of silver nitrate. The fabrication of those two nanosilver-doped films has been prepared using spin-coating method on nickel substrates of 1 × 1 cm^2 with 1500 rpm speed for 60 s. Each of the resulted film then follows annealing for repeating the process for concentrations of 0.2, 0.3, 0.4, and 0.5 M. The films finally annealed at 50°C for 5 min. Then those two series films were characterized using X-RD using Cu-Kα, FTIR, and four-probe electrical conductivity measurements.

3. Results and discussion

3.1. The influence of MSA on AgNP structures

Except for $NaBH_4$ for reducing agent, to synthesize nanometallic state, MSA is used as a reducing agent that also acts as a stabilizer agent of Ag^+. The synthetic silver nanoparticles are more stable and not easily oxidized. In addition, MSA also affects the size of the resulting silver nanocrystals. **Figure 1** shows the TEM results of spherical silver on the nanometer scale. The particle size of the TEM shows a yield of about 30 nm.

The TEM diffraction pattern of the sample was reported in our previous work [35]. It is shown that the sample is polycrystalline, which is indicated by the clear spots together with accompanying weak rings also reported by Majeed [36].

The X-ray diffraction pattern of obtained samples is displayed in **Figure 2**. Several identified peaks of intensity I-2θ are 38.10, 44.29, 64.43, 77.37, and 81.52°, associated to Bragg's planes

http://dx.doi.org/10.5772/intechopen.75682

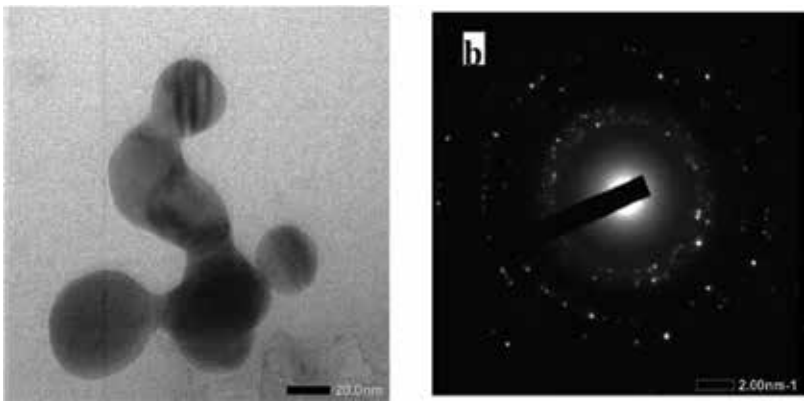

Figure 1. TEM image of silver nanoparticles and associated diffraction [35].

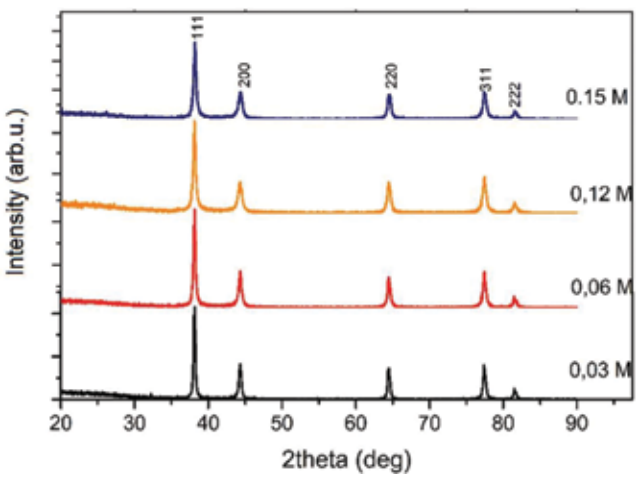

Figure 2. XRD pattern of AgNPs at various MSA concentration.

of (111), (200), (220), (311), and (222), respectively. There is apparently no other peaks, except the silver crystal peaks. All of the peaks shown in **Figure 2** can readily fit in a model of FCC structures, as also reported previously [37] for various PEG [23], for the different surfactant, and [38] for urea, PVP, and dextrose. Further refined to the lattice parameter gives rise to a = 4.0876 Å. This result insignificantly differs from the model of a = 4.0872 Å [36]. Detailed investigation to the same peak positions 2θ of all the diffraction patterns, even the peaks are not distinguished, it looks that the higher the fraction of MSA the broader the peaks. Broadening of diffraction peaks β, measured as FWHM, may show smaller crystal size (L) according to Scherrer's equation (Eq. (1)). Since crystal dimension L is just inversely proportional to its broadness of the peaks β.

$$L = \frac{K\lambda}{\beta \cos\theta} \tag{1}$$

It is also possible that one found different values of L from the same pattern. The origin of the discrepancies is mostly due to the K_α splitting, selecting the peaks, and fitting method of calculating β.

Based on the result of XRD as shown in **Figure 2**, the crystal size was calculated using Eq. (1). It shows that the size is in the range of 20–30 nm, which decreases with increasing concentration of MSA, as shown in **Figure 3**.

Of the two characterization analyses between TEM and XRD showed the size of the crystal is somewhat different results. The problems of crystal size calculation obtained from TEM, XRD, and/or probably SEM characterization is discussed in our work [35]. The crystal size obtained from XRD pattern calculation may be smaller than that derived from TEM. The discrepancy mostly not only originated from the di erent method of both types of equipment, but also due to the choosing peaks, implementing units of β and θ, as well as using the range of K in Eq. (1). The smaller diffraction angle we choose, the bigger the size we obtain. When the higher shape constant of K in the Scherrer formula, we may also get the bigger size. Sometime β is taken using degrees instead of radians. The crystal size calculation using a more compact software such as GSAS [39] or Fullprof [40]. In such software, they use the more rigid equation in Rietveld analyses with different compared to Eq. (1). The crystal size under GSAS or Fullprof is more comprehensive since they involve the strains, various profile functions as well as the anisotropy, or the crystal. The result of the crystal size obtained from the method is also slightly different from the manual using Scherrer equation. An example of manual crystal size calculation using a more complex equation is reported by Khan et al. [36]. It looks that there is a discrepancy of AgNP crystal size obtained by Scherrer and obtained from HRTEM. The average crystal size obtained by HRTEM shows a much bigger than that of using Scherrer equation. This result is similar to the work of Diantoro et al. [35].

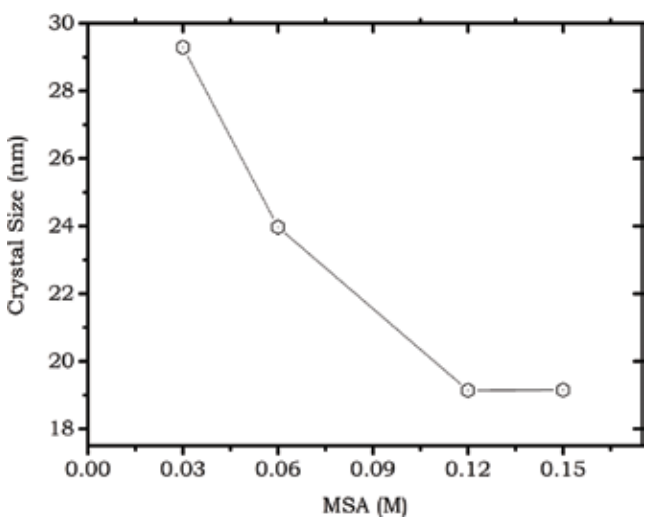

Figure 3. The influence of MSA concentration on AgNP crystal size.

Another capping agent such as polyethylene glycol (PEG) will be discussed briefly. We have obtained several AgNP samples which were prepared under the influence of PEG. The results are displayed in **Figure 4**.

Figure 4 shows the result of AgNP crystal size with increasing of PEG concentration. The silver crystal size lies around 12–24 nm. Based on **Figure 4**, it is seen that excluding of 0.075 M, increasing PEG concentration slightly decrease the crystals size. It could be indicated that PEG plays a role in controlling the crystal size. The researcher also uses PEG as a template for synthesizing nanoparticles [37]. One purpose of the use of PEG as a template or as a capping agent is not only to control the size, but also the distribution [41]. The effect of PVP repeating unit to the obtained crystal size of AgNPs was reported [18]. Many other solvents have been used for the synthesis of various size and shape of AgNPs, such as PEG [42], citrate [33, 43], and MSA [35].

3.2. The influence of AgNPs on crystal size and conductivity of PANI

It is shown that the size and shape of particles are affected by its physical properties [31, 32]. At the nanometer scale, the properties or characteristics of silver will change its electrical properties. Therefore, in the exploration of organic materials for electronics, silver nanoparticles can be incorporated with various conductive polymers such as PANI, JML, and PIW. The three polymers are conductive polymers with electric charge mechanisms of single- and double-conjugated bond hopping in the polymer. Although they said to be a conductive polymer, the pristine one is in the semiconductor range. So researcher expects that by controlling the metallic or oxidic nanoparticles may influence the electrical properties. In this report, we focus on the modification of the electrical conductivity. The following shows the effect of AgNP concentration on the electrical conductivity of PANI film as indicated in **Figure 5**.

The PANI composite with AgNPs indicates an increase in electrical conductivity by increasing the concentration of AgNPs used, as shown in **Figure 5**. The increased electrical conductivity of PANI is due to the increased electrical mobility derived from AgNPs in the compound. This

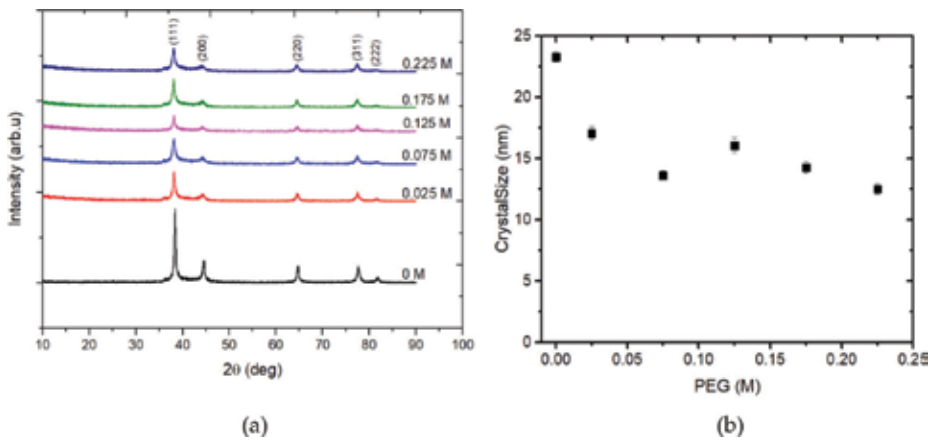

Figure 4. The influence of PEG template (a) XRD and (b) crystal size.

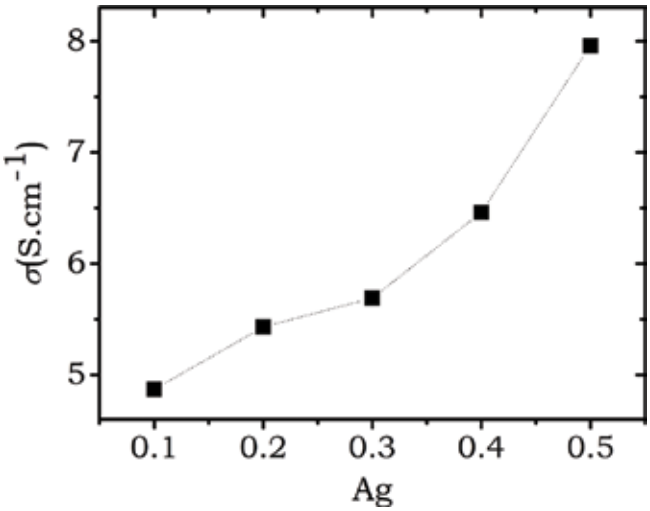

Figure 5. The influence of AgNPs on electrical conductivity of PANI.

result is comparable with the works reported by Wankhede et al. [44]. Unfortunately, they reported only for one composition of PANI-AgNPs, at various temperatures. Our results are far higher than that of PANI/PS/AgNPs nanocomposite samples [45].

The stability of electrical conductivity to PANI and AgNP composites were measured under the influence of ultrasonic irradiation. The various irradiation time was employed to the mixture of PANI-EB-AgNP solution prior to the deposition process. The electrical conductivity measurements of dwelling time are depicted in **Figure 6**.

It shows that the electrical conductivity of PANI-AgNP film has the stability of electrical conductivity values in the range 0.5–0.7 $S.cm^{-1}$. Out of that range, the duration of irradiation time

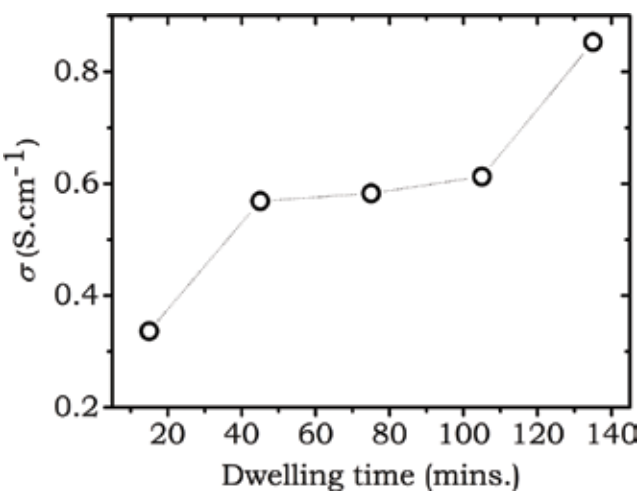

Figure 6. The stability electrical conductivity of PANI-AgNPs under ultrasonic irradiation.

is followed. It suggests that the intrinsic structure may also be changed by the ultrasonic irradiation dwelling time.

3.3. The influence of AgNPs on crystal size and conductivity of JML and PIW

Flavonoids of JML [46, 47] or PIW [48] are potential for the conductive organic polymer. Initially, the conductive polymer is in/below the semiconductor range after oxidizing or reducing process [49]. Also, the general polymer has an amorphous phase. When flavonoids extracted from JML are composited with AgNPs, we may expect that its electrical conductivity will increase. Here, we report the results of electrical conductivity measurement of AgNPs doped of JML and PIW flavonoids extracts. The crystallinity of the sample may be affected by the electrical conductivity, **Figure 7**. It indicates that the crystallinity of the sample increases with the increase of AgNP concentration in the composite.

As indicated in **Figure 7**, it is seen that the feature of AgNPs vs. crystallinity is not a linear, simple relationship. It shows a significant change in the range of 0.2–0.4 M of AgNPs, while substantial difference above or below that range. To look further, we plot the relation between AgNP concentration to its electrical conductivity, as shown in **Figure 8**.

The electrical conductivity of extracted JML flavonoid-AgNPs exponentially increases as the AgNPs increase. By comparing **Figure 8** with **Figure 7**, it is found that the rise in electrical conductivity does not merely support its crystallinity. It means that there is no direct or simple relationship.

AgNP-doped PIW flavonoid may show a similar feature. Roughly speaking, the role of AgNPs induced in the flavonoids' PIW-AgNP film also increases its crystallinity, as shown in **Figure 9**.

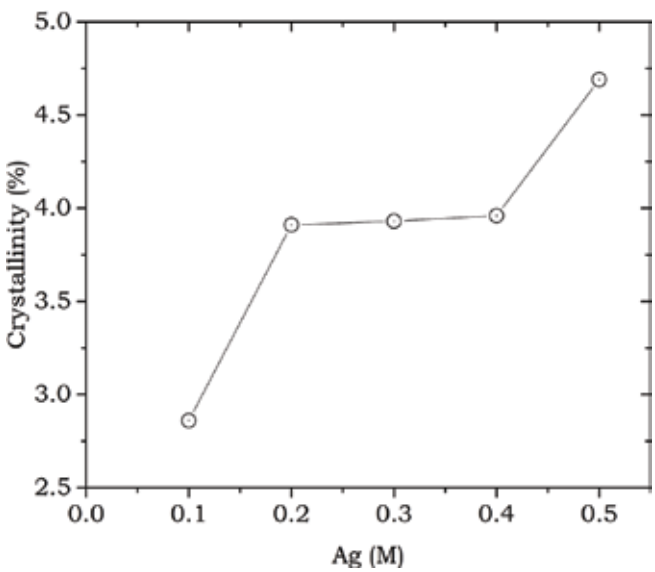

Figure 7. The influence of AgNPs on crystallinity JML.

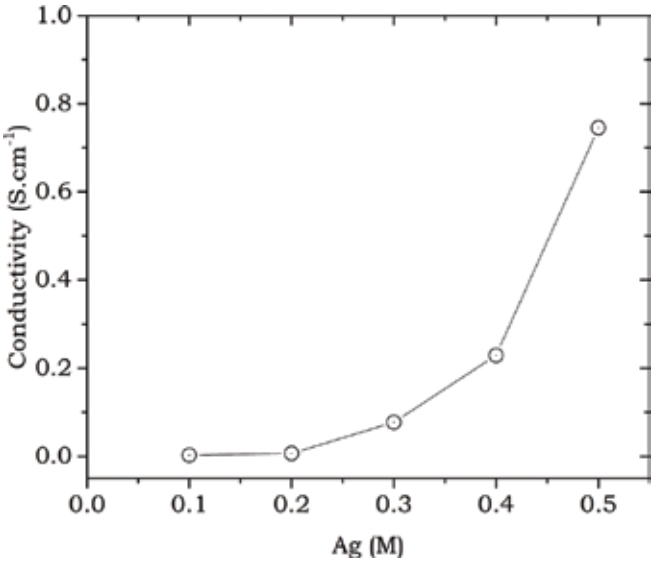

Figure 8. The influence of AgNPs on film JML-AgNPs.

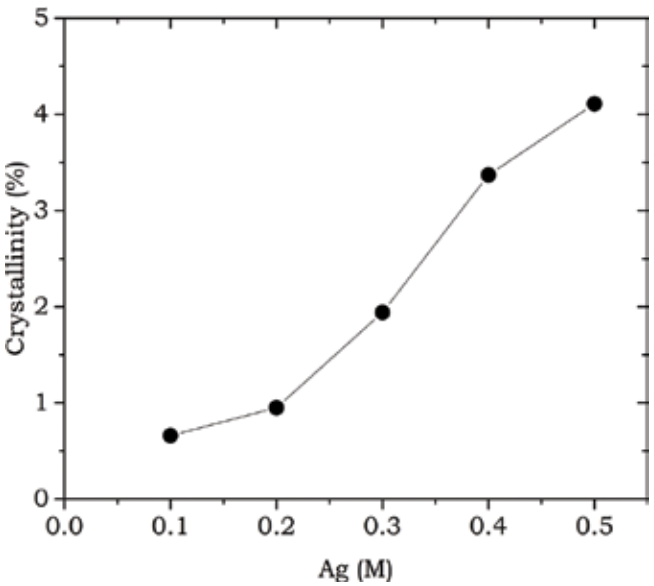

Figure 9. The influence of AgNPs on crystallinity flavonoid's PIW-AgNP film.

It is similar to its increase of crystallinity, the electrical conductivity of flavonoid's PIW-AgNP film is also increased as the increase of AgNPs, as illustrated in **Figure 10**.

By comparing **Figures 9** and **10**, it can be inferred that its crystallinity may characterize the increase of electrical conductivity of flavonoid's PIW-AgNP film. In another words, the role of AgNPs on the electrical conductivity of flavonoid's PIW-AgNP film is reflected by its

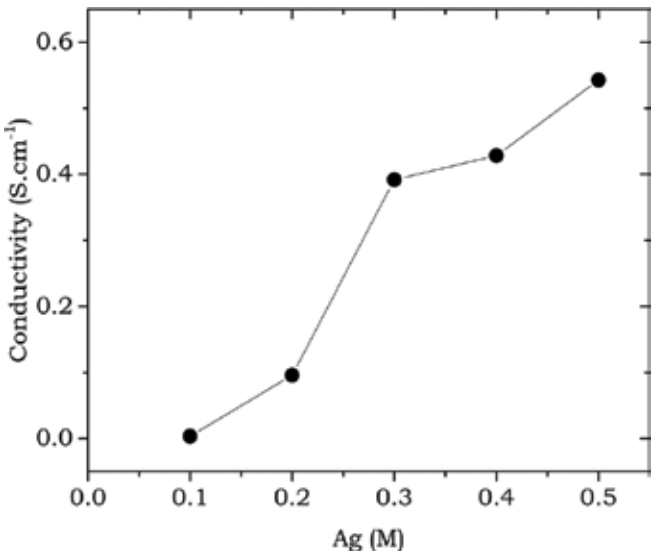

Figure 10. The influence of AgNPs on electrical conductivity of flavonoid's PIW-AgNP film.

crystallinity. As the electrical conductivity of flavonoids of PIW and JML shows different features, the type of flavonoid of both plants is possibly different. It is also possible that technically the distribution, or where the AgNPs interreact with, is also different.

Study of the role of AgNPs and polymers has been widely reported for many routes of synthesis and their applications [45, 50, 51]. Recently, AgNPs containing nanostructure nanocomposite have also been investigated for supercapacitors [52], polymer solar cells [53], or thin film silver-TiO_2 thermoelectric [54].

4. Conclusion

Some factors are influencing the size and the conductivity of AgNPs, i.e., the MSA concentration, ultrasonic irradiation time, as well as the concentration of PEG. In general, the increase of AgNP concentration gives rise to an increase in its electrical conductivity. Although the conductivity of polymers depends on AgNP concentration, the conductivity of the AgNPs doped of polymers does not directly reflect its crystallinity or crystal size.

AgNPs have excellent potential applications in medical, environment, electronics, dielectrics, and optical solar cell application. It is urgently required to perform an extensive research of various AgNPs and its derivatives for multiple applications.

Acknowledgements

The author thanks the Ministry of Research and Higher Education for the Research grants of University Excellent Research Grants, HUPT 2016, 2017, Primary Individual National Innovative Research Grant INSINAS 2017.

Author details

Markus Diantoro[1,2]*, Thathit Suprayogi[1], Ulwiyatus Sa'adah[1], Nandang Mufti[1,2], Abdulloh Fuad[1,2], Arif Hidayat[1] and Hadi Nur[3]

*Address all correspondence to: markus.diantoro.fmipa@um.ac.id

1 Department of Physics, Faculty of Mathematics and Natural Sciences, Universitas Negeri Malang, Malang, Indonesia

2 Center Laboratory for Minerals and Advanced Materials, Faculty of Mathematics and Natural Sciences, Universitas Negeri Malang, Malang, Indonesia

3 Centre for Sustainable Nanomaterials, Ibnu Sina Institute for Scientific and Industrial Research, Universiti Teknologi Malaysia, Skudai, Johor, Malaysia

References

[1] Lide DR. CRC Handbook of Chemistry and Physics: A Ready-Reference Book of Chemical and Physical Data. New York: CRC Press; 2008

[2] Ma R, Kang B, Cho S, Choi M, Baik S. Extraordinarily high conductivity of stretchable fibers of polyurethane and silver nanoflowers. ACS Nano. 2015;**9**:10876-10886. DOI: 10.1021/acsnano.5b03864

[3] Basak D, Karan S, Mallik B. Significant modifications in the electrical properties of poly(methyl methacrylate) thin films upon dispersion of silver nanoparticles. Solid State Communications. 2007;**141**:483-487. DOI: 10.1016/J.SSC.2006.12.014

[4] Gupta K, Jana PC, Meikap AK. Optical and electrical transport properties of polyaniline–silver nanocomposite. Synthetic Metals. 2010;**160**:1566-1573. DOI: 10.1016/J.SYNTHMET.2010.05.026

[5] Suganuma K, Sakamoto S, Kagami N, Wakuda D. Low-temperature low-pressure die attach with hybrid silver particle paste. Microelectronics. 2012;**52**:375-380

[6] Faddoul R, Reverdy-Bruas N, Blayo A, Haas T, Zeilmann C. Optimisation of silver paste for flexography printing on LTCC substrate. Microelectronics and Reliability. 2012;**52**:1483-1491. DOI: 10.1016/J.MICROREL.2012.03.004

[7] Bhattarai B, Chakraborty I, Conn BE, Atnagulov A, Pradeep T, Bigioni TP. High-yield paste-based synthesis of thiolate-protected silver nanoparticles. Journal of Physical Chemistry C. 2017;**121**:10964-10970. DOI: 10.1021/acs.jpcc.6b12427

[8] Diantoro M, Tjia MO, Kováč P, Hušek I. Pinning mechanisms in Bi-2223 tapes with reinforced Ag sheath and oxide additives in the core. Physica C: Superconductivity and Its Applications. 2001;**357-360**:1182-1185

[9] Kovác P, Husek I, Pachla W, Diantoro M, Bonfait G, Maria J, Fröhlich K, Kopera L, Diduszko R, Presz A. Material for resistive barriers in Bi-2223/Ag tapes. Superconductor Science and Technology. 2001;**14**:966-972. DOI: 10.1088/0953-2048/14/11/313

[10] Diantoro M, Loeksmanto W, Tjia M, Gömöry F, Šouc J, Hušek I, Kováč P. AC loss and critical current density in Bi-2223 tapes with oxide additives and reinforced Ag sheaths. Physica C: Superconductivity. 2002;**378-381**:1143-1147. DOI: 10.1016/S0921-4534(02)01728-8

[11] Oemry F, Diantoro M, Sutjahja IM, Tjia MO, Kopera L, Bonfait GMJ, Kovac P. Variation of vortex structure characteristics of Bi-2223/Ag superconducting tapes with respect to applied magnetic field direction. Physica C: Superconductivity. 2005;**426-431**:396-401. DOI: 10.1016/J.PHYSC.2005.02.051

[12] Jabur AR. B2223 high-temperature superconductor wires in silver sheath, filament diameter effect on critical temperature and current density. Energy Procedia. 2012;**18**:254-264. DOI: 10.1016/j.egypro.2012.05.037

[13] Rosarin FS, Mirunalini S. Nobel metallic nanoparticles with novel biomedical properties. Journal of Bioanalysis & Biomedicine. 2011;**3**:085-091. DOI: 10.4172/1948-593X.1000049

[14] Szczepanowicz K, Joanna S, Robert PS, Piotr W. Preparation of silver nanoparticles via chemical reduction and their antimicrobial activity. Physicochemical Problems of Mineral Processing. 2010;**45**:85-98

[15] Zhou W, Jia Z, Xiong P, Yan J, Li Y, Li M, Cheng Y, Zheng Y. Bioinspired, and biomimetic AgNPs/gentamicin-embedded silk fibroin coatings for robust antibacterial and osteogenetic applications. ACS Applied Materials & Interfaces. 2017;**9**:25830-25846. DOI: 10.1021/acsami.7b06757

[16] Dai X, Guo Q, Zhao Y, Zhang P, Zhang T, Zhang X, Li C. Functional silver nanoparticle as a benign antimicrobial agent that eradicates antibiotic-resistant bacteria and promotes wound healing. ACS Applied Materials & Interfaces. 2016;**8**:25798-25807. DOI: 10.1021/acsami.6b09267

[17] Leelavathi A, Bhaskara Rao T, Pradeep T. Supported quantum clusters of silver as enhanced catalysts for reduction. Nanoscale Research Letters. 2011;**6**:123. DOI: 10.1186/1556-276X-6-123

[18] Liang H, Wang W, Huang Y, Zhang S, Wei H. Controlled Synthesis of Uniform Silver Nanospheres. The Journal of Physical Chemistry C. 2010;**114**:7427-7431. DOI: 10.1021/jp9105713

[19] Zhang H, Duan T, Zhu W, Yao WT. Natural chrysotile-based nanowires decorated with monodispersed Ag nanoparticles as a highly active and reusable hydrogenation catalyst. Journal of Physical Chemistry C. 2015;**119**:21465-21472. DOI: 10.1021/acs.jpcc.5b05450

[20] Sarkar AK, Saha A, Midya L, Banerjee C, Mandre N, Panda AB, Pal S. Cross-linked biopolymer stabilized exfoliated titanate nanosheet-supported AgNPs: A green, sustainable

ternary nanocomposite hydrogel for catalytic and antimicrobial activity. ACS Sustainable Chemistry & Engineering. 2017;**5**:1881-1891. DOI: 10.1021/acssuschemeng.6b02594

[21] Elzey S, Grassian VH. Agglomeration, isolation and dissolution of commercially manufactured silver nanoparticles in aqueous environments. Journal of Nanoparticle Research. 2010;**12**:1945-1958. DOI: 10.1007/s11051-009-9783-y

[22] Purushotham E, Krishna NG. Preparation, and characterization of silver nanoparticles. Indian Journal of Physics. 2014;**88**:157-163. DOI: 10.1007/s12648-013-0396-z

[23] Reyes PY, Espinoza JA, Treviño ME, Saade H, López RG. Synthesis of silver nanoparticles by precipitation in bicontinuous microemulsions. Journal of Nanomaterials. 2010;**2010**:1-7. DOI: 10.1155/2010/948941

[24] Koski KJ, Kamp NM, Smith RK, Kunz M, Knight JK, Alivisatos AP. Structural distortions in 5-10 nm silver nanoparticles under high pressure. Physical Review B. 2008;**78**:165410. DOI: 10.1103/PhysRevB.78.165410

[25] Bahadory M. Synthesis of Noble Metal Nanoparticles. Pennsylvania: Drexel University; 2008 (Doctoral Thesis)

[26] Song KC, Lee SM, Park TS, Lee BS. Preparation of colloidal silver nanoparticles by chemical reduction method. Korean Journal of Chemical Engineering. 2009;**26**:153-155. DOI: 10.1007/s11814-009-0024-y

[27] Zielińska A, Skwarek E, Zaleska A, Gazda M, Hupka J. Preparation of silver nanoparticles with controlled particle size. Procedia Chemistry. 2009;**1**:1560-1566. DOI: 10.1016/J.PROCHE.2009.11.004

[28] Malekzadeh M, Halali M. Method of producing high purity silver nanoparticles. 2012. No. US 20120060649A1

[29] Esfahani NN, Toghraie D, Afrand M. A new correlation for predicting the thermal conductivity of ZnO–Ag (50%–50%)/water hybrid nanofluid: An experimental study. Powder Technology. 2018;**323**:367-373. DOI: 10.1016/J.POWTEC.2017.10.025

[30] Meng Y, Su F, Chen Y. Effective lubricant additive of nano-Ag/MWCNTs nanocomposite produced by supercritical CO_2 synthesis. Tribology International. 2018;**118**:180-188. DOI: 10.1016/J.TRIBOINT.2017.09.037

[31] Tan M, Wang X, Hao Y, Deng Y. Novel Ag nanowire array with high electrical conductivity and fast heat transfer behavior as the electrode for film devices. Journal of Alloys and Compounds. 2017;**701**:49-54. DOI: 10.1016/J.JALLCOM.2017.01.086

[32] Anandhakumar S, Sasidharan M, Tsao C-W, Raichur AM. Tailor-made hollow silver nanoparticle cages assembled with silver nanoparticles: An efficient catalyst for epoxidation. ACS Applied Materials & Interfaces. 2014;**6**:3275-3281. DOI: 10.1021/am500229v

[33] Liu J, Hurt RH. Ion release kinetics and particle persistence in aqueous nano-silver colloids. Environmental Science & Technology. 2010;**44**:2169-2175. DOI: 10.1021/es9035557

[34] Ghosale A, Shankar R, Ganesan V, Shrivas K. Direct-writing of paper based conductive track using silver nano-ink for electroanalytical application. Electrochimica Acta. 2016;**209**:511-520. DOI: 10.1016/J.ELECTACTA.2016.05.109

[35] Diantoro M, Fitrianingsih R, Mufti N, Fuad A. Synthesis of silver nanoparticles by chemical reduction at various fraction of MSA and their structure characterization. In: AIP Conference Proceedings; 2014. pp. 257-261. DOI: 10.1063/1.4868795

[36] Majeed Khan MA, Kumar S, Ahamed M, Alrokayan SA, AlSalhi M. Structural and thermal studies of silver nanoparticles and electrical transport study of their thin films. Nanoscale Research Letters. 2011;**6**:434. DOI: 10.1186/1556-276X-6-434

[37] Shameli K, Bin Ahmad M, Jazayeri SD, Sedaghat S, Shabanzadeh P, Jahangirian H, Mahdavi M, Abdollahi Y. Synthesis and characterization of polyethylene glycol mediated silver nanoparticles by the green method. International Journal of Molecular Sciences. 2012;**13**:6639-6650. DOI: 10.3390/ijms13066639

[38] Lu YC, Sen Chou K. A simple and effective route for the synthesis of nano-silver colloidal dispersions. Journal of the Chinese Institute of Chemical Engineers. 2008;**39**:673-678. DOI: 10.1016/j.jcice.2008.06.005

[39] Larson A, Von Dreele R. General Structure Analysis System. New Mexico: Los Alamos; 1994

[40] Rodriguez-Carvajal J, Roisnel T. FullProf-Manual. Grenoble, France: Institute Laue-Langevin; 1992

[41] Mishra S, Shimpi NG, Sen T. The effect of PEG encapsulated silver nanoparticles on the thermal and electrical property of sonochemically synthesized polyaniline/silver nanocomposite. Journal of Polymer Research. 2013;**20**:49. DOI: 10.1007/s10965-012-0049-5

[42] Abou El-Nour KMM, Eftaiha A, Al-Warthan A, Ammar RAA. Synthesis and applications of silver nanoparticles. Arabian Journal of Chemistry. 2010;**3**:135-140. DOI: 10.1016/j.arabjc.2010.04.008

[43] Mansouri SS, Ghader S. Experimental study on effect of different parameters on size and shape of triangular silver nanoparticles prepared by a simple and rapid method in aqueous solution. Arabian Journal of Chemistry. 2009;**2**:47-53. DOI: 10.1016/j.arabjc.2009.07.004

[44] Wankhede YB, Kondawar SB, Thakare SR, More PS. Synthesis and characterization of silver nanoparticles embedded in polyaniline nanocomposite. Advanced Materials Letters. 2013;**4**:89-93. DOI: 10.5185/amlett.2013.icnano.108

[45] Youssef AM, Mohamed SA, Abdel-Aziz MS, Abdel-Aziz ME, Turky G, Kamel S. Biological studies and electrical conductivity of paper sheet based on PANI/PS/Ag-NPs nanocomposite. Carbohydrate Polymers. 2016;**147**:333-343. DOI: 10.1016/J.CARBPOL.2016.03.085

[46] Falodun A, Imieje V, Erharuyi O, Joy A, Langer P, Jacob M, Khan S, Abaldry M, Hamann M. Isolation of antileishmanial, antimalarial and antimicrobial metabolites from *Jatropha multifida*. Asian Pacific Journal of Tropical Biomedicine. 2014;**4**:374-378. DOI: 10.12980/APJTB.4.2014C1312

[47] Rampadarath S, Puchooa D, Ranghoo-Sanmukhiya VM. Antimicrobial, phytochemical and larvicidal properties of *Jatropha multifida* Linn. Asian Pacific Journal of Tropical Medicine. 2014;**7**:S380-S383. DOI: 10.1016/S1995-7645(14)60262-5

[48] Khan MR, Omoloso AD. Antibacterial activity of *Pterocarpus indicus*. Fitoterapia. 2003;**74**: 603-605. DOI: 10.1016/S0367-326X(03)00149-7

[49] Lange U, Roznyatovskaya NV, Mirsky VM. Conducting polymers in chemical sensors and arrays. Analytica Chimica Acta. 2008;**614**:1-26. DOI: 10.1016/j.aca.2008.02.068

[50] Ragachev AA, Yarmolenko MA, Xiaohong J, Shen R, Luchnikov PA, Rogachev AV. Molecular structure, optical, electrical and sensing properties of PANI-based coatings with silver nanoparticles deposited from the active gas phase. Applied Surface Science. 2015;**351**:811-818. DOI: 10.1016/j.apsusc.2015.06.008

[51] Abbasi NM, Yu H, Wang L, Zain-Ul-Abdin, Amer WA, Akram M, Khalid H, Chen Y, Saleem M, Sun R, Shan J. Preparation of silver nanowires and their application in conducting polymer nanocomposites. Materials Chemistry and Physics. 2015;**166**:1-15. DOI: 10.1016/j.matchemphys.2015.08.056

[52] Luo S, Yu S, Sun R, Wong CP. Nano Ag-deposited $BaTiO_3$ hybrid particles as fillers for polymeric dielectric composites: Toward high dielectric constant and suppressed loss. ACS Applied Materials & Interfaces. 2014;**6**:176-182. DOI: 10.1021/am404556c

[53] Tran QT, Thu HT, Tran VS, Cuong TV, Hong C. Solution-processed rGO/AgNPs/rGO sandwich structure as a hole extraction layer for polymer solar cells. Materials (Basel). Journal of Materials. 2015;**2015**:1-5. DOI: 10.1155/2015/652645

[54] Jung SY, Ha TJ, Park CS, Seo WS, Lim YS, Shin S, Cho HH, Park HH. Improvement in the conductivity ratio of ordered mesoporous Ag-TiO_2 thin films for thermoelectric materials. Thin Solid Films. 2013;**529**:94-97. DOI: 10.1016/j.tsf.2012.03.087

Chapter 13

Antimicrobial Effect of Silk and Catgut Suture Threads Coated with Biogenic Silver Nanoparticles

Saraí C. Guadarrama-Reyes,
Rogelio J. Scougall-Vilchis, Raúl A. Morales-Luckie,
Víctor Sánchez-Mendieta and
Rafael López-Castañares

Additional information is available at the end of the chapter

http://dx.doi.org/10.5772/intechopen.75074

Abstract

Two bionanocomposites based on suture threads, silk-silver nanoparticles (Ag NPs) and catgut-Ag NPs, were prepared through a green chemistry methodology using *Chenopodium ambrosioides* (Mexican Epazote) as reducing agent. UV-Vis spectrophotometry (UV-Vis), Scanning Electron Microscopy (SEM) and Transmission Electron Microscopy (TEM), were used for their characterization. UV-Vis confirmed the synthesis of silver nanoparticles. Micrographs showed polydisperse, mostly spherical, Ag NPs attached to both suture threads. The bionanocomposites antimicrobial properties were evaluated through cultures and inhibition zones tests. The *Chenopodium ambrosioides*-assisted synthesized bionanocomposites have proved antibacterial effect against *S. aureus* and *E. coli* in both sutures (silk and catgut) and could be potentially useful for oral or periodontal surgery. There was no significant difference statistically in inhibition of *Staphylococcus aureus versus Escherichia coli*.

Keywords: nanotechnology, silver nanoparticles, antimicrobial suture, oral microorganisms, *Staphylococcus aureus*, *Escherichia coli*

1. Introduction

In recent years, nanotechnology has become an issue of major importance because of its wide range of applications in different disciplines [1]. Rapid advances in medicine and biomaterials have become evident [2]. Nanomedicine supports the diagnosis, monitoring, prevention,

and treatment of diseases [3, 4]. Silver nanoparticles have been widely used because they have proven to have significant antimicrobial activity [5–7]; therefore, they play a significant role in the field of biological systems, and in modern medicine [8–11].

It is known that properties of silver nanoparticles depend on their size and shape, consequently, their controllable synthesis represents a key challenge to achieve their more desirable characteristics [12]. The conventional approaches of nanoparticle synthesis use highly toxic chemicals which result in toxic side effects upon administration [13]. Hence, an alternative method is required to overcome these toxic effects. According to green chemistry, there is an increasing necessity for industries to become more sustainable through developing more environmentally friendly products [14, 15]. Green chemistry offers biological approaches incorporating the use of plant extracts for the synthesis of silver nanoparticles [16, 17]. *Chenopodium ambrosiodes* (Mexican Epazote) is native to the Mesoamerican region, belongs to the *Chenopodiaceae* family. It has been utilized in traditional cuisine and folk medicine [18]. Epazote is an aromatic herb, which has diverse pharmacological applications in the treatment of influenza, cold and respiratory ailments, [19], it has been widely used as vomiting and antihelmintic [20], also in gastrointestinal problems and worms [21], and healing of skin ulceration, and anti-inflammatory and antitumor properties. Therefore, accordingly to our previous experience, the biomolecules present in epazote may act as reducing reagents of silver ions and as passivation agents of the biogenic silver nanoparticles.

Sutures used in oral surgery should avoid or limit bacterial colonization to those parts exposed to oral fluids [22]; nevertheless, they offer adhesion in their surface to bacteria, increasing the susceptibility to postoperative infections [23, 24]. Suture knots are believed to be the principal site of bacterial colonization [25]. Silk and catgut have been used for the closure of wounds with acceptable results. However, a suture-based on natural fibers may increase the risk for the development of infectious processes [26]. Once suture material becomes colonized, local mechanisms to avoid infection become ineffective [27], in addition, some of the oral pathogens are antibiotic resistant [28–30]. Thus, efforts have been made to add some antiseptics to sutures, such as triclosan and chlorhexidine [31], a few cases have confirmed allergies to chemical substances, though [32–35]. Current trends suggest that the direct drug delivery from the suture to the surgical site can improve recovery and patient comfort [36].

The aim of this study was to evaluate the antimicrobial effect of two natural suture threads coated with biogenic silver nanoparticles, against two main representative microorganisms of the Gram-positive and Gram-negative groups: *Staphylococcus aureus* and *Escherichia coli*.

2. Experimental

2.1. Synthesis of Ag NPs

Chenopodium ambrosioides was acquired from the surrounding fields and washed and dried in the shade at room temperature for 24 hours. The leaves were mashed to a powder and mixed

to obtain a homogeneous sample. *Chenopodium ambrosioides* powder was used as a green-reducing agent. About 1gram of each powder was immersed in 100 mL of distilled water, and underwent a boiling process. Afterwards, the solution was filtered through a filter paper. A 10 mM silver nitrate solution ($AgNO_3$, Sigma-Aldrich) was prepared. Both solutions were mixed in a 1: 2.5 ratio to generate Ag NPs.

2.2. Formation of bionanocomposites

To follow the nanoparticles formation, UV-Vis analysis was carried out every hour, during 6 hours after preparing each solution (*vide supra*). After this time, suture threads (Silk and Catgut USP 3-0, Atramat®) were totally immersed in the solution for 1 hour, then taken out and dried at room temperature.

2.3. Characterization of Ag NPs and bionanocomposites

2.3.1. UV-Vis spectroscopy

UV-Vis spectra measurements were recorded on a Cary 5000 UV-Vis-NIR Scanning Spectrophotometer using a quartz cell and the wavelength range from 300 to 600 nm.

2.3.2. SEM analysis

Assessment of Ag NPs impregnated suture threads was performed through scanning electron microscopy (SEM) and energy dispersive spectroscopy (EDS) analysis in a JSM-6510-LV microscope (JEOL) at 20 kV of acceleration and using secondary electrons.

The samples were coated with a thin film of gold (c.a. 20 nm) using a Denton Vacuum DESK IV sputtering equipment.

2.3.3. TEM analysis

Shape and size of silver nanoparticles solution were evaluated with a Transmission Electron Microscope (TEM, JEOL JEM-2100-Tokyo, Japan). The specimens were sonicated during 4 hours to detach the nanoparticles from the fibers. Samples for the TEM observation were prepared by placing a drop of the sample solution on a copper grid (300 mesh) coated with carbon film and let it dry at room temperature. A 200 keV-accelerating voltage, was used in Brightfield mode, and high resolution.

2.4. Determination of the antibacterial activity of bionanocomposites

Streptococcus aureus and *Escherichia coli* strains were obtained from the Biochemistry Laboratory of the School of Dentistry, at the National Autonomous University of Mexico (UNAM). They were characterized by appropriate biochemical tests, and cultured by the agar well diffusion method, first, on a selective agar; mannitol salt agar or eosin methylene blue agar (EMB) respectively, and then in Muller Hinton agar plates.

To determine the antibacterial effect, paper discs were put on Petri plates. In each plate, three different paper disks were placed, embedded in the silver nanoparticles solution, a paper disc containing the infusion of *Chenopodium ambrosioides* was used as a control, and a bared paper disc was used as a blank control. Each plate was prepared in triplicate.

Silk and Catgut suture threads were cut into pieces of approximately 10 mm in length and put on the petri plates, prepared as previously described. Each plate contained: one suture thread (silk and catgut separately) embedded in the silver nanoparticles solution, and a silk suture thread (silk and catgut separately), without Ag NPs, used as blank control. Each plate was prepared in triplicate. The plates were incubated at 37°C in a Felisa® incubator for 24–48 hours. After incubation lapse, the diameter of the bacterial zone of inhibition was measured in millimeters.

3. Results

A characteristic and well-defined plasmon-band for silver nanoparticles was obtained at around 455 nm, as shown in **Figure 1**. Ag NPs synthesized by *Chenopodium ambrosioides* produced polydisperse and stable nanoparticles.

Transmission electron microscopy (TEM) study demonstrated the size and the spherical or quasi-spherical shape of biogenic Ag NPs (**Figure 2**). The average particle size was determined to be around 8 nm, as shown in **Figure 2**.

Scanning electron microscopy (SEM) micrographs revealed that Ag NPs were formed on the surface of both suture threads, silk and catgut (**Figure 3**). It is possible to assume that the cavities in the suture threads can act as nanoreactors to attach, firstly, the silver ions to subsequently form the nanostructures when the reducing agent acts.

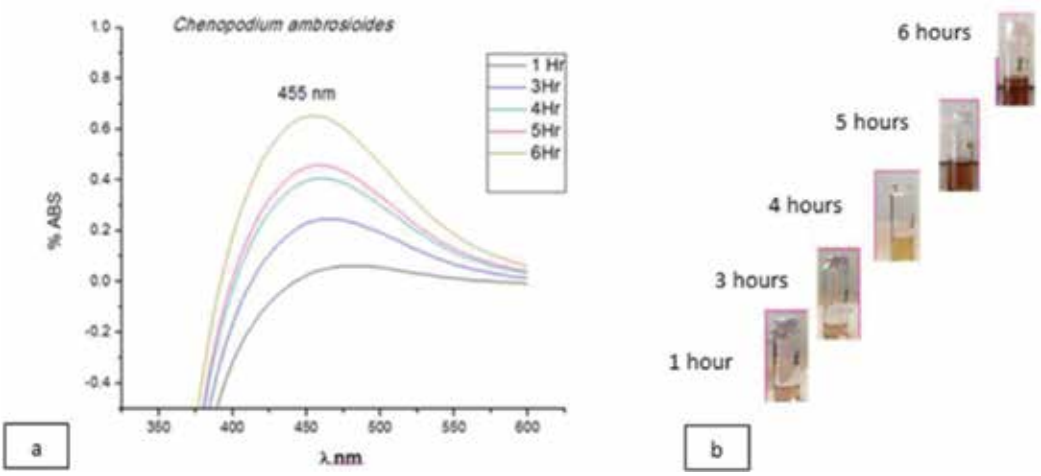

Figure 1. (a) UV-Vis Spectra showing that the surface plasmon resonance wavelength lies around 455 nm in Ag NPs synthesized by *Chenopodium ambrosioides*. (b) The flasks show the color change upon formation of silver nanoparticles; the solution changed from a light yellow to a light brown.

http://dx.doi.org/10.5772/intechopen.75074

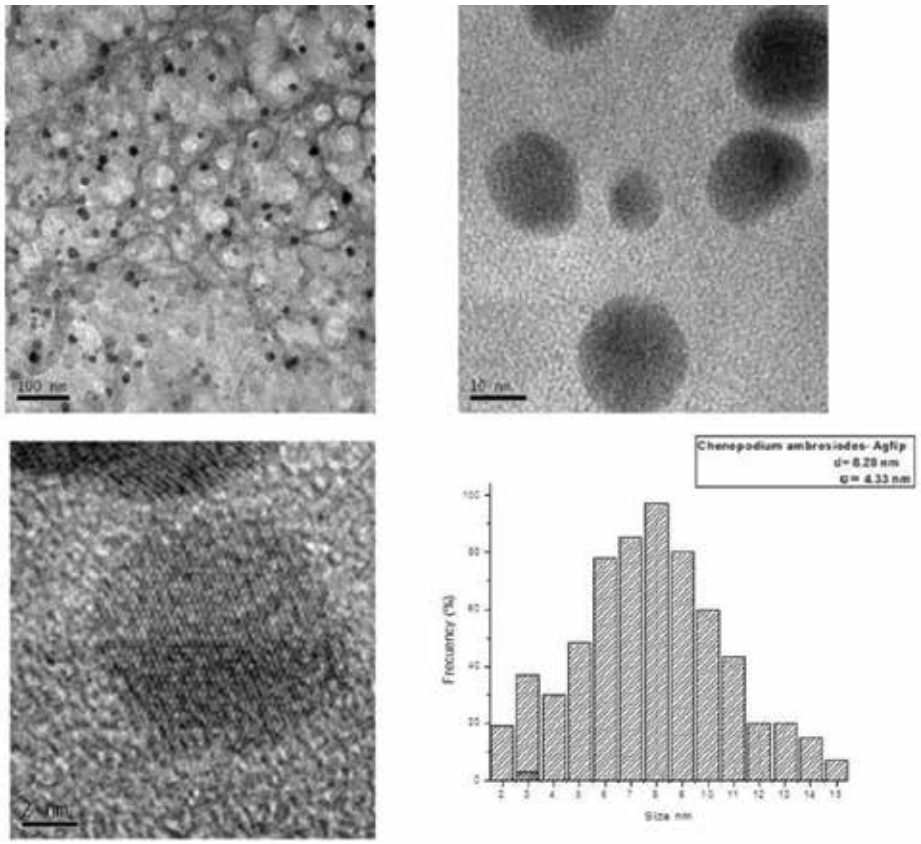

Figure 2. TEM images show that Ag NPs have a spherical shape, and the particle size distribution histogram shows that Ag NPs synthesized by *Chenopodium ambrosiodes* have a mean diameter of approximately 8 nm.

The antimicrobial activity of the biogenic Ag NPs, generated using *Chenoposium ambrosioides* infusion as reducing and capping agent, against *Staphylococcus aureus*, can be seen in **Figure 4**. The antibacterial effect of these biogenic Ag NPs can be observed clearly by the inhibition halo formed around the disk impregnated with the nanoparticles solution.

In **Figure 5**, the antimicrobial activity of both bionanocomposites against *S. aureus* and *E. coli* is observed. The suture threads (silk and catgut) were cut into small pieces and put on the Petri dishes, as mentioned in the experimental section. Some suture threads samples were used as a blank.

The inhibition growth of bacteria by the biogenic Ag NPs and the two bionanocomposites are shown in **Table 1**, revealing a strong antimicrobial effect of silver nanoparticles embedded in the corresponding suture threads against Gram-positive and Gram-negative bacteria.

As can be seen in **Table 1**, the growth inhibition of *Staphylococcus aureus* by disks impregnated with biogenic Ag NPs was on average 2.75 mm, compared to its control (*Chenopodium ambrosiodes* infusion with the same concentration). Also, the growth inhibition of *Escherichia coli* was

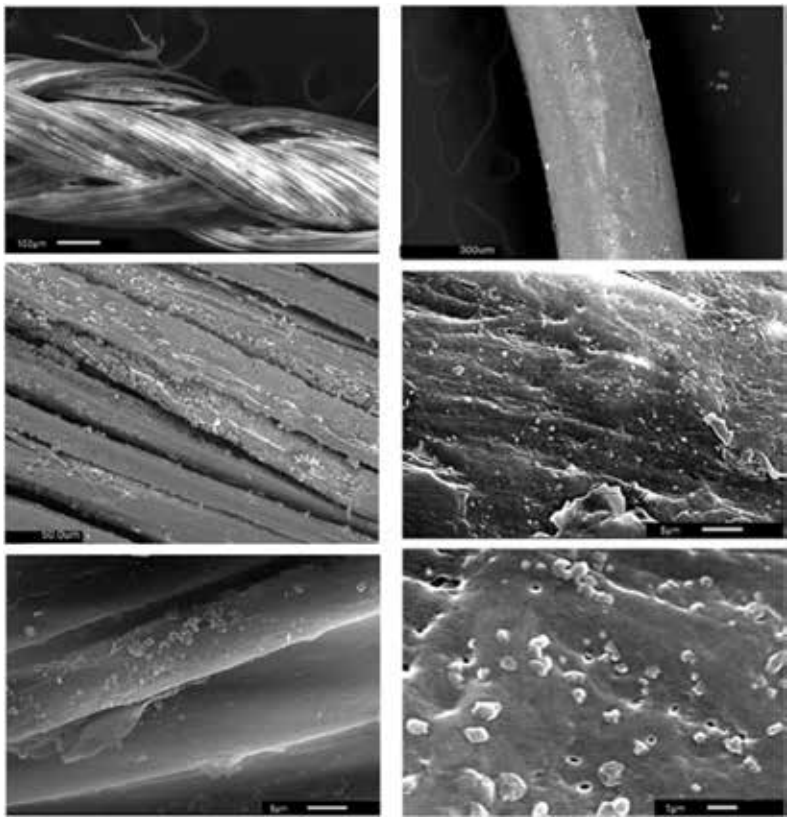

Figure 3. SEM micrographs showing Ag NPs embedded on silk (left images) and on catgut (right images) suture threads.

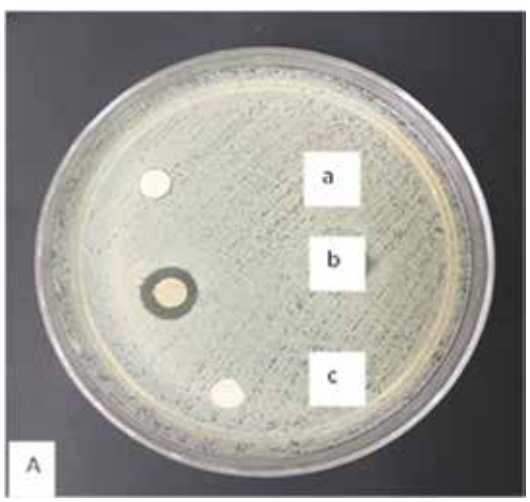

Figure 4. Ag NPs against *Staphylococcus aureus:* (a) blanc disc, (b) disc containing Ag NPs synthesized by *Chenopodium ambrosioides*, (c) disc with *Chenopodium ambrosioides* infusion as a control.

http://dx.doi.org/10.5772/intechopen.75074

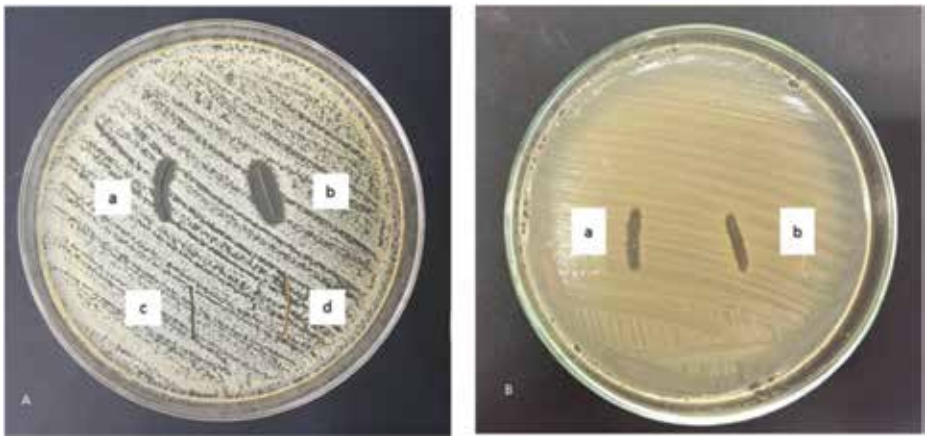

Figure 5. (A) Antibacterial effect of bionanocomposites against *Staphylococcus aureus*. (a) Silk suture thread-Ag NPs; (b) catgut suture thread-Ag NPs; (c) silk suture thread; (d) catgut suture thread. (B) Antibacterial effect of bionanocomposites against *Escherichia coli*. (a) Silk suture thread-Ag NPs; (b) catgut suture thread-Ag NPs.

Table 1. Inhibition of bacterial growth

	Staphylococcus aureus				Escherichia coli				
Discs and sutures	n	Mean (SD)		Minimun Value	Maximum Value	n	Mean	SD	Minimun value	Maximum value
AgNP C.a.	4	2.75 (0.5)%		2	3	4	2.5	0.577	2	3
Control C.a.	4	0	0	0	0	4	0	0	0	0
Blank control	4	0	0	0	0	4	0	0	0	0
Silk AgNP C.a.	15	2.533	0.516	2	3	15	2.467	0.516	2	3
Catgut AgNP C.a.	15	2.667	0.488	2	3	15	2.467	0.516	2	3

Table 1. Inhibition of bacterial growth.

on average 2.5 mm, compared to its control (*Chenopodium ambrosiodes* infusion with the same concentration). With the use of silk impregnated with biogenic Ag NPs the growth inhibition of *Staphylococcus aureus* was on average 2.53 mm, compared to the control solution. When silk impregnated with biogenic Ag NPs was used, the growth inhibition of *Escherichia coli* was on average 2.46 mm, compared to its control solution. For catgut impregnated with biogenic Ag NPs, the growth inhibition of *Staphylococcus aureus* was on average 2.6 mm; and the growth inhibition of *Escherichia coli* was on average 2.46 mm. There was no growth inhibition with

blank or control discs, neither with silk and catgut blank sutures, as can be seen in **Figures 4** and **5**. All the measurements were replicated three times for each treatment. Minimum and maximum value for each Petri sample is shown. The effect on both types of bacteria was similar. No statistically significant differences were found in both sutures with Ag NPs embedded.

4. Discussion

Periodontal and oral surgical procedures, in combination with the presence of foreign materials, may develop infectious processes when bacteria lodge on the suture material invading the suture track [22]. In the oral cavity, sutures are placed within high vascularity tissues, in a moist bacteria-rich environment. When performing surgical procedures using natural sutures, such as catgut or multifilament threads, as silk, the risk of infection may increase because bacteria are housed in the interstices [23]. Therefore, the choice of the kind of material for the closure of surgical wounds is paramount. Catgut, a monofilament suture made from the submucosa layer from the intestines of animals has been banned in Europe and Japan, due to health concerns [24, 25]. Silk is a natural protein fiber created by the *Bombyx mori* silk worm. It is well known for its water absorbency, which may favor bacterial growth [26]. Although both types of sutures have suitable properties for use, such as biocompatibility, flexibility and endurance, and sutures are designed to meet different needs, nowadays, more surgeons are opting for the use of synthetic suture materials [27]. We believe that the use of a suture thread bionanocomposite could prevent the colonization of pathogenic microorganisms. In this context, Ag NPs were selected in this study for decorating conventional sutures. It has been proved that the use of chemical elements such as silver is an alternative to multiple microorganisms. Silver is a nontoxic, safe inorganic antibacterial agent that can kill about 650 types of disease-causing microorganisms; silver nanoparticles can inhibit bacterial growth [5, 28]; therefore, they are currently being used in a variety of potential applications in pharmaceutics, medicine [6, 29] and we have recognized its use in dentistry [30, 31].

Although the precise antibacterial action of silver nanoparticles is not completely understood, it is believed that electrostatic attraction between negatively charged bacterial cells and positively charged nanoparticles is important for their antibacterial activity [32]. Ag NPs can interact with disulfide bonds of the glycoprotein/protein contents of microorganisms such as viruses, and bacteria, exerting an antimicrobial effect on Gram-positive and Gram-negative producing lysis in the peptides of the membrane of microorganisms. Certain studies have proposed that Ag NPs prompt neutralization of the surface electric charge of the bacterial membrane and change its penetrability, leading to bacterial death [33, 34]. On the other hand, the size of bacteria is measured in microns, three orders of magnitude greater than the nanoparticles obtained by green synthetic methods; therefore, the probability that the nanoparticles meet bacteria is higher when the size of Ag NPs is smaller. As it is known, the properties of Ag NPs depend on their size and shape, consequently, their controllable synthesis represents a key challenge to achieve their more desirable characteristics [13]. The development of reliable,

eco-friendly processes for the synthesis of nanomaterials is an important aspect of nanotechnology [35]. The synthesis of Ag NPs by eco-friendly agents represents an environmental and economically sustainable biological method that minimizes the costs and provides the benefits and properties of native plants and herbs such as *Chenopodium ambrosioides.* We have studied that there is huge potential of Mexican medicinal plants [36], among them, *Chenopodium ambrosioides* (Mexican Epazote) has been utilized in traditional cuisine and folk medicine since ancient times [18], it has demonstrated diverse pharmacological applications, it is also useful for healing of skin ulceration, and shows anti-inflammatory and antitumor properties [19, 37]. It is difficult to assign a single component of being responsible for the bioreduction; however, it is considered that the main chemical constituents involved in this process are mainly monoterpenoids, sesquiterpenoids, and flavonoids, among others [38].

To understand the way by which the nanoparticles adhere to the suture threads, it is necessary to describe the composition of the threads. Catgut was the first bioabsorbable suture made from animal intestines braided together to constitute a single strand, consisting mainly of collagen [39]. The collagen helix is a type of secondary structure protein consisting of amino groups. It is well known that silk is formed by two main proteins (sericin and fibroin). Fibroin consists mainly of recurrent amino acids sequence, containing carboxylic functional groups besides amino groups. Both show affinity to metallic atoms and cations, also, possess reducing properties. For this reason, carboxylic and amino groups could be responsible for the stabilization and capping of the silver nanoparticles [40].

It is important to consider that by electrostatic attraction the silver nanoparticles remain adhered to the threads, ensuring that there are not released into the oral environment. Besides, high surface area to volume ratio, allows Ag NPs to be effective in very small amounts [41], thus, we consider that the use of these type of bionanocomposites is an alternative approach to combat the bacterial resistance toward conventional antibiotics [42, 43], reducing as much as possible, the exaggerated prescription antibiotic schemes, affecting the systemic health of the patient; nonetheless, *in vivo* studies are required.

5. Conclusions

One of the pillars of oral surgery is based on a surgical procedure in an aseptic field, so it is essential to implement all means to achieve it, the bionanocomposites here presented can be effective for the treatment of periodontal surgery, being a useful tool against resistant bacteria. In this study, *Chenopodium ambrosiodes* turns out to be an appropriate reducing agent for coating natural suture threads with Ag NPs. The formed bionanocomposites possess important antibacterial activity against *S. aureus* and *E. coli.* This is an option that may help to reduce the harmful effect of the major pathogens while representing an attractive option as part of the eco-friendly materials, which would result not only in less expensive drugs but also in substances with a minor risk to human health and the environment.

Acknowledgements

We are indebted to Dr. Gloria Gutierrez-Venegas, Head of the Department of Biochemistry, Faculty of Dentistry, National Autonomous University of Mexico, for her guidance in the antimicrobial studies.

Conflict of interest

The authors declare that they have no conflict of interest.

Author details

Saraí C. Guadarrama-Reyes[1], Rogelio J. Scougall-Vilchis[1], Raúl A. Morales-Luckie[2]*, Víctor Sánchez-Mendieta[2] and Rafael López-Castañares[2]

*Address all correspondence to: ramoralesl@uaemex.mx

1 School of Dentistry, Autonomous University of the State of Mexico, Toluca, State of Mexico, Mexico

2 Joint Center for Research in Sustainable Chemistry (CCIQS), Autonomous University of the State of Mexico, Toluca, State of Mexico, Mexico

References

[1] Faramarzi MA, Sadighi A. Insights into biogenic and chemical production of inorganic nanomaterials and nanostructures. Advances in Colloid and Interface Science. 2013; **189-190**:1-20. DOI: 10.1016/j.cis.2012.12.001

[2] Zeeshan S, Kiran U, Ishtiaq M, Jamal A, Hameed A, Ahmed S, Ali N. Combine efficacy of biologically synthesized silver nanoparticles and different antibiotics against multi-drug-resistant bacteria. International Journal of Nanomedicine. 2013;**8**:3187-3195. DOI: 10.2147/IJN.S49284

[3] Coccia M, Wang L. Path-breaking directions of nanotechnology-based chemotherapy and molecular cancer therapy. Technological Forecasting and Social Change. 2015;**94**:155-169. DOI: 10.1016/j.techfore.2014.09.007

[4] Falzarano MS, Flesia C, Cavalli R, Guiot C, Ferlini A. Nanodiagnostics and nanodelivery applications in genetic alterations. Current Pharmaceutical Design. 10 Jan, 2018. DOI: 10.2174/1381612824666180110151318. [Epub ahead of print]

[5] Ibrahim HMM. Green synthesis and characterization of silver nanoparticles using banana peel extract and their antimicrobial activity against representative microorganisms.

Journal of Radiation Research and Applied Sciences. 2015;**8**:265-275. DOI: 10.1016/j.jrras.2015.01.007

[6] Beyth N, Houri-Haddad Y, Domb A, Khan W, Hazan R. Alternative antimicrobial approach: Nano-antimicrobial materials. Evidence-Based Complementary and Alternative Medicine. 2015;**2015**:246012. DOI: 10.1155/2015/246012

[7] Najafi-Taher R, Ghaemi B, Kharrazi S, Rasoulikoohi S, Amani A. Promising Antibacterial Effects of Silver Nanoparticle-Loaded Tea Tree Oil Nanoemulsion: a Synergistic Combination Against Resistance Threat. AAPS PharmSciTech. Jan 11, 2018. DOI: 10.1208/s12249-018-0950-2

[8] Kora AJ, Sashidhar R.B. Biogenic silver nanoparticles synthesized with rhamnogalacturonan gum: Antibacterial activity, cytotoxicity and its mode of action. Arabian Journal of Chemistry. March 2018;**11**(3):313-323. DOI: 10.1016/j.arabjc.2014.10.036

[9] Mat ZN, Stapley AGF, Shama G. Green synthesis of silver and copper nanoparticles using ascorbic acid and chitosan for antimicrobial applications. Carbohydrate Polymers. 2014;**112**:195-202. DOI: 10.1016/j.carbpol.2014.05.081

[10] Murugan K, Balakrishnan S, Senbagam D, Al-Sohaibani S. Biosynthesis of silver nanoparticles using acacia leucophloea extract and their antibacterial activity. International Journal of Nanomedicine. 2014;**9**:2431-2438. DOI: 10.2147/IJN.S61779

[11] Ramesh PS, Kokila T, Geetha D. Plant mediated green synthesis and antibacterial activity of silver nanoparticles using Emblica officinalis fruit extract. Spectrochimica Acta Part A: Molecular and Biomolecular Spectroscopy. 2015;**142**:339-343. DOI: 10.1016/j.saa.2015.01.062

[12] Shinde NM, Lokhande AC, Lokhande CD. A green synthesis method for large area silver thin film containing nanoparticles. Journal of Photochemistry and Photobiology B: Biology. 2014;**136**:19-25. DOI: 10.1016/j.jphotobiol.2014.04.011

[13] Roy N, Gaur A, Jain A, Bhattacharya S, Rani V. Green synthesis of silver nanoparticles: An approach to overcome toxicity. Environmental Toxicology and Pharmacology. 2103;**36**:807-812. DOI: 10.1016/j.etap.2013.07.005

[14] Bindhu MR, Umadevi M. Antibacterial and catalytic activities of green synthesized silver nanoparticles. Spectrochimica Acta Part A: Molecular and Biomolecular Spectroscopy. 2015;**135**:373-378. DOI: 10.1016/j.saa.2014.07.045

[15] Anastas P. Green Chemistry: Theory and Practice. Oxford University Press; 2000. 135 p. ISBN: 9780198506980

[16] Kumar K, Anand H, Mandal BK. Activity study of biogenic spherical silver nanoparticles towards microbes and oxidants. Spectrochimica Acta Part A: Molecular and Biomolecular Spectroscopy. 2015;**135**:639-645. DOI: 10.1016/j.saa.2014.07.013

[17] Liu L, Liu T, Tade M, Wang S, Li X, Liu S. Less is more, greener microbial synthesis of silver nanoparticles. Enzyme and Microbial Technology. 2014;**67**:53-58. DOI: 10.1016/j.enzmictec.2014.09.003

[18] Blanckaert I, Paredes-Flores M, Espinosa-Garcia FJ, Piero D, Lira R. Ethnobotanical, morphological, phytochemical and molecular evidence for the incipient domestication of Epazote (*Chenopodium ambrosioides* L.: Chenopodiaceae) in a semi-arid region of Mexico. Genetic Resources and Crop Evolution. 2012;**59**:557-573. DOI: 10.1007/s10722-011-9704-7

[19] Barros L, Pereira E, Calhelha R, Dueñas M, Carvalho AM, Santos-Buelga C, Ferreira I. Bioactivity and chemical characterization in hydrophilic and lipophilic compounds of *Chenopodium ambrosoides* L. Journal of Functional Foods. 2013;**5**:1732-1740. DOI: 10.1016/j.jff.2013.07.019

[20] Carrillo-López L, Zavaleta-Mancera H, Vilchis-Nestor A, Soto-Hernández M, Arenas-Alatorre J, Trejo-Téllez L, Gómez-Merino F. Biosynthesis of Silver Nanoparticles Using *Chenopodium ambrosioides*. Journal of Nanomaterials. 2014;**2014**:9. Article ID: 951746. DOI: 10.1155/2014/951746

[21] Kiuchi F, Itano Y, Uchiyama N, Honda G, Tsubouchi A, Nakajima-Shimada J, Aoki T. Monoterpene hydroperoxides with trypanocidal activity from *Chenopodium ambrosioides*. Journal of Natural Products. 2002;**65**:509-512. DOI: 10.1021/np010445g

[22] Banche G, Roana J, Mandras N, Amasio M, Gallesio C, Allizond V, et al. Microbial adherence on various intraoral suture materials in patients undergoing dental surgery. Journal of Oral and Maxillofacial Surgery. 2007 Aug;**65**(8):1503-1507

[23] Leknes KN, Selvig KA, Bøe OE, Wikesjö UM. Tissue reactions to sutures in the presence and absence of anti-infective therapy. Journal of Clinical Periodontology. 2005;**32**(2):130-138. DOI: 10.23736/S0026-4970.17.03966-8

[24] Niaounakis M. Biopolymers: Applications and Trends. Plastics Design Library series. PA, USA: Elsevier; 2015. 604 p. ISBN: 9780323353991

[25] Frost & Sullivan Market Insight. Does the Suture have a Future? [Internet]. 2002. Available from: http://www.frost.com/prod/servlet/market-insight-print.pag?docid=MBUT-5FGQ8S [Accessed: Dec 1, 2017]

[26] Srisuwan Y, Srisaard M, Sittiwet C, Baimark Y, Narkkong N-A, Butiman C. Preparation and characterization and characterization of nanocomposite and nanoporous silk friboin films. Journal of Applied Sciences. 2008;**8**(12):2258-2264. DOI: 10.3923/jas.2008.2258.2264

[27] Srinivasulu KN. Dhiraj K. A review on properties of surgical sutures and applications in medical field. International Journal of Research in Engineering & Technology. 2014;**2**:85-96. ISSN(P): 2347-4599

[28] Jayshree A, Thangaraju N. Green synthesis of silver nanoparticles: Characterization and determination of antibacterial potency. Applied Nanoscience. 2016;**6**:259-265. DOI: 10.1007/s13204-015-0426-6

[29] Jannathul M, Firdhouse L. Biosynthesis of Silver Nanoparticles and Its Applications. Journal of Nanotechnology. 2015;**2015**(2):18. Article ID: 829526. DOI: 10.1155/2015/829526

[30] García-Contreras R, Argueta-Figueroa L, Mejía-Rubalcava C, Jiménez-Martínez R, Cuevas-Guajardo S, Sánchez-Reyna P, Mendieta-Zerón H. Perspectives for the use of

silver nanoparticles in dental practice. International Dental Journal. 2011;**61**:297-301. DOI: 10.1111/j.1875-595X.2011.00072.x

[31] Mattos-Corrêa J, Mori M, Lajas-Sanches M, Dibo da Cruz A, Edgard Poiate Jr E, Venturini-Pola-Poiate A. Silver nanoparticles in dental biomaterials. International Journal of Biomaterials. 2015;**2015**:9. Article ID: 485275. DOI: 10.1155/2015/485275

[32] Guzmán M, Dille J, Godet S. Synthesis and antibacterial activity of silver nanoparticles against gram-positive and gram-negative bacteria. Nanomedicine: Nanotechnology, Biology and Medicine. 2012;**8**:37-45. DOI: 10.1016/j.nano.2011.05.007

[33] Dakal TC, Kumar A, Majumdar RS, Yadav V. Mechanistic basis of antimicrobial actions of silver nanoparticles. Frontiers in Microbiology. 2016;**7**:1831. DOI: 10.3389/fmicb.2016.01831

[34] Wang L, Hu C, Shao L. The antimicrobial activity of nanoparticles: Present situation and prospects for the future. International Journal of Nanomedicine. 2017;**12**:1227-1249. DOI: 10.2147/IJN.S121956

[35] Vilchis-Nestor AR, Sanchez-Mendieta V, Camacho-Lopez MA, Gomez-Espinosa RM, Camacho-Lopez MA, Arenas-Alatorre JA. Solventless synthesis and optical properties of Au and Ag nanoparticles using Camellia sinensis extract. Materials Letters. 2008;**62**:3103-3105. DOI: 10.1016/j.matlet.2008.01.138

[36] Rosas-Piñóna Y, Mejía A, Díaz-Ruiz G, Aguilar MI, Sánchez-Nieto S, Rivero-Cruz JF. Ethnobotanical survey and antibacterial activity of plants used in the altiplane region of Mexico for the treatment of oral cavity infections. Journal of Ethnopharmacology. 2012;**141**:860-865. DOI: 10.1016/j.jep.2012.03.020

[37] Carrillo-López L, Zavaleta-Mancera H, Vilchis-Nestor A, Soto-Hernández M, Arenas-Alatorre J, Trejo-Tellez L, Gómez-Merino F. Byosinthesis of silver nanoparticles using Chenopodium ambrosioides. Journal of Nanomaterials. 2014;**2104**:9. ID: 951746. DOI: 10.1155/2014/951746

[38] Hou S-Q, Li Y-H, Huang X-Z, Li R, Lu H, Tian K. Polyol monoterpenes isolated from *Chenopodium ambrosioides*. Journal of Natural Product Research. 2017;**31**:2467-2472. DOI: 10.1080/14786419.2017.1314278

[39] Vilchis-Nestor AR, Nolasco-Arizmendi V, Morales-Luckie RA, Sánchez-Mendieta V, JP Hinnestroza JP, Castro-Longoria E. Formation of silk-gold nanocomposite fabric using grapefruit aqueous extract. Textile Research Journal. 2012;**83**(12):1229-1235. DOI: 10.1177/0040517512461697

[40] Zhang D, William G, Hong T, Lin H, Yu Yue C. In situ synthesis of silver nanoparticles on silk fabric with PNP for antibacterial finishing. Journal of Materials Science. 2012;**47**:5721. DOI: 10.1007/s10853-012-6462-7

[41] Mahendra R, Ranjita S. Metal Nanoparticles in Pharma. Czech Republic: Springer; 2017. 493 p. ISBN: 978-3-319-63790-7

[42] Tillotson GS, Theriault N. New and alternative approaches to tackling antibiotic resistance. F1000Prime Reports. 2013;**5**:51. DOI: 10.12703/P5-51

[43] Richter K, Van den Driessche F, Coenye T. Innovative approaches to treat Staphylococcus aureus biofilm-related infections. Essays in Biochemistry. Mar 3, 2017;**61**(1):61-70. DOI: 10.1042/EBC20160056

Chapter 14

Electrochemical Formation of Silver Nanoparticles and Nanoclusters on Multiwall Carbon Nanotube Electrode Films

Andrés Alberto Arrocha Arcos and
Margarita Miranda-Hernández

Additional information is available at the end of the chapter

http://dx.doi.org/10.5772/intechopen.74056

Abstract

The Ag nanoparticles and nanoclusters (AgNP, AgNC) have been widely used due to their multiple applications, for example, in catalysts for CO_2 to CO electrochemical reduction, O_2 reduction in fuel cells, interface design for plasmonic resonance experiments and H_2O_2 or glucose sensors. The chemical methods most used to obtain AgNP, reported in the literature are: borohydride reduction, the Tollens method or the sonication at high concentrations of $AgNO_3$. One important disadvantage of these methods is the multiple steps required for electrode design, especially in carbon materials, and one of them is MWCNTs, used in some applications mentioned above. Electrodeposition has been reported in the preparation of metallic particles. In this chapter, we described the electropolishing method in the preparation of AgNP and AgNC supported on MWCNT film. An advantage of this proposed method is that it allows obtaining AgNP and AgNC in situ, supported on carbon matrices, ready to use as electrodes in different applications.

Keywords: silver nanoparticles, silver nanoclusters, electropolishing method, multiwall carbon nanotubes, carbon film electrode

1. Introduction

Ag nanoparticles (AgNP) have been widely used in multiple applications related to energy and storage, in the electrocatalytic conversion of CO_2 to CO [1]; in the spectroscopic analysis by enhancing the plasmonic resonance effect [2]; in the environmental remediation by

degrading highly toxic compounds [3]; for biosensor design with H_2O_2 detection systems [4], and in many molecular interaction technologies with DNA, RNA and proteins [5].

Different methods for the synthesis and preparation AgNP have been reported; one of the most implemented technologies is the physical methods based on evaporation-condensation and laser ablation; these methods offer high reproducibility and no chemical contamination. The AgNP size achieved by the physical methods is around 10–100 nm layers [6, 7].

The chemical methods normally used convey a reduction step; one of the most widely used is the borohydride reduction in which the injection method is preferred to provide AgNP of 17 ± 2 nm by using a polymeric template [8, 9]. In the borohydride method, the silver cation is reduced by the free electron pairs on borohydride molecule [10, 11]. In the same way, the Tollens reagent for $[Ag(NH_3)_2]^+$ reduction with saccharides is a chemical reduction method; this method allows 50 nm as the smallest size by controlling the ammonia and saccharide concentration [12–14].

Other methods, as the assisted methods, implement techniques of radiation like the photoinduced method in which AgNP are synthesized with Ag^+ by exposure to UV light and nucleate around a polymer matrix as polyvinyl alcohol. Other polymers as carboxymethylated chitosan or Triton molecules allows AgNP synthesis by changing the light intensity [15]. Similar to this UV light, the microwave-assisted synthesis is possible using the same reducing agents and the same silver ion source [16]. Finally, the greener methods are based on the reduction principle by the implementation of polymers and polysaccharides. These methods are similar to the chemical reduction technologies; nevertheless, the reduction is performed in a biodegradable polymer source like starch and the reaction is performed in mild conditions [17, 18].

The biological organism like bacteria, fungi, algae and plants allows the synthesis of silver nanoparticles in mild conditions. Nevertheless, these organisms need to be tolerant to the presence of silver on water. Moreover, these syntheses are in the real sense working as the previously discussed chemical and polymer-assisted methods. Biological-assisted synthesis is complex but in general terms the living organism provides several reducing agents or templates for silver cations as example proteins and peptides provide several amino acids with free electron pairs as Tyr residues and carboxyl groups in Asp/Glu residues [19], enzymes like Cyt C, NADH-dependent reductase, nitroreductase are able to transfer electrons and reduce free silver cations [20–22]. Different cells which produce polysaccharides in the cell's wall are perfect nucleation sites for silver proliferation. Also, chitosan and other biopolymers are suitable as templates for particle arrangement. In the case of plants and algae, the plethora of organic xenobiotics is cumbersome, and many molecules as flavonoids, catechols and polyphenols are able to reduce silver [23, 24].

In the previous paragraphs, different methods have been described for the synthesis of AgNPs. However, in the practical use of nanomaterials, some difficulties must be overcome; one of them is to avoid the formation of aggregates when they are handled directly. The presence of aggregates often overrides their unique functionalities. Therefore, it is very important to implement immobilization techniques for metallic NPs on easily handled supports.

The immobilization of AgNP into several matrices of synthetic and natural polymers has been reported with some success. One of the methods of incorporation and direct immobilization is the electrodeposition of AgNP on different matrices. Silver electrocrystallization studies have been reported in the last decades, and the understanding of silver electrodeposition process is reached on plane electrodes. The role of electrode nature and the effects of ionic metal concentration determine the kinetic, morphology, nucleation and growth during the electrodeposition process [25–27]. In the same way, carbon nanomaterials such as graphene and MWCNT provide a nanostructure which may facilitate the AgNP immobilization and the established procedures can be transferred to design AgNP. Techniques as potentiostatic double pulse (PDP) and chronoamperometry [28] have been implemented to obtain silver nanoclusters in different modified carbon materials like graphene intercalated with poly(sodium 4-styrenesulfonate) [29, 30]. The electrodeposits obtained by these techniques on substrates like MWCNT are commonly in the range of 100 nm to 1 mm [28]. Likewise, the obtainment of AgNP of controlled sizes by applying potential sweeps has been achieved in the presence of the chloride ion, which acts as an "abrasive" that modulates the nanoparticle to the required size from massive silver electrodes to obtain AgNP of 10–100 nm [31, 32].

It is clear that the direct immobilization and the specific size of the AgNP become a challenge for the different applications, in addition to the growing interest of conjugating the activity of these nanoparticles with nanostructured carbon materials.

This chapter describes the obtainment of silver nanoparticles and silver nanoclusters (AgNC) by the electropolishing of micrometer silver obtained with electrodeposition on MWCNT film electrodes. The procedure involves anodic stripping voltammetry in the presence of chloride ions as a polishing agent. The effect of the MWCNT functionalization in the formation of AgNP and AgNC is shown. This method is a straightforward proposal which enables the redesign of micrometric Ag deposits to nanometric size and is adaptable to already existing electrodeposition procedures. An advantage of this method is the obtainment electrodes with AgNP or AgNC supported on MWCNT films ready for direct use in different applications.

2. General techniques

2.1. Silver electrodeposition

An electrochemical three-electrode cell was used, with a Pt mesh as a counter electrode, reference electrode sulfate saturated electrode (SSE, 0.644 V vs. NHE). As working electrodes, different carbon film electrodes (CFEs) were used, prepared from an ink containing MWCNT and Nafion (see below) and supported on glassy carbon (GC) as a current collector. The silver electrodeposition is carried out in 10 mM $AgNO_3$/1 M KNO_3, pH = 7 system. Different potential values were selected (between −0.05 and −0.100 V range) and applied a potential pulse during 30 s to obtained silver deposits on the different CFEs. The AgNP and AgNC were obtained through the remodeling and sculpturing of Ag deposits using anodic stripping voltammetry in a system free of silver ions:100 mM KCl/100 mM K_2HPO_4/KH_2PO_4, pH = 7

at 20 mV/s; the scan was initiated from open circuit potential (OCP) to positive direction. All the electrochemical measurements were taken with a Basic Autolab W/PGSTAT30 & FRA equipment using Nova 3.1 software; all the electrolytes were prepared with analytical-grade reagents and deionized water (18 MΩcm) using a Milli-QTM system.

2.2. Electrode preparation

The carbon film electrodes (CFEs) were prepared from an ink containing 3 mg MWCNT, 1 ml Nafion (0.05%) and isopropylic alcohol, mixed by sonication for 1 h. After, 3 μl of this ink was applied by dropping cast on GC and dried at room temperature. Before the dropping cast step, the GC surface was polished with fine 600 grit silicon carbide sandpaper, once rinsed GC was polished with cloth and alumina of 0.3 and 0.05 μm. MWCNTs were commercial with the following characteristics: 95% purity, 5–15 μm long, 2–7 nm ID and 10 nm OD (Nanostructured & Amorphous Materials Inc.). The MWCNTs were functionalized using reflux in 65% HNO_3 at different times: 2, 10 and 24 h. After the reflux step, the MWCNTs were washed with MiliQ water until pH 7 was reached, filtrated with 50 nm nitrocellulose filters. CFEs elaborated with functionalized MWCNT were identified in the manuscript as CFE2, CFE10 and CFE24, and the number corresponds to the reflux time.

2.3. CFE morphology and Ag particle size

Scanning electronic microscopy (SEM) is used to describe the morphology of the MWCNT as CFE after chemical treatment for every single reflux time, besides silver deposits were analyzed before and after electropolishing procedure. A scanning electron microscope (FE SEM Hitachi S-5500) was used to determine particle size, and distribution was obtained using the ImageJ 1.50i software.

2.4. X-ray photoelectron spectroscopy

Finally, an X-ray photoelectron spectroscopy (XPS) was used to perform the quantification of Cs1 and Os1, the spectra obtained from the average of three zones with a 400-μm^2 randomly selected area on the surface of each MWCNT material. The oxidize groups (hydroxyl, carbonyl and carboxyl) were quantified by deconvolution performed with GNUPLOT Free Software License 4.6 by multiple Gaussians fit.

3. Results and discussion

3.1. MWCNT morphology characterization

Figure 1 shows the SEM images corresponding to MWCNT with different reflux times (all images show the same magnification). The morphology and structure change as reflux time increases are presented. MWCNT in CFE2 shows few imperfections preserving structure possibly due to the treatment time reduction (**Figure 1A**). In the case of CFE10, the structures

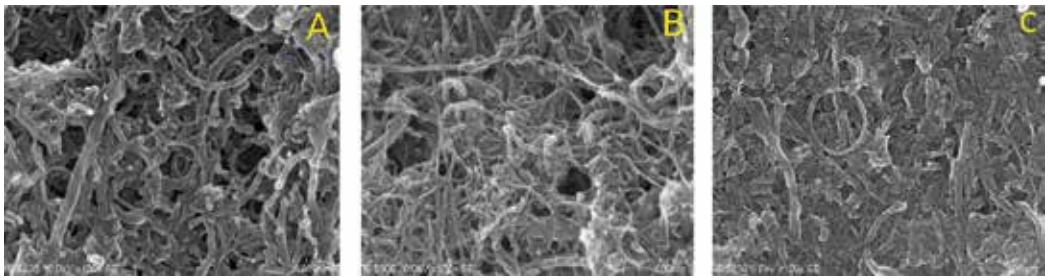

Figure 1. SEM images showing the morphology on: (A) CFE2, (B) CFE10 and (C) CFE24.

of MWNCT are preserved, but with lower diameter against CFE2, also many defects are observed on the MWNCT surface (**Figure 1B**). Finally, CFE24 presents a drastic loss of structure with aggregate formation tendency (**Figure 1C**). It is well known that long functionalization times affect MWCNT structure as has been already reported [33, 34].

3.2. X-ray photoelectron spectroscopy analysis

The MWCNT chemical surface composition was carried out through an XPS study. **Figure 2** shows the XPS spectra in the Cs1 and Os1 regions corresponding to MWCNT treated with acid reflux at different times. The intensity of Cs1 decreases as the reflux time increases, in contrast to the increase of Os1 peak in direct relation to the reflux time increase (**Figure 2A**, **B**). The deconvolution of Os1 for the MWCNT at 24 h is provided in **Figure 2C**. Four different peaks are presented in every O1s signal, and the functional group positions used for the deconvolution are C=O (531.2 eV), O-C=O* (531.6 eV), C-OH (532.8 eV) and O=C-O (534.5 eV) according to previous reports [33, 34]. **Table 1** shows the ratio of oxygenated group intensities on MWCNT with treatment against pristine MWCNT. At the treatment times of 2, 10 and 24 h in which case, the OH− and COO− groups are favored as time increases.

The XPS results show that reflux treatment provokes an increase in oxygen content with the concomitant carbon decrease; the only difference is the oxygenated functional groups content on every MWCNT. The generation of defects observed on SEM images is in direct correlation

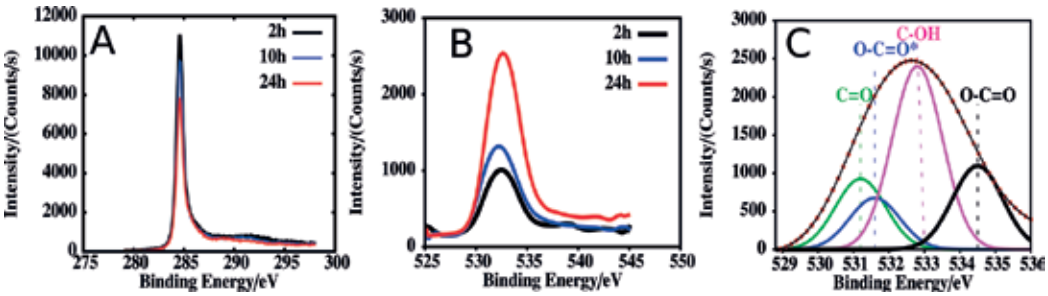

Figure 2. XPS spectra corresponding to MWCNT treated with acid reflux at different time. (A) Cs1, (B) Os1 and (C) deconvolution of Os1 for CFE24.

MWCNT functionalization time (h)	$MWCNT_f/MWCNT_p$		
	C-OH	C=O	COO^-
2	1.88	0.27	0.46
10	2.90	0.99	1.94
24	5.15	2.21	3.57

Table 1. Relative appearance of functionalized groups against pristine MWCNT obtained by deconvolution of O1s shown in **Figure 2B**.

with the surface functionalization produced by this treatment. The relationship of these oxidized MWCNT surfaces on the silver electrodeposition process and remodeling will be discussed in further sections.

3.3. Electrodeposition of micro silver particles on MWCNT

With the aim of establishing the conditions for the silver electrodeposition process, a cyclic voltammetry study (CV) in 10 mM $AgNO_3$/1 M KNO_3 system was carried out to describe the potential range of silver electrodeposition at 20 mV/s. The scan initiates at open circuit potential (OCP) in the negative direction up to the potential limit of −0.6 V where the sweep direction is reversed to the uppermost potential at 0.6 V vs. SSE. **Figure 3** shows the responses corresponding to the different CFE (indicated in the figure); in all cases, two reduction steps are depicted by Red1 and Red2. In the reverse direction, the Ox1 peak is observed which corresponds to the redissolution process of the previously deposited silver. Noteworthy, density currents descend with MWCNT functionalization time; it is important to note that the deposition potentials are dependent on the electrode type. In **Table 2**, potential values for Red1 and Red2 are shown. This proves that silver deposition involved two processes. The

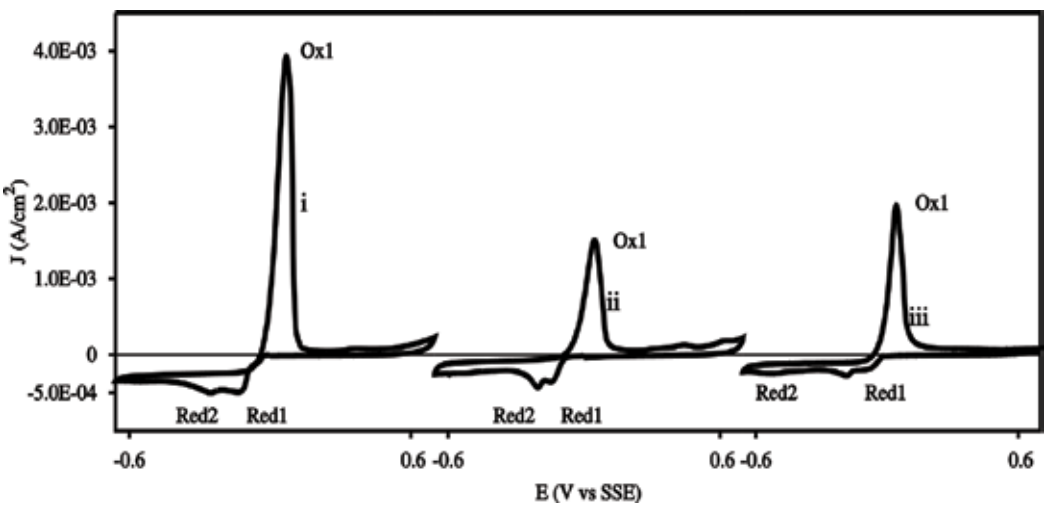

Figure 3. Cyclic voltammetry responses obtained in 10 mM $AgNO_3$/1 M KNO_3 system correspond to silver deposition on: (i) CFE2, (ii) CFE10 and (iii) CFE24. The scan started from OCP to negative direction at 20 mV/s, in the potential range −0.6 to 0.6 V vs. SSE.

Electrode	Red1(V vs. SSE.)	Red2 (V vs. SSE.)
CFE2	−0.133	−0.256
CFE10	−0.144	−0.200
CFE24	−0.186	−0.350

Table 2. Voltammetry parameters obtained of cyclic voltammetry studies for silver deposit.

lower reduction potentials observed at Red1 are possibly related to an energetically favor step due to more accessible physical sites. The higher electrodeposition potentials observed at Red2 indicate sites with difficult access for Ag^{+} cation into the MWCNT matrix. The presented results show that there is a clear influence of the MWCNT surface chemistry on the silver electrodeposition process.

Considering the CV results discussed above, different potentials values were selected for Ag electrodeposition applying a 30 s pulse on every matrix. The electrodes obtained from this procedure are defined as $Ag°_{micro}$/CFE2, $Ag°_{micro}$/CFE10 and $Ag°_{micro}$/CFE24 for the applied potential of −0.083, −0.09 and −0.130 V vs. SSE, respectively. SEM images allow a description of the micrometric deposits; in all the cases, it is clear that MWCNTs are gradually covered by Ag° (**Figure 4A**-**C**). Silver intercalation is observed in MWCNT's matrix. In other areas, the presence of agglomerates is such that MWCNTs are no longer visible, and they are covered up in the silver deposits.

No matter the functionalization and the imperfections on the MWCNT surface, the micrometric silver electrodeposition was successful in three electrodes. The results presented here indicate that the silver micrometric electrodeposition process is independent of the MWCNT chemical surface moieties. Similar results have been previously reported, showing the micrometric silver on MWCNT after electrodeposition process which indicates that other steps may be needed to achieve AgNP by these techniques [29, 30]. An electropolishing procedure is proposed to take advantage of the different MWNCT chemical surface, and it is evinced that this procedure will act as a modulator for AgNP obtainment; the results are discussed in the next section as the following step after the electrodeposition process.

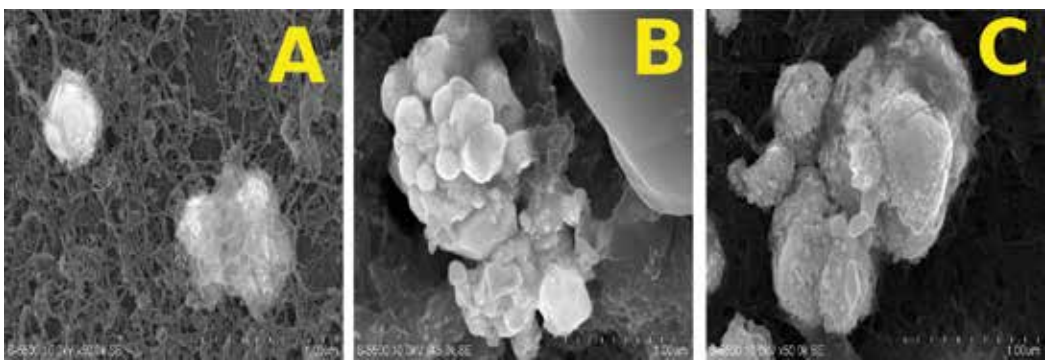

Figure 4. SEM images corresponding to (A) $Ag°_{micro}$/CFE2, (B)$Ag°_{micro}$/CFE10 and (C)$Ag°_{micro}$/CFE24.

3.4. Electropolishing of micrometric silver particles toward achieving AgNP and AgNC

To obtained AgNP and AgNC, a program of anodic stripping cycles in 100 mM KCl/100 mM K_2HPO_4/KH_2PO_4,pH = 7, at 20 mV/s was applied. **Figure 5** shows SEM images corresponding to AgNP obtained after the remodeling process. For AgNP/CFE2, dispersed particles of approximately 10 nm size (**Figure 5A**) are observed. On the other hand, for AgNP/CFE10 particles are around 20 nm, and a low population of them is observed (**Figure 5B**). Finally, the particles presented in AgNP/CFE24 are preferentially in the 10–20 nm range, and they are covering most of the MWCNT matrix (**Figure 5C**).

The formation of Ag nanocluster (AgNC) on MWNCT surface by electrochemical methods is scarcely reported [29, 30]. In our case, AgNC can be obtained from the electrodeposition process on CFE24 in the system 1 mM $AgNO_3$/1 M KNO_3 pH = 7 applying a − 0.070 V vs. SSE during 30 s. After anodic stripping voltammetry in similar experimental conditions described previously, AgNC/CFE24 was obtained (**Figure 6A**). The AgNC are well dispersed with a size between 1.2 and 1.8 nm (**Figure 6B**). Considering the atomic radii of Ag (0.144 nm), AgNC contains approximately 8–12 silver atoms. These AgNC are even smaller than the ones obtained by with poly(sodium4-styrenesulfonate) and oligonucleotides as intercalated agents, respectively [29, 30].

The advantage of the electrochemical method for the obtainment AgNP/CFE and AgNC/CFE is that these electrodes are ready for immediate use in different processes, such as electrocatalysis, specifically in the electrochemical reduction of CO_2 and O_2.

3.5. Steps involved in the formation of silver nanoclusters

What is the mechanism involved in the obtainment of AgNP and AgNC? When anodic stripping voltammetry was applied to the MWCNT with silver microdeposits, the Ag^+ is liberated to the bulk solution; in the presence of chloride anions, a AgCl(s) layer is formed (reaction 1).

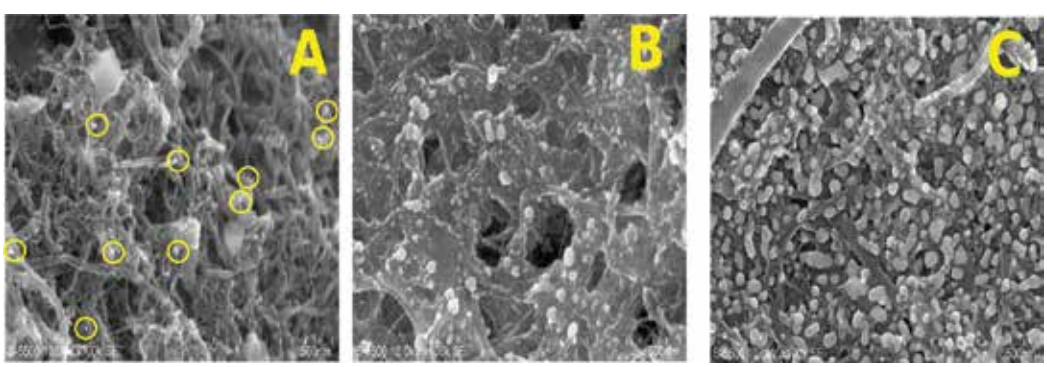

Figure 5. SEM images of AgNP supported on different CFE: (A) AgNP/CFE2, (B) AgNP/CFE10 and (C) AgNP/CFE24 after electropolishing by anodic stripping voltammetry procedure.

http://dx.doi.org/10.5772/intechopen.74056

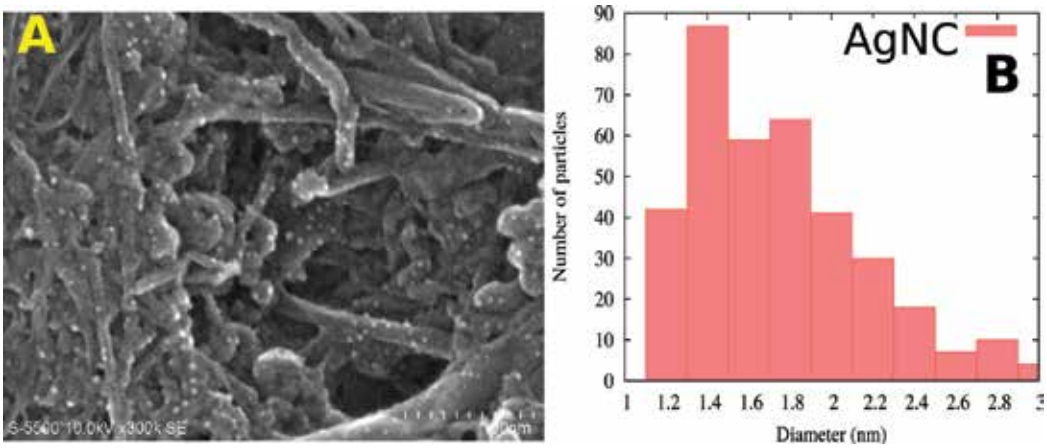

Figure 6. (A) SEM images of AgNC/CFE24 with deposit at 1 mM $AgNO_3$ after anodic stripping voltammetry procedure. (B) Particle distribution histogram.

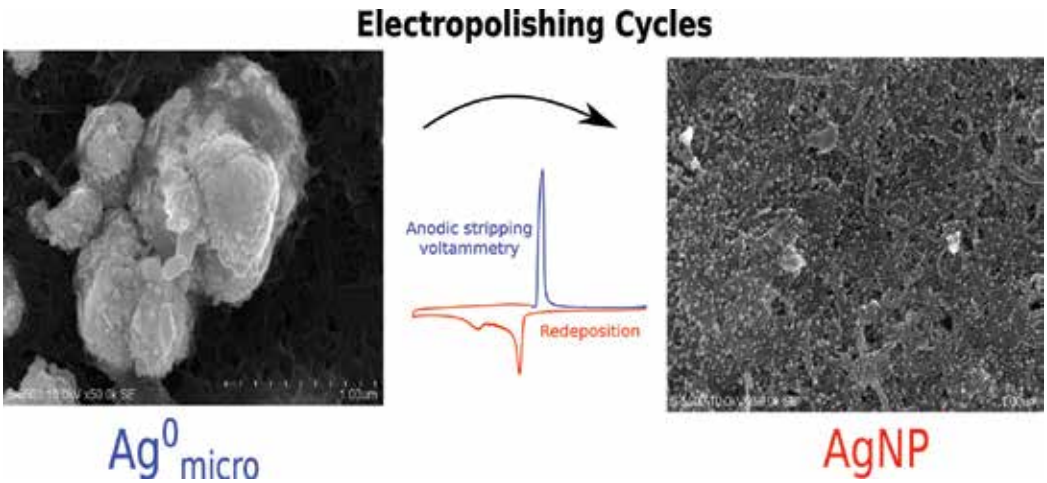

Figure 7. Squematic representation of the electropolishing process for the obtainment of AgNP from Ag^0_{micro} in 100 mM KCl/100 mM K_2HPO_4/KH_2PO_4 pH = 7 at 20 mV/s.

The direction of the scan is reverse to promote the reduction of AgCl(s) to obtain AgNP or AgNC (reaction 2), and a representation of the process is presented in **Figure 7**. Then, the 10 consecutive stripping cycles allow the size modulation and the particle distribution of MWCNT matrix. The catalytic activity of these AgNP and AgNC has been recently reported for the electrochemical formate synthesis from CO_2 [35].

$$Ag^0_{micro} - e^- \rightarrow Ag^+ + Cl^- \rightarrow AgCl_{(s)} \quad (1)$$

$$AgCl_{(s)} + e^- \rightarrow Ag^0_{NP} + Cl^- \quad (2)$$

4. Conclusions

This chapter describes an outstanding methodology for the obtainment of in situ generating AgNP and AgNC on MWCNT film electrodes. This methodology allows the size modulation and the immobilization of the immediate application in catalytic processes such as the electrochemical reduction of O2 and CO2. The silver electrodeposition process is facilitated by the proper MWCNT functionalization; an original electropolishing process is applied for the AgNP and AgNC obtainment. This method markedly outstrips the existing procedures which are characterized by being more expensive and with multiple synthesis steps.

Acknowledgements

The authors acknowledge the financial support of PAPIIT-DGAPA-UNAM-IN201815 and Engineer Rogelio Elvira Morán for technical support in obtaining SEM images. Andrés A. Arrocha Arcos thanks the PhD scholarship granted by CONACYT.

Author details

Andrés Alberto Arrocha Arcos and Margarita Miranda-Hernández*

*Address all correspondence to: mmh@ier.unam.mx

Institute of Renewable Energies, National Autonomous University of Mexico, Temixco, Morelos, México

References

[1] Kim C et al. Achieving selective and efficient electrocatalytic activity for CO_2 reduction using immobilized silver nanoparticles. Journal of the American Chemical Society. 2015;**137**:13844-13850. DOI: 10.1021/jacs.5b06568

[2] Sun R, Li SJ, Yao JL, Gu RA. Surface enhanced Raman spectroscopy and theoretical studies on the electrochemical transformation processes of 4-aminothiophenol on au electrode. Acta Chimica Sinica. 2007;**65**:1741-1745

[3] Cesarino I et al. Electrochemical degradation of benzene in natural water using silver nanoparticle-decorated carbon nanotubes. Materials Chemistry and Physics. 2013;**141**: 304-309. DOI: 10.1016/j.matchemphys.2013.05.015

[4] Wan Q et al. In situ synthesized gold nanoparticles for direct electrochemistry of horseradish peroxidase. Colloids and Surfaces. B, Biointerfaces. 2013;**104**:181-185. DOI: 10.1016/j.colsurfb.2012.12.009

[5] Jin J et al. Nucleic acid-modulated silver nanoparticles: a new electrochemical platform for sensing chloride ion. The Analyst. 2011;**136**:3629-3634. DOI: 10.1039/c1an15283a

[6] Yu A et al. Silver nanoparticle-carbon nanotube hybrid films: Preparation and electrochemical sensing. Electrochimica Acta. 2012;**74**:111-116. DOI: 10.1016/j.electacta.2012.04.024

[7] Tsierkezos NG et al. Nitrogen-doped multi-walled carbon nanotubes modified with platinum, palladium, rhodium and silver nanoparticles in electrochemical sensing. Journal of Nanoparticle Research. 2014;**16**:1-13. DOI: 10.1007/s11051-014-2660-3

[8] Zamiri R et al. Laser based fabrication of chitosan mediated silver nanoparticles. Applied Physics A: Materials Science & Processing. 2011;**105**:255-259. DOI: 10.1007/s00339-011-6525-7

[9] Chen RH, Phuoc TX, Martello D. Effects of nanoparticles on nanofluid droplet evaporation. International Journal of Heat and Mass Transfer. 2010;**53**:3677-3682. DOI: 10.1016/j.ijheatmasstransfer.2010.04.006

[10] Noordeen S, Karthikeyan K, Parveen MN. Synthesis of silver nanoparticles by using sodium borohydride as a reducing agent. International Journal of Engineering Research Technology. 2013;**2**:388-397. DOI: 10.13140/2.1.3116.8648

[11] Van Hyning DL, Klemperer WG, Zukoski CF. Silver nanoparticle formation: Predictions and verification of the aggregative growth model. Langmuir. 2001;**17**:3128-3135. DOI: 10.1021/la000856h

[12] Soukupová J, Kvítek L, Panáček A, Nevěčná T, Zbořil R. Comprehensive study on surfactant role on silver nanoparticles (NPs) prepared via modified Tollens process. Materials Chemistry and Physics. 2008;**111**:77-81. DOI: 10.1016/j.matchemphys.2008.03.018

[13] Pal S et al. Site-specific synthesis and in situ immobilization of fluorescent silver nanoclusters on DNA nanoscaffolds by use of the tollens reaction. Angewandte Chemie - International Edition. 2011;**50**:4176-4179. DOI: 10.1002/anie.201007529

[14] Dondi R, Su W, Griffith GA, Clark G, Burley GA. Highly size- and shape-controlled synthesis of silver nanoparticles via a templated tollens reaction. Small. 2012;**8**:770-776. DOI: 10.1002/smll.201101474

[15] Huang L et al. UV-induced synthesis, characterization and formation mechanism of silver nanoparticles in alkalic carboxymethylated chitosan solution. Journal of Nanoparticle Research. 2008;**10**:1193-1202. DOI: 10.1007/s11051-007-9353-0

[16] Perelaer J, Klokkenburg M, Hendriks CE, Schubert US. Microwave flash sintering of inkjet-printed silver tracks on polymer substrates. Advanced Materials. 2009;**21**:4830-4834. DOI: 10.1002/adma.200901081

[17] Raghavendra GM, Jung J, Kim D, Seo J. Step-reduced synthesis of starch-silver nanoparticles. International Journal of Biological Macromolecules. 2016;**86**:126-128. DOI: 10.1016/j.ijbiomac.2016.01.057

[18] Kim B et al. Novel synthesis of porous silver nanostructures using a starch template and their applications toward plasmonic sensors. Chemphyschem. 2013;**14**:2663-2666. DOI: 10.1002/cphc.201300278

[19] Zaheer Z, Rafiuddin. Nucleation and growth kinetics of silver nanoparticles prepared by glutamic acid in micellar media. International Journal of Chemical Kinetics. 2012;**44**: 680-691. DOI: 10.1002/kin.20711

[20] Wallace JM et al. Silver-colloid-nucleated cytochrome c superstructures encapsulated in silica nanoarchitectures. Langmuir. 2014;**20**:9276-9281. DOI: 10.1021/la048478u

[21] Talekar S et al. Preparation of stable cross-linked enzyme aggregates (CLEAs) of NADH-dependent nitrate reductase and its use for silver nanoparticle synthesis from silver nitrate. Catalysis Communications. 2014;**53**:62-66. DOI: 10.1016/j.catcom.2014.05.003

[22] Syed B et al. Synthesis of silver nanoparticles by endosymbiont pseudomonas fluorescens CA 417 and their bactericidal activity. Enzyme and Microbial Technology. 2016;**95**: 128-136. DOI: 10.1016/j.enzmictec.2016.10.004

[23] Banerjee P, Satapathy M, Mukhopahayay A, Das P. Leaf extract mediated green synthesis of silver nanoparticles from widely available Indian plants: synthesis, characterization, antimicrobial property and toxicity analysis. Bioresource Bioprocess. 2014;**1**:3. DOI: 10.1186/s40643-014-0003-y

[24] Prasad R. Synthesis of silver nanoparticles in photosynthetic plants. Journal of Nanoparticles. 2014:1-8. DOI: 10.1155/2014/963961

[25] Miranda-Hernández M, González I. Effect of potential on the early stages of nucleation and growth during silver electrocrystallization in ammonium medium on vitreous carbon. Journal of the Electrochemical Society. 2004;**151**:C220. DOI: 10.1149/1.1646154

[26] Miranda-Hernández M, Palomar-Pardavé M, Batina N, González I. Identification of different silver nucleation processes on vitreous carbon surfaces from an ammonia electrolytic bath. Journal of Electroanalytical Chemistry. 1998;**443**:81-93. DOI: 10.1016/S0022-0728(97)00487-7

[27] Miranda-Hernández M, González I, Batina N. Silver electrocrystallization onto carbon electrodes with different surface morphology: Active sites vs surface features. The Journal of Physical Chemistry. B. 2001;**105**:4214-4223. DOI: 10.1021/jp002057d

[28] Ding YF, Jin GP, Yin JG. Electrodeposition of silver nanoparticles on MWCNT film electrodes for hydrogen peroxide sensing. Chinese Journal of Chemistry. 2007;**25**:1094-1098. DOI: 10.1002/cjoc.200790204

[29] Jin S et al. Stable silver nanoclusters electrochemically deposited on nitrogen-doped graphene as efficient electrocatalyst for oxygen reduction reaction. Journal of Power Sources. 2015;**274**:1173-1179. DOI: 10.1016/j.jpowsour.2014.10.098

[30] Lopes JH, Ye S, Gostick JT, Barralet JE, Merle G. Electrocatalytic oxygen reduction performance of silver nanoparticle decorated electrochemically exfoliated graphene. Langmuir. 2015;**31**:9718-9727. DOI: 10.1021/acs.langmuir.5b00559

[31] Hsieh YC, Senanayake SD, Zhang Y, Xu W, Polyansky DE. Effect of chloride anions on the synthesis and enhanced catalytic activity of silver nanocoral electrodes for CO_2 electroreduction. ACS Catalysis. 2015;**5**:5349-5356. DOI: 10.1021/acscatal.5b01235

[32] Zhang L, Wang Z, Mehio N, Jin X, Dai S. Thickness- and particle-size-dependent electrochemical reduction of carbon dioxide on thin-layer porous silver electrodes. ChemSusChem. 2016;**9**:428-432. DOI: 10.1002/cssc.201501637

[33] Wepasnick KA et al. Surface and structural characterization of multi-walled carbon nanotubes following different oxidative treatments. Carbon N. Y. 2001;**49**:24-36. DOI: 10.1016/j.carbon.2010.08.034

[34] Lehman JH, Terrones M, Mansfield E, Hurst KE, Meunier V. Evaluating the characteristics of multiwall carbon nanotubes. Carbon N. Y. 2011;**49**:2581-2602. DOI: 10.1016/j.carbon.2011.03.028

[35] Arrocha-Arcos AA, Cervantes-Alcalá R, Huerta-Miranda GA, Miranda-Hernández M. Electrochemical reduction of bicarbonate to formate with silver nanoparticles and silver nanoclusters supported on multiwalled carbon nanotubes. Electrochimica Acta. 2017;**246**:1082-1087. DOI: 10.1016/j.electacta.2017.06.147./j.electacta.2017.06.147

Edited by Khan Maaz

Silver nanoparticles are the subject of immense interest because of their distinct chemical and physical properties that are different from their bulk counterpart. This makes these nanoparticles very important in many fields including antimicrobial applications, biosensor materials, composite fibers, cryogenic superconducting materials, cosmetic products, and electronic components. This book aims to provide in-depth study and analysis of various fabrication, characterization, and application techniques of silver nanoparticles that lead these nanoparticles very important in the recent technology. This book presents deep understanding of the new techniques from basic to the advanced level. This book addresses scientists, engineers, doctoral and postdoctoral fellows, and technical professionals working in specialized fields.

Published in London, UK

IntechOpen

ISBN 978-1-83881-546-2